

DSE Final Report

AE3200 - Design Synthesis Exercise
Wings For Aid

Group 18



DSE Final Report

by

Group 18: Wings for Aid

Torben Aalbers	5297672
Maxime Biolders	4794877
Tim den Blanken	5294525
Théo Huegens	5073502
Ties Leniger	5258456
Linda Mahajna	5229529
Jarno Platenburg	5321484
Bram Staps	5315131
Jan Vonken	5324890
Jan Wiącek	5215102

Institution: Delft University of Technology
Place: Faculty of Aerospace Engineering, Delft
Project Duration: April 2023 - June 2023

Cover Image: Wings for Aid - Render of Aircraft
Source: Own Work

Executive Overview

Wings for Aid is a company focused on solving the 'last mile' problem in humanitarian aid delivery. Disaster-stricken areas often prove to be hard to navigate on land. The approach Wings for Aid takes to solve the last mile problem is aerial delivery of boxes that contain 20 kilograms of aid with pinpoint accuracy. To fulfil this mission, Wings for Aid uses remotely piloted aircraft. The present report describes the design process of such an aircraft capable of delivering 10 to 12 boxes of aid at a distance of 250 kilometres. The main objective of this design is to minimize the cost of delivery and the unit cost of the aircraft. With the help of Wings for Aid, humanitarian aid delivery becomes quicker, safer and more efficient.

The present report documents the detailed design phase of this project. This entails the system engineering and project planning as well as the design of all subsystems; propulsion, fuselage, wing, empennage, and undercarriage. Analysis of the flight performance, operations and logistics of the project is performed. Subsequently, all aspects of the design are brought together and integrated. As cost is a crucial parameter in this project, the total cost of the aircraft and the delivery is analysed. Finally, verification and validation is performed on the models that were used in the design process.

Systems Engineering

Systems engineering is the key to any project's success. It provides a foundation upon which the project is built. The project description is created first. The mission objective is to deliver 10 to 12 aid packages containing 20 kilograms of aid at a range of 250 kilometres. The project entails designing a new remotely piloted aircraft that is able to fulfil this objective. From this, the project objective flows down. The objective is to design a remotely piloted aircraft, able of delivering 10 to 12 boxes of aid at a range of 250 kilometres, with 10 students in 10 weeks.

To get an overview of the functionality of the system, tools such as the Functional Flow Diagram (FFD) and Functional Breakdown Structure (FBS) are used. The mission is subdivided into a number of top-level phases; setting up the ground base and transporting aircraft there, the operational phase and the end of mission phase. Setting up the ground base covers the selection of a location, setting up equipment, defining a runway and arranging a loading area. The functionality of the aircraft in the first and last top-level phase entails the modularity of the aircraft. The main wing and horizontal stabiliser can be dismantled from the aircraft in order for it to fit in a 40 foot ISO container. The majority of the functions fall under the operational phase. This phase is, again, subdivided into sub-phases. These sub-phases are ground operations like loading, fueling and maintenance, take-off, climb, cruise, descent, loitering and dropping manoeuvres. At the end of mission phase, the state of the aircraft is assessed from which a decision is made whether the aircraft can be used for another mission or whether it enters the end-of-life phase. The goal of the end-of-life phase is to recycle as much as possible.

After the functional analysis, the requirement analysis is performed. This analysis provides a framework defining the goals and boundaries of the project. The following requirements play a large role in the design process and eventual outcome. The importance of cost for this project is defined in two requirements. The unit cost of an aircraft shall not be more than €25,000 and the cost of delivering a kilogram of payload shall be not more than two to four times higher than that of a truck. The size of the operation is dictated by the requirement that the daily payload delivery capacity shall be equal to that of a C130 Hercules aircraft. Additionally, the first boxes have to be delivered within 72 hours of Wings for Aid being contracted to deliver aid.

In the design process, contingencies are applied in order to cover uncertainties. These contingencies appear in the form of margins and safety factors. The magnitude of the contingencies decrease throughout the project. On the result of the design phase, contingencies of 5% are applied to most parameters. These contingencies are expected to decrease more when the design process is continued past this stage.

Next, the technical risk assessment is performed. The technical risks that can occur, or are expected to occur, are defined for the development and operational stages. The risks are scored one through five for both impact and likelihood. For the highest ranking risks, mitigation is applied to get the likelihood and impact of it down. The aim is to get all the risks that have been identified to a risk of a 1 or 2 in likelihood and impact. The most significant two risks are staying under the budget requirement and the safety of operations.

Sustainability is an integral part of this design process. The three elements of sustainability considered are environmental, social and economical. The environmental aspect is split up into three life phases: the design and production phase, operational phase and end-of-life (EOL) phase. The main objective of the environmental sustainability is reducing the CO₂ emissions, reducing energy consumption and making use of renewable energy. The end-of-life phase also covers recycling of the materials used in the aircraft. The social aspect covers the integration of local organisations and people in the project. This creates job opportunities and builds trust. The economical aspect is about being as efficient as possible. For example, integrating the lean philosophy into the manufacturing process.

The market in which Wings for Aid aims to operate is a growing one. Between the years 2013 and 2023, the total worldwide aid value delivered increased from 8.6 billion US dollars to 51.5 billion US dollars [1]. Climate change may increase the frequency and severity of disasters even more. This means that the demand for aid delivery is projected to increase. A number of competitors are active within the market. These competitors can be group into urban delivery drones, low payload mid-range drones, high payload mid-range drones and existing aircraft like the C130 Hercules. Trucks are included in the market analysis as a control group. The Wings for Aid group falls within the high payload mid-range group. Within this group, Wings for Aid has the second highest payload. The competitive advantage of the present project lies in the higher range, higher payload, semi-autonomy and operating capabilities.

Design Approach

The first step in the design process was the generation of design options. These were generated using logical combinations from the Design Option Trees. The design options are presented in Table 1.

Table 1: Overview of all feasible design concepts from the Design Option Tree

Identifier	Fuselage type	Configuration	Number of engines and position	Tail
CON-1	Double	Conventional	2 nose-mounted engines	conventional tail
CON-2	Single	Canard	1 rear-mounted engine	wing-mounted tail
CON-3	Single	Conventional	1 nose-mounted engine	conventional tail
CON-4	Single	Conventional	1 nose-mounted engine	boom-mounted conventional tail
CON-5	Single	Conventional	1 nose-mounted engine	flying tailplane
CON-6	Single	Conventional	1 nose-mounted engine	boom-mounted flying tailplane
CON-7	Single	Conventional	1 rear-mounted engine	Y-tail
CON-8	Single	Conventional	1 rear-mounted engine	H-tail
CON-9	Single	Conventional	1 rear-mounted engine	boom-mounted inverted V-tail
CON-10	Single	Conventional	1 fuselage mounted engine	V-tail

The choice for the final concept was based on two trade-offs. The first trade-off was a general, qualitative, trade-off based on higher level system parameters. This narrowed down the design options to seven options; namely concepts 3, 4, 5, 6, 7, 9 and 10. Concepts 3, 4, 5 and 6 are very similar, the only difference between them being a boom-mounted tail or not and a full-moving tailplane or not. These design options were analysed to a class II level of detail, where component weights are computed based on geometry and semi-empiric relations. The Class II values were found by iterating over Class I estimations, which use statistics as their basis, geometry determination using initial sizing rules and the Class II weight estimation. The iteration stopped when the maximum take-off weight between the current and last iteration was lower

than 1%. Using these values, a detailed trade-off was performed. The detailed trade-off was performed on the fuselage and propulsion system, the tail configuration, wing support and a material trade-off. Combining the best outcome of every trade-off leads to the best final design option, which is CON-6 in Table 1. That is an aircraft with a front-mounted engine on the fuselage, a boom tail, pitch regulated by a stabilator and simple, light-braced, detachable high wings.

This design is worked out in more detail by five departments: aerodynamics, control and stability, flight performance, operations and structures. Each department performs their own calculations, as described in the coming sections. These calculations are then integrated into an overall iteration code, in order to find a converged design, which satisfies all requirements from all departments.

Operations

The operating principle of Wings for Aid is shown in Figure 1. The UAVs are shipped in by plane and ship as soon as a disaster happens and the service for aid delivery is requested by an agency (World Food Program, Red Cross). Within 72 hrs, the first airframes are unpacked, assembled and prepared for operational sorties. Drop zones are set up and organized by the contractor and authorize the pilot to drop via radio.

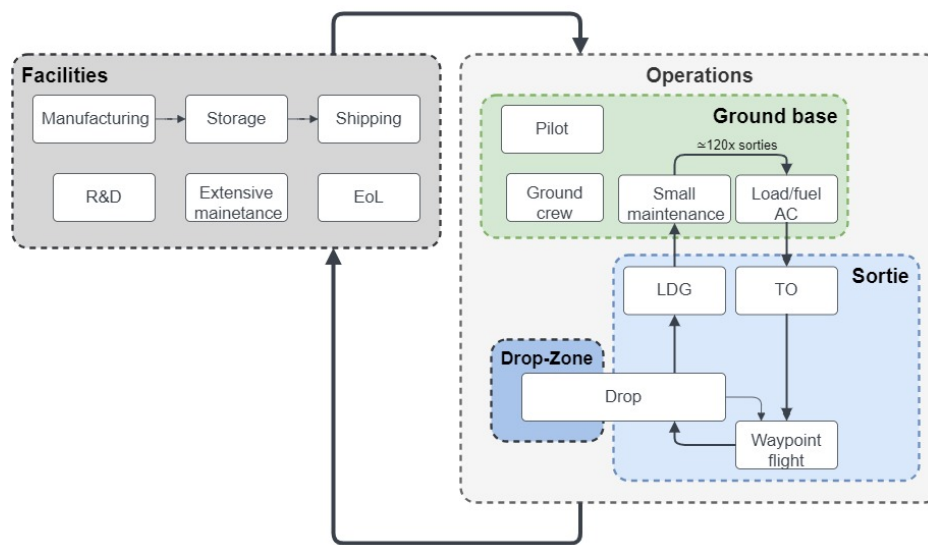


Figure 1: Schematised representation of operations' logistics

The aircraft is semi-autonomous: a pilot remotely controls the taxi, take-off and landing while most of the flight is done through waypoint flight and preset maneuvers such as climb-out, loiter, approach and the package drop itself. A relay satellite is used for communications to ensure a reliable link regardless of distance and terrain. Indeed, Wings for Aid intend to operate in a wide variety of countries ranging from the flat hot plains of South-Sudan to the mountainous regions of Nepal.

Flight Performance

The assessment of the flight performance of the aircraft covers a number of aspects. The most important aspects are take-off and landing and overall sortie performance in terms of fuel consumption and time. These are the aspects that can be coupled to high-level requirements like payload delivery capacity, delivery cost and operating capabilities.

The aircraft is required to be able to operate from runways with a maximum length of 750 m. For take-off, the aircraft is able to do this in a clean configuration for a variety of headwind and tailwind maximum value of 11 m/s, a runway slope of maximum 11°, and airport altitude of 1,000 m. For landing, the aircraft needs extra lift in order to comply with the 750 m requirement. For this, a longer runway is needed than for take-off. A runway slope of -5°, headwind and tailwind of 11 m/s, and airport altitude of 1,000 m. The aircraft is designed with high lift devices to cope with landing, but after iterations it turned out that no high lift devices

are needed. They are still included in the design and can be used for missions with more severe conditions where extreme maneuvers are needed.

The flight time and fuel consumption over a sortie were obtained through simulation. This simulation takes different flight profiles, which are defined by cruising altitude and number of drops, into account. Climbing is assumed to be done at maximum continuous power, the cruise speed is used as an input and descent are performed at maximum lift-to-drag ratio with idle power. The fuel consumption over a sortie was found to be around 40 kg or between 50 and 55 litres of petrol. The sensitivity of the fuel consumption to the number of drops is low. This is due to the fact that a large part of the aircraft's take-off weight is the payload. When more drops are performed, weight is lost earlier in the flight. The model automatically alters the cruising altitude based on the number of drops as the distance between the drops becomes smaller. The flight time of the sortie, on the other hand, is sensitive to the flight profile as performing multiple climbs and descents hampers the average speed.

Propulsion Subsystem

The flight performance analysis that is performed on the concept yields a required power of $95 \text{ hp} \pm 5 \text{ hp}$. Possible engine options should thus have a power around 100 hp. With this power requirement, the following engines are found.

- Used 100 hp Rotax 912
- Jabiru 3300
- UL260 Power
- Lycoming O-235

A trade-off was performed between the different engine options based on cost, weight, fuel consumption, certification and lifetime. The propulsion subsystem is one of the biggest contributors to the unit cost of the aircraft. One of the user requirements states that the engine that is selected for the design should be similar to a Rotax 912. Certified Rotax 912 engines cost up to €25,090 ¹. Because of this, cost plays a big part in the engine trade-off. Cost is also the reason why the UL260 Power and Lycoming O-235 are eliminated. The price of a used Rotax engine is the lowest. This does, however, come with the deficit of reduced lifetime and uncertainty. The Jabiru 3300 has a unit price of €10,658 ². The main difference between the Jabiru engine and Rotax engine is the fact that the Jabiru has six cylinders instead of the Rotax' four. Because of this, the fuel consumption of the Jabiru 3300 is higher than the fuel consumption of the Rotax. All trade-off criteria considered, the Rotax 912 engine is selected for the design, the used option should be preferred, followed by the non-certified new Rotax 912 when used ones are not available. The used engines should be inspected and maintained before implementation in an aircraft. Using used engines also improves the sustainability of the design, lowering the energy used for production and adhering to a circular economy.

Fuselage Subsystem

The fuselage is composed of a truss structure sized around the payload and designed to transfer loads between payload, engine, empennage, wing and landing gear. A truss fuselage choice follows an analytical mass-strength comparison of different fuselage concepts including load-bearing skin, truss structure and load-transferring spine boom. Because of large cutouts needed for voluminous payload loading and lack of pressurization, the truss structure concept is chosen. A truss layout is proposed around the payload, consisting of lateral frames each 1-2 box rows, connected via longitudinal and diagonal struts, with a custom Rotax 912 engine mount also constituting the nose cone, tail cone and tail boom support strut. The truss structure is modelled in Ansys Mechanical FEA, where wing, landing gear, wing strut, engine, tail and payload loads are applied to the structure, simulating critical load scenarios of $n=6.67$ and $n=-3.67$ in flight as well as single landing gear touch-down at $n=2$ and nose gear static loading of $n=2.25$. The axial forces in respective truss members are determined, allowing for cross-sectional design of truss elements, with column buckling as the critical failure mode. As a result, the fuselage is composed of thin-walled tubes of five different cross sections: $t=0.6$ and $r=10$, $t=0.7$ and $r=15$, $t=0.9$ and $r=18$, $t=1.0$ and $r=24$, $t=1.2$ and $r=30$, all in mm.

¹ Rotax engine prices

² Jabiru engine price

The empennage transfers loads to the fuselage via a tail boom, idealised as a beam, sized with the maximum maneuvering loads exerted on the vertical and horizontal tail. Internal bending moment being the critical failure mode, the cross section should be maximised, yet a compromise has to be made for aerodynamic purposes, setting the cross sectional shape of the tail boom to a thin walled tube of $r=7.5$ cm. For a given total length of $l=2.95$ m, the default material is chosen as steel 4130. The main fuselage and tail boom characteristics are summarised in Table 2.

Table 2: Summary of systems' materials and masses with alternative boom designs

Structure	Shape [mm]	Thickness [mm]	Material	Corrosion	Mass [kg]
Truss fuselage	Circular tubes	-	Steel 4130	-	45.0
Tail boom	Tube \varnothing 150	0.7	Steel 4130	No	7.6
Tail boom	Tube \varnothing 150	0.3	S. steel 410	Yes	3.3
Tail boom	Tube \varnothing 150	1.2	Al 5052 H38	Yes	4.5

Wing Subsystem

The planform of the wing is designed with overall goal of minimum cost per kg delivered in mind. This has been incorporated in many of the design decisions. Therefore a relatively thick NACA 4415 airfoil was chosen as this showed greatest compliance with the high $C_{L_{max}}$ required, therefore limiting flap weight, cost and complexity. However, drag, weight and stability were also considered in the airfoil selection. Next, it was decided to not include any sweep, while both taper ratio and twist were found to outweigh the increased unit cost over the lifetime of the aircraft. Moreover, the drag decrease by implementation of taper showed to decrease fuel cost more than the added manufacturing cost of the entirety of the mission. Further, the addition of twist was deemed necessary to assure crashes do not occur often, which both harm the image of the company and add cost to the mission. A relatively slender aspect ratio has been selected, as lower aspect ratios show significant cost increase required within the flap and or aileron design, whereas higher aspect ratios show an increase in cost per kg of payload delivered. The incidence angle of the main wing is set such that the fuselage is not required to fly at any angle of attack during cruise, as this makes up the biggest phase of the flight profile.

Next, it was also found that in order to perform better in spiral stability it was required to add a dihedral angle of 1.5° . With this angle the current design is however still spirally unstable. Nonetheless, the dihedral angle was not increased further as the spiral eigenmotion is slow, meaning that correct implementation of auto pilot software assures that this instability does not impose any threat.

The current aerodynamic analysis has been performed using traditional methods of Roskam and Torenbeek, together with Lifting Line Theory. After the design has been refined and partly validated by simulations in AVL. These were mainly used to adjust the incidence angle, $C_{L_{max, clean}}$, dihedral angle and stability derivatives of the entire aircraft. The most important final wing planform parameters are given in Table 3.

Table 3: Summary of main final wing planform parameters.

<i>Airfoil</i>	<i>S</i>	<i>b</i>	<i>AR</i>	λ	i_w	α_t	$\Lambda_{c/4}$	C_{root}	<i>MAC</i>	$C_{L_{max, clean}}$
[—]	[m^2]	[—]	[—]	[—]	[deg]	[deg]	[deg]	[m]	[m]	[—]
NACA 4415	10.4	9.11	8.00	0.66	3.10	-2.00	0.00	1.37	1.15	1.42

The wing is modelled through a wingbox, consisting of a front spar, aft spar and top and bottom plates connecting the spars. Through optimisation the optimal wingbox is found, with minimum thicknesses to meet all failure modes, together with the best combination of the number of stringers and ribs. 18 failure modes are assessed, including column buckling of stringers, panel buckling because of compression and spar buckling because of shear. The final values for all its elements can be found in Table 4

Table 4: Summary of structural parameters of final wingbox

Parameter	Value	Unit	Parameter	Value	Unit
Airfoil	NACA 4415	-	Base length stringer	7.5	mm
Location front spar	20%	chord	Flange length stringer	15	mm
Thickness front spar	1.3	mm	Thickness stringer	0.5	mm
Location aft spar	75%	chord	Number of stringers	26	-
Thickness aft spar	1	mm	Number of ribs	14	-
Thickness top panel	0.5	mm	Thickness ribs	1	mm
Thickness bottom panel	0.5	mm			

To relieve loads and thus reduce the wing weight a wing strut is attached to the wing from the fuselage. The wing strut significantly reduces the shear forces and moments within the wingbox, connecting the front spar of the wing at 1.50 m away from the fuselage to the bottom part of the fuselage frame. The strut is designed so that it withstands critical tension and compression loads, while having a thin-walled elliptical cross-section of semi-major $a = 4$ cm and semi-minor $b = 2$ cm for aerodynamic purposes. It is made of steel 4130 with a thickness $t = 1.0$ mm, resulting in a unit mass of $m = 2.57$ kg. By altering the length of the strut, the dihedral angle of the wings can be tuned.

The wings and struts are connected to the fuselage via pins supports, allowing to transfer transnational forces, but not bending moments. The design of attachments favours simplicity of assembly and is sized for pin failure, shear out, net section failure and bearing failure. The principle of both wing and strut attachment is to align plates with holes in them, such that a pin can be inserted through. The attachment plates of the wings are connected to the front and rear spar, located at 20% and 75% of the chord, while fuselage attachment plates are directly welded on assigned truss nodes. The mass of an individual strut (two per strut) and wing attachments (two per wing) is 0.61 kg and 0.82 kg respectively.

Connected to the rear spar are the high lift devices and the ailerons. Ailerons are sized based on requirements set for Class-I aircraft. For a Class-I aircraft, it has to adhere to three requirements that state that the aircraft has to perform a certain bank angle in a specified time, of which 60° in 1.3 s was the most constraining case. For this requirement it was found that for a aileron spanning 25% of the chord, the aileron has to stretch from 2.10 to 4.45 m with respect to the root of the wing.

The high lift devices are sized based on the difference between the $C_{L_{max}}$ required and the $C_{L_{max}}$ generated by the wing. Plain flaps, single slotted flaps and fowler flaps have been considered, with preference for plain flaps due to their simplicity. However, due to the large size of the ailerons, plain flaps were not feasible resulting in single slotted flaps to be chosen. This leads to a flap spanning 2.03 m starting from the root of the aircraft. As a single slotted flap is used, the chord of the flap is reduced by 3% to account for the gap, resulting in a flap chord of 22% of that of the wing. In total, this high lift device is capable of delivering an additional $\Delta C_{L_{max}}$ of 0.58.

Empennage Subsystem

Next, the design of the empennage of the aircraft will be justified. In order to size the empennage, a more thorough analysis of the stability and control of the aircraft has to be performed. As a first step, a better estimation of the most forward and backward position of the centre of gravity has to be found. The centre of gravity of the operational empty weight of the aircraft was found to be at 0.0690 MAC. Then, knowing this position, the loading diagram of the aircraft was created with which the minimum and maximum position of the centre of gravity were found to be from 0.012 to 0.391 of the MAC. In order to get to this this range, and operational constraint had to be applied, making configurations 000022, 000222, 002222 and 022222 unfeasible. To drop the payload, it is advised to first drop the most aft row, then the most forward row, continuing going back and forth until empty.

The found range in centres of gravity was then positioned on a scissors plot in which the limits on controllability and stability are indicated. From this analysis, it was found that the minimum required S_h/S to be 0.162, for which both the controllability and stability of the aircraft is limiting. With the required size in mind, the other characteristics of the horizontal tailplane can be found.

The most optimum design for the horizontal tailplane showed to be very simplistic when taking the goal of minimising cost per kilo payload delivered in mind. Moreover, no twist, sweep or taper is added. An aspect

ratio of $2/3^{th}$ of the wing's aspect ratio was chosen as this deemed high aerodynamic efficiency with limited weight increase drawbacks. A NACA 0012 airfoil was selected as both negative and positive lift generation can be desired from the horizontal tailplane. Next to that, high stall angles were found to be needed, limiting reduction of the thickness even more to decrease drag. The incidence angle was set to generate the lift required in cruise to trim the aircraft, therefore reducing force required over the entire sortie. This incidence angle was obtained by using downwash estimations of AVL. The final most important planform values are given in Table 5.

Table 5: Summary of main final horizontal tailplane parameters.

<i>Air foil</i>	S_h	b_h	AR_h	λ_h	i_h	α_h	α_{th}	$\Lambda_{c/4_h}$	C_{root_h}	MAC_h
[—]	[m ²]	[—]	[—]	[—]	[deg]	[deg]	[deg]	[deg]	[m]	[m]
NACA 0012	1.79	3.09	5.33	1.00	2.44	-0.0555	0.00	0.00	0.580	0.580

The horizontal tail should be able to fully rotate, imposing a circular thin tube spar, common for both tail surfaces, passing through the tail boom on plain bearings. Approached as a beam, the spar is sized for manoeuvring loads on the tail surface, whose net force acts at $1/3$ of the horizontal tail half span away from the boom, laterally, and a maximum 0.25 tail rootchord length away from the spar, longitudinally. 10 cm are added on both sides of the spar, the length of which is sized between the net force occurrence, resulting in $l=1.23$ m. Because the spar passes through the tail boom, its radius is limited to $r=3.5$ cm. Limiting the twist angle of the boom to 1° , the bending moment becomes critical, resulting in a thickness of $t=0.6$ mm, mass $m=1.27$ kg and twist $\theta = 0.81^\circ$, when made of steel 4130.

In the same way, the horizontal tailplane is sized to improve longitudinal stability, the vertical tailplane is sized for lateral stability. This was done by setting a minimum directional stability coefficient for the aircraft and then computing the minimum required surface area of the vertical tailplane needed. The vertical tailplane is required to compensate for the destabilizing effects of the fuselage, propeller and high wing. For a required directional stability coefficient of 0.065, it was found that S_v/S has to be at least 0.074.

Firstly, the aspect ratio of the vertical tail was limited to comply with a span of 1.2 m such that it can fit within a 40 ft ISO container without disassembly. The sweep and taper ratio of the vertical tail were chosen by trading off the aerodynamic performance, structural weight and increased stability as the moment arm increases. The incidence angle was seized to resist the engine torque in cruise condition, to limit the required rudder deflection. Compared to the horizontal tailplane less limiting stall angles were needed and therefore a thinner NACA 0009 airfoil was selected. The most important final planform parameters of the vertical tailplane are presented in Table 6

Table 6: Summary of main final vertical tailplane parameters.

<i>Air foil</i>	S_v	b_v	AR_v	λ_v	i_v	$\Lambda_{LE_{c/4}}$	C_{root_v}	MAC_v
[—]	[m ²]	[m]	[—]	[—]	[deg]	[deg]	[m]	[m]
NACA 0009	0.76	1.20	1.92	0.70	1.44	35.00	0.74	0.63

As the concept aircraft is a Class-I aircraft, the design of the rudder will be determined by the requirement for cross-wind. This implies that the aircraft is able to counter a side slip angle, β , by deflecting the rudder to a maximum rudder deflection of 30 degrees. This analysis resulted in a chosen chord fraction, $\frac{C_r}{C_v}$, of 0.50. For this ratio, the maximum allowable crosswind is 20 kts, this value could be increased to 22 kts when the chord fraction $\frac{C_r}{C_v}$ is set to 0.70.

Undercarriage Subsystem

Considering the conceptual layout of the aircraft and the corresponding range in the centre of gravity, the type, position and structure of the landing gear are selected. Firstly, a trade-off is performed to determine the landing gear configuration. For the design concept, the decision was taken to use the nose-gear configuration as it scores high in stability and manufacturability. Secondly, the landing gear type was chosen

to be a fixed landing gear as it will be cheaper, lighter and easier to manufacture in comparison to retractable landing gear. Then the nose gear and main landing gear were positioned. The longitudinal and lateral position of the landing gear is constrained by a number of limits. The results of the placement of the landing gear are presented in Table 7.

Table 7: Summary of estimations of the landing gear position. X-position with respect to the nose tip of the aircraft. Y-position with respect to the centre line of aircraft.

Parameter	Estimation	Unit
$X_{lg_{nose}}$	0.18	m
$Y_{lg_{nose}}$	0	m
$X_{lg_{main}}$	2.39	m
$Y_{lg_{main}}$	± 0.82	m

The undercarriage structure is sized according to the critical loading scenarios, namely single main wheel landing at $n=2$, nose gear loading at $n=2.25$, assuming 15% of MTOW carried by it and 46% of MTOW static load at each of the main gears. For aerodynamic purposes, the main landing gear structure consists of thin elliptical tubes with semi major $a=6$ cm and semi minor $b=4$ cm. The nose strut is circular, with a radius $r=2.5$ cm. Made of stainless steel 4130, same as the fuselage to avoid corrosion, the thickness of main and nose struts is 2.5 mm and 1 mm respectively, with masses of 14.2 kg and 0.6 kg.

Onboard Equipment

Aside from the structural and aerodynamics considerations, equipment selection plays a key role in the power and cost budgets. Because of the conceptual nature of the design at this stage, a statistical approach was taken to estimate the mass, cost, power and volume of the following:

- On-Board Computer: made up of the air-data computer, navigation unit, flight-data recorder and the autopilot. The system is estimated that the mass of the entire onboard computer is $3.6 \text{ kg} \pm 1.5 \text{ kg}$, the power required is $210 \text{ W} \pm 130 \text{ W}$, the volume estimated is $3.6 \text{ L} \pm 1.5 \text{ L}$ and the cost to be $\text{€}11300 \pm \text{€}4300$.
- Communications: the UAV's transmitter power and antenna diameter is sized with respect to a series of SATCOM relays options (geostationary, traditional and low-earth constellation). The resulting system amounts to about 1500€ for a 4 W transmission (excluding video stream) and 12 cm antenna.
- Control actuators: Since the aircraft is unmanned, electro-mechanical actuators are used to move the ailerons, flaps, elevator, rudder and nose gear. Together with the redundant elevator needed to satisfy the CS-23 regulations, the system weighs about 22 kg and consumes 16 W on average with a peak power of 1200 W.
- Power: To satisfy the power needs, an alternator of 1560 W was chosen along with a 650 Wh battery which can supply the aircraft with startup and emergency power for 30 min.

The combined systems account for a significant part of the costs and are a prime target for cost reduction in the next phases of the design.

Integration Summary

The subsystems are designed with eventual integration having a big role. After all the subsystem designs have been finalised, they are brought together. After integration, parameters like the stability derivatives and total aircraft drag can be calculated. First, some top level parameters are presented in Table 8.

Table 8: Summary of top level design parameters

Parameter	Value	Unit	Parameter	Value	Unit
Operational Range	250	km	Payload capacity	276 / 12	kg / boxes
Ferry Range	1077	km	Runway length	750	m
Endurance	12.8	hr	n_{ult}	6.6	[-]
Power	100	hp	V_{cruise}	105 / 54.012	kts / m/s
Service ceiling	20500	ft	V_{stall}	46.83 / 24	kts / m/s
MTOW	688	kg	Fuel type	RON 95 / 100LL	[-]
OEW	367	kg	Lifetime	10000	hours
Fuel capacity	75	L	Maintenance interval	100	hours

The zero lift drag estimation of the aircraft is based on skin friction drag, pressure drag and interference drag, at the wing fuselage connection for example. To capture the drag from misaligned sheets, antennas and skin roughness, a 20% excrescence drag factor is included. Accounting for all the drag types described, the calculated total C_{D_0} of the aircraft is 0.0303. The total drag coefficient in cruise condition including lift induced drag is; $C_D = 0.0421$.

User requirement REQ-USER-AC-S&C-01 states that the UAV should be at least as stable as a Cessna 172. To assess whether this requirement is met, the stability derivatives of the aircraft have been calculated using a vortex lattice model called AVL. The analysis yields comparable values for most stability derivatives. However the C_{l_β} , which is an important factor in the spiral stability of the aircraft, UAV is lower in magnitude than the Cessna 172. Because of this, the UAV has spiral instability. This is not a big problem as spiral instability is a slow, minor instability. If desired this could however be changed by adding dihedral as mentioned before. This would also increase the magnitude of C_{Y_β} , which now also performs less than the Cessna 172. In order to have both values equal or bigger in magnitude than the Cessna 172 a dihedral angle of five degrees is needed. Because of this spiral instability the UAV is currently graded slightly less stable than the Cessna 172, but other eigenmodes show similar stability and the UAV is statically more stable.

With the integration of the design, the final cost can be calculated. The cost breakdown per subsystem is shown in Table 9.

Table 9: Summary of UAV system parameters

	Mass [kg]	Cost [€]	Power [W]	Volume[L]
STR	199	8520	0	0
PRO	93.7	15000	100	10
GNC	20.4	11600	35	3.5
COM	2.2	1910	6.4	4.1
PWR	18.2	2330	109.2	1.1
OBC	3.7	11240	212	0
UAV OEW	337	50,600	462.6	18.7
COTS		34120		

At this design stage, the requirements for cost are not met. The projected unit cost is 65% higher than the requirement of €25,000. In order to get closer to the goal, in further design, cost reduction by mass ordering and production will have to be analyzed. Next to this, the cost per kilogram exceeds the limit of €0.96 by 56%. As a large part of the cost is due to transport it would be an option to store aircraft close to high-risk areas. Having aircraft spread does in turn require a more decentralised organisation. Lastly, the aircraft is not spirally stable and hence it does not meet that stability requirement. This can however be compensated by the autopilot of the aircraft and therefore this is seen as feasible for the design.

Final Design Evaluation

The evaluation of the final design covers the production cost, operational cost assessment, the return on investment and RAMS analysis.

With the materials, geometry and equipment known, an estimation of the cost to produce the aircraft can be done. Each part is either manufactured by Wings for Aid or bought off the shelf from external supplier companies. Manufacturing costs are estimated part-wise by considering the costs of cutting, forming, welding and joining the stock material into its final shape. The combined cost of these amounts to 50,600€, 33,000€ of which are COTS Table 9. The assembly process then accounts for a 20% increase in unit cost. Since the plan is to produce 500 aircraft, scale reductions such as discounts for COTS parts and reduction in assembly time due to the learning curve of employees can be considered. The cumulative average unit cost should be about 43,000€. The total investment cost to produce all UAVs is thus estimated at 23M€.

The cost to use these aircraft, or operational costs are split into three parts according to Figure 1: Facilities cost include storage, UAV overhauls and shipping to and from ground bases. The ground base itself needs to be setup and some small maintenance is done on-site. Most of the operational costs come from the sortie itself, through fuel and pilot wages. A breakdown of each category is used and estimations of the activities' time, cost, labor and recurrence is used to find their cost. Accounting for the complete lifetime of the full fleet and fulfilling all user requirements, the cost of payload delivery is between 1.4 and 1.6 €/kg. Finally, in order to make a profit, a return on investment analysis is performed which finds a target profit margin of 1.4 is sustainable for this project.

Reliability, availability, maintenance and safety are instrumental to determining the number of aircraft lost and maintained per operation. They are assessed together in RAMS using a repairable, component-level model based on statistical subsystem reliability. It is found that 20-30 aircraft are needed to deliver 20,000kg/day of aid. The planned and unplanned maintenance are done about 500 times per operation, most of which is minor and can be done at the ground-base, but some aircraft need to be grounded and shipped back for extensive repairs. The resulting fleet availability is computed and the required amount of aircraft shipped per operation is obtained along with the number of maintenance activities. The safety of the system is evaluate with respect to the expected crashes and ground operations of the crew. Mitigation measures such as avoiding flying over cities and training the local labor to Wings for Aid's safety standards were found to be sufficient to meet our goals.

Verification & Validation

Verification and validation is performed on the models used to justify the use of the results these models give. For the models that were produced by the design team the verification & validation process entails static testing, dynamic testing, a design output comparison, a global input-output analysis and a FEA model verification.

The static testing that is performed on the code consists of checking the structure, variables and logic in the models. Because of the size of the project, this includes a lot of updating of the variables used. The dynamic testing of the code covers running different modules. Tests that are run are boundary value tests, expected value tests and sensitivity analyses on smaller blocks of code. Some of the modules can be validated by using existing aircraft as input.

A design output comparison is done by comparing the output values of the iteration program to the same parameters for a Piper PA 18-150, a Piper PA 22 and a Cessna 152. At the same time a global input-output analysis of the code has been performed, checking logical changes of output with changes of input. At last the finite element analysis software used for the design of the truss structure and the tail boom is also verified. This verification is performed using a convergence study based on the mesh size and an analytical value comparison.

Contents

Executive Overview	i	5 Flight Performance	36
1 Introduction	1	5.1 Take-off	36
2 Systems Engineering	2	5.2 Climb Performance	37
2.1 Project Description	2	5.3 Cruise	38
2.2 Functional Analysis	2	5.4 Descent	38
2.2.1 Functional Flow Diagram	2	5.5 Approach & Landing	39
2.2.2 Functional Breakdown Structure	3	5.6 Sortie Performance	40
2.3 User Requirements	6	5.7 Drop Maneuver	40
2.4 Contingencies	9	6 Propulsion Subsystem	42
2.5 Technical Risk Assessment	9	6.1 Engine Selection	42
2.5.1 Risk Likelihood and Impact Identification	9	6.2 Propeller Selection	44
2.5.2 Risk Mitigation and Contingency	12	6.2.1 Number of Blades	44
2.6 Sustainable Development Strategy	14	6.2.2 Type of Propeller	45
2.6.1 Environmental Strategy	14	6.2.3 Propeller Cost Estimation	46
2.6.2 Social Strategy	16	6.3 Fuel Equipment Sizing	46
2.6.3 Economic Strategy	17	7 Fuselage Subsystem	48
2.6.4 Sustainability Evaluation	17	7.1 Frame Structure	48
2.7 Market Analysis	18	7.1.1 The Fuselage Concept	48
2.7.1 Competition Market	18	7.1.2 Truss Layout	49
2.7.2 Market Trend	19	7.1.3 Critical Loading Scenarios	49
2.7.3 Competitor Companies	19	7.1.4 Fuselage Truss Geometry	50
2.7.4 Product Differentiation of the Market and Market Gap	21	7.1.5 Tail Boom Geometry	52
2.7.5 SWOT Analysis	21	7.1.6 Materials & Integration	53
3 Design Approach	23	7.2 Outside Fairing	53
3.1 Design Options	23	7.2.1 Sizing	53
3.1.1 Transportation Configuration	23	7.2.2 Lofting	54
3.1.2 Design Concepts	23	7.2.3 Fairing Structure	54
3.2 Trade-off	24	8 Wing Subsystem	57
3.2.1 General Trade-off	24	8.1 Design of the wing	57
3.2.2 Detailed Trade-off	26	8.1.1 Airfoil Selection	57
3.2.3 Material Trade-off	29	8.1.2 Sweep	59
3.3 First Order estimation	30	8.1.3 Dihedral	59
3.3.1 Class I	30	8.1.4 Twist	60
3.3.2 Preliminary Geometry and V-n diagram	30	8.1.5 Aspect Ratio, Taper Ratio and Incidence Angle	60
3.3.3 Class II and CG estimation	31	8.1.6 Winglet Consideration	62
3.4 Design Organisation	31	8.1.7 AVL Refinement	62
3.5 Iteration Description	32	8.2 Wingbox	64
4 Operations	33	8.2.1 Loading Diagrams	64
4.1 Operations Model	33	8.2.2 Material	66
4.2 Ground Base Layout	34	8.2.3 Structure	66
4.3 Box Loading	34	8.2.4 Calculations	67
4.4 Operational parameters	35	8.2.5 Optimisation and Final Design	68
		8.2.6 Wing Strut	70
		8.2.7 Attachment to Fuselage	70
		8.3 Aileron Design	71
		8.4 High-lift Devices	72
		9 Empennage Subsystem	74
		9.1 Position of Centre of Gravity	74
		9.2 Horizontal Tailplane	77
		9.2.1 Elevator Design	77
		9.2.2 Planform	77
		9.2.3 Structure	79
		9.2.4 Aeroelastic behaviour	80

9.2.5 Option Without Detachment	81	13 Final design overview	105
9.3 Vertical Tailplane	82	13.1 Total Drag.	105
9.3.1 Sizing	82	13.2 Stability and Control of Entire Aircraft	106
9.3.2 Planform	82	13.3 Friendly-Look Assessment.	107
9.3.3 Rudder Design	83	13.4 Resource budgeting	108
10 Undercarriage Subsystem	85	13.5 Requirement Compliance	109
10.1 Landing Gear Selection	85	13.6 Feasibility Analysis	111
10.1.1 Landing Gear Configuration	85	13.7 Modularity.	112
10.1.2 Landing Gear Storage	86	14 Final Design Evaluation	114
10.2 Placement	86	14.1 Production Plan.	114
10.3 Structure	87	14.1.1 Manufacturing	114
10.3.1 Critical Load and Geometry	87	14.1.2 Aircraft Unit Cost	116
10.3.2 Materials and Integration.	88	14.1.3 Container fitting.	117
10.3.3 Tires and Shock Absorber	88	14.1.4 End-Of-Life Procedures	118
11 Onboard Equipment	89	14.2 Operational Cost	118
11.1 System Interactions	89	14.3 Return on Investment	120
11.2 Onboard Computer.	90	14.4 RAMS	121
11.3 Communications Subsystem.	91	14.4.1 Reliability	122
11.4 Controls Actuators	93	14.4.2 Maintenance	123
11.5 Power Electronics	95	14.4.3 Availability	124
12 Verification & Validation	97	14.4.4 Safety	125
12.1 Static Testing	97	15 Post Project Plan	127
12.2 Dynamic Testing	97	15.1 Client Recommendations	127
12.3 Design Output Comparison	101	15.2 Project Design and Development Logic	127
12.4 Global Input-Output Analysis	103	15.3 Project Gantt Chart.	128
12.5 FEA Model Verification.	103	15.4 Cost Breakdown Structure	128
12.5.1 Setup	103	16 Conclusion & Recommendations	131
12.5.2 Convergence Study	103	References	135
12.5.3 Analytical Value Comparison	104	A Task division	136

Introduction

Due to global warming, the frequency and intensity of natural disasters over the world are increasing. In many of these disasters, a large number of people are cut off from essential life supplies. Hence, ensuring that humanitarian aid is available for everyone is crucial. Wings for Aid aims to be an integral part of the humanitarian aid market in which it provides a solution for the 'last-mile problem'. The term last-mile problem is used for the distribution of small quantities of humanitarian aid to isolated communities. The proposed mission concept is an aircraft that can deliver 10 to 12 standardised boxes over a range of 250 km. The driving factor in the design will be the cost per kilogram of humanitarian aid delivered. Next to this, the aircraft shall be able to be transported in a 40 ft ISO container. In order to solve this problem, multiple concepts were developed in the Baseline Report [2]. Next, in the Midterm Report, a concept was chosen and a first design iteration was performed [3]. In this phase of the design, the conceptual design is worked out in more detail.

This report aims to document and justify the design choices made for the design concept and the concept of operation. At the heart of the design will be an iterable design model that sizes the main subsystems of the aircraft. Once the model is verified and validated, a conceptual design is found that is then analysed on its flight performance, market position and sustainability.

The report is structured in the following way. At first, in Chapter 2, the project will be organised by establishing project objectives, user requirements and contingencies. Next to this, the position of Wings for Aid in the market will be analysed and a Sustainable Development strategy is developed. In Chapter 3, the approach to the design is presented. In this section, also the results from previous reports will be summarised. Next, in Chapter 4, the concept of operations will be discussed. Having defined a desired mission profile from operations, the individual subsystems can be designed. In Chapter 5, the required flight performance of the aircraft will be established. Then, in Chapter 6, the method of selecting a propulsion system is described. The design of the main components of the aircraft; the fuselage, the wing and the empennage will be discussed consecutively in Chapter 7, Chapter 8 and Chapter 9. In these chapters, the location, planform, structures and control surfaces of these elements are analysed. In Chapter 10, the position and structure of the undercarriage are taken into account. As a last subsystem, the onboard equipment is sized in Chapter 11. The model and results are verified and validated in Chapter 12. Combining all elements, Chapter 13 gives a summary of the integration process and presents all results. Moreover, once the results are presented, this allows for evaluating the results and estimating the cost which is done in Chapter 14. Also, the production plan will be discussed in this chapter. Afterwards, in Chapter 15, the tasks that have to be performed after the DSE are presented. And at last, in Chapter 16, conclusions are drawn based on the design process and a number of recommendations are given for further design.

Systems Engineering

To start, the project was organised by the use of systems engineering. This is discussed in Section 2.1 by clearly stating the goal of the project and in Section 2.2 by presenting the functional flow diagram and the functional breakdown structure. Combining this project goal and these diagrams, the user requirements were then stated in Section 2.3. This is then followed by the contingencies of the important variables in these user requirements in Section 2.4. Two more important aspects of system engineering are the technical risk assessment and the sustainable development strategy which are discussed in Section 2.5 and Section 2.6 consecutively. At last, the competitive advantages of Wings for Aid in the humanitarian aid market are analysed in the market analysis, which is done in Section 2.7.

2.1. Project Description

The first step before the design process can start is to define and understand the system and its required capabilities according to the needs of the stakeholders. Wings for Aid is currently testing its most recent design. During the design iterations, several improvements have been identified and a new mission objective is formulated for the next design iteration: 'The mission objective is to deliver 10-12 aid packages of 20 kg within a range of 250 km.' [4]. The main point of concern that needs attention along the entire design and operation process is to optimise for cost per kilogram of payload (\$/kg), and the sustainability of the project, this comes from the nature of the project and its goals to aid people in need with as minimum cost as possible.

This project aims to come up with a new iteration of the system that satisfies the new mission objective. From there, a project objective has been defined as: "The project aims to design an unmanned aircraft that delivers 10 to 12 aid packages of 20 kg within a range of 250 km, with ten students in ten weeks".

From the project objective, a need statement is defined: "The unmanned aircraft shall deliver 10-12 aid packages of 20 kg each to pinpoint locations within a range of 250 km." The user requirements flow from the need statement and will be presented in Section 2.3.

2.2. Functional Analysis

To get an overview of what the system will do, tools such as the Functional Flow Diagram (FFD) and Functional Breakdown Structure (FBS) can be used. This will help with coming steps, such as risk analysis and assessment, in addition to the design option tree. Section 2.2.1 shows the functional flow diagram, while Section 2.2.2 shows the functional breakdown structure.

2.2.1. Functional Flow Diagram

The Functional Flow Diagram captures the performing logical order of the functions for the system as a whole. When two streams originate or split it can be done either with an OR or an AND. When it is an OR one of the two streams has to be followed depending on the scenario. While in the case of an AND both streams have to be followed.

For this project, the system's performance is split up into eight top-level functions. Which are given at the top with an identifier of a two-digit number ending with a zero. One level further down is second-level functions given with dashed boxes, again with two number identifiers ending with a number presenting the sequence order of that function. The third and last levels are small functions with no colour. To make it accessible for colour-blind people, the colours are given an indicator; 1: Red = RE, 2: Orange = OR, 3: Yellow = YE, 4: Green = GR, 5: Turquoise = TU, 6: Blue = BL, 7: Purple = PU and 8: Pink = PI.

Some of the functions are in a loop, for example, function 3.2.1 - Climb to cruise altitude and 3.2.2 - Monitor

climb rate and altitude. This means that as long as the aircraft did not reach cruise altitude yet, the climb rate and altitude have to be monitored. Box 2.2.5 has 3 colours, yellow, green and turquoise, which correspond to functions 3, 4 and 5 respectively. This means that the scout drone first needs to take off (function 3), fly to the drop zones (function 4) and drop the equipment (function 5). Once this has been done, and the aid UAVs are loaded, then the aid UAVs can start taking off.

The post-flight operations, function 8.0, has a lot of possible scenarios. An explanation is as follows: Once the UAV has landed it will be inspected for any defects (function 8.1.1), if there is a problem it goes into maintenance (function 8.1.2). The next step is checking the remaining mission plan (function 8.1.3). This will lead to four options:

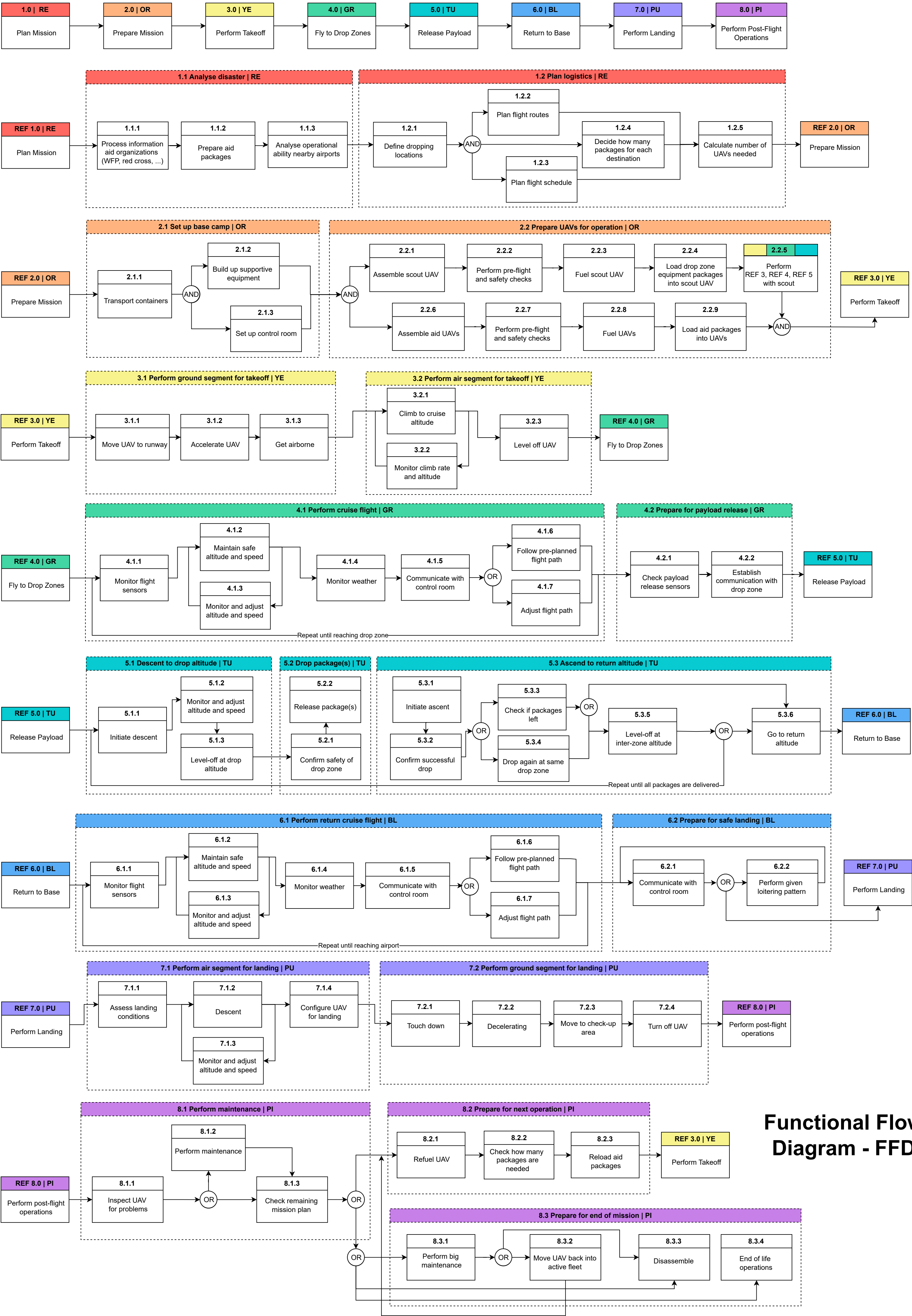
1. The UAV is prepared and loaded again, such that it can deliver more aid packages (in functions: 8.2.1 - 8.2.2 - 3.0)
2. The UAV needs big maintenance, after which it is moved back into the active fleet (in functions: 8.3.1 - 8.3.2 - 8.2.1 - 8.2.2 - 3.0)
3. The UAV needs big maintenance, after which it is disassembled and put into the transport container again, ready to be used in a new mission (in functions: 8.3.1 - 8.3.3)
4. The UAV is moved to end-of-life operations (in functions: 8.3.4)

The functional flow diagram can be found on page 5. In Section 2.2.2 the FFD is further broken down into one deeper level of functions.

2.2.2. Functional Breakdown Structure

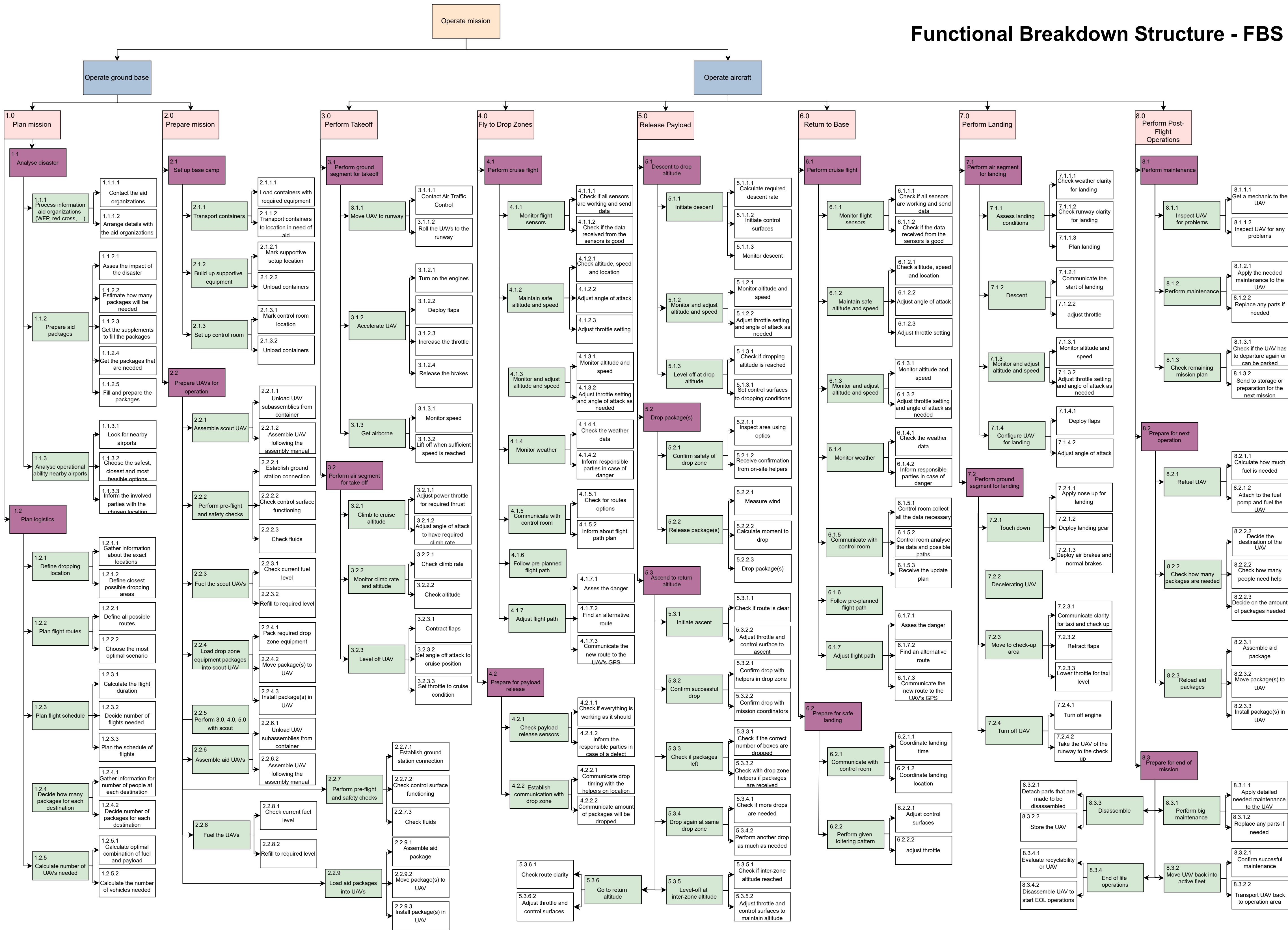
The Functional Breakdown Structure (FBS) is a function-oriented tree, not product-oriented. It is a structured, modular breakdown of every function that must be addressed to perform a generic successful mission [3]. Unlike the FFD, it is not time sequence driven. The order of presenting the functions is by breaking them down from general into more detailed functions. The purpose is to reach a level where by looking at the FBS an operator can understand what has to be done from the most basic tasks to achieving the mission of the project.

The FBS is presented to further elaborate the functions that are mentioned in the FFD. The project is split into two main categories, operating the ground base and operating the aircraft. The functions that follow are the eight top-level functions explained in Section 2.2.1 with an identifier shown in the top left corner of the light pink coloured boxes, they are to present the general function division of the mission. One deeper level is the purple boxes, which are to explain the actions that have to be taken to achieve the top-level functions. The third level is the green boxes, which contain detailed functions that can be enough to reach the goal but still not accurate. Thus, the white boxes follow, which tells the reader exactly what has to be done and what actions have to be performed to get the mission done in high accuracy, avoiding communication misunderstandings. The diagram can be read by following a path that comes in a numbering sequence. For example, starting from the box that says "operate mission" to the category specification box "operate ground base", going further down to "1.0 - Plan mission", followed by "1.1 - Analyse disaster" and then "1.1.1 - Process information aid organisations (WFP, red cross, ...)" finally, the lowest level which says "1.1.1.1 - Contact the aid organisations". From this action sequence, it can be understood that to operate the ground base a mission plan has to be made, amongst other functions. To plan a mission the disaster has to be analysed and information from aid organisations has to be processed, for that the aid organisations have to be contacted. The full FBS can be found on page 6.



Functional Flow Diagram - FFD

Functional Breakdown Structure - FBS



2.3. User Requirements

The design has to comply with a set of requirements given by the user of the system and all involved stakeholders, from these requirements, more detailed requirements flow down to a system and subsystem technical level. These user requirements are presented in Table 2.3. Each requirement has an ID, verification method, and remarks if there are any. The ID for all requirements starts with REQ which stands for requirement. Then it is USER which shows that the requirements are formulated from the user's need. Following that, there are seven different identifiers, which are as follows:

- OPS - Indicates requirement that constrains the operations
- MANV - Indicates requirement that constrains the manufacturability of the aircraft
- COST - Indicates requirement that constrains the cost budget
- AC-S&C - Indicates requirement that constrains the stability and control performance of the aircraft
- PL - Indicates requirement on the payload that constrains the aircraft
- F-ENV - Indicates requirement on the operating environment that constrains the aircraft
- AC-PROP - Indicates requirement that constrains the propulsion subsystem of the aircraft.

Table 2.1: User requirements together with their verification method

ID	Requirement	Verification	Remark
REQ-USER-OPS-01	The aircraft shall be able to fit into a 40 ft ISO container.	Demonstration on a scale or CAD model and demonstration on a full-scale prototype of the aircraft.	The container may be equipped with dedicated transport jigs.
REQ-USER-OPS-02	The aircraft shall be able to operate 24/7.	Demonstration of a prototype flight during daytime and nighttime.	
REQ-USER-OPS-03	The aircraft and its systems shall be operable in a temperature range of -5 to 50°C.	Testing that each of the individual subsystems can operate in this temperature range, subsequently testing the entire aircraft.	
REQ-USER-OPS-04	The aircraft and its systems shall be able to operate during rain.	Testing the entire aircraft on the ground (water ingestion) and in flight.	
REQ-USER-OPS-05	The aircraft shall be able to perform at least three aid missions within 24 hrs.	Demonstration of three sorties within 24 consecutive hours.	Enough time within this 24 hrs has to be reserved for maintenance, refueling and loading.
REQ-USER-OPS-06	The aircraft without payload shall have an endurance of at least 10 hrs.	Analysis through calculations validated by prototype demonstration in flight.	Additional fuel tanks may be installed to satisfy this requirement.
REQ-USER-OPS-07	The aircraft shall be able to operate in conditions similar to a UH1 helicopter.	Demonstration of aircraft capabilities at the operational limits of the UH1.	Hardly specific, to be reformulated when deriving technical requirements. Operational conditions can be expressed by air humidity, temperature, particle suspension etc.
REQ-USER-OPS-08	The aircraft shall be able to operate in mountainous regions.	Demonstration of a typical mission profile in mountainous regions.	Hardly specific, to be reformulated when deriving technical requirements. Can be expressed in minimum air pressure or rate of climb.

REQ-USER-OPS-09	The aircraft shall be able to operate in desert conditions.	Demonstration of a typical mission profile in desert conditions.	Hardly specific, to be reformulated when deriving technical requirements. Can be expressed in temperature, air humidity or suspended particles.
REQ-USER-OPS-10	The design of the aircraft shall guarantee the cargo loading to be performed outside of the propulsion system zone.	Inspection of the placement of the propulsion system with respect to the cargo hold.	
REQ-USER-OPS-11	The design of the aircraft shall guarantee fueling to be performed outside of the propulsion system zone.	Inspection of the placement of the propulsion system with respect to the fuel tank infusion.	
REQ-USER-OPS-12	The visual inspection of the cargo bay shall be possible by opening hatches or clear windows.	Inspection of the designated cargo bay visual areas.	
REQ-USER-OPS-13	The aircraft shall look friendly.	Demonstration of operation of the prototype to a larger group of individuals and assessment of their reaction.	Hardly specific, to be reformulated when deriving technical requirements.
REQ-USER-OPS-14	The aircraft shall be able to take off and land on paved runway surface.	Demonstration of operations by prototype aircraft.	
REQ-USER-OPS-15	The aircraft shall be able to take off and land on grass runway surface.	Demonstration of operations by prototype aircraft.	
REQ-USER-OPS-16	The aircraft shall be able to take off and land on gravel runway surface.	Demonstration of operations by prototype aircraft.	
REQ-USER-OPS-17	The avionics system of the aircraft shall be swarm compatible.	Demonstration of swarm compatibility of prototype aircraft.	
REQ-USER-OPS-18	The aircraft shall use as many standard of the shelf parts as possible	Inspection of the part documentation and analysis of their availability in the local market.	Hardly specific, to be reformulated when deriving technical requirements. Can be quantified by stating the net worth of commonly available parts.
REQ-USER-MANV-01	The aircraft shall be able to fly at a minimum altitude of 15 m within fly-in and drop zone.	Demonstration of a prototype flying a dropping profile at minimum altitude.	
REQ-USER-MANV-02	The aircraft shall be able to accurately deliver a package within a drop-zone of 25 m by 25 m.	Demonstration of payload delivery of a prototype aircraft.	
REQ-USER-MANV-03	The aircraft shall be operable at a visibility condition of at least 100 m during take-off and landing.	Testing of guidance sensors and demonstration by prototype aircraft in flight.	

REQ-USER-MANV-04	The maximum runway length for take-off and landing shall be 750 m.	Analysis through flight performance calculations validated by prototype demonstration.	
REQ-USER-MANV-05	The aircraft shall have a maximum stall speed at an airspeed of 50 kts at its maximum take-off weight.	Analysis through flight performance calculations validated by prototype demonstration.	
REQ-USER-MANV-06	The aircraft shall be able to climb at a rate of at least 500 ft/min at sea level.	Analysis through flight performance calculations validated by prototype demonstration.	
REQ-USER-COST-01	The unit cost of one aircraft shall not exceed €25,000.	Inspection of the total costs of the bill of materials and the production costs.	The unit cost is excluding the development cost.
REQ-USER-COST-02	The operational costs shall at maximum be 2-4 times the operational costs of a truck per delivered kg.	Inspection of the operational costs for a typical mission and analysis of operational costs for aid delivery by truck.	Hardly specific, to be reformulated when deriving technical requirements. Operational costs can be expressed per unit mass distance
REQ-USER-AC-S&C-01	The aircraft shall be at least as stable as a Cessna 172.	Analysis through flight dynamics calculations validated by prototype demonstration.	This requirement will have to be quantified using stability derivatives data from the Cessna 172. Can be measured for example in terms of $dC_m/d\alpha$.
REQ-USER-PL-01	The aircraft shall be able to carry a payload of at least 10-12 boxes of 20 kg each.	Demonstration of a prototype flight with full payload capacity	
REQ-USER-PL-02	The total operational aid delivery capacity per 24 hrs shall be comparable with the aid delivery capacity of a C-130 Hercules.	Demonstration of operational aid delivery capacity by prototype aircraft and analysis of operational aid delivery capacity by C-130.	This requirement will have to be quantified using payload capacity data of the C-130 Hercules. Delivery capacity can be measured in unit mass per unit time.
REQ-USER-F-ENV-01	The aircraft that is loaded with payload shall have a range of at least 500 km.	Analysis through flight performance calculations validated by prototype demonstration.	
REQ-USER-F-ENV-02	The aircraft shall have a ferry range of at least 1000 km.	Analysis through flight performance calculations validated by prototype demonstration.	Additional fuel tanks may be installed to satisfy this requirement.
REQ-USER-F-ENV-03	The aircraft shall have a maximum operational altitude of 18,000 ft.	Analysis through flight performance calculations validated by prototype demonstration.	
REQ-USER-F-ENV-04	The aircraft shall have a cruise speed in the range of 100 to 110 kts.	Analysis through flight performance calculations validated by prototype demonstration.	

REQ-USER-AC-PROP-01	The aircraft shall be powered by an engine equivalent to the Rotax-912.	Inspection of the engine main characteristics.	This requirement will have to be quantified using the main characteristics of the Rotax 912.
REQ-USER-AC-PROP-02	The aircraft propulsion unit shall be powered by AVGAS or gasoline.	Testing the propulsion unit using the dedicated fuel.	

2.4. Contingencies

The user requirements allow for determining the important design variables. These variables and the corresponding contingencies throughout the design are shown in Table 2.2.

Table 2.2: Contingency in percentages applied per variable, depending on the project phase

Variable	Conceptual	Class I	Class II	Class III	detail
Cruise drag	±20	±15	±10	±5	±2
Maximum lift coefficient	±20	±15	±10	±5	±2
UAV unit production cost	±30	±20	±15	n/a	n/a
COM cost	n/a	n/a	±10	±5	±1
OBC cost	n/a	n/a	±10	±5	±1
Labour cost	n/a	n/a	±10	±5	±1
Propulsion cost	n/a	n/a	±10	±5	±1
Propulsion mass	n/a	n/a	±10	±5	±1
Structure mass	n/a	n/a	±10	±5	±1
Payload rate	±20	±15	±10	±5	±2
Number of packages	±20	±15	±10	±10	±10
Specific fuel consumption	±30	±20	±15	±10	±5
Delivery range	±20	±15	±10	±5	±2
Ferry range	±20	±15	±10	±5	±2
Operational range	±20	±15	±10	±5	±2
Time to first delivery	±20	±15	±10	±5	±2
MTOW	±30	±20	n/a	n/a	n/a
OEW	±30	±20	n/a	n/a	n/a
Fuel weight	±30	±20	±15	±10	±5

The variables chosen to apply the contingency are mostly requirements which help ensure the final design meets these in the event some characteristics were over or under-estimated in earlier phases. Class I is especially coarse as it relies on statistical approximation concerning aircraft that operate radically differently. It should be noted that although the last phase shown here is called "detailed design", the specifications shown in Section 13.4 i.e. the outputs of this DSE, are still those of a preliminary design. If approved, a new contingency plan should be made such that the production aircraft fulfills the requirements.

2.5. Technical Risk Assessment

With a more detailed design new risks appear on top of the risks identified and mitigated in the Midterm Report [3]. In Section 2.5.1 the likelihood as well as the impact severeness of the existing risks are updated, in addition to new risks that are identified, while some of the risks are discarded for the fact of being insignificant anymore. Furthermore, the risks are mitigated and a contingency is proposed allowing to assign post-mitigation likelihood and impact severeness to each risk in Section 2.5.2.

2.5.1. Risk Likelihood and Impact Identification

Each identified risk event is qualified by its likelihood of occurrence on a scale between 1 and 5, the same is done to evaluate the impact of consequence in case the risk happens, as defined on Table 2.3.

Table 2.3: The definition of likelihood and impact metrics

Likelihood metrics		Impact metrics	
Improbable	1	Negligible	1/5
Remote	2	Low	2/5
Occasional	3	Moderate	3/5
Probable	4	Significant	4/5
Frequent	5	Catastrophic	5/5

The risks are divided into two types; Technical development risks, which are risks that may occur in the design and development phase. These have an identifier that starts with RT. And technical operational risks, which are risks that may occur when the system is operated. These have an identifier that starts with RO. The scoring of impact severeness and qualification of the likelihood of a risk to happen is based on own judgement and discussion between a group of the team members. In case of a disagreement on the seriousness of the risk, a further investigation has been done. The risk of an event is quantified by multiplying the likelihood L with the severity S as shown in $RS = L \cdot I$. It should be noted that one risk event can have more than one consequence, in that case, they have the same likelihood to happen. While different risks with the same consequence will have the same impact. All are presented in Table 2.4.

Table 2.4: Identified risk events with their likelihood and consequence quantified and identified impact

ID	Risk event	L	Impact	S	RS
RT-AC-GNC-2.4	Underestimated cost budget for avionics system prevents the use of advanced collision avoidance	2	The avionics system of the aircraft is not swarm compatible.	2	4
RT-AC-PLB-1.3	Fuel accommodation needs to limit the achievable payload mass and volume	2	The aircraft is unable to carry a payload of 10-12 boxes of 20 kg each.	3	6
RT-AC-PRO-1.1	Performance and practicality design is prioritised over aerodynamic drag	1	The aircraft requires a significantly higher power than a Rotax 912 can provide	3	3
RT-COST-2.1.1	Performance and practicality design is prioritised over aerodynamic drag, causing an increase in fuel consumption	2	The operational costs exceed by 2-4 times the operational costs of a truck per delivered [\$/kg].	4	8
RT-COST-2.1.2	Drastic increase in global AVGAS or gasoline price	2	The operational costs exceed by 2-4 times the operational costs of a truck per delivered [\$/kg].	3	6
RT-ENV-2.1	Waterproof design is not properly accounted for and the aircraft fails the water ingestion test	1	The aircraft is inoperative in the rain	3	3
RT-ENV-4.1	Remote control and autonomous landing system performance is overestimated under low visibility condition	2	The aircraft is unable to operate in visibility conditions of 100 m	3	6
RT-ENV-6.1	Underestimated mass budget for landing gear prevents a structurally suitable design	1	The aircraft is unable to take off and land on paved runway surface	5	5
RT-ENV-6.2	Underestimated mass budget for landing gear prevents a structurally suitable design	1	The aircraft is unable to take off and land on grass runway surface	4	4
RT-ENV-6.3	Underestimated mass budget for landing gear prevents a structurally suitable design	1	The aircraft is unable to take off and land on gravel runway surface	4	4
RT-ENV-6.4	Underestimated mass budget for landing gear prevents a structurally suitable design	1	The aircraft is unable to take off and land on unprepared runway surface	4	4

RT-ENV-6.5.2	Remote control and autonomous landing system performance is overestimated under low visibility condition	2	The landing distance needed is higher than 750 m	4	8
RT-FR-OPS-LOG-1.4	Trade-off favours performance over modularity	1	The system first sortie happens later than 72h after deployment decision	3	3
RT-FR-OPS-MIS-2.4	Part choice makes the aircraft dependent on a single supplier	1	The system does not have an operational availability of 100%	3	3
RT-LEG-1.1	Safety policies are not taken seriously	3	The aircraft is not deemed airworthy	5	15
RT-MRKT-1.1	Aircraft parts on the market are more expensive than budgeted for	2	The unit cost is higher than required, reducing the strength of market position.	3	6
RT-MRKT-1.2	Incomplete statistical data set drives the class I weight estimation too high	1	The unit cost is higher than required, reducing the strength of market position.	4	4
RT-OPS-GB-1.1	Structural performance design is prioritised over maintenance, causing particular load paths preventing inspection hatches	2	The key systems of the aircraft are not easily accessible for ground maintenance.	2	4
RT-OPS-MIS-1.1	Engine overheating is not accounted for in the design	1	The aircraft is unable to perform three aid missions within 24 hours.	2	2
RT-OPS-MIS-2.1	Remote control and autonomous landing system performance is overestimated under low visibility conditions	1	The aircraft is inoperable at night	3	3
RT-ORG-1.1	Deadlines during the development phase are not met	1	The whole project is delayed	3	3
RT-REQ-1	Stability requirements not met	2	The aircraft is not stable enough to operate	4	8
RT-REQ-2	Overall cost requirements not met	4	The aircraft is too expensive to be produced	5	20
RT-REQ-3	Operational requirements not met	2	The aircraft is unable to carry a payload of 10-12 boxes of 20 kg each.	3	6
RO-TIME-1	Ground base parts and equipment delivering delay	2	The system first sortie happens later than 72h after deployment decision	3	6
RO-TIME-2	Assembling and loading delay	2	The system first sortie happens later than 72 hrs after deployment decision	3	6
RO-TECH-1	Failure of aileron actuator	4	Control and stability difficulty	3	12
RO-TECH-2	Failure of flap actuator	4	Not able to take-off or land because of low lift coefficient	3	12
RO-TECH-3	Failure of one of the horizontal tail actuator	4	Control and stability difficulty	3	12
RO-TECH-4	Failure of both horizontal tail actuators	2	Lose control and stability	5	15
RO-TECH-5	Failure of rudder actuator	4	Control and stability difficulty	3	12
RO-TECH-6	Failure of dropping mechanism	3	The aid boxes are not delivered	3	9
RO-TECH-7	Failure of engine during flight	2	Glide and descend in an undesirable location	4	8

RO-TECH-8	Failure of communication system between aircraft and ground control	3	Lose control over the aircraft, which leads to no dropping, landing, and take-off commands, thus aircraft crash	5	15
RO-TECH-9	Failure of the communication system with dropping zone	3	No information about dropping zone clearance, thus no dropping possible	3	9
RO-TECH-10	Failure in hardware system	3	losing a subsystem	4	12
RO-TECH-11	Occurrence of short circuit	2	Losing a subsystem, or can lead to a fire	4	8
RO-TECH-12	Error in the software system	3	Aircraft crash	5	15
RO-TECH-13	Weak batteries	1	Not enough power to start up the engine	4	4
RO-TECH-14	Alternator failure	2	Subsystems power relies on the batteries, which have limited capacity	4	8
RO-D-1	Propeller damage	2	Not enough thrust generation	3	6
RO-D-2	Landing gear damage	3	Fuselage or propeller damage from landing impact	3	9
RO-D-3	Wing structural damage	1	Not enough lift generation, or drag for landing	3	3
RO-D-4	Horizontal tail structural damage	1	Control and stability difficulty	3	3
RO-D-5	Vertical tail structural damage	1	Control and stability difficulty	3	3
RO-D-6	Tires explosion	1	Landing gear damage	5	5
RO-P-1	Pilot mistake that leads to a crash	2	Losing an aircraft	4	8
RO-O-1	Dropping at wrong location	2	The aid boxes are not delivered	3	6

2.5.2. Risk Mitigation and Contingency

Preferably, the team would like to have the likelihood and the impact of any risk as low as possible. For that reason mitigation is applied to the risks with a likelihood larger than 1, risks with likelihood of 1 are negligible but have to be monitored, and an impact of 3 or higher, which means a risk value of maximum 6 is accepted.

Being at the end of the design phase, which means iteration is being conducted, the models of all departments are combined. Thus, there will be a low likelihood of almost all development risks. Risks that have a likelihood of 2 are not of a big significance but can not be neglected. They all can be mitigated by being careful in the iterations and verifying the code and iteration results and all design steps and choices. For the risk of the increase in the price of AVGAS, it can be treated by decreasing operating costs as contributing to the design value as the performance, and analysing local fuel market sensitivity.

There are two risks that have a likelihood higher than 2; risk RT-LEG-1.1 about safety policies and RT-REQ-2 about exceeding the cost requirement. The first one is very important and can be mitigated by raising awareness about the importance of safety and providing training and coaching to achieve the level of safety desired, furthermore, analysing the risk assessment for intended operation (SORA) and verifying the requirement for an aircraft to be judged airworthy. While the second risk is about meeting the cost requirement, this is very difficult to achieve because of the very low value that is specified as a maximum cost by the customer, €25,000. This can be mitigated by for example negotiating with the customer about increasing the cost limit by presenting the reasoning behind not meeting the cost specified, which has been done and the customer agreed on a higher cost in case of convincing reasons, or having less expensive parts or fewer functional abilities and accept the quality of the product going down.

Furthermore, all technical risks, which are the ones that have TECH in their identifier, that are about the failure of an actuator are of high likelihood because of the much lower reliability of the actuators than the engine. Mitigating these risks is done by redundancy; if an aileron actuator fails, the other aileron and the flaps take over, the same for flaps failure, and in case of ruder failure the ailerons take over. For the horizontal tail, there is the redundancy of two actuators, thus the likelihood of the two actuators failing is half.

IMPACT	Catastrophic 5	RT-ENV-6.1 RO-TECH-4 LG	RT-LEG-1.1 YE	RT-REQ-2 OR	RE	RE
	Significant 4	RT-COST-2.1.1 RT-ENV-6.2 RT-ENV-6.3 RT-ENV-6.4 RO-TECH-7 RO-D-6 LG	RO-TECH-8 RO-TECH-12 YE	OR	OR	RE
	Moderate 3	RT-AC-PRO-1.1 RT-ENV-2.1 RT-ENV-4.1 RT-ENV-6.5.2 RT-FR-OPS-LOG-1.4 RT-OPS-MIS-2.1 RT-ORG-1.1 RT-REQ-3 RO-TIME-1 RO-TIME-2 RO-TECH-13 RO-TECH-14 RO-D-1 RO-D-3 RO-D-4 RO-D-5 DG	RT-AC-PLB-1.3 RO-TECH-9 RO-TECH-10 RO-TECH-11 RO-D-2 LG	YE	OR	OR
	Low 2	RT-FR-OPS-MIS-2.4 RT-OPS-GB-1.1 RT-OPS-MIS-1.1 RT-REQ-1 RO-P-1 RO-O-1 DG	RT-AC-GNC-2.4 RT-MRKT-1.1 RT-MRKT-1.2 RO-TECH-6 DG	RO-TECH-1 RO-TECH-2 RO-TECH-3 RO-TECH-5 LG	YE	YE
	Negligible 1	DG	RT-COST-2.1.2 DG	DG	LG	LG
		Improbable 1	Remote 2	Occasional 3	Probable 4	Frequent 5
LIKELIHOOD						

Figure 2.1: Risk map of identified risk events

All the actuators' risk failures can be mitigated, in addition to redundancy, by means of maintenance.

The failure of the dropping mechanism is important because it causes the failure in delivering the packages, and will need to design for a heavier aircraft and more fuel consumption if the flying back tour to the ground base will be with a full payload. Thus the dropping mechanism will need double or maybe triple redundancy. The probability of an engine failure is relatively low, but its impact is high, thus inspection and maintenance are required to be on the safe side. While, failure in the communication system is considered likely to happen with big consequences, especially since the failure between aircraft and ground control will lead to the loss of the aircraft. That is why redundancy is needed in the communication system parts, in addition to inspection and testing before taking off. From risk RO-TECH-10 till risk RO-TECH-14 can be avoided by testing the parts before taking off and inspection after landing, the part has to be changed in case of any sign of damage.

The structural damage risks, which have a D in their identifier, all have a low likelihood to happen. An exception to this is the propeller which can be damaged by a bird strike, and the landing gear is exposed to more damage because of the runway types for take-off and landing. The tire explosion has a small risk to happen but with a significant impact on the landing gear. These risks can be avoided by inspecting the structure and the tires before taking off and after landing. In case of any crack indication, the part has to be immediately treated or, worst case, switched. For the tire explosion case redundancy in shock absorbers can be added.

Finally, the pilot's mistake is of low likelihood but can cause losing the aircraft. Thus, the pilots have to be trained well, and fully informed about the systems and operations of the aircraft. Next to that, the autopilot can be enhanced to assist the pilot and detect if a mistake is being done. Dropping at a wrong location can happen but can be prevented by making the communication accurate and clear between the dropping zone and the ground base, furthermore, securing high reliability on the GPS system.

After the risks have been mitigated, a risk map is made to clearly show if any risk is still threatening and needs extra attention. The risk map is shown in Figure 2.1

As can be seen in the risk map, risk RT-REQ-2 about exceeding the cost requirement for one aircraft, has a

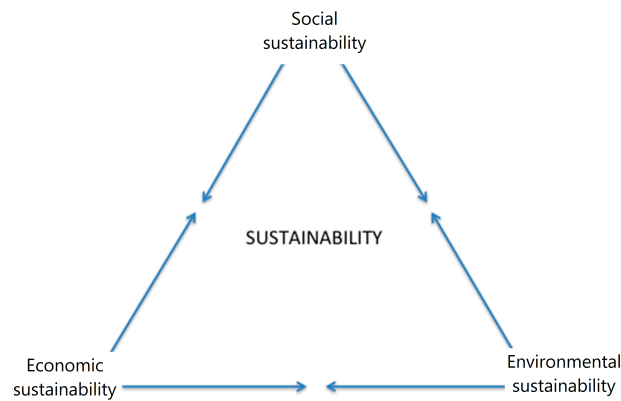


Figure 2.2: The triangle of sustainability

risk of 15, which means that it's likely to happen with big consequences. Thus it has to be treated carefully and the customer has to be aware of it. The three risks in the yellow boxes are RT-LEG-1.1 about safety, that is for the importance of safety and even though further mitigation is applied it still needs attention all the time during the designing, manufacturing and operating. Further mitigation and caution can always be applied. The second one is RO-TECH-8 about failure in communication between the ground base and the communication system because of the likelihood of it happening and losing the aircraft in case it does happen. That is why more redundancy and verification tests are needed for this system. The last risk in yellow is RO-TECH-12 about an error in the software, this risk is of big importance since it can affect the entire mission. Thus validation and testing for the software can be ignored or done poorly.

2.6. Sustainable Development Strategy

Sustainability is an aspect of growing importance in any type of project. It combines three significant and leading variables in design processes. These variables are environmental impact, social effects, and cost-effectiveness, which are each explained in Section 2.6.1, Section 2.6.2 and Section 2.6.3 respectively. Shown in Figure 2.2. The sustainability plan presented in this report is taken from the midterm report [3] and updated to meet the deeper level of design reached so far.

Having a detailed design and operations analysis, which are presented further in the report, allows for a more detailed sustainability strategy. Which should aim to strike a balance between the different aspects of sustainability. The nature of the project dictates the relative importance of each of the three concepts, with emphasis on keeping the cost as low as possible.

2.6.1. Environmental Strategy

Global warming and climate change cause an increase in temperature. Because of this, the frequency of natural disasters is increasing¹. Because of the clear effects of global warming on the environment, the team's vision is to reduce the footprint of the project in all aspects possible, from design to production and manufacturing to operation.

In the following subsections, the strategy for environmental sustainability regarding the project is divided into three life phases: Initial phase, Operational phase, and End-of-Life.

Initial Phase

The initial phase of the project starts from the designing step to the production and manufacturing methods and materials chosen for the aircraft.

- Being sustainable already starts with the means of transportation used to get to the meetings. bikes and public transportation are preferred over cars.
- While no direct emissions are present in the designing phase, energy is still consumed for software and hardware computer use. To increase sustainability, a building that uses reusable energy sources,

¹IMF: Climate Change Will Bring More Frequent Natural Disasters & Weigh on Economic Growth, [cited on 22 May 2023]

such as solar or wind power is preferred. Renewable energy systems can be installed on-site or purchased from the grid.

- The next step is the production and manufacturing phase of the aircraft. The Lean Manufacturing approach will be used. This philosophy aims to minimise waste during the manufacturing phase. Which reduces the total footprint of the project [5].
- During the design and manufacturing, the production methods have to be chosen. Methods that are universal for different shapes are favourable over others, for example, rubber forming is preferred over deep drawing.
- Supply Chain Management: Choosing to work with suppliers and partners that adhere to ethical and environmentally responsible practices, following a policy of transparency for the sources of the raw materials.
- Regarding the material to be used in manufacturing the aircraft, the property of kg of CO₂ emission per kg of material or product produced is considered. This property also takes into account recyclability; field disposal, open loop or closed loop. Each option has an effect on the amount of CO₂ emitted per kg of material used. A closed loop means the material will be recycled and used in the same industry. Open loop means the material will be recycled and used in any industry. Recycled material may lower the CO₂ footprint, but it could be heavier and less reliable. This is due to the fact that recycled material loses some of its properties, which is impactful in the aerospace industry. This balance requires a trade-off to optimise the CO₂ emission per kg produced while preserving the material properties needed for the aircraft. The option of using recycled plastic has to be always considered, if not possible now or then for a future iteration.
- Another aspect considered in the process of choosing the material is resource depletion. The material to be chosen has to be a material that can be replenished at least as fast as it is being consumed. This can also make the design cheaper, as depleted materials are taxed more. This criterion is measured in the cost of tax per kg of material. For the purpose of this project, this variable is preferred to be minimum to have a cheap and sustainable design.
- The final aspect to consider is eco-toxicity. This entails any harmful effect on both the environment and organisms. It is quantified in the same way as the resource depletion mentioned previously, which means that the lower the value of the chosen material the better.

Operational Phase

The operational phase's impact is mostly driven by the energy consumption of equipment transport and aircraft fuel consumption since fuel is burned proportionally to the energy required. A common way of measuring this is by computing the energy intensity (EI) ² in MJ/ton-km. Using an energy density of 4.27 MJ/kg ³ for AVGAS, it is possible to compute the current concept's EI at 4.22 MJ/kgkm. This is higher than other types of freight delivery such as sea, rail and truck but lower than the current average for air freight as can be seen in Table 2.5 [6]. However, the complete Wings for Aid system relies on the transport of aircraft, ground base and equipment (see Chapter 4). This contribution can be included by using the previously mentioned energy intensity along with the mass and number of aircraft and ground bases shipped per operation by air, sea and road.

Table 2.5: Energy intensity of the system for different transport options

Transport	M[kg]	R[km]	EI [MJ/kgkm]	E [MJ]	Notes
Air	0	10,019	10	0	10% of fleet flown to GB
Sea	1,125,000	1,822	0.2	409,857,955	the rest + equipment by boat, all shipped back
Road	1,125,000	1000	2	2,250,000,000	500 km between harbour and GB assumed, for everything
W4A fuel/op	20,131,728	250	0.03	149,813,609	with 25 operational AC on avg, flying 180 sorties each and using 60 kg of fuel per sortie-AC assuming 44.65 MJ/kg of fuel energy density
W4A total/op	20,131,728	250	0.56	2,809,671,564	and including shipping energy

²EAA Europa, [cited on 22 May 2023]

³Energy density of aircraft fuel

As seen in Table 2.5, the transport contribution is driving the energy consumption of the system optimised for the payload weight and the range to a value of 0.56 MJ/kgkm. Since the customer requires the use of gasoline or AVGAS for the aircraft, the sustainability strategy used going forward can include the following:

- Decrease the number of aircraft shipped by air in the initial phase of the operation as much as possible since air freight has the highest EI. An alternative can be by sea or by road, preferably by sea.
- Decrease the shipping distance from storage to the ground base. This can be achieved by increasing the number of locations where the system is stored around the world. However, this would increase cost and complexity which is a negative effect on the economic strategy.
- Package optimisation: Optimise the container loading for the amount of equipment transported to the time and distance of transportation which affects the emissions. For example, in addition to the aircraft, fill the containers with tools and boxes.
- Use clean transport whenever possible. Efficient, carbon-neutral or zero-emission (e.g. hydrogen or electric) ships, trucks or even aircraft may become available during the project's lifetime. Using these would greatly reduce or nullify the environmental effects of the energy consumed.
- Increase the concept's fuel efficiency. Designing for efficiency would mitigate the consumption of AVGAS and reduce the EI of the overall system. This would have the added benefit of reducing operational costs.
- Shipment collaboration: especially effective for sea transportation, where sharing container space with other shipments can lead to significant efficiency gains. Collaborate with other companies or businesses in the same region to merge shipments. Which reduces the number of individual trips required, maximizing the load capacity of each transportation mode and reducing overall emissions.

End-of-Life

Aircraft maintenance after each operation contributes to reducing the probability of it failing during the operation and crashing, thus increasing the possibility of reusing the aircraft more times. After the aircraft has reached the end of its usable lifetime (in flight hours or the number of sorties or operations), it is important to plan how to approach the end-of-life in terms of environmental sustainability.

- This starts with the choice of material used, as mentioned previously, the material has three options of recycling: field disposal, closed loop and open loop. The best option for the aerospace industry is to go with the open loop option since recycled material is not the best option because of the quality of the material. With this option, the material that is used will be recycled and reused, which is a step closer towards sustainability.
- Hazardous material: there are materials in the aircraft that are hazardous, such as fuel, lubricants, batteries, and chemicals. A plan for safe handling, removing, and disposing of these materials should be developed to prevent environmental contamination.

2.6.2. Social Strategy

The social aspect of the sustainability of the project concerns the communities targeted by Wing for Aid's aid strategy, as well as the ones involved in the project throughout its lifetime, not only immediate aid but also contribute to the long-term well-being of the affected communities. The following guidelines have been established such that these populations are helped in a manner that benefits them the most.

- Aid strategy: The basis for the project is to provide aid quickly to communities targeted by natural or man-made disasters. However, the amount of payload that can be delivered along with the operational concept means that everything cannot be done by this system alone. Indeed, Wings for Aid intends to be part of a larger system which includes many types of aid delivery (truck, ship, train, C-130 Hercules and others) coordinated by the Red Cross and the World Food Program (WFP) [4]. This integration plays a large role in the operations Chapter 4 and is reflected in the whole design.
- Local population contacts: Involving the local population is of primary importance to the success of the project. Indeed, contacts in the zone are required before any disaster happens as the means of communications established and training given enables the WFP to pack what is needed the most and the drop zones to be defined, secured and monitored without extra resources and time needed.
- Local labour: Involving the local population in the project allows Wings for Aid to gain their trust and

respect, which helps with the overall coordination and acceptance of the project. Furthermore, using local labour allows people to have a job and wages after large disasters, which alleviates the large economic impact of these events.

- Collaboration with a local organisation: collaboration in the targeted areas where a disaster happened, or is very likely to happen, with local organisations can provide valuable insights, local knowledge, and existing network for effective execution of the operations. In addition to better integration with the communities, thus gaining the people's trust.
- Material choice: Manufacturing also has a social impact, which is most prevalent in the sourcing of materials (metals in particular). Mining of certain resources sometimes exploits populations and endangers workers. In order to minimize the project's impact and contribution to these practices, social sustainability will be considered when deciding which materials to use in the structure of the aircraft.
- Cultural consideration: Respect and consider the cultural values of the communities being helped. Set the communication methods, the equipment and aid delivered, to meet the cultural code and rules to help the communities accept the aid and make full use of it.

2.6.3. Economic Strategy

The economic aspect of sustainability is about developing a strategy that supports long-term economic growth without negatively impacting social and environmental aspects⁴. A few strategies can be followed to assure economic sustainability:

- Optimise the use of resources, whether in terms of material, energy, man-hour or knowledge. This optimisation will increase efficiency, which serves the goal of economic growth. For example, minimising the sortie time can maximise the number of sorties per day, which results in more efficient use of the ground base and man-helping power.
- The philosophy of Lean Manufacturing can be adopted in the context of economic sustainability since it counts for as minimum waste as possible, which again increases efficiency and thus economic growth.
- Funding sources: seek for diverse funding sources to not have a dependence on a single funding stream. For example, governments, organisations, companies, etc.
- Another aspect is distributing the funding from aid organisations, such as the Red Cross and the World Food Program, as effectively as possible. This can be achieved by minimising the cost per kilogram of aid payload delivered.
- Cost per kg of payload delivered: The objective of the design is to reduce the cost per kg of payload to be delivered which keeps the cost as low as possible.
- Business Model Innovation: explore different business models to ensure income flow and sustain the project. In other words, economic sustainability can be enhanced by diversifying revenue streams and strengthening the project's capabilities.

2.6.4. Sustainability Evaluation

In order to evaluate the sustainability of the final design, sustainability metrics need to be defined. The metrics are aimed at evaluating the three aspects of sustainability presented before in terms of whether they are met or not at this point of the design, whether they will be implemented in a later stage in the design, and whether they affect any of the other sustainability aspects. The metrics and the evaluation are shown in Table 2.6.

Table 2.6: Overview of sustainability strategy compliance

	Sustainability strategy	Compliance	Notes
	Groups members transportation means	Yes	Bikes or train
	Use of reusable energy	Yes	Solar panels
	Lean manufacturing approach in production	In further stage	When production phase starts
	Production methods	In further stage	-

—Environmental

⁴Economic Sustainability, [cited on 22 May 2023]

	Suppliers	In further stage	May affect the cost sustainability positively
	Material CO ₂ production	Yes	As least as possible CO ₂ emissions per kg produced together with important material properties
	Use of recycled material	No	Maybe in the future but now the recycled material are not compatible with the design. May affect the cost sustainability positively
	Number of aircraft shipped by air	In further stage	-
	Decrease shipping distance	In further stage	May affect the cost sustainability positively looking at long term
	Package optimisation	In further stage	-
	Use of clean transport	In further stage	-
	Increase fuel efficiency	Yes	Efficient engine choice, designing for least drag possible. May affect the cost sustainability negatively
	Shipment collaboration	In further stage	-
	Recycling plan	Yes	Open recycling loop strategy
	Hazardous material disposal	In further stage	The plan will be made in a further stage in the design
Social	Aid strategy	Yes	The system is designed to deliver aid as quickly as possible
	Local population contacts	In further stage	-
	Local labour	Yes	When testing in another countries local pilots are hired. May affect the cost sustainability positively
	Collaboration with local organisation	In further stage	-
	No choice of mined material	Yes	GFPR is chosen so less metal is used
	Cultural consideration	In further stage	This can be executed when operating the system
Economic	Optimise the use of resources	In further stage	Is more significant when production and operation starts. May affect the environment sustainability positively
	Lean manufacturing approach	In further stage	When production phase starts

2.7. Market Analysis

Before designing and engineering a product, its potential should be assessed by exploring the market gap that it aims to fill and identifying existing competitors it will challenge or use as a design basis. The market analysis, therefore, consists of the specific market identification, together with competing competitors and what differentiates the product from existing ones, exploring market trends and establishing the strengths, weaknesses, opportunities and threats of the future product. The market analysis is built upon the analysis conducted in the Baseline Report [2], with improvement and modification.

2.7.1. Competition Market

Wings for Aid is a humanitarian initiative company, that aims to help people in need by delivering aid as quickly as possible in a disastrous situation. This is done to pinpoint accurate locations with minimum cost

and maximum sustainability to inaccessible areas, by the means of unmanned aerial vehicles. That is what makes Wings for Aid compete in the so-called Humanitarian Market. This market emerged because of the help that multiple international stakeholders want to provide to affected populations in case of any type of crisis happening, such as conflicts, natural or industrial disasters. This international response triggers the development of new products and services to deliver the help needed. The market is mainly dominated by international and national nongovernmental organizations (NGOs). But it also includes donors, service providers, and enterprises [1].

The humanitarian share of international official development assistance (ODA) has shown a significant growth between the years 2001 and 2005, from 7.5% to 10.2%. The orientation of donor governments has clearly been shifted towards the private sector of humanitarian aid for cost-effective solutions, due to the increase in frequency, complexity and length of humanitarian crisis [1].

The humanitarian market is considered challenging for enterprises because of the lack of knowledge development in the private sector, for the following main reasons [1]:

- High level of uncertainty; poor oversight and unclear authority.
- Time pressure to respond to an immediate need.
- Limited human and capital resources

Another factor that makes the humanitarian market challenging is the intense media involvement in a highly political situation and environment.

2.7.2. Market Trend

Between the years of 2013 and 2023, the United Nation's aid delivery budget increased from 8.6 billion \$ to 51.5 billion \$ ⁵. Part of this money has been spent to provide help to people who became victims of man-made or natural disasters. When these events occur, communities can be cut off from the outside world due to the destruction of infrastructure or, for example, floods. To avoid the need to travel to get to humanitarian aid supply, there is a need for fast, low-cost, pinpoint delivery of aid supply. Aerial delivery is a good candidate to fulfil this need as it does not require extensive infrastructure. The market that is aimed at providing these services is still in its startup phase. The growth in the demand for humanitarian aid combined with the young market projects provides sufficient room for growth.

The distress locations can usually be reached from the established logistical centres ⁶, and, even if an earthquake and war cannot be well predicted, disasters tend to occur within fixed, susceptible geographical locations.

The Wings for Aid project is aiming to fill the aforementioned niche in the market with a largely off-the-shelf, low-cost, certified and fossil fuel-powered unmanned aerial vehicle. This is done to cut development time and costs. Potential new markets that aim to attend to the need for pinpoint aid delivery are markets in which the deliveries are performed by certified drones or drones that are not powered by fossil fuels. These types of drones could have a competitive edge over the Wings for Aid design. To avoid being competed out of the market, the design could be made ready for certification. In this way, the deficit due to not being certified could be overcome quickly. Furthermore, by integrating modularity into the design, the aircraft could be prepared for renewable energy sources when the technology becomes available.

2.7.3. Competitor Companies

The humanitarian market is a big title to analyse competitors, thus a more specific sector of the market has been identified, which is the field of innovative and technology-driven solutions for aid delivery and disaster response. The competitors for Wings for Aid are companies or projects that have the technology and ability to deliver aid in a short time to specific locations, the main competitors are listed in Table 2.7.

The competitors' performance can be quantified by comparing their operating range, payload and cost of a kilogram delivered over a kilometre. The cost has been calculated by dividing the operating costs of a single flight by range and payload.

⁵OCHA, [cited 2 May 2023]

⁶UN, [cited 2 May 2023]

Table 2.7: List of selected key competitors of Wings for Aid with their product's payload, range and cost per kgkm

Project	Cost [€/kgkm]	Payload [kg]	Range [km]	Label
Zipline ⁷	0.28	1.8	80	1
Swoopaero conf. 1 ⁸	no data	3	175	2
Swoopaero conf. 2	no data	5	130	3
Manna ⁹	no data	3,5	20	4
Antwork TR9 ¹⁰	0.046	9	27	5
Antwork TR7S	0.046	6	18	6
Antwork RA3	0.046	4.5	15	7
Matternet ¹¹	no data	2	20	8
Spirit drones ¹²	no data	150	500	9
Elroy air ¹³	no data	226	480	10
Bayraktar TB2 ^{14 15}	0.010	150	300	11
Cloudline ¹⁶	0.018	100	200	12
Dronamics Black Swan ¹⁷	0.0020	350	2500	13
Windracers ¹⁸	no data	100	1000	14
Volansi ¹⁹	no data	no data	563	15
Pablo air ²⁰	no data	30	no data	16
Cessna Caravan ²¹	0.0024	1393	1982	17
Pilatus PC12 ^{22 23}	0.0061	458	2424	18
Mil Mi-8 ²⁴	0.0013	4000	519	19
Bell 212 ²⁵	0.0045	2286	439	20
Airbus H125 ²⁶	0.0044	973	629	21
C-130 Hercules ²⁷	0.00068	15422	3330	22
UH1 Huey ²⁸	0.0015	2120	556	23
Truck (class 5, two axis, single unit) ^{29 30}	0.000044	5000	600	25
Truck (class 7-8, six axis, sep. trailer)	0.000011	30000	800	26

The gathered projects from Table 2.7 can be visualised in Figure 2.3 which plots them based on their range and payload performance. The market area for Wing for Aid is also identified with a red dot, which is the same point as in the beginning of the project because of the fixed payload and range designed for. Furthermore, the products' cost/kgkm can be compared with payload and range in Figure 2.3a and Figure 2.3b, respectively. Again, the Wings for Aid aim to be placed within the red dashed rectangle, while the current cost of Wings for Aid is shown by the continuous red rectangle. The range and payload are a requirement defined in Section 2.3.

From Figure 2.3 it can be seen that Wings for Aid is doing relatively well in terms of amount of payload delivered for the specified range. It is important to remember that even though these companies and

⁷ Zipline, [cited 2 May 2023]

⁸ Swoopaero, [cited 2 May 2023]

⁹ Manna, [cited 2 May 2023]

¹⁰ Antwork, [cited 2 May 2023]

¹¹ Matternet, [cited 2 May 2023]

¹² Unmanned Systems Technology, [cited 2 May 2023]

¹³ Elroy air, [cited 2 May 2023]

¹⁴ Bayraktar, [cited 2 May 2023]

¹⁵ Military Today, [cited 2 May 2023]

¹⁶ Cloudline, [cited 2 May 2023]

¹⁷ Dronamics, [cited 2 May 2023]

¹⁸ Windracers, [cited 2 May 2023]

¹⁹ SNC, [cited 2 May 2023]

²⁰ Pablo Air, [cited 2 May 2023]

²¹ Cessna, [cited 2 May 2023]

²² Aircraft Cost Calculator [cited 2 May 2023]

²³ Pilatus Aircraft, [cited 2 May 2023]

²⁴ Military Today, [cited 2 May 2023]

²⁵ Army Technology, [cited 4 May 2023]

²⁶ Airbus H125, [cited 2 May 2023]

²⁷ C-130 Hercules, [cited 2 May 2023]

²⁸ UH1 Huey, [cited 2 May 2023]

²⁹ The Truck Expert, [cited 2 May 2023]

³⁰ Fraikin, [cited 2 May 2023]

organisations are considered competitors, sometimes it is necessary to collaborate with them in order to deliver the aid in the most efficient and helpful way for the people that are in need of the help, which is, of course, the first and most important aim of all these companies.

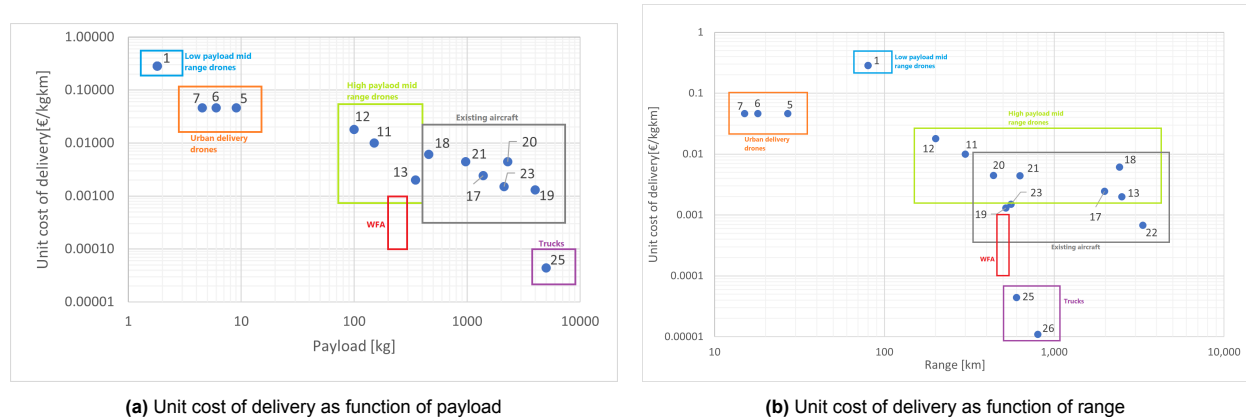


Figure 2.3: The segmentation of the competition within the target market

From Figure 2.3 it can be seen that Wings for Aid is doing relatively well in terms of amount of payload delivered for the specified range. It is important to remember that even though these companies and organisations are considered competitors, sometimes it is necessary to collaborate with them in order to deliver the aid in the most efficient and helpful way for the people that are in need of the help, which is, of course, the first and most important aim of all these companies. Still, competition is there. To visualise the market position Wings for Aid is aiming to fill more, the unit cost is graphed as a function of payload and range in Figure 2.3. As can be seen in the graphs, Wings for Aid aims at a lower unit cost of delivery compared to solutions with similar payload and similar range. If this can be realised, Wings for Aid will have a competitive edge.

2.7.4. Product Differentiation of the Market and Market Gap

The existing solutions to rapid aerial cargo pinpoint delivery can be categorised by similarities in their capabilities. Urban delivery drones are usually VTOL rotorcrafts with low range and payload, not fulfilling the Wings for Aid user requirements, while sharing a relatively saturated market. Thus appears the market gap that Wings for Aid is planning to conquer. Which is a solution for the last mile problem in humanitarian aid, delivering aid packages as quick as possible to pinpointed locations with minimum cost. What differentiates Wings for Aid product than the other existing products can be identified as follows:

1. Semi-autonomous: Semi-autonomy is used as it differentiates a big part of the market since there is low human risk, allowing to relax safety requirements on the design.
2. Aerial: The aid delivery systems discussed are used in areas that could be inaccessible by roads.
3. Minimum capacity of 100 kg: This eliminates smaller drones that can not deliver large quantities/products needed for aid.
4. Minimum range 200 km: This eliminates drones that cannot reach a large zone within the impacted areas.
5. Multiple drops per sortie: Allows for a different mission profile by delivering to multiple, smaller drop zones which do not need large-scale aid delivery.
6. Remote/unprepared landing strip: Eliminates large amount of existing aircraft that need extensive infrastructure e.g. regular landing strips.

For the reasons mentioned previously, Wings for Aid can make a big advantage in the humanitarian market, and in the field of innovative and technology-driven solutions for aid delivery and disaster response in specific. Which draws the attention of customer and will give the lead in the market.

2.7.5. SWOT Analysis

In Table 2.8, the Strengths, Weaknesses, Opportunities and Threats are shown. The table is based on a table from [2], and is updated to the current stage of the project.

Table 2.8: SWOT analysis for the Wings for Aid aircraft, as for the final stage of the design

Strengths	Weaknesses
<p>High payload – advantage with respect to competition</p> <p>Long range – advantage with respect to competition</p> <p>Low human risk – any danger for the pilot is eliminated, allowing to relax the safety requirements on the design</p> <p>Low turnaround time – optimising for payload delivered per day increases competitiveness on the market</p> <p>Broad range of operating environments – universality attracts customers and reduces logistic and manufacturing costs</p> <p>Dismantlability – favours logistics and reduces the response time by increasing the range of transporting solutions</p> <p>Simplicity of design – facilitates maintenance and reduces its costs</p> <p>Use gasoline - currently commonly available</p> <p>Medium unit price - less competitive than expected, but still in the market</p>	<p>Currently no certification – gives disadvantageous position of when requesting access to airspace</p> <p>Low target unit price – limits the technology that can be implemented</p> <p>Limited operational range – 300 km range from origin by law. Otherwise, more extensive import process</p> <p>Required to obey to safety regulations – local CAA requirements and precautions to prevent military use require specific design solutions which slows down the development process</p> <p>High speed of falling packages – can pose danger to humans and wildlife, but the design of the box will protect the cargo inside from damage</p> <p>Dismantlability – eliminates the benefits of integral structures from the design and imposes the need for connector implementation, which increases complexity</p>
Opportunities	Threats
<p>Unmanned aircraft market growth – expected dynamic growth of UAV market can boost technology development and decrease some subsystems costs</p> <p>Modularity – possibility to use for different purposes than aid delivery which increases the range of potential customers</p> <p>Increase humanitarian aid delivery – the global worth of humanitarian aid delivered increases every year which indicates a growing market</p> <p>Social acceptance of the project – potential to attract partners and investors because of the high moral status of humanitarian aid concept</p>	<p>High performing existing solutions – some existing aircraft already provide good solutions to large scale aid delivery</p> <p>Operation in unstable environments – increases the risk of crashes caused by external human and environmental factors.</p> <p>Indirect involvement in conflicts of interests - unwillingness to share all developments advancements and costs because of confidentiality requirements slows down the development process</p> <p>Use of gasoline – can become obsolete, manufacturer to stop maintenance support and discourage investors with high sustainability expectations</p> <p>Low payload capacity given the needs – the UN recognise the payload as low, compared to the needs</p>

It can be observed that, because of the increase in price per kilogram of payload delivered, and the increased unit cost, some of the expected strengths have weakened. Wings For Aid still has a high potential of taking a significant market share with the simplistic solution to the last mile problem. The main weaknesses remain the price restrictions and certification. With the biggest opportunity staying the increasing market growth, which allows for more opportunities to enter and stay in the market. The possibility for modularity to utilize the fleet for non-aid purposes when there is less need for aid can significantly increase revenues. This extra profit can then be used to create a more efficient and cost-effective design to further decrease unit costs. Over time, this can increase Wings For Aids's place in the market.

Design Approach

This chapter aims to inform on the approach of the design process. Moreover, the process from generating initial concepts to the final design will be elaborated. This will be done first by discussing the generated design concepts in Section 3.1. The trade-off of these concepts will be discussed next in Section 3.2, which is a summary of the Midterm Report [3]. Then in Section 3.3, a first-order estimation is done on the chosen concept, and the organisation for the design process is explained in Section 3.4. Lastly, the method for the detailed design is explained in Section 3.5, with a focus on the workings of the code used in this stage.

3.1. Design Options

In the Midterm Report [3], logical combinations of aircraft configurations are generated using a flow-down method through the design option trees, made in the Baseline Report [2]. This method lead to the 10 design concepts in Table 3.1.

Table 3.1: Overview of all feasible design concepts from the Design Option Tree

Identifier	Fuselage type	Configuration	Number of engines and position	Tail
CON-1	Double	Conventional	2 nose-mounted engines	conventional tail
CON-2	Single	Canard	1 rear-mounted engine	wing-mounted tail
CON-3	Single	Conventional	1 nose-mounted engine	conventional tail
CON-4	Single	Conventional	1 nose-mounted engine	boom-mounted conventional tail
CON-5	Single	Conventional	1 nose-mounted engine	flying tailplane
CON-6	Single	Conventional	1 nose-mounted engine	boom-mounted flying tailplane
CON-7	Single	Conventional	1 rear-mounted engine	Y-tail
CON-8	Single	Conventional	1 rear-mounted engine	H-tail
CON-9	Single	Conventional	1 rear-mounted engine	boom-mounted inverted V-tail
CON-10	Single	Conventional	1 fuselage mounted engine	V-tail

3.1.1. Transportation Configuration

To get to a complete design concept, the transportation configuration also has to be evaluated. Using the design option tree for the transport configuration of the wing, which is indicated as tree 6, a trade-off has been performed in the Baseline Report. This has led to the choice of using detachable wings. However, the decision for a detachable or fixed empennage is not made yet at this stage. This will be investigated within this report, as this trade-off requires more detailed design information.

3.1.2. Design Concepts

Combining the results from Table 3.1 and Section 3.1.1, the total design concepts are generated, where every concept uses detachable wings for the transport configuration. Strawman figures of each concept can be found in Figure 3.1, the blue arrow with the annotation 'DOF' indicates the direction of flight. These designs enter the trade-off that will lead to a final configuration which is described and performed in Section 3.2.

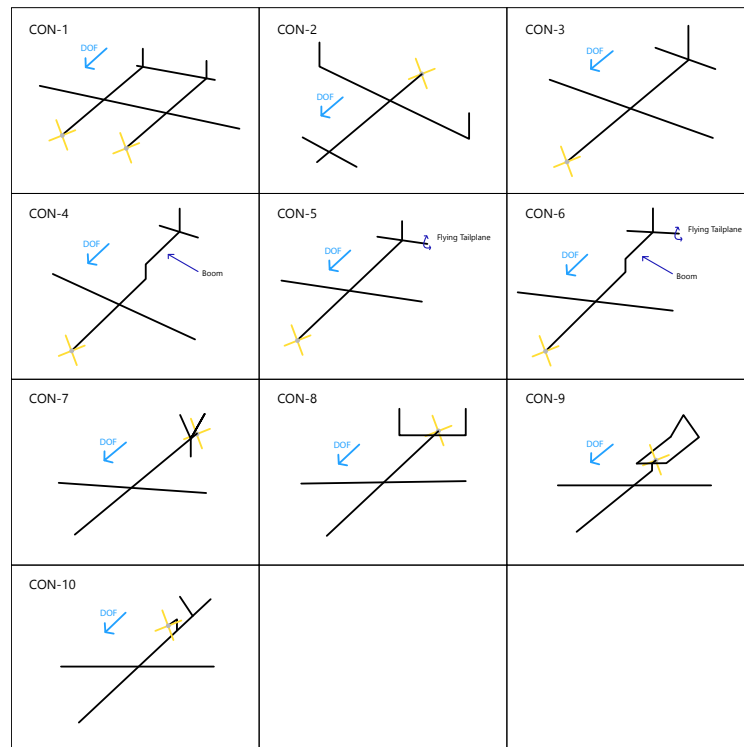


Figure 3.1: Strawman figures of the design concepts [7, Fig. 8.1a]

3.2. Trade-off

With the configurations defined in Section 3.1 a trade-off has to be performed in order to come up with one final configuration that will be further designed. As explained in detail in the Midterm Report [3], the trade-off is done in two steps; first a general trade-off, followed by a detailed trade-off.

3.2.1. General Trade-off

At this point, ten concepts are left and there are not enough resources to work out each concept in more detail. Therefore it is chosen to first perform a qualitative trade-off between the concepts, which assesses global criteria, such as 'design simplicity'.

The graphical trade-off method is used, where each concept is assessed on each criterion using 'Excellent; exceeds requirements', 'Good; meets requirements', 'Correctable deficiencies', 'Unacceptable'. This leads to a ranking between the ten design concepts. On page 25 the criteria, weights and results are presented. From the score in the second-last row in the table on page 25, it can be seen that configurations CON-3, CON-4, CON-5 and CON-6 are the clear winners. The configuration numbers correspond to the configurations defined in Table 3.1. However, because these configurations are very alike (the only differences are the presence of a boom and or flying tailplane), the three highest ranking configurations after concepts CON-3 to CON-6 are considered as well. This results in configurations CON-3, CON-4, CON-5, CON-6, CON-7, CON-8 and CON-10 moving to the detailed trade-off. The reason behind this decision is that the tail of, for instance, configuration CON-7 could outweigh that of configuration CON-3, but its method of propulsion makes the overall design significantly worse. Using this method the best components of each design are selected and combined together to create the best design.



	GEN-CON-1	GEN-CON-2	GEN-CON-3	GEN-CON-4	GEN-CON-5	GEN-CON-6	GEN-CON-7	GEN-CON-8	GEN-CON-9	GEN-CON-10
Structural Mass	1; double fuselage requires more mass to carry payload, two engines add weight	2; wing structural mass slightly higher due to wing mounted tail	2; conventional configuration	3; boom tail structure is lighter than conventional tail structure	2; see CON-3	3; see CON-4	2; comparable with conventional configuration	1; H-tail is relatively big, horizontal stabiliser needs reinforcement	1; double boom adds extra weight, V-tail usually heavy	1; V-tail is usually heavy, extra structure needed for engine placement
Stability	1; double fuselage aircraft are less stable due to boom flexibility (cte) and flutter	1; allowable cg range is smaller	2; conventional configuration	2; comparable to conventional configuration	2; comparable to conventional configuration	2; comparable to conventional configuration	2; drawbacks of v tail but directional stability better due to extra fin	2; increased longitudinal stability, but decrease in directional stability	1; spiral and dutch roll stability problems,	1; spiral and dutch roll stability problems
Controllability	2; sufficient controllability	1; smaller possible cg range, possible difficulties with dropping and HLDs	2; sufficient controllability	2; sufficient controllability	3; moving tailplane is effective which increases controllability	3; moving tailplane is effective which increases controllability	1; control is more complex	2; sufficient controllability	1; control is more complex	1; control is more complex
Fuselage - Propulsion interaction	1; two engines increase fuel burn and smaller propellers are less efficient	1; pusher propeller is less efficient than propeller in tractor configuration	2; propeller in tractor configuration has good efficiency	2; propeller in tractor configuration has good efficiency	2; propeller in tractor configuration has good efficiency	2; propeller in tractor configuration has good efficiency	1; pusher propeller is less efficient than propeller in tractor configuration	1; pusher propeller is less efficient than propeller in tractor configuration	1; pusher propeller is less efficient than propeller in tractor configuration	1; propeller needs to operate in flow disturbed by fuselage and wing
L/D	1; double fuselage generates more drag	3; Canard provides positive lift and less tip vortices due to vertical tail	2; little surface area, so good drag performance	2; comparable to conventional configuration	2; comparable to conventional configuration	2; comparable to conventional configuration	2; comparable to conventional configuration	2; comparable to conventional configuration, more surface area but also less tip vortices	2; comparable to conventional configuration	2; comparable to conventional configuration
Reliability	2; no projected reliability issues	1; more complex control connections to wing mounted tail rudder surfaces	2; no projected reliability issues	2; no projected reliability issues	2; no projected reliability issues	2; no projected reliability issues	1; Y-tail produces higher structural stresses; fatigue life	1; Y-tail produces higher structural stresses; fatigue life	1; V-tail requires complex mixer of elevator and rudder input. Also high structural stresses	1; V-tail requires complex mixer of elevator and rudder input. Also high structural stresses
Turnaround time	1; loading via the sides increases loading time. Heavier/larger aircraft may take more fuel	1; loading via the sides increases loading time	2; loading is possible from the back (with limited space) or sides	3; boom gives a lot of room for loading from the back. Possible to load and fuel simultaneously	2; loading is possible from the back (with limited space) or sides	3; boom gives a lot of room for loading from the back. Possible to load and fuel simultaneously	2; loading from the front possible with limitations at the rear. Otherwise from the sides	2; loading from the front possible with limitations at the rear. Otherwise from the sides	2; loading from the front possible with limitations at the rear. Otherwise from the sides	2; loading from the front possible with limitations at the rear. Otherwise from the sides
Accessibility for maintenance	1; difficulty accessing the structure in between the two fuelages	3; all control surfaces and lift surfaces at accessible height, easy engine access	2; sufficient access to engine and other important parts	2; sufficient access to engine and other important parts	2; sufficient access to engine and other important parts	2; sufficient access to engine and other important parts	2; sufficient access to engine and other important parts	2; sufficient access to engine and other important parts	1; engine is positioned in an inconvenient location in the aircraft.	1; engine is located on top of the fuselage
Modularity	1; requires splitting of wing, unstable in storage (single LG per fuselage), but can save space in container	1; potentially more complex to separate tail from wing x two, canard width can be driving	2; concept requires partial disassembly of wings. Possibly of vertical tail	3; boom configuration allows for more easy disassembly	2; potential need for one/two cut for wing and complex tail attachment, with risk of damage to prop	3; boom configuration allows for more easy disassembly	2; potential need for one/two cut for wing and complex tail attachment, with risk of damage to prop	2; potential need for one/two cut for wing and complex tail attachment, with risk of damage to prop	2; potential need for one/two cut for wing and complex tail attachment, with risk of damage to prop	2; potential need for one/two cut for wing and complex tail attachment, with risk of damage to prop
Terrain capabilities (ground ops)	3; landing gear track can be larger so more uneven terrains can be traversed	1; canard must be high up on the fuselage to have sufficient clearance	2; sufficient ground clearance	3; boom configuration can positively impact tail clearance	2; sufficient ground clearance	3; boom configuration can positively impact tail clearance	1; Y-tail lower fin is at risk of hitting the ground at take off and landing	2; sufficient ground clearance due to length	1; booms may impact pitch angles on landing and take-off due to length	2; sufficient ground clearance
Friendliness	1; unconventional design can come across as dangerous	2; canard has friendly appearance	2; conventional configuration is what people are used to seeing	2; conventional configuration is what people are used to seeing	2; conventional configuration is what people are used to seeing	2; conventional configuration is what people are used to seeing	1; Y-tail is used in MQ-9 Reaper, thus it can come across as unfriendly	1; military drones often have pusher propeller, which might come across as unfriendly	1; unconventional design can come across as dangerous	1; V-tail is used in MQ-1 Reaper, thus it can come across as unfriendly
Loading solutions	1; two engines limit loading possibilities	1; canard (front) and propeller (back) complicate loading	2; both loading from the back and sides is possible	2; both loading from the back and sides is possible	2; both loading from the back and sides is possible	2; both loading from the back and sides is possible	2; both loading from the front and sides is possible	2; both loading from the front and sides is possible	2; both loading from the front and sides is possible	2; both loading from the front and sides is possible
Handling safety	1; two engines increase chance of incidents	1; canard and wing mounted tail makes manoeuvring around the aircraft more complicated	2; handling of conventional aircraft is common, therefore safe procedures are known	2; handling of conventional aircraft is common, therefore safe procedures are known	2; handling of conventional aircraft is common, therefore safe procedures are known	2; handling of conventional aircraft is common, therefore safe procedures are known	3; Y-tail gives extra protection against engine	3; H-tail gives extra protection against engine	3; double boom mounted tail encases engine	3; engine is placed where crew cannot accidentally come too close
Design simplicity	1; two fuselages increase the amount of parts and the amount of rigging connections	1; canard and wing mounted tail increase design complexity	2; conventional configuration	3; conventional configuration and boom instead of stiff structure	2; conventional configuration	3; conventional configuration and boom instead of stiff structure	1; Y-tail and pusher propeller make the design more complex	1; H-tail and pusher propeller make the design more complex	1; V-tail requires complex mixer of rudder and elevator inputs	1; V-tail is usually heavy, extra structure needed for engine placement
Certification possibilities	1; less reference data available on double fuselage concept and uncommon proof of concept.	1; less reference data available on wing mounted tail and uncommon proof of concept, canard limits controllability and HLD use	3; Conventional configuration, common proof of concept	3; Conventional configuration, common proof of concept	3; Conventional configuration, common proof of concept	3; Conventional configuration, common proof of concept	2; aircraft with Y-tail concept is less common and thus there is less proof of concept	2; aircraft with H-tail concept is less common and thus there is less proof of concept	2; aircraft with V-tail concept is less common and thus there is less proof of concept	2; aircraft with V-tail concept is less common and thus there is less proof of concept
Rank:	1.2337	1.3562	2.0450	2.5464	2.0780	2.5794	1.6755	1.7234	1.3905	1.4881
	10	9	4	2	3	1	6	5	8	7

Table: Results of the general trade-off with each concept's score in specific category, together with a brief explanation

3.2.2. Detailed Trade-off

As the remaining concepts from the general trade-off share some commonalities, the detailed trade-off process is divided into three independent trade-off's with the following three system groups:

- The fuselage shape and propulsion system placement - these two influence each other, therefore are assessed together.
- The tail configuration.
- The wing support (braced wings or not).

In each system group, four to five criteria have been defined and each criterion has received a percentage weight. All design options within the independent groups have been assigned a score, which, multiplied by the criteria weight, allows for determining the best design option from each independent system group. Because of the more precise ordering need of the Fuselage + Prop design options and wing support, the options are ranked according to the scoring scheme on Figure 3.2b, while tail design options trade-off employs the ranking scheme defined on Figure 3.2a.

3	Excellent; Better than conventional	5	Excellent; Much better than conventional
2	Good; Equal to conventional	4	Very good; Better than conventional
1	Okay; Worse than conventional	3	Good; Equal to conventional
		2	Okay; Worse than conventional
		1	Bad; Much worse than conventional

(a) On a 1-3 scale

(b) On a 1-5 scale

Figure 3.2: Ranking definition of design options

The so-called conventional design is always defined as a single propeller engine mounted at the nose of the aircraft, in line with the fuselage-mounted conventional tail configuration with stabilisers in front of control surfaces.

Fuselage and propulsion system

The following options have been identified to choose from to combine the fuselage and propulsion functions within the aircraft:

- DET-CON-1: Pull propeller in front of fuselage, with fuselage mounted tail - considered a conventional configuration, an example of this configuration is the Cessna 152
- DET-CON-2: Pull propeller in front of fuselage, with boom-mounted tail - a single beam transferring all tail (and potentially engine) loads to the fuselage, an example is the current Wings for Aid prototype
- DET-CON-3: Push propeller at the rear of the fuselage, with fuselage mounted tail - potentially implies placing the tail in front of the propeller, such as on the MQ9 Reaper
- DET-CON-4: Push propeller at the rear of the fuselage, with boom-mounted tail - potentially implies the use of two booms on both sides of the propeller, such as on the Bayraktar TB2
- DET-CON-5: Propeller mounted on the top of the fuselage, with fuselage mounted tail, such as on the SH Duo Discus glider
- DET-CON-6: Propeller mounted on the top of the fuselage, with boom-mounted tail

The trade-off criteria, weights, and scoring are presented in Figure 3.3.

REQ Rationale	Criteria	Explanation	Weight	Pull prop, fuselage	Pull prop, boom	Push prop, fuselage	Push prop, boom	Top prop, fuselage	Top prop, boom
SYS-FR-AC-PRO-3.1	Propulsive efficiency	Push versus tractor propeller	15%	3	3	1	1	2	2
SYS-CO-COST-1.1	Aircraft structure	Mass of design (boom or fuselage), mass of propulsive structure, manufacturability	20%	3	3	2	2	3	3
SYS-FR-AC-GNC-3.1/3.2/3.3/3.4	CG Range	Center of gravity range during operations, stability	25%	3	3	1	1	1	1
SYS-FR-FP-1.2	Aerodynamics	Drag of design, shape of fuselage	10%	3	2	4	4	2	2
SYS-FR-OPS-MIS-1.1	Operations	Loading flexibility, assembly and storing ease, maintenance	30%	3	4	4	5	2	2
Total			100%	3	3.2	2.4	2.7	1.95	1.95

Figure 3.3: Trade-off of the propulsion system placement and fuselage configuration

As can be seen in Figure 3.3, the winning configuration is the pull propeller, boom-mounted tail. That is because the pull propeller causes the engine mass to shift the centre of gravity forwards, as well as leads to a shorter forebody, thus allowing for a smaller tail area [8, p. 261]. It operates in undisturbed air, making it more efficient, while the fuselage is in the propeller wake. A pull propeller has a better ground clearance when the aircraft rotates during take-off. It also provides easier reach for maintenance. Regarding the fuselage configuration, the use of a boom tail allows for simplifying the structure that transfers the tail loads into the fuselage. This can have operational advantages, should the tail be dismantled from the main body, as well as allowing to access the main body from behind, underneath the tail. It decreases the total wetted area of the aircraft, thus decreasing the friction drag.

Tail

The following options have been identified to choose from to fulfill the tail functions of the aircraft:

- Conventional - the fixed vertical stabiliser is in front of the rudder, and the fixed horizontal stabiliser is in front of the elevator, an example is the Cessna 152
- V-tail - two fins inclined in approximately 45° from vertical pointing upwards, with stabilisers in front of ruddervators, an example is the Cirrus Vision
- Inverted V-tail - two fins inclined in approximately 45 deg from vertical pointing downwards, with stabilisers in front of ruddervators, an example is the Bayraktar TB2
- Y-tail - two longitudinal stability stabilisers inclined in approximately 45° from horizontal pointing upwards and a vertical stabiliser pointing downwards, an example is the MQ9 Reaper
- H-tail - two vertical stabilisers with rudders attached at the tips of a single horizontal stabiliser with an elevator, an example is the B-25 Mitchell
- Flying tailplane (stabilator) - the entire horizontal stabiliser rotates as a single body, taking over the role of the elevator, an example is the current Wings for Aid prototype

The trade-off criteria, weights, and scoring are presented in Figure 3.4.

REQ Rationale	Criteria	Explanation	Weight	Conventional	V-tail	Inverted V-tail	Y-tail	H-tail	Flying tailplane
SYS-FR-AC-GNC-3.1/3.2/3.3/3.4	Control & Stability	Tail effectiveness of design	30%	2	1	3	3	3	2
SYS-FR-FP-1.2	Aerodynamics	Wetted area tail, shape of tail	15%	2	2	2	1	1	3
SYS-FR-AC-PRO-1.1	Structural Mass	Mass of design	35%	2	2	2	1	1	2
SYS-CO-COST-1.1	Complexity	Effort in manufacturing and design	20%	2	1	1	2	2	3
Total			100%	2	1.5	2.1	1.8	1.8	2.35

Figure 3.4: Trade-off of the tail configuration

The winning tail from the trade-off is the flying tailplane (also called stabilator). This can be considered a simpler design, as it consists of a big moving surfaces, which also favours dismantability. It allows a more

effective control response, yet requires an unusual pitch trim design. Drag can be reduced, as lift by the control surface is created by the change in angle of attack rather than change in airfoil camber ^{1 2}.

Wing support

The following options have been identified to choose from to fulfil the structural support of the wing function of the aircraft:

- Non-braced wing - the conventional design, the wing transfers all loads to the fuselage on its own and creates all lift on its own (assumed fuselage lift insignificant), an example can be the Antonov An-225
- Light-braced wing - struts connect the mid-wing to the fuselage to transfer some of the lift and weight loads from the wing structure to the fuselage, an example can be the current Wings for Aid prototype
- Lift generating braced wing - struts connecting the wing to fuselage are airfoil shaped and contribute to the lift generation of the aircraft, an example can be the Boeing Truss-Braced Wing concepts

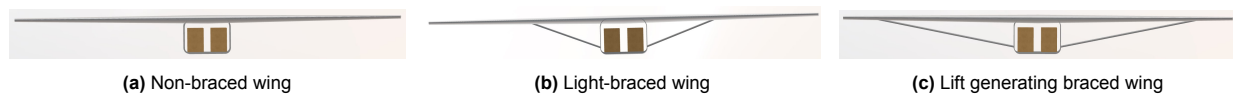


Figure 3.5: Bracing configurations

The trade-off criteria, weights, and scoring are presented in Figure 3.6.

REQ Rationale	Criteria	Explanation	Weight	Non-braced	Light-braced	generating braced
SYS-FR-AC-PRO-1.1	Aircraft structure	Mass of design	27.50%	3	5	4
SYS-FR-FP-1.2	Aerodynamics	L/D ratio	20.00%	3	2	5
SYS-CO-COST-1.1	Complexity	Ease of manufacturing, assembly on site and cost	27.50%	3	4	1
SYS-FR-AC-GNC-3.1/3.2/3.3/3.4	Control and stability	Influence on control	10.00%	3	3	2
SYS-FR-OPS-MIS-1.1	Operations	Ease to load, maintenance	15.00%	3	2	1
Total			100%	3	3.475	2.725

Figure 3.6: Trade-off of the wing support configuration

From the trade-off, the chosen option is the light-braced wing support. This option allows for decreasing the structural mass of the wing by taking over some of the lift and weight distribution from the wing to the fuselage. As a result, the spar or wingbox at the root can decrease in mass (decrease in wing group mass by up to 30%, [9]). Although struts can be made thin, the struts generate additional drag (increase in frontal area, interference drag), while the lift is kept constant. Simple struts do not add significant manufacturing effort and cost, compared to the overall wing group, however, the attachment of the detachable wing to the fuselage can be greatly simplified. The addition of the strut essentially transforms a cantilever beam-type structure (non-trussed) into a truss structure (light-trussed). This means that fixed attachments bearing shear and moment loads can be replaced by simple pin attachments. Because of its passive performance function, it does not change significantly the controllability, but limits the ground operations, reducing access to potential side hatches.

Final design concept

To conclude, combining results from Figure 3.3, Figure 3.4 and Figure 3.6, the final design concept chosen is similar to the current Wings for Aid prototype, mainly a front-mounted engine on the fuselage with boom tail, pitch regulated by a stabilator and simple, light-braced, detachable high wings.

¹ Stabilators vs Elevators, AOPA, [cited on 17 May 2023]

² What is the Difference Between a Stabilator and an Elevator?, [cited on 17 May 2023]

3.2.3. Material Trade-off

Apart from trade-offs for design decisions, a trade-off for material selection is important too. Therefore a consistent method is established to choose materials for individual subsystems, that allows avoiding design bias and reduces the time spent on the detailed trade-off of individual subsystem material. Initially, a list of 50 commonly used aerospace materials is assembled, including eight aluminium alloys, eight stainless steels, two steel alloys, two nickel alloys, five titanium alloys, five composites, nine thermoplastics, four woods, four ceramics and a number of other types of metals. Material properties are assembled, namely the density ρ , yield stress σ_y , elastic modulus E , fracture toughness K_{ic} ³ [10], raw cost ⁴, ecological cost (cost of recycling) and CO₂ emissions (mass of CO₂ released per mass of material produced) ⁵. It is always aimed to retrieve the same properties from a single website to ensure consistency. If available, either US or EU material quality is chosen, assuming the highest purity of material (non-recycled when entering the manufacturing facility). Average values are taken, if data differs for the same material produced under different conditions (heat treatment or cold reduction of metals).

The array of 50 materials is subsequently ranked from 1 (worst) to 50 (best) for each of the quantitative properties by numerical comparison, resulting in seven rankings of 50 materials. This ranking should be independent of the target subsystem of the application, but based on material characteristics only. Each property is subsequently given a weight, which is based on the design requirements of a subsystem of application and attributed subjectively. Material indices specific for subsystems can be defined from combinations of the properties assembled. The criteria weight can also be decided to be null, to reduce complexity. Once all the ten rank arrays are multiplied by the agreed weights of ten properties, the material with the highest sum of scores (one among 500, = 50 × 10) shall perform the best, given the required properties. The first couple of materials should be assessed, to determine how close the winner is to second and third-place alternatives.

Ranking materials has the advantage of giving a uniform scale of difference between ranked positions, which decreases the final score differences. An elastic modulus of metals that is several orders of magnitude greater than the one of the wood automatically prevents the wood from winning in nearly all cases, no matter the assigned weights. Therefore, using a ranking solution allows for realistically including all available materials in the trade-off. It also allows ranking materials based on properties, even though exact physical values might not be available (fracture toughness of wood). On the other hand, materials outperforming others in some properties can still be identified as potential solutions, therefore the output of the program should be closely monitored.

The material properties of some key materials that are selected for the aircraft design later in the report are summarised in Table 3.2. Shear strength of steels is assumed 0.58 of tensile strengths ⁶.

Table 3.2: Summary of properties of the key materials chosen in the aircraft design

	ρ [kg/m ³]	Raw cost [€/kg]	Eco-cost [€/kg]	CO2 emis. [kg/kg]	σ_y [MPa]	E [GPa]	K_{ic} [MPa m ^{1/2}]
Al-5052-H38	2680	2.81	2.66	8.82	255	70.3	28.50
S-steel-410	7800	3.99	1.38	3.94	1225	200	75.00
Steel-4130	7850	1.23	0.21	0.96	460	205	61.50
GFRP ⁷	1500	29	0.07	0.34	216	9	15

It is recommended to assemble more materials and their properties for future design process. Raw cost and ecological performance of materials should be confirmed for local markets of application.

³Matweb - Physical material properties, [cited on 19 June 2023]

⁴Indiamart, [cited on 19 June 2023]

⁵Idemat, [cited on 19 June 2023]

⁶Roytech - shear and tensile stress, [cited on 19 June 2023]

⁷Properties of the particular material used for fuselage fairing, see Section 7.2.3

3.3. First Order estimation

In order to begin the detailed phase of the design, an initial sizing is needed, which has been performed in the Midterm Report [3] using, first the Class I weight estimation, and built upon that, some preliminary geometry determination. This then allows for a more detailed, Class II weight estimation.

3.3.1. Class I

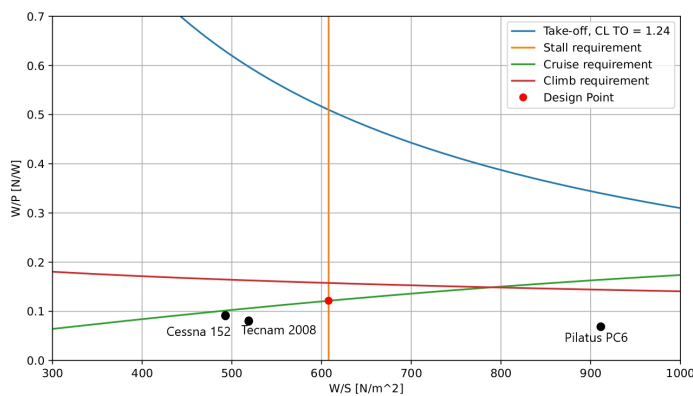
Class I weight estimation aims to calculate the Maximum Take-Off Weight (MTOW), Operating Empty Weight (OEW) and Fuel Weight (W_F) based on the mission definition, fuel fraction, Lift-to-Drag ratio (L/D), Specific Fuel Consumption (SFC) of the engine, and the OEW/MTOW ratio. It is based on empirical equations, derived from existing aircraft databases. A total number of 70 aircraft are assembled in the database, including general aviation aircraft with a single, piston engine driven propeller, ultralight general aviation aircraft, with MTOW of about 500 kg and single combustion engine powered UAVs, mostly of military purpose, with no strict limit on MTOW.

By plotting the OEW against the MTOW of each aircraft from the assembled database, a linear trend can be observed between the two parameters and expressed as $OEW = 0.5249 \cdot MTOW + 42.049$, with a coefficient of determination R^2 of 0.97. This results in an initial MTOW, OEW and W_F of 720 kg, 421 kg and 59 kg respectively.

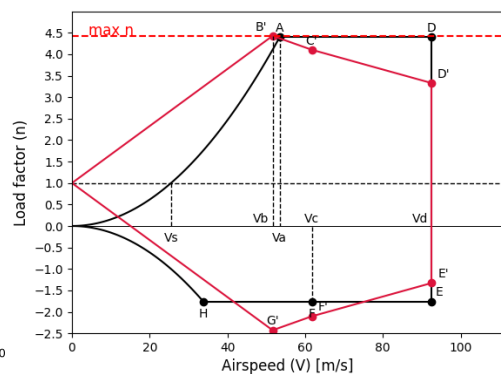
3.3.2. Preliminary Geometry and V-n diagram

The geometry determination is an initial sizing of external geometry parameters based on the Class I weight estimation. Based on this preliminary geometry, the Class-II weight estimation can be performed. One of the key outcomes of the initial sizing covers the creation of a W/P - W/S diagram, which shows the relation between the weight-to-power ratio and the weight-to-surface area ratio as well as a V-n diagram, allowing to define ultimate load factors.

From the W/P - W/S diagram, the design point can be selected. With the preliminary take-off weight found in the Class-I weight estimation, the required power and wing surface area can be determined. The W/P - W/S diagrams incorporate a stall limit, take-off limit, landing limit, cruise limit and climb limit. For a propeller engine, both the weight per horsepower (W/P) as well as the weight per wing surface area (W/S) should be as large as possible. The W/P - W/S diagram for the selected design concept is shown in Figure 3.7a. In this diagram, the landing requirement is not displayed as it falls outside of the diagram. Three reference aircraft are also placed on the graph for comparison. Figure 3.7b shows the V-n diagram, built from the manoeuvre envelope and gust envelope, based on CS-23 requirements [11]. The ultimate load factors are obtained by multiplying the maximum and minimum load factors by 1.5. These maximum and minimum load factors are 4.45 and -2.45.



(a) W/S-W/P diagram including the optimal design point and reference aircraft



(b) V-n diagram, used to determine the limit loads

As can be seen from Figure 3.7a, the cruise performance is limiting for the present design project. This is likely due to the fact that low speeds must be obtained during dropping manoeuvres. Because of this, the wing loading is limited, resulting in larger wings and thus a higher drag. To mitigate this, the implementation of high-lift devices for dropping manoeuvres should be investigated.

3.3.3. Class II and CG estimation

The Class II weight estimation is performed after doing the Class I estimation and determining the aircraft geometry and V-n diagram. It uses the OEW, 3D view geometry and the ultimate load factor as inputs. The output is an updated value for the OEW, which is then used in the Class I estimation for the iteration process. The calculated weights are also used in the CG calculation. The method used is taken from Torenbeek, where the formulas to calculate the weights of subsystems are listed, based on statistical data [12, pp. 277–294]. Iterating through Class I and Class II calculations leads to a converged design, which gives some initial design parameters.

An initial CG estimation can be performed using the weights calculated using Class II relations from Torenbeek. This gives a first insight into the weight distribution of the aircraft, and shows possible limitations in loading and dropping procedures. In order to calculate the CG, the weights are divided into a wing group and a fuselage group. The wing group consists of the wing and the control surfaces, while the fuselage group consists of the rest. First assuming that the OEW CG is at 25% of the MAC, the absolute location of the leading edge of the MAC can be calculated using Equation 3.1. As a result, the absolute location of the OEW CG is at the leading edge of the mean aerodynamic chord plus 25% of the mean aerodynamic chord.

$$X_{LEMAC} = X_{FCG} + \bar{c} \left[\left(\frac{x}{\bar{c}} \right)_{WCG} \frac{M_W}{M_F} - \left(\frac{x}{\bar{c}} \right)_{OEWCg} \left(1 + \frac{M_W}{M_F} \right) \right] \quad (3.1)$$

In Equation 3.1: X_{FCG} is the CG location of the fuselage group, $\left(\frac{x}{\bar{c}} \right)_{WCG}$ is the CG location of wing group as a fraction of MAC, M_W is the wing group mass, M_F is the fuselage mass and $\left(\frac{x}{\bar{c}} \right)_{OEWCg}$ is the CG location of the operative empty weight as a fraction of the MAC. Table 3.3 summarizes the outcomes of the Class II weight estimation, the baseline for detailed design.

Table 3.3: Class II results for weights, geometry and cg estimations

Table 3.4: Class II weights and geometry

Parameter	Estimation	Unit
W_{TO}	730 ± 50	kg
W_F	60 ± 10	kg
W_{OE}	430 ± 30	kg
S	12 ± 1	m ²
b	11 ± 0.3	m
l_{fus}	5.5 ± 0.7	m
l_{boom}	2 ± 0.4	m
l_{MAC}	1.0 ± 0.1	m
W_w	55 ± 5	kg
W_{fus}	96 ± 15	kg

Table 3.5: Class II cg estimations

Parameter	Estimation	Unit
$\frac{x_{c.g.}}{l_{MAC \text{ front}}}$	0.17 ± 0.05	-
$\frac{x_{c.g.}}{l_{MAC \text{ after}}}$	0.53 ± 0.05	-
$\frac{x_{c.g.}}{l_{MAC \text{ TO}}}$	0.41 ± 0.05	-
$\frac{x_{c.g.}}{l_{MAC \text{ range}}}$	0.36 ± 0.1	-

3.4. Design Organisation

The detailed design of aircraft subsystems is performed by five departments, each composed of two team members. The operations department is responsible for the conceptual design of the logistics of the Wings For Aid project, onboard equipment as well as ground handling and base layout and estimating costs. Finally the operations department investigates the dropping manoeuvre. The flight performance and propulsion department computes flight characteristics at each mission phase and selects the engine and propeller. The control and stability department sizes the required control surfaces, the landing gear position, and defines a mass distribution, ensuring the centre of gravity is correctly placed with respect to other subsystems. The aerodynamics department conceptually designs the wing characteristics required for flight, seized the fuselage shape, estimates the drag components of subsystems as well as defines the stability derivatives of the aerodynamic design. Finally, the structures department is responsible for the design of the wingbox, fuselage, tail boom design, landing gear, wing strut structure, the connections of detachable struts and wings onto the fuselage, as well as the fuselage fairing, together with material assignment.

3.5. Iteration Description

Class I and Class II weight estimations are performed iteratively until the OEW converges to a difference of less than 1% between two consecutive loops. After, these values are used as initial inputs for the more detailed design. Once this stage of the design got more refined, Class I and Class II have been run once more with the more accurate values. The outputs of this were then used as the input of the final design stage.

This final design stage is broken up into different departments, as mentioned in Section 3.4. As a first step of the final design stage the outputs of class I and class II are supplemented by additional important initial values for each department. For example, the wing incidence angle is not an output of Class I / Class II, yet still an important value to have an initial sizing of. This enlarged list of variables is then used for the full design iteration, captured in Figure 3.8.

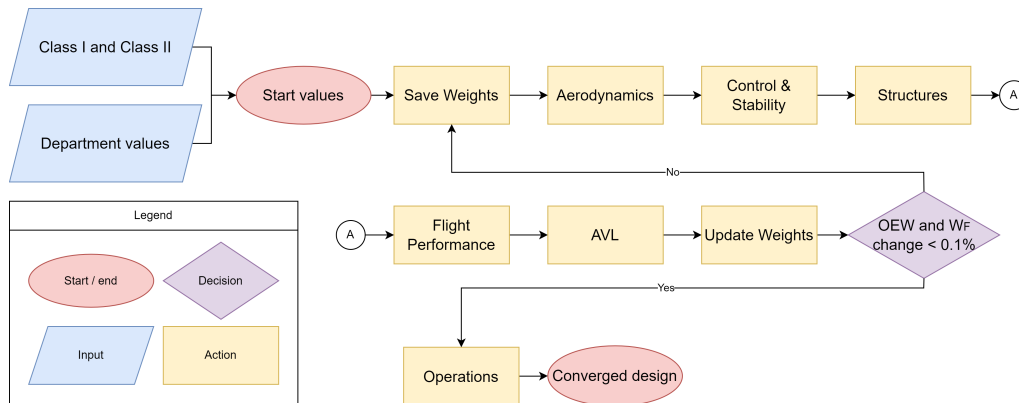


Figure 3.8: Schematised iteration process in conceptual design phase

This design iteration is performed in the form of a Python program, which integrates all calculations from all departments into one large program. This will ensure that the values of all departments will be consistent with each other, which is important when evaluating a full design.

At the start of the iteration the fuel weight and operative empty weight are saved. These weights will be used to check the convergence of the design, since these are the top-level weights that change throughout the iterations. The maximum take-off weight is the sum of the operative empty weight, fuel weight and payload. Since payload is a constant value, there is no benefit to using the MTOW as convergence check. The design is deemed converged if the weights that are actually updated, change less than 0.1% between two consecutive iterations.

First all calculations for the aerodynamics department are performed, these include airfoil selection, defining the wing, horizontal and vertical tail planform and performance and the total aircraft's drag estimation. Throughout the aerodynamics code the relevant parameters are updated. Next up is the control and stability department, which performs calculations such as the control surface sizing and landing gear placement. When also these parameters are updated, the code of the structures department is ran. This finds the optimum wingbox parameters and updates those. Other structure components are calculated separately using FEM and therefore are not incorporated in the iteration. Afterwards the flight performance department updates parameters concerning their department, specifically important is the fuel use per sortie, as this directly influences the fuel weight loaded in the aircraft. Finally AVL is ran in order to assess the CL max clean, check the stability parameters and update the incidence angles.

Throughout all these calculations weights such as the wing weight and tail weight are updated, leading to a new operative empty weight and fuel weight. If the change in these weights is less than 0.1 percent, the loop is exited. If not the iteration loop is continued, performing the same calculations over and over, until the design converges. When the design has converged, the operations department uses the output values to assess the costs, and detail the operational procedures further. Once this final step has been performed, a fully converged final design is set.

Operations

Before the subsystems of the aircraft will be discussed, it will first be analysed how the aircraft interacts with other elements of the system. This is done in this chapter by defining an operational model for the system in which the different phases of the mission are explained.

4.1. Operations Model

The designed system does not only consist of aircraft. In order to be most effective, the concept of operation has to be thought through. This is done by developing a model of operations and indicating the critical elements of the mission, allowing for an accurate cost estimation. Three main components of the operations are indicated, namely ground base (GB), sortie and facilities. Within these main components, all elements of the operational mission are shown. These elements are worked into functions of the system in Figure 4.1.

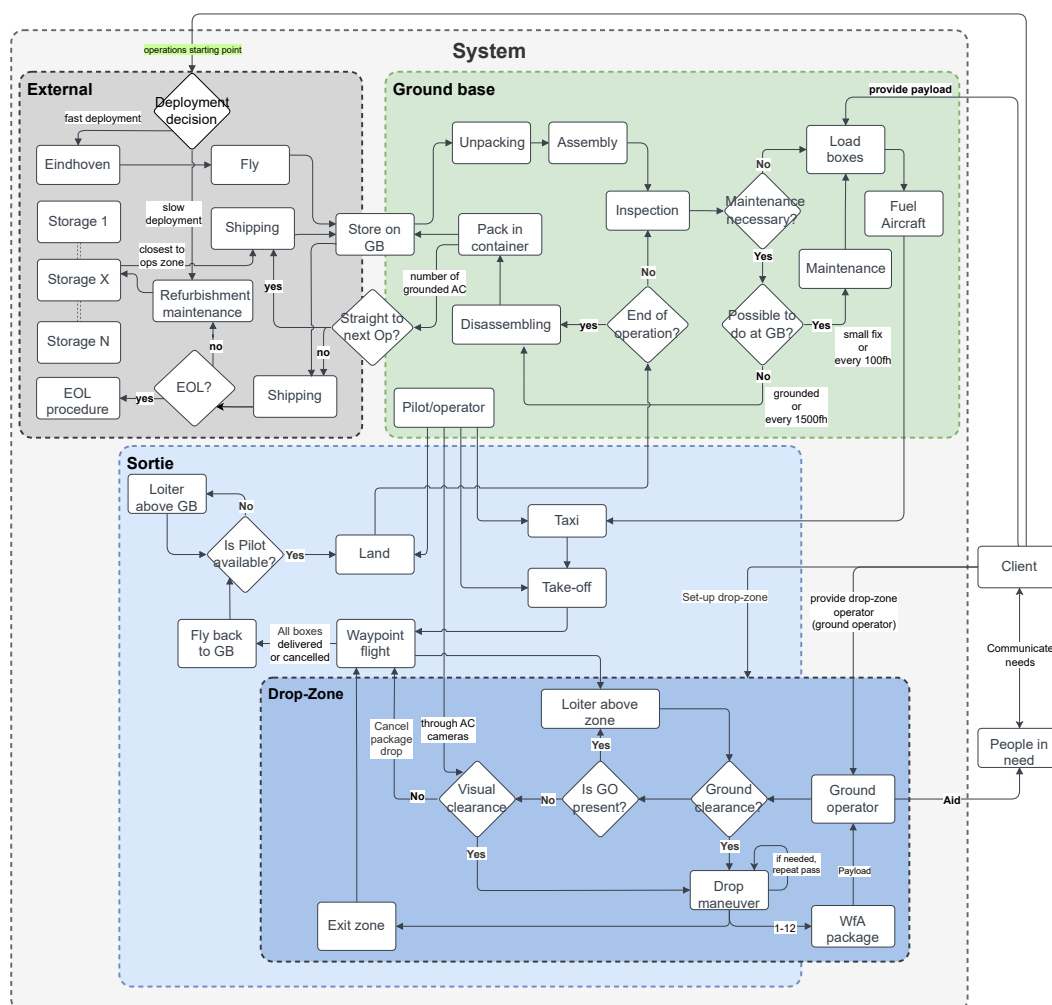


Figure 4.1: Schematised representation of operations' logistics

The starting point of the operation is on the left of the figure when the decision is taken to deploy the Wings for Aid aircraft in the regions affected by a disaster. To provide aid as soon as possible, fast deployment will

be used by flying over containers with disassembled aircraft to the ground base. The remaining aircraft will be shipped over to the ground base which will take significantly longer.

Once containers reach the ground base, the container will be unpacked and the aircraft will be assembled. The two most important parts of the assembly will be the assembly of both halves of the main wing to the fuselage and the horizontal tailplane to the boom. After assembly, the aircraft will be inspected carefully. If necessary maintenance has to be performed on the aircraft, it is done either at ground base if possible or at the facilities. Once the aircraft is ready to be loaded with boxes and fueled. Once the aircraft is completely loaded and fuelled and a mission profile is selected, the aircraft is ready for take-off.

The aircraft will take-off from the runway that is available at the ground base. It will then climb towards cruise height and fly autonomously by waypoint flight. Once the aircraft gets near the drop zone, it will request ground clearance from the ground operator to drop the boxes. If clearance is given, the aircraft will start the dropping manoeuvre and it will drop the boxes in the dropping zone. The process is repeated until all boxes are dropped. Once close to the ground base again, the control of the aircraft will partially be taken over by a pilot to perform the landing.

4.2. Ground Base Layout

In order for the operations to go smoothly, the ground base is essential. Some necessities are already at the ground base and do not have to be brought in by Wings for Aid. These include, but are not limited to, the ground staff, a runway (this can be anything from a grass field to a gravel road), fuel and oil for the aircraft and the payload to be delivered.

Other essentials will have to be transported to the ground base by Wings for Aid. Other than the aircraft themselves and the empty cardboard boxes, there are more things necessary to smoothly run the ground base. Starting with the pilot, it will be able to control the aircraft from the ground base. In order to do this, a control system is also brought in. The 40 ft ISO containers, in which the aircraft and other equipment are shipped, can be used as dry and safe rooms from which the operations can be controlled. Next to this, tents need to be available at the ground base to protect the aircraft. Finally, the carts described in Section 4.3 along with spare parts and tools will be shipped with the aircraft inside the containers. This is further explained in Section 3.1.1.

4.3. Box Loading

A big part of the operation is dropping the boxes filled with aid. To get the boxes inside the aircraft, some steps need to be taken beforehand. When the containers arrive at the ground base, and they are unloaded, the empty and folded boxes are taken out. These are subsequently folded into the correct shape and filled with aid. Once filled with aid, the weight of the boxes ranges from 13 kg (3 kg of the box and 10 kg payload) to 23 kg.

To transport the boxes from the filling station at the ground base, to the aircraft, they need to be moved. There are a multitude of ways to transport the boxes from A to B. The most logical of these is to use a cart. Because of the possible rough terrain, the cart needs to be very stable. A trade-off was made between six different types of trolleys. The criteria analysed in the trade-off are the weight, cost, balance and, if applicable, the amount of force needed to increase the height of the cart. It was decided that a cart with adaptable height is most effective, as the boxes can be put on the cart at a different height than they will be, when put in the aircraft. This minimises the force needed to lift the boxes. At the maximum payload of 20 kilograms, this is a significant practicality for the workers on site. In the trade-off, the most important aspects are the cost and stability. From this, the results were that a single scissor cart is the most applicable for these types of operations.

Once the boxes are folded and filled with payload, they are put on the trolley and rolled towards the aircraft. The height of the trolley is then adjusted for the loading bay and the carts are pushed into the belly of the aircraft. Once they are in the correct spot, a pin is taken out, which will allow the hatches to open when the signal is given. Finally, the loading bay doors are closed, and the trolley is rolled back for new boxes to be loaded.

Some operational limits should be considered to prevent tipover and ensure stability regardless of the

payload: boxes are always loaded from the front to the back. In case the packages are unevenly loaded ($15 \pm 5 \text{ kg}$) the lightest should be stored in the back. Dropping done from back to front according to Section 5.7.

4.4. Operational parameters

The approach taken to estimate cost, time and performance over an operation are driven by choices made at an operation level. These are left as parametric values that can be changed depending on the desires of the customer, delivery conditions (disaster, conflict, commercial use) and logistics decisions. Default values are defined in parentheses such that a comparison can be done consistently throughout analyses.

- Payload delivery rate (20,400 kg/day): the amount of payload that is to be delivered by a fleet. This defines the number of aircraft to be sent as explained in Section 14.4.3.
- Payload mass per package (20 kg): the maximum load of a box is used, any lower value would thus take a cost/kg penalty.
- Number of packages per drop (2): the wings for Aid concept's main strength is the combination of a high payload capacity and high accuracy and resolution in the packages delivered. The possible range is limited by the aircraft's design: an operational limit is set at a minimum 2 boxes per drop such that there is no transverse weight shift and a maximum of 6 in order to allow the boxes to deploy their brakes and flaps without interfering with each other on descent.
- Number of aircraft produced (500): a higher number would require higher initial investment and yield a cheaper aircraft on average thanks to the economies of scale discussed in Figure 14.2.
- Number of concurrent operations (2): determines the required number of ground base equipment sets to be produced and stored as well as the minimum number of aircraft that need to be ready at any given moment.
- Number of harbour storage locations (5): this variable is mostly defined by the World Food Programme and Red Cross accommodations of the project. More storage locations reduce the delivery time of aircraft to the disaster area. A privately owned storage can be considered in the case of a commercial use of the UAV.
- World coverage in 72 h (100%): determines the maximum distance to be covered by the shipping containers between contracting and start of operations.
- AC shipped by air (2): the number of aircraft that are sent to the disaster location via C130 (or similar) for first response deliveries and ground crew training.
- AC per ship (20): determines the size of each shipment of aircraft delivered to the ground base. The time between shipments is such that all previous AC are assembled and operational.
- Operation duration (28 days): The duration of an operation is critical to the cost of an operation as the shipping and setup costs are fixed. Disaster reliefs can range from 4 weeks to a year of aid delivery.
- Storage time (30 days): The time between operations during which the UAVs are not generating any revenue. This is somewhat outside of the company's control since they are contracted when disasters happen but it can be changed by deciding to turn down smaller, less profitable ventures (higher storage time) or by using aircraft in private operations for non-aid cases.
- MTBM (100 fh): the mean time between maintenance (in flight hours) define the interval between small fixes on each UAV - oil changes, filters cleaning, general health check - and is a trade-off between recurring costs and unplanned failures occurring.
- MTBO (1500 fh): similarly, the mean time between overhaul defines the interval between large and costly refurbishments of the airframe.
- MTTR (30 h): the time between a failure or deficiency is detected on an aircraft and the point at which it re-enters the operational fleet. A smaller number increases the fleet efficiency but increases running maintenance costs as a larger team is needed to keep up with the inspections, diagnostics, parts orders and repairs.
- Operational Lifetime (5,000 fh): amount of flight time an airframe is allowed to do before being retired or refurbished. Given a fixed design, increasing the lifetime will increase the end-of-life failure rate while decreasing it will reduce the number of operations possible with a set number of UAVs and thus increase the cost.

Flight Performance

This chapter presents the methods and results of the assessment of the flight performance of the conceptual design. This covers take-off, climb, cruise, descent, and approach and landing that are discussed in Section 5.1 to Section 5.5 consecutively. These performance figures determine operating capabilities which can be checked against requirements to see whether the design lives up to them. Afterwards, the total sortie performance and the dropping manoeuvre are analysed in more detail in Section 5.6 and Section 5.7.

5.1. Take-off

The sizing the control surfaces depends on the highest value of $C_{L_{max}}$, the maximum lift coefficient, needed for take-off, landing or cruise. In this section, the method used to determine $C_{L_{max}}$ for take-off is presented. The method is taken from lecture slides of the course for Flight and orbital mechanics - take-off and landing [13]. Multiple conditions are taken into account to satisfy all user requirements as shown in Section 2.3. The aircraft will be designed for a certain runway slope, headwind, tailwind and airport altitude. In case of headwind facing the aircraft, the lift and drag will increase due to the increase of airspeed of the aircraft which is integrated in the equations of motion with the air speed calculated as shown in Equation 5.1.

$$V = \frac{\sqrt{V_{LOF}^2 + V_{wind}^2}}{\sqrt{2}} \quad (5.1)$$

The V_{LOF} is lift off speed in for take-off, which is 1.05 times the stall speed [13]. It is important to note that tailwind has a negative effect on lift and drag, which means it causes their magnitude to go down, Equation 5.1 becomes as follows:

$$V = \frac{\sqrt{V_{LOF}^2 - V_{wind}^2}}{\sqrt{2}}$$

To incorporate the wind speed in the calculation of runway needed to decelerate the aircraft, the correct ground speed has to be considered. The correct integration form is shown in Equation 5.2.

$$S = \int_0^{V_{LOF} - V_{wind}} V dt \quad (5.2)$$

For all cases the runway friction coefficient considered is of the worst case scenario, which is with the highest friction coefficient of 0.08 on wet grass for take-off [14, p. 564]. After iteration, the result showed that a $C_{L_{max}}$ of 1.42 for take-off is enough, and the aircraft will take-off with a C_L of 0.41. Which means no extra high lift devices are needed for take-off since this value is the same maximum lift coefficient as for the clean configuration.

The transition distance is also calculated to secure the take-off. This is done by Equation 5.3[13]. The result is 28.54 m, with a climb angle of 3 degrees considered.

$$X_{trans} = \frac{V_{LOF}^2}{0.15g} \sin \gamma_{climb} \quad (5.3)$$

Figure 5.1 shows the plots of the runway length required for each of the restriction conditions designed for.

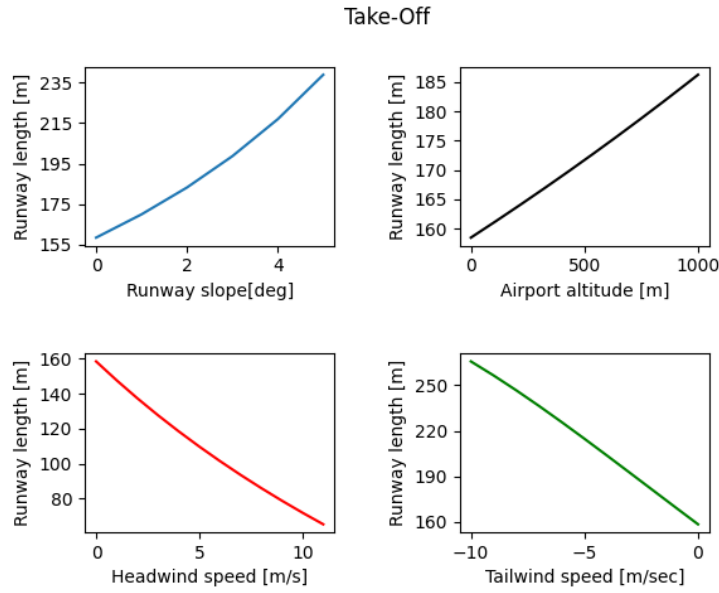


Figure 5.1: Runway length required for take-off for different conditions

As can be seen in Figure 5.1 the runway length needed for acceleration to take-off with nominal conditions; is approximately 160 m.

The trend for runway slope and airport altitude graphs are increasing, which is as expected since the weight will be acting as a drag force when there is a positive slope. In the case of higher airport altitude the air density goes down which effects the lift, but the effect in the first 1,000 m is not very significant and as can be seen in Figure 5.1 the runway length only increases about 30 m. A value of 1,000 m is taken because 85% of airports over the world are below 1,000 m altitude¹. When the aircraft is facing headwind, the required runway length goes down. That trend comes from the fact that the airspeed is higher than the groundspeed when the aircraft encounters headwind. The increased airspeed helps the aircraft take off with less distance. As is visible in the figure, the runway length goes down to about 65 m with headwind of 11 m/s. The value reaches this low because the headwind considered is about 40% of the take-off speed, normally the headwind speeds considered are close to 10% of the take-off speed. A rule of thumb says that 10% headwind w.r.t lift-off speed decreases the required runway length by 20%. This is also the case for this design. The last aspect to look at is in case of tailwind present. Tailwind has the opposite effect of headwind, decreasing airspeed w.r.t groundspeed. Because of this, an increase in tailwind causes an increase in ground roll length. The maximum tailwind considered is 11 m/s as being a reasonable value to design for.

In conclusion, with the addition of the transition distance to the ground accelerating distances shown in Figure 5.1 and a contingency of 5%, the requirement of a runway length of 750 m is comfortably met.

5.2. Climb Performance

This section presents the climb performance of the conceptual design and the methods used to determine it. As the aircraft is aimed at operating with the lowest cost possible, it should operate as efficiently as possible. This means minimizing the power per unit weight and maximizing the surface area of the wings per unit weight. Because of this, in terms of flight performance, the climb angle will remain small. This is an important assumption in the assessment of the climb performance. Because of the assumption made, the climb rate can be expressed as in Equation 5.4.

$$ROC = \frac{P_a - P_r}{W} \quad (5.4)$$

The climb rate is calculated from sea level up until the service ceiling. The service ceiling is defined as the altitude above which the climb rate is lower than 100 ft or 0.5 m/s [15]. The service ceiling of the aircraft is

¹ Airports altitude over the world

equal to 20000 ft with a contingency of 1000 ft. The climb rate as a function of altitude, altitude as a function of time and weight as a function of time are shown in Figure 5.2.

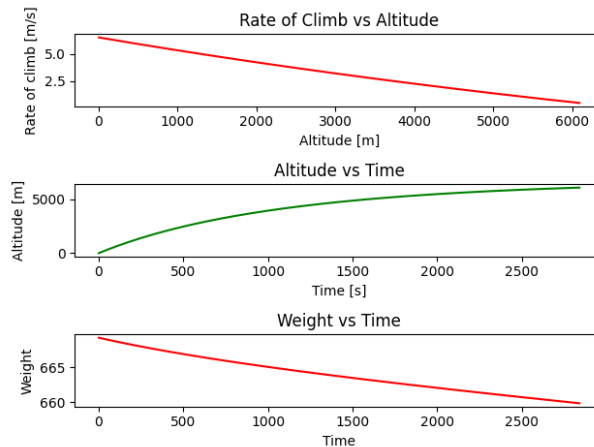


Figure 5.2: Climb performance of the aircraft as function of time

5.3. Cruise

The cruise phase for this aircraft is a fuel-intensive phase, meaning it has a large effect on overall performance. The Wings for Aid UAV will encounter many different cruise scenarios. These scenarios depend on the range for a specific sortie, the number of drops that are performed and the spatial density of the drops. Namely, the last one dictates cruise distance and cruise altitude. At lower altitudes and shorter cruise distances, it is more fuel-efficient to fly slower. Operations-wise, a trade-off has to be performed between fuel efficiency and cruise speed. A higher cruise speed will decrease sortie time and thus payload rate at a higher cost in fuel.

An important figure for the cruise performance is the fuel mass used per kilogram of payload delivered per kilometre flown. For the design, this figure lies around 0.00056 1/km. It should be noted that this is calculated using the operational range of 250 kilometres. This choice is made as the boxes are only carried over the operational range. This figure is dependent on the flight profile. Total sortie fuel lies between 38 and 43 kg of fuel per sortie. At moderate speeds, multiple drops are nearly as efficient as dropping only one time as the possibilities of a high, fast and fuel-efficient cruise are not used to the full extent. At higher speeds, it is visible that dropping only once is more efficient.

5.4. Descent

When descending from a certain altitude, the rate of descent and descending angle are important to know. The approach is the same as for climbing except that the angle and rate of descent are now negative due to the power required being higher than the power available. The results are shown in Figure 5.3.

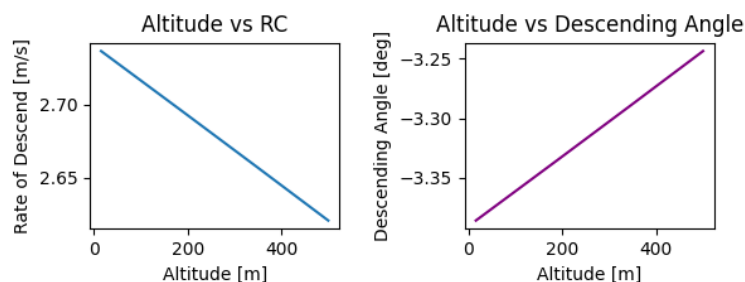


Figure 5.3: Descending rate and angle as function of altitude

5.5. Approach & Landing

The landing phase starts when the aircraft reaches the screen altitude, which is 15.4 m, and lands at 3 degrees, with an approach speed of 1.2 times the stall speed [13]. The approach for calculation the landing distance is the same as for take-off except that there is no thrust in landing (the throttle is set on idle). In this design there will be no negative thrusters that work to slow down the aircraft. Another difference from take-off is the friction coefficient, which is now a higher value that takes into account braking of the wheels. To design for the worst case scenario, the lowest friction is taken with a value of 0.2 for wet grass [14, p. 563].

The equations presented in Section 5.1 apply for landing as well, now the lift off speed, V_{LOF} , is the touchdown speed which is 1.2 times the stall speed [13]. Figure 5.4 presents the plots of the runway length required for each of the restriction conditions that it is designed for.

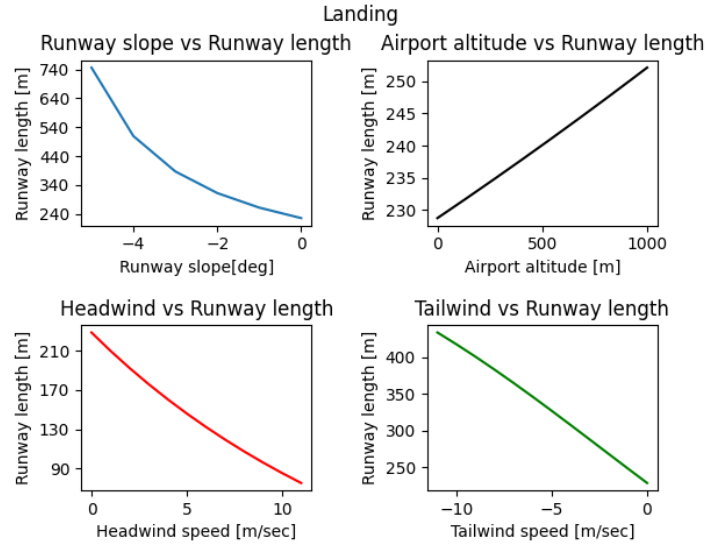


Figure 5.4: Runway length required for landing for different conditions

As can be seen in Figure 5.4, the required runway length in nominal conditions is approximately 225 m. Nominal conditions means no wind, no runway slope and landing at an airport at sea level.

When the aircraft lands on a runway with a downwards slope, the required runway length is longer. This is due to the weight acting in the direction of travel. The maximum downward slope for which the aircraft can adhere to the requirement of 750 m runway length is 5 degrees. If the airport is situated higher than sea level, the air density is lower. This causes a higher required approach speed which increases the landing distance. For the same reason mentioned in Section 5.1 it is designed for airport altitudes up to and including 1,000 m. When the aircraft has to perform a tailwind landing, the ground speed is higher than the airspeed. This also increases the required runway length. The UAV is designed for a maximum tailwind of 11 m/s, which is a reasonable value to cope with. The presence of headwind has the opposite contribution compared to a tailwind landing. 11 m/s is also used as a maximum value for headwind. At sea level, this wind speed is around 50% of the touchdown speed. Because of this, the required runway length for landing in these conditions is very low. The aircraft would only have a groundspeed of around 40 km/h. Another explanation for the steep reduction in runway length with the presence of wind, is the very low weight of the aircraft which at landing is almost half of the take-off weight in case all 12 boxes are dropped. If there still are two boxes on board when landing then the runway length with 11 m/s headwind is around 90 m. This is 15 m increase, which is significant. The transition distance for landing is 23.2 m from Equation 5.3. Considering all factors, with a contingency of 5%, the requirement for the runway length of 750 m is comfortably met with $C_{L_{max}}$ 1.42, which is the maximum clean configuration lift coefficient, and landing at C_L of 1.35, except for a slope of -5 degrees. The aircraft is designed with high lift devices. These may not be necessary for some landing cases. Including them in the design, however, increases the operating capabilities of the aircraft, allowing it to land on shorter runways. This is not unusual and is also seen in general aviation aircraft, which also do not need to deploy high lift devices to meet certain runway lengths.

5.6. Sortie Performance

The overall performance over a sortie was assessed using a simulation of the sortie. The flight profile was defined based on the distance to the furthest drop, the number of drops and a possible drop region. Possible flight profiles are shown in Figure 6.1.

The flight simulation is aimed at finding the fuel used during the sortie. This is based on cruise height, cruise speed, range to furthest drop, the number of drops, the number of boxes that are loaded and whether a drop region is defined. If a drop region is not defined, the drops are assumed to be evenly spaced. For the climb phases, the aircraft flies at the optimum climb speed. This is the situation where $\frac{P_a - P_r}{W}$ is the largest. The C_L connected to this situation is equal to $\sqrt{3C_{D_0}\pi Ae}$. For the cruise phase, the speed can be varied to see what the effect is on fuel consumption and sortie time. In the descending phases, the power is set to idle and the aircraft flies at $(\frac{L}{D})_{max}$. In this situation, the C_L is equal to $\sqrt{C_{D_0}\pi Ae}$. Throughout the simulation, the fuel flow is calculated based on the power setting at that moment. For climb, 100% power is used. For cruise, the required power is set and for descent, the power is set to idle. The weight of the aircraft is continuously updated. At the dropping points, the aircraft weight is lowered by the number of boxes dropped times the weight of a single box. This is equal to 20 kg of contents and 3 kg of the weight of the box itself.

5.7. Drop Maneuver

Once the aircraft has reached its designated dropping point, a drop manoeuvre has to be performed in such a way that it ensures the requirements on zone size (25x25 m) and impact velocity (95% probability of landing under 50 kph). These requirements apply to the complete operational envelope, i.e. for conditions variations of the box mass (10-20 kg payload +3 kg box), wind speed (0-15 m/s), wind heading (0-180°) and the number of boxes (1-12).

In order to verify this, the box is simulated as a point mass with varying drag over time following the brake and flaps opening. The reference frame is defined with X+ in the direction of flight and Z+ upwards, right-handed. The origin is the position of the aircraft at the moment of release, projected to ground level. The manoeuvre currently used by Wings for Aid, level flight at minimum altitude (15 m) and drop speed limit (50 kts) is defined as the "reference" manoeuvre. Assuming the UAV can also simulate Figure 5.5a and drop at such a time that it hits the center of the dropzone, Figure 5.5b would be the possible zone the package drops in.

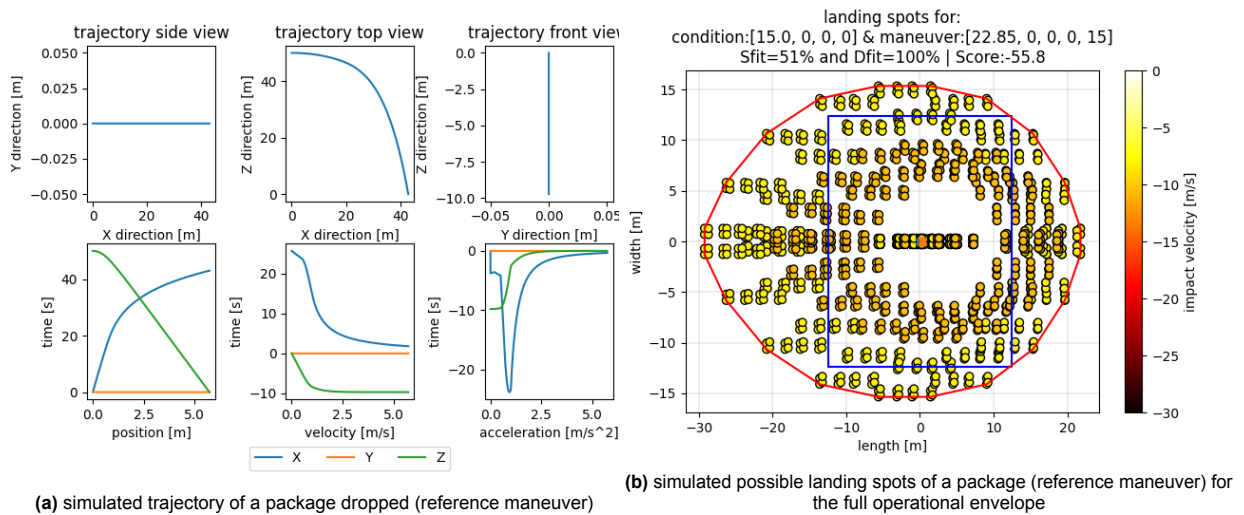


Figure 5.5: Initial results of a standard drop maneuver

A first mitigation measure is to use the aircraft's instruments in order to estimate the environmental conditions such as wind speed and heading. This can be done either by using meteorological data broadcasted from the GB or on-board estimations using GPS and flight dynamics behaviour. However, some uncertainties will remain (assumed 5%, or 2-sigma certainty) along with deviations inherent to the box such as hatch, brake and flaps timings which are outside of the system's control. Computing the resulting landing zone by adding

each combination of uncertainty results in Figure 5.6.

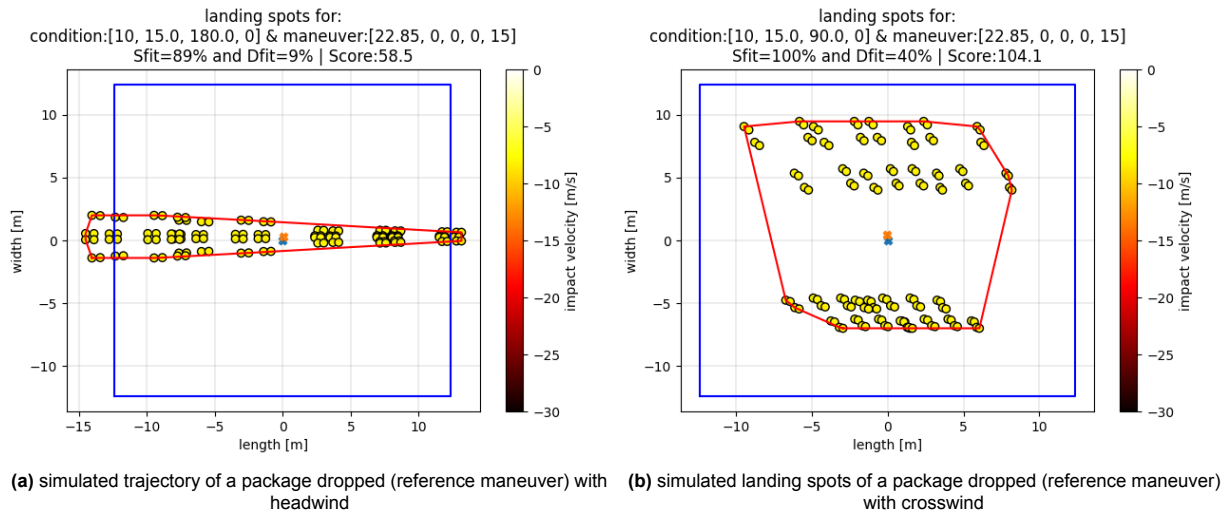


Figure 5.6: Mitigated drop results with active guidance and navigation assistance in determining the conditions

The expected zones computed for all conditions combinations using this GNC assistance are in Figure 5.7a. Additional improvements can be made by executing more aggressive manoeuvres such as reducing the drop altitude to a hard-deck of 15 m or dropping in a dive or at an angle. A number of manoeuvres were tried and evaluated based on technical performance measures (TPM) where a score above 100 meant requirements was passed, the best manoeuvre was chosen per condition and its envelope was added to Figure 5.7b. It used the following criteria and weights:

- Requirements passed(100): fits within drop-zone, lands under maximum impact speed.
- Drop performance (10): accuracy, impact speed.
- Aircraft (40): load factor, approach pitch and speed in the manoeuvre.

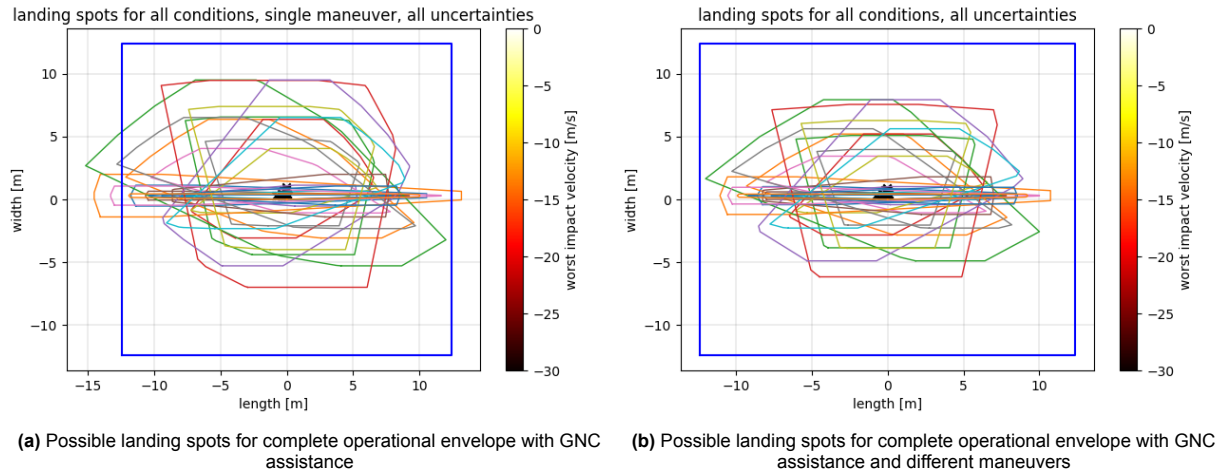


Figure 5.7: Final mitigation ²

Finally, in cases where the payload is dropped multiple boxes at the same time, a delay between each drop needs to be added such that the flaps opening do not interfere with each other. This obviously leads to a landing zone much larger than the required 25x25m but allows for a higher payload rate (kg/day) since a single drop pass is needed. Wings for Aid [W4A] has determined through drop tests that 0.5 s is a safe delay. The resulting envelope for such a drop would be similar to Figure 5.6 (no approach angle allowed) but stretched out about $= V_{AC}(N_{boxes} \cdot \Delta_t) \approx 22.85(12 \cdot 0.5) \approx 140$ m.

Propulsion Subsystem

An engine and propeller selection is a very wide and long procedure because of the big market and many different options. Due to the time limit that the project is restricted by, extensive and detailed research is not possible, thus the suggested engine by the cooperative company Wings for Aid, the Rotax 912, is considered first. Further options for engines are looked into and investigated in Section 6.1. Following is the propeller selection, done by analysing the number of blades needed and propeller type that serves best the design purpose presented in Section 6.2.

6.1. Engine Selection

A driving requirement of the project is the cost of one aircraft, which is bounded by a maximum price of €25,000 as can be seen in Section 2.3. Looking at new certified Rotax 912 iS engine, the price reaches €25,090¹. Which is very high considering the budget limitation. An alternative is a non-certified engine, which is applicable since certification of the aircraft is not required. The price of a new non-certified Rotax engine of 80 hp, Rotax 912 UL, is €17,485¹. From preliminary Class I and Class II estimation, the aircraft will need 95 hp. The 100 hp non-certified Rotax engine, Rotax 912 ULS, reaches a price of €21,403¹. Because of the power required and the high cost with a limited budget, further research is conducted to check for the option of an alternative engine that meet the requirements but for a lower cost.

From the research, four alternatives have been found:

1. Used 100 hp Rotax engine
2. Jabiru 3300 engine
3. UL260 Power
4. Lycoming O-235

Table 6.1 summarises the properties of the engines looked into, they are to be compared so that the most suitable option can be chosen. The type of fuel that the engines take is not included in this table. All engines can operate on AVGAS (100LL) or petrol (RON95).

²Rotax 912 characteristics

³Rotax 912 fuel consumption

⁴Used Rotax 912 cost

⁵Jabiru 3300 characteristics

⁶Jabiru 3300 fuel consumption

⁷Jabiru 3300 cost

⁸UL Power 260 characteristics

⁹UL Power 260 cost

¹⁰UL Power 260 fuel consumption

¹¹Lycoming O-235 Characteristics

¹²Lycoming O-235 cost

¹³Lycoming O-235 fuel type

¹Rotax engine prices

Table 6.1: Properties of engines included in the research

	Rotax 912	Used Rotax 912	Jabiru 3300	UL260 Power	Lycoming O-235
Power [hp]	100 ²	100 ²	120 ⁵	107 ⁸	115 ¹¹
Weight [kg]	56.6 ²	56.6 ²	83.5 ⁵	72.3 ⁸	109 ¹¹
Speed [rpm]	5800 ²	5800 ²	3300 ⁵	2800 ⁸	2800 ¹¹
SFC [l/h]	12.3 ³	12.3 ³	18.93 ⁶	13 ¹⁰	27.63 ¹¹
Cost [€]	17,485 ¹	6,843 ⁴	10,658 ⁷	20,386 ⁹	22,395 ¹²

Used 100 hp Rotax engine

The cost of used engines is not constant, it depends on its flight hours, condition, and of course the shipping cost. But resulting from the research, the price averages around €6,843, which is less than half of the new engine price. Furthermore, there are used engines that are for this low price and certified⁴. This is a cost-efficient option which can get important if competitor companies enter the market and manufacture certified aircraft, which is obviously favourable over non-certified ones.

This option also has its disadvantage, which are as follows:

- Limited number available on the market
- Inspection on the engine is needed before implementing in the aircraft
- Shorter lifetime

Even though the used engines need a check-up before using them, the cost of the check-up and condition evaluation will for sure be less than the cost difference compared to a new non-certified engine. The engine bought will have papers with documentation of maintenance and condition, which makes the process of evaluation easier and quicker. The shorter lifetime of the used engine is less of a problem because of the lower-than-usual reliability and higher risk of crashing of the aircraft. While the limited number of used engines, especially certified engines, is the biggest problem. For that, the option of used engines has to be prioritised and when this option is not available anymore, a new non-certified engine can be used. With this approach, thousands of euros will be saved when manufacturing larger amounts of aircraft.

Jabiru 3300

The Jabiru 2200 is an equivalent engine to the Rotax 912 but with 80-85 hp. As mentioned before, 95 hp is required, thus a more powerful version of the Jabiru engines have to be used, the Jabiru 3300 reaches the requirement of the power 120 hp⁵.

The main difference between the Jabiru 3300 and the Rotax 912 is the number of cylinders in the engines. The Rotax 912 is a four-cylinder engine, while the Jabiru 3300 is a six-cylinder engine which results in higher fuel consumption, this has to be taken into account in the detailed design of the subsystems to see if it is manageable. Even though it is heavier than the Rotax 912, with the extra weight of about 26.9 kg, the cost of a new engine, not original from the company, is €10,658⁷, which is significantly less than a new 100 hp Rotax 912 engine. The extra weight has again to be taken into account in the detailed design of the subsystems to see if the extra is manageable. Next to the cost difference between the two engines, the Jabiru engines are manufactured in Australia while the Rotax are manufactured in Austria. The certification of Jabiru engines depends on the specific type chosen; The Jabiru UL-D and J160-C are CASA certified (Civil Aviation Safety Authority), The J230D, J170-D, J160-D and J120-C are designed to CASA accepted ASTM standards for Light Sport Aircraft¹⁴. The Rotax is certified by EASA (European Union Aviation Safety Agency)¹⁵.

UL260 Power & Lycoming O-235

Further in the research, the UL Power engines are taken into consideration, in addition to the Lycoming engines. From the UL Power engines, an applicable option is the UL260 with 107 hp. And from the Lycoming engines, the O-235 is found to be the most applicable with 115 hp. The cost of the UL Power is relatively

¹⁴Jabiru engine certification

¹⁵Rotax engine certification

high, while the weight of the Lycoming is significantly higher than all the other options.

Research Results and Conclusion

As a result of the research the following can be concluded:

- The Lycoming can be ruled out because of its significantly higher weight than the Rotax 912. In addition to the high price, which doesn't solve the problem of budget limit.
- The UL Power engine has a good power-to-weight ratio, but just like the Lycoming, the price issue is not solved. Unless the company Wings for Aid has connections to find a distributor that sells for a lower price than the Rotax 912 price, in that case, this option is recommended.
- With the found distributor of the Jabiru 3300 that sells at a relatively low price, which is a positive point for the objective of budget requirement. Because of the fact that this engine has 6 cylinders instead of 4, it will have a higher fuel consumption, with the iteration in the design code it can be seen if the extra fuel needed is possible or not.
- The last option is the used Rotax 912 engines. This option is very recommended, because of the big price cut which helps to meet the budget requirement. The only uncertainty about this option is the flight hours left for the engine, which is not available information on the websites. Contact was tried to be done with the sellers, however, no response is received in the short time span available.

From the conclusions mentioned above and the iteration with implementing the different engines with their different weights, fuel consumption, and size, the result was opting for the used Rotax 912 100 hp engine as much as there is available, otherwise use the new non-certified Rotax 912 100 hp engine. With the recommendation of further investigation for the option of Jabiru 3300 and UL Power 260.

6.2. Propeller Selection

The current design of Wings for Aid has a four-blade propeller. An analysis is conducted in order to make a decision of what type of propeller matches the best and the optimal number of blades.

6.2.1. Number of Blades

The number of blades affects the efficiency of the propeller, noise, vibrations, ground clearance and stability. Table 6.2 shows the advantages of the number of blades to be chosen.

Table 6.2: Overview of different propeller type advantages (blade number)

Less blades	More blades
<ul style="list-style-type: none"> - Higher efficiency due to lower interference - Faster tips because longer blades - limits the RPM to not get to sonic speeds thus very high drag - Lighter - Usually used for under 300 hp 	<ul style="list-style-type: none"> - More stability - Less noise - Less affected by wind - Reduces vibration - Smaller diameter - thus better ground clearance - More thrust - More drag

Stability

From the requirement, the stability of the aircraft has to be the same as the Cessna 172 as discussed in Section 2.3. Looking at the Cessna 172, it has a 2-blade propeller, and from Table 6.2 it can be seen that more blades assure a higher stability, which means in terms of sufficient stability it does not matter if 2, 3, or 4 blades are used. On the other hand, too much stability is not desired since it affects controllability negatively, for that reason 4 blades might be over stabilising thus not the best choice.

Noise and Vibrations

Looking again at the Cessna 172, which is a piloted aircraft with a two-blade propeller, that means that the vibrations and noise of a two or three-blade propeller are definitely enough in terms of vibrations and noise, four blades are not necessarily needed for this purpose.

Clearance

The ground clearance can be a problem since the design has to be suitable for all types of runways as mentioned in the requirements in Section 2.3; paved, grass, gravel, unprepared, etc. which means that shorter blades will be a better option. Then from Table 6.2 it is seen that the more blades in the propeller the shorter they are. So for this purpose, three or four blades are a better option than two blades.

Efficiency

Table 6.2 shows that fewer blades are better in terms of efficiency. Since the current design of Wings for Aid has four blades, that shows that the efficiency needed for the mission of the aircraft is achieved by four blades, thus 2 blades are not necessary to get the efficiency desired.

Weight

Lower number of blades results in a lighter propeller, as shown in Table 6.2. The lighter the aircraft the better, which means two or three blades are a better choice than 4 blades.

From the arguments and discussion above, it has been chosen to opt for a three-blade propeller.

6.2.2. Type of Propeller

Three types of propellers are available to opt from: fixed pitch, controllable pitch - constant speed propeller, and ground adjustable. To choose which one fits the best to comply with the mission objective, a small analysis has to be done to know the advantages of each option.

In Table 6.3 the results of the research are presented.

Table 6.3: Overview of different propeller features advantages

Fixed pitch	Constant speed	Ground adjustable
- Low speed	- Controllable pitch	- Pitch adjustable manually when the propeller is not in use
- Limited range	- Adjustable for changing conditions	- Not seen in modern aircraft
- Limited altitude	- Usually for high performance aircraft	- Easier for maintenance and change since it has the clamping mechanism that connects the propeller to be able to adjust the pitch angle
- Performance affected under varying conditions	- Good for safety (which is not necessarily important for our case)	- Cruise speed is low so it is possible to optimize the pitch for take-off and climb, so that it will still be good enough for cruise
- Run more easily in problems due to vibrations		- Since the aircraft has to operate under different weather conditions, this allows efficient adjustment for an optimum climb and lower cost

Resulting from the research, the fixed pitch is not a good option because of the requirement to fly in different weather conditions as discussed in REQ-USER-OPS-04 and REQ-USER-OPS-07 in Section 2.3. Nevertheless, controllable pitch all the time during flight is not necessarily needed for several reasons:

- The dropping distance is within 250 km, in that distance the weather does not change significantly which means no need to change the propeller pitch.
- The most important phase of the flight is climb, since the aircraft has to operate in mountainous places

as well as flat places, and every time after dropping the aircraft has to pull up again to get back to cruise altitude. So if the propeller pitch is set to be most efficient for climb depending on the current weather, no controllable pitch is needed for during flight.

- As shown in Table 6.3, controllable pitch is usually used in high performance aircraft, which is not the case for this mission.

Because of the reasons mentioned above and the positive aspects of ground adjustable propeller shown in Table 6.3 and the results from the number of blades research, it is chosen to use a ground adjustable three-blade propeller.

6.2.3. Propeller Cost Estimation

To be able to choose a propeller, an estimation of the propeller diameter is required, which is done with Equation 6.1[14].

$$d = 1.5\sqrt[4]{HP} \quad (6.1)$$

From the primary design, the power required is 95 hp, which gives a propeller diameter of approximately 1.44 m.

Getting a price estimation for the propeller is tricky because of the lack of prices available on the internet. The available information is for very few propellers that are standard for engines. An attempt to get in touch with multiple manufacturing companies and distributors was done but no response was received.

Example for three propellers for which the price is available are:

- Rotax ground adjustable propeller, 3 blades, 1.65 m to 1.83 m, €2,400².
- UL Power ground adjustable propeller, 3 blades, 1.56 m to 1.66 m, €3,253³.
- UL Power and Jabiru ground adjustable, 2 blades, 1.52 m to 1.63 m, €2,455⁴.

Clearly the Jabiru propellers are more expensive, that is also because they are high-speed propellers, which is not needed for the case of this project. Since the propeller size is smaller than the Rotax, the Jabiru or the UL Power, the price will also be less. Thus the estimation will be in between the Rtoax and the UL Power, 3 blades, but closer to the Rotax, which means around €2,500.

6.3. Fuel Equipment Sizing

In order to get the weight and cost of the fuel management subsystem, the fuel consumption has to be computed for nominal missions, requirements, and contingencies. Section 5.6 is used to simulate the following:

- Nominal sortie: 12 packages with 20 kg of payload dropped in two manoeuvres at 250 km. This is the design case of the aircraft
- Low-altitude sortie: 12 packages with 20 kg of payload dropped in two manoeuvres with a ceiling of 500 ft. Such a mission can be required by the local authorities when flying a new aircraft in their airspace.
- High-altitude sortie: 12 packages with 20 kg of payload dropped in two manoeuvres with a minimum ceiling of 5000 ft. Such a mission can be beneficial in unstable regions where the aircraft may be shot down - flying higher reduces the probability of being hit.
- Scattered delivery: 12 packages dropped with 20kg of payload delivered with equal spacing over 250 km. This allows for private clients, tailored missions, and the possibility of higher ROI and revenue.
- Failed drop: in case the aircraft cannot, for some reason, drop the packages at the designated drop-zone and needs to fly back to GB, a sufficient fuel reserve will be needed. Follows the nominal case.
- Ferry range: following the requirement SYS-FR-FP-1.3, 1000 km ferry mission can be assessed to size the fuel tanks accordingly.
- Extended ferry range: replacing the boxes with fuel yields the extended ferry range of the aircraft. This assesses whether flying the aircraft to the GB could be an option.

²Rotax propeller, 3 blades

³UL Power propeller, 3 blades

⁴UL Power and Jabiru propeller, 2 blades

- Increased payload nominal: increasing the payload from 12 to 16 boxes, the results should be considered carefully as the aircraft is not redesigned for this step - simply increasing the carried mass. This assesses whether an extended fuselage version could be an option.

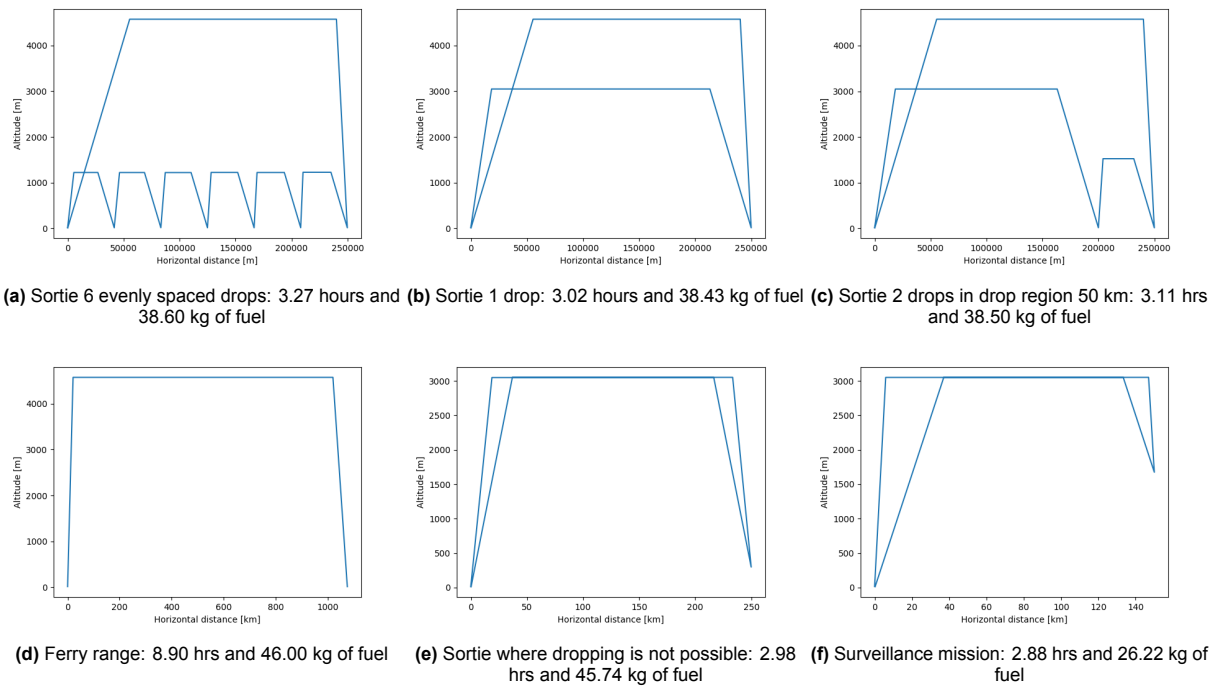


Figure 6.1: Mission profiles and fuel consumption for different cases

The minimum fuel needed to be capable of executing all profiles is 47.63 kg. This fuel consumption occurs when the aircraft arrives at a dropzone 250 km from the ground base but can not drop. This can be due to an unsafe dropzone or a faulty dropping mechanism. Using a margin of 5%, this yields around 52.5 kg or 70.00 L load. Sizing the fuel tank is done using linear-relation with respect to volume presented in Figure 6.2, using COTS data⁵⁶. The complete feed system including ignition, throttle, flow management, refuelling, venting, pumps and mixture control, are estimated, as a 1.25% fraction of MTOW [16], to be about 3.45 kg. Finally, some extreme profiles are assessed for future developments, using the chosen fuel volume as a basis.

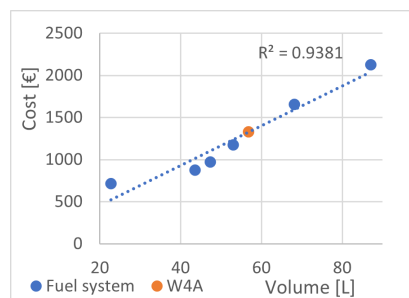


Figure 6.2: Fuel system cost estimation

⁵AircraftSpruce

⁶DakotaCub - fuel tanks

Fuselage Subsystem

In this chapter, the design of the structure of the fuselage is discussed. It will be discussed in two parts. First, the frame structure will be discussed in Section 7.1. In this section, the truss geometry of the aircraft is also presented. Then, also the structure of the outside fairing is sized in Section 7.2.3. Together, the frame structure and fairing structure will form the basis to which all other subsystems will be connected.

7.1. Frame Structure

The fuselage transfers and distributes all the loads in the aircraft, creating a load path for empennage, landing gear, payload, engine and onboard equipment loads. This chapter describes the design process of the fuselage and tail boom, from the concept selection, to the individual trusses thickness.

7.1.1. The Fuselage Concept

Three concepts have been evaluated in order to choose the lightest fuselage configuration: a load-bearing skin fuselage (Figure 7.1a) and two truss structure fuselages. One of the truss fuselages relies on a continuous spinal boom connecting the engine, wings and empennage (Figure 7.1b, spinal boom in blue), while the other truss fuselage distributes loads among multiple equally sized members (Figure 7.1c).

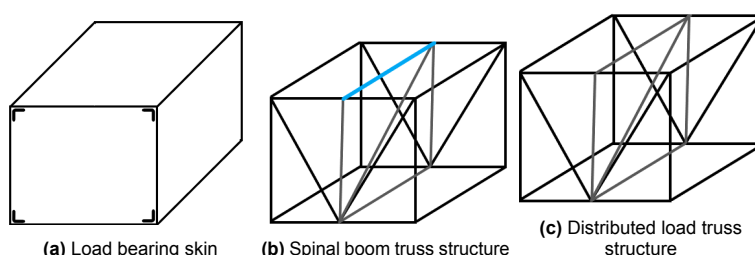


Figure 7.1: Three concepts of fuselage configuration in equally sized modules

In order to compare the mass-strength performance of the proposed concepts, loads imitating the ones induced from the wing structure in flight, payload load and landing gear are applied to modular, equally sized structures, as presented on Figure 7.1 and analysed analytically. The spinal boom is directly loaded with most engine and wing loads, in contrast to the distributed load truss structure. Column as well as compression and shear sheet buckling occurred as critical loads for skin and truss structure respectively, yielding a higher mass of the modules for a zero-lift loading scenario. The load-bearing skin module is outperformed by the truss structure, being approximately four times heavier in both loading scenarios. The spinal boom is lighter in flight conditions but heavier in zero lift conditions, however, the mass differences are hardly higher than 10%.

The simplified modular comparison of fuselage configuration aims at choosing the lightest concept, and not accurately determining the mass of the module. Once the arbitrary loads are applied to the structures, reaction forces have been calculated and subsequently minimum structural characteristics are derived, based on which mass can be computed. The simplified modular comparison concludes that a truss structure shall be used, which goes along the quantitative arguments of no cabin pressurisation needed together with a need of voluminous payload loading via large cutouts.

7.1.2. Truss Layout

The next step of the fuselage design is a quantitative trade-off between the trusses layout, the concepts of which are presented on a front view of the fuselage cross section on Figure 7.2. Truss connections are represented by circles, the spinal boom by a blue circle, main load-bearing trusses in black, while assisting trusses in yellow. Although not to scale, the boxes are drawn for reference in brown.

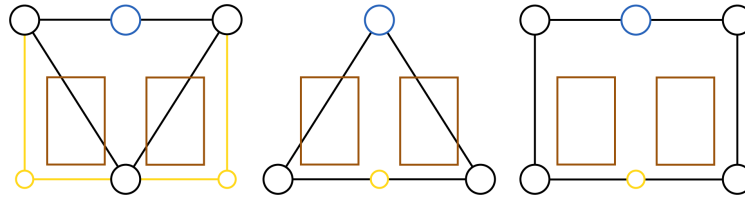


Figure 7.2: Front view of fuselage truss layout concepts

It can be observed, that the truss layout is related to how the wings are attached to the fuselage. The triangular truss cross-section (middle of the 3 options) favours an attachment of both detachable wings to the fuselage in a single pin, while the remaining two concepts allow the attachment of the wings to separate sides of the fuselage. The first concept from the left on Figure 7.2 is chosen, given the following advantages:

- Two pins available for wing attachment from both fuselage sides, easier for assembly
- Two pins available for wing strut attachment, easier for assembly
- Inverted triangular structure beneficial for stability

Since the wings are not connected to a single pin, the main advantage of the spinal boom disappears, leading to the choice of a distributed truss structure with the first left cross-section from Figure 7.2. The tail boom is therefore integrated directly into the fuselage structure, as the maximum storage dimensions do not implement a need to detach it (Chapter 4). Its length strictly follows from the control requirements described in Chapter 9.

The truss layout can therefore be decided upon, based on the payload geometry, with the assumption that the boxes are loaded from the side and dropped from the bottom of the fuselage. The engine mount is integrated into the structure and fits the Rotax 912 engine, which should be supported from the bottom at four points and incorporates a propeller ground clearance of 30 cm. Figure 7.3 shows the front and side view of the fuselage truss layout and tail boom, together with the dimensions. The geometry has been created as a line body in Ansys Design Modeler CAD, with the purpose to be used as input into the FEA program Ansys Mechanical (Static Structural). A brief assessment of the Ansys program is elaborated upon in Section 12.5.

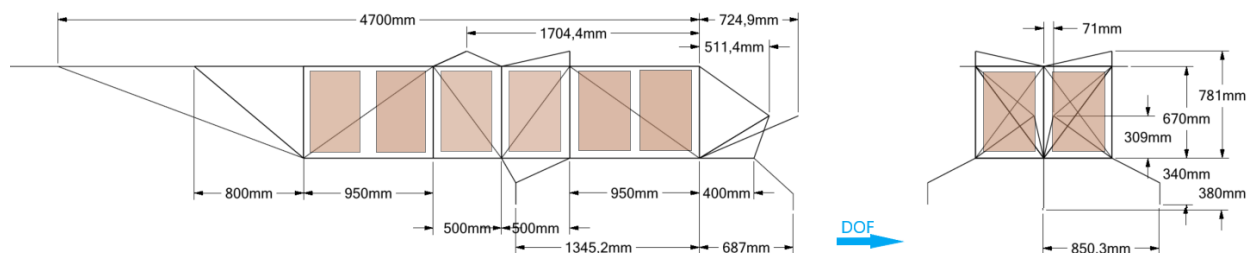


Figure 7.3: Geometry and dimensions of the fuselage, front and cropped side view with payload boxes for reference and indicated direction of flight

7.1.3. Critical Loading Scenarios

It is important to underline the assumption that the fuselage is treated as a truss structure, with every strut being a line body carrying either tension or compression loads. This implies that the connections of trusses transfer forces, but are not designed to transfer moments. On the other hand, the tail boom is idealised as a beam, carrying both forces and moments induced from the empennage. Although the tail boom (beam) is directly connected (via fixed connections) to the fuselage (truss structure), the behaviour of those elements is structurally different.

The proposed fuselage and boom geometry is exposed to critical loads, which are identified from the aircraft loading diagram Figure 3.7b as well as gust, maneuvering and landing impact loads as described in Certification Specification for Normal, Utility, Aerobatic, and Commuter Category Aeroplanes amendment 3 [17] and elaborated upon in the Standard Specification for Design Loads and Conditions [18]. The increment on the horizontal and vertical tail load ΔL_t (in lb) due to gust be estimated with Equation 7.1 [18, p. 6]

$$\Delta L_t = \frac{K_g U_{de} V a_t S_t}{498} \left(1 - \frac{d\epsilon}{d\alpha} \right) \quad (7.1)$$

where U_{de} is the derived gust velocity (25 kts), V the airplane equivalent speed (kts), a_t the slope of respective tail lift curve (per radian), S_t the respective tail area (ft²), $(1 - \frac{d\epsilon}{d\alpha})$ the downwash factor (1 for vertical tail) and K_g the gust alleviation factor, defined as follows [18, pp. 7–8, 3];

$$K_g = \frac{0.88\mu_g}{5.3 + \mu_g} \quad (7.2)$$

$$\mu_g = \frac{2(W/S)}{\rho c a_g} \quad (7.3)$$

Where W/S is the wing loading (psf), c the mean aerodynamic chord (ft), ρ the air density ((slugs/ft³), g the acceleration due to gravity (ft/s²) and a a slope of the airplane normal force coefficient curve.

The maneuvering aerodynamic horizontal tail load increment ΔP_h can be estimated by Equation 7.4

$$\Delta P_h = \Delta n M g \left[\frac{x_{cg}}{l_{t.arm}} - \frac{S_h a_h}{S_a} \left(1 - \frac{d\epsilon}{d\alpha} \right) - \frac{\rho_0}{2} \left(\frac{S_h a_h l_{t.arm}}{M} \right) \right] \quad (7.4)$$

where Δn is the load factor increment, M the aircraft mass, x_{cg} the longitudinal distance of aircraft CG aft of the aerodynamic center of aircraft less horizontal tail and $l_{t.arm}$ the tail arm, all in SI units. Because of the lack of explicit expression for manoeuvring vertical tail load increment, Equation 7.4 has been scaled by the ratio of vertical to horizontal tail gust loads defined by Equation 7.1. It has been observed, that the result of Equation 7.4 varies significantly with iterations, mainly due to changes in x_{cg} and $l_{t.arm}$. The final value used, estimated for boom and horizontal tail spar sizing is $\Delta P_h = 1987$ N.

Furthermore, the landing load factor n_{impact} has been estimated as the difference between inertia load factor $n_{inertia} = 2.67$ (minimum value) and landing $L/W = \frac{2}{3}$ [18, p. 11], with a single main wheel touch down at 0.95 MTOW. The nose wheel shall withstand a landing load of $n = 2.25$ [18, p. 12], while carrying 15% (requirement from stability and control, Chapter 9) of the 0.95 MTOW at landing. The engine torque load is applied at maximum power, scaled by a common safety factor of 1.5 [17, p. 1C1]. This leads to an application on the fuselage and tail boom of the critical load cases, summarised in Table 7.1.

Table 7.1: Summary of the applied critical loads on the fuselage and tail boom

n	Condition	Weight	Tail load	Engine torque
+6.67	in flight	MTOW	\pm maneuvering ΔP	1.5 T_{max} at P_{max}
-3.67	in flight	MTOW	\pm maneuvering ΔP	1.5 T_{max} at P_{max}
+2.0	single l.g. landing	0.95 MTOW	\pm maneuvering ΔP	1.5 T_{max} at P_{max}
+2.25	nose l.g. static load	0.15 - 0.95 MTOW	\pm maneuvering ΔP	1.5 T_{max} at P_{max}

It should be noted, that in flight load conditions are simulated by applying pre-calculated reaction forces from wings and struts (from the wing loading, see Chapter 8) on their points of attachment, while the "fix support" of the aircraft (treated as a free body) is the midpoint between the wing attachment. During the landing impact, the fix support is the attachment point of one of the main landing gear.

7.1.4. Fuselage Truss Geometry

Once all the critical load cases are applied, the compression or tension force can be computed in every truss member and their maximum absolute value is taken to size the truss cross section. Equation 7.5 and Equation 7.6 define the minimum cross sectional area A_{min} for tension and minimum moment of inertia $I_{xx,min}$ for column buckling of truss members, given a load P , yield strength σ_y and elastic modulus E .

$$A_{min} = \frac{P}{\sigma_y} \quad (7.5)$$

$$I_{xx,min} = \frac{PL^2}{n\pi^2 E} \quad (7.6)$$

Here, n is the clamping factor, chosen as 1 for the design (pinned ends). Since trusses are welded to each other, they could be treated as fixed on both sides ($n=4$)¹, yet because of non ideal conditions (structure deformation and potential weakness of weld), the conservative approach is taken with $n=1$. Figure 7.4 plots the A_{min} and $I_{xx,min}$ for the fuselage truss members. The tail cone and boom support beams require cross sections of an order of magnitude higher, thus have been omitted to facilitate comparison of lower load bearing trusses.

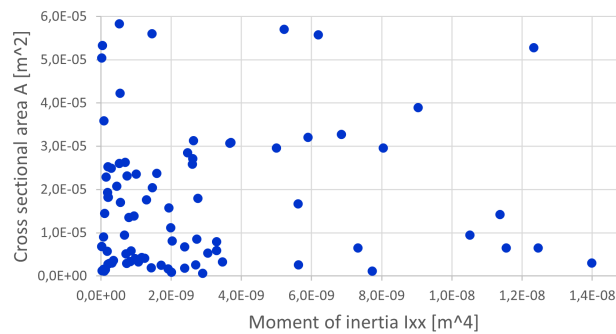


Figure 7.4: The minimum moment of inertia and cross sectional area of the analysed truss tubes, excluding outliers

Based on Figure 7.4, one can propose five different thin-walled tube geometries that can be used to assemble the fuselage, as listed on Table 7.2. Note, that this excludes the sizing of the tail boom, the geometry of which is described Section 7.1.5. Figure 7.5 pictures which tubes shall be applied to which truss on the fuselage, by applying a colour code.

Table 7.2: The cross-sectional definition of tubes used to assemble the fuselage

	Tube 1 (A)	Tube 2 (B)	Tube 3 (C)	Tube 4 (D)	Tube 5 (G)
A [mm ²]	37.7	66.0	101.8	150.8	226.2
I [mm ⁴]	$1.89 \cdot 10^3$	$7.43 \cdot 10^3$	$1.65 \cdot 10^4$	$4.35 \cdot 10^4$	$1.02 \cdot 10^5$
t [mm]	0.6	0.7	0.9	1.0	1.2
∅ [mm]	20	30	36	48	60

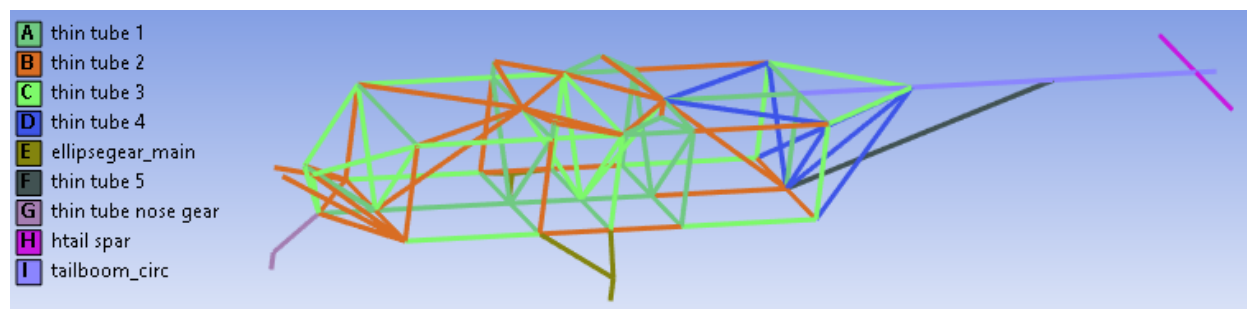


Figure 7.5: The layout of the tubes within the fuselage structure

¹The Engineering ToolBox - Euler's Column Formula, [cited on 26 June 2023]

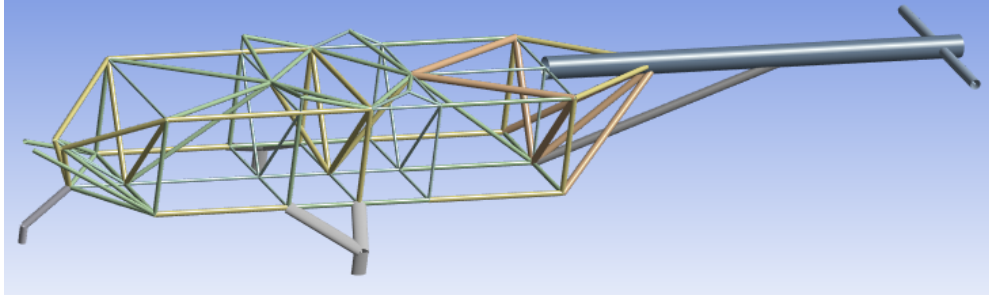


Figure 7.6: The actual shape of the tubes within the fuselage structure

The column buckling is most constraining for all trusses, with no exception, as all tubes are in compression in at least one of the loading cases. The tube diameter \varnothing shall thus be maximised for minimal mass, however the trusses should be thin enough to allow for payload loading and prevent interference with the systems. This is why a compromise has been made, limiting the maximum truss radius. Thickness t is rounded up to the nearest 1/10 mm, with a minimum value of 0.5 mm, which is also a design choice. The resulting fuselage mass is 45.0 kg.

7.1.5. Tail Boom Geometry

In contrast to the fuselage structure, the tail boom is treated as a beam. This means, it shall transfer not only axial forces, the sizing for which is described by Equation 7.5 and Equation 7.6, but also shear force F_s (Equation 7.7) and bending moment M_x (Equation 7.8). Similarly, the minimum cross sectional properties can be derived, however the distance from the bending neutral axis y is a cross sectional property, thus no explicit expression of $I_{xx,min}$ is available.

$$\sigma_{y,shear} = \frac{F_s}{A_{min,shear}} \quad (7.7)$$

$$\sigma_y = \frac{M_x y}{I_{xx,min}} \quad (7.8)$$

Since the tail boom is attached to the fuselage in three points (see Figure 7.3), it could be called statically undetermined. However, after performing a FEA simulation of all the load cases, the dominating reaction forces occur at the boom support truss (tube 5 (G)) and tail cone trusses (tubes 4 (D)), and thus the vertical reaction of the attachment of the boom to the fifth fuselage frame can be neglected. The forces used to define maximum shear force and moments are the horizontal (critical) and vertical maneuvering and gust loads, as well as structural weight given ultimate load factors, as defined in Table 7.1. The FEM program maximum axial force (maximum between both attachment, compression) and shear force (constant maximum between end and last attachment) as well as bending moment (maximum at rear truss attachment) outputs are used to determine the cross-section of the boom (see landing gear design in Section 10.3.1 for reference). The tail boom shall thus be made of a $t=1.4$ mm tube with a $d=15$ cm diameter. Figure 7.7 completes Figure 7.3 by a top view including the entire length of the tail boom. The horizontal tail spar sizing and geometry is elaborated upon in Chapter 9.

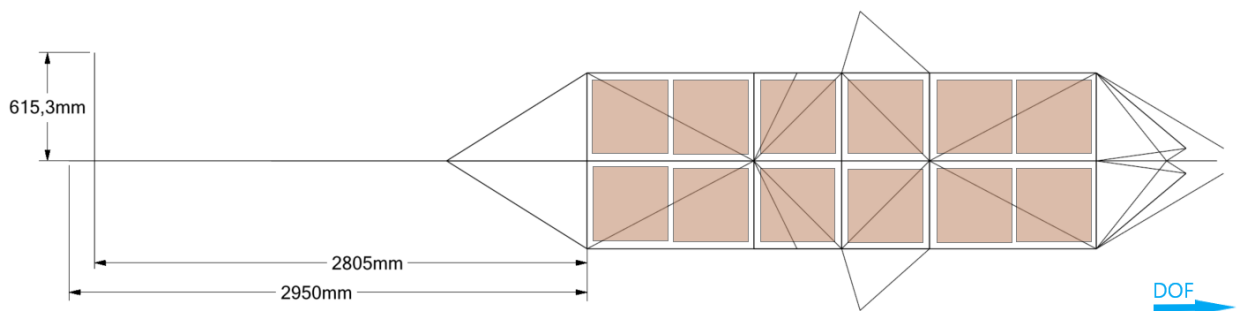


Figure 7.7: Top view of the fuselage, tail boom and horizontal tail spar with payload boxes for reference and the direction of flight indicated

7.1.6. Materials & Integration

The material choice is performed using the convention as described in Section 3.2. For the fuselage structure, the weights of material properties are: raw cost (4), ecological cost (1), CO₂ (0.5), fracture toughness (0.5), buckling material index (4), and tension material index (1). Given the buckling material index for lightweight design (most critical) is defined as \sqrt{E}/ρ and the tension one as σ_y/ρ , both of which should be maximised. This yields the material choice of steel 4130 for the fuselage.

For the tail boom, the critical failure mode is yielding by moment-induced stress, thus the most critical material index is σ_y/ρ , given a weight of 4, while the buckling material index is discarded. This yields the most optimal material choice of stainless steel 410. However, connecting by welding or bolts the boom to the fuselage creates a high risk of corrosion, therefore the default design assumes the tail boom is made from steel 4130, as the fuselage. As it is not stainless, both the tail boom and fuselage shall be painted to provide protection from the environment. An alternative tail boom design can be proposed, with the use of stainless steel 410. Because of a relatively high mass difference between the booms made of the two types of steels, Table 7.3 proposed alternative designs of the boom. The total length of the boom is $l_{boom}=2.95$ m.

Table 7.3: Summary of system's materials and masses with alternative boom designs

Structure	Shape [mm]	Thickness [mm]	Material	Corrosion	Mass [kg]
Truss fuselage	Circular tubes	-	Steel 4130	-	45.0
Tail boom	Tube \varnothing 150	0.7	Steel 4130	No	7.6
Tail boom	Tube \varnothing 150	0.3	S. steel 410	Yes	3.3
Tail boom	Tube \varnothing 150	1.2	Al 5052 H38	Yes	4.5

It should be noted that thickness values below 0.5 mm can pose a challenge for structural integration of the vertical and horizontal tail. The thickness might thus have to be artificially increased. Because the vertical tail induces less load than the horizontal one, an elliptical boom ($a=75$, $b=50$ mm) cross-section could be used, this allows for saving approximately 3 kg of mass. Aluminum 5052 allows for saving weight, however, is over twice as expensive as Steel 4130, which is why ranks lower than both steels in the material trade-off ranking. For future design steps, a detachable version of the tail can be considered, where aluminum use could be better motivated, together with an investigation of its attachment to the main fuselage. The aeroelastic behaviour of the integral tail boom and empennage should be addressed, preferably by numerical simulation or experimentally.

7.2. Outside Fairing

An outside fairing is constructed over the frame structure. This is mainly for aerodynamic purposes but also for protecting the payload from rain, wind and dust. The fairing design consists of sizing the shell and lofting. Sizing determines the length and diameter of the fuselage. Lofting is done to make the design more streamlined at fewer aerodynamic points such as connections.

7.2.1. Sizing

The fuselage sizing is split into three sections: The main section, where the payload is placed, the nose and tail section. For initial sizing purposes, it is assumed the nose section is an elongated semisphere, the tail a cone and the main section a circular connection. As mentioned in Section 7.1.2, the main section is 2.9 meters long and has a rectangular cross-section with height and width of 0.67 m and 1 m, respectively. The main section's sizing is mostly determined by payload requirements and is therefore rectangular. However, assuming a circular section makes calculations easier and an effective diameter is used to make sure the results are still accurate.

The nose and tail sections have more freedom in their design and have initial lengths of 0.8 and 0.9342 m. Furthermore, the sections are used to optimise the fuselage aerodynamically while keeping the weight low. The weight is considered through the wetted surface area (S_{wet}) as it is assumed the added weight is equal to S_{wet} multiplied by the thickness and density. The main aerodynamic focus is on minimising the zero-lift drag by choosing the length of the fuselage. The zero-lift drag is given by Equation 7.9. [19, p. 372]

$$C_{D_{0f}} = C_f f_{LD} f_M \frac{S_{wet_f}}{S_{ref}} \quad (7.9)$$

where C_f is the skin friction coefficient, f_M a function of airspeed, S_{ref} the wing reference area and f_{LD} a function of the total fuselage length-to-diameter ratio. Only this and the wetted area are functions of aircraft geometry. As the middle section's cross-section and thus effective diameter is known, only the length of the nose and tail sections have to be determined. In Figure 7.8, the fuselage zero-lift drag is plotted for variations of the nose and tail section. The left plot varies the nosecone length and the right varies the tailcone to separate their influences. Both plots have a red dot indicating the initial value based on structural requirements. The fuselage section cannot be made shorter than this point as there would not be enough storage space for the payload.

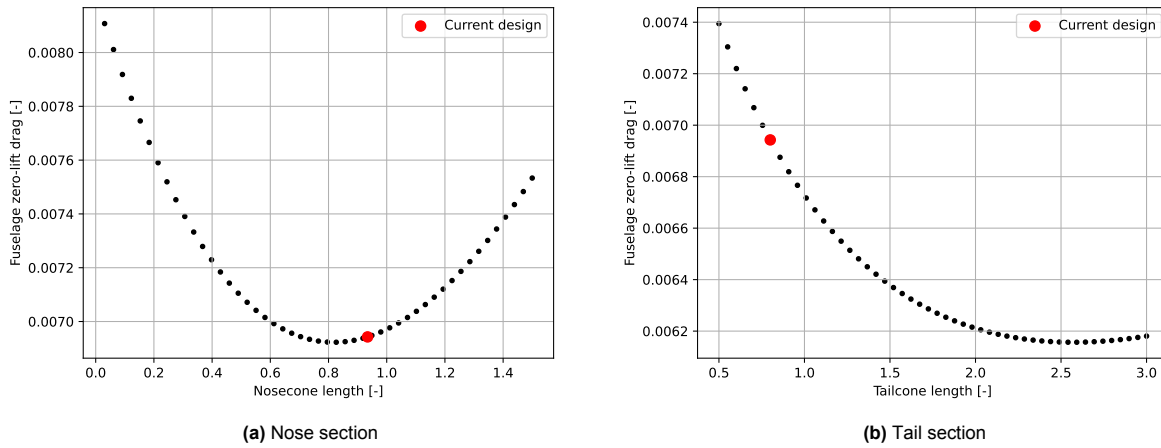


Figure 7.8: Zero-lift drag plotted as function of fuselage section length

In Figure 7.8, it can be seen that the design has a fuselage zero-lift drag of 0.0094. For the nose section, the initial length is already very close to the minimum drag obtainable. A small reduction is obtainable by reducing the nosecone length. This would impede on the required engine space and is therefore omitted. The tail section can benefit from getting extended from 0.8 to 2.6 meters. However, this comes with a large increase in weight as S_{wet} goes from 13.0 m² to 15.9 m². In fact, all attempts at reducing drag come with a significant weight penalty. It is thus decided to keep the fuselage length the same as the drag is already near its minimum value.

7.2.2. Lofting

Finally, lofting is applied at the least aerodynamic positions. The least aerodynamic sections and their respective lofting solution are listed below:

- The corners of the main fuselage section are made circular instead of sharp edges.
- The engine sticks out of the fuselage cross-section. The transition between engine and fuselage is made smooth.
- The struts attached to the fuselage for undercarriage and wing are made in an oval shape.
- The wing is attached to the fuselage with a smooth transition.
- The boom has a circular shape.

The sizing and lofting combine for the fuselage design as shown in Figure 14.3 where the final renders are displayed.

7.2.3. Fairing Structure

The fairing is designed to protect the payload from the external environment and withstand the aerodynamic loads. As it does not have to withstand structural loads, more freedom can be used in the material choice,

allowing for the transparency of the structure, thus the material is selected among thermoplastics, glass and GFRP. The glass fibre-reinforced plastic outperforms thermoplastics by being approximately 10 times as rigid, 5 times as tough in fracture, and 3 times as strong but 3 times as expensive while having a similar density. In order to guarantee transparency, a specific composition of the GFRP is required. The specific material properties presented on Table 3.2 in Section 3.2 are obtained by using a sol-gel derived cycloaliphatic epoxy-functionalized siloxane hybrid (EPSH) resin with short fiber (5 wt% of chopped strands glass fibers) and long fibre (10 layers of glass fabric) [20], allowing for high optical transparency (80% at 550 nm) [20].

The fuselage consists of three parts, the nose cone, main fuselage part and tail cone. While the nose and tail cone are mainly determined by aerodynamic efficiency, the main part fulfills a role of protecting the payload. Moreover, the sides of the main part should allow for the opening of loading doors to supply the aircraft with boxes. Six loading doors (hatches) are placed on the sides (three per side), each door (0.67 m × 0.95-1.0 m depending on the frame spacing) allowing to load two boxes, hinged horizontally on the top edge of the door panel. An indentation is needed in the first two rows of doors (boxes rows 1 to 4) because of the wing strut at the second frame, counting from the nose. Furthermore, the bottom fairing requires holes for the hatch mechanism to drop boxes. These edges are therefore also all sized differently, whereas the tail and nose cones consist of a homogeneous design from a structural perspective. While the doors shall be transparent, the top fairing should protect any electronics within the fuselage from exposure to sunlight and heat, therefore the fibres and resin used for it should be opaque, otherwise painting is recommended. The nose cone is subject to engine oil spray and insect strikes, thus its transparency is also discouraged. Figure 7.9 shows a simplified side and bottom fairing layout for reference.

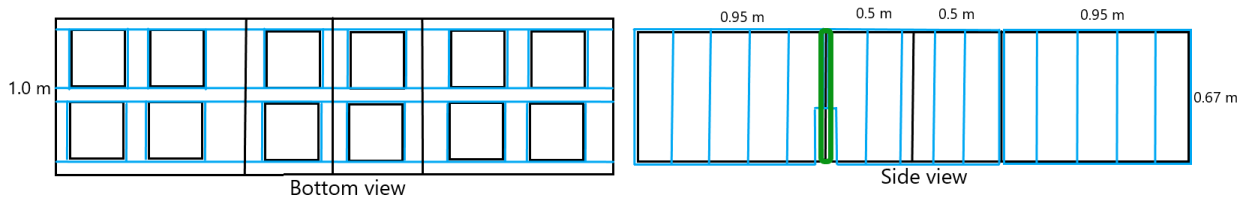


Figure 7.9: A simplified layout of the fuselage fairing loading doors, stringers (blue) with the fuselage frame (black) and wing strut (green)

The fairing encloses the fuselage at about 3 cm away from the center line of truss structure tubes, which assumes that it can be bolted to plates welded to the fuselage. This allows for preventing buckling of the fairing under aerodynamic loads or own weight. In the sizing, the worst-case impact modelled is a severe hail storm. Because of the propeller in front of the nose cone, sizing for bird impact energy absorption is not necessary. The energy the fuselage is required to be able to absorb without failure is found using Equation 7.10. Besides this, the area of impact has to be specified as described above. Note that hail is assumed perfectly circular with a radius of 2.54 cm, 1.7 g and an impact velocity of 25 mph², resulting in 0.107 J over an area of 5.07 cm². The hail impact velocity excludes the flight speed, yet this has no influence on top and side fairings and the tail cone. Both the tail and nosecone are reinforced, because of the challenge to place stringers on the folded shape, however the nose cone also has to withstand hail impact at increased velocity, including air speed.

$$E_{kin} = \frac{1}{2} \cdot m \cdot v^2 \quad (7.10)$$

In order to estimate the required fuselage thickness from the energy of impact, a computation of the material toughness is needed. Toughness, the ability to absorb kinetic energy E_{kin} per unit volume V [21], can be estimated by the area below the stress-strain curve of the material, as described by Equation 7.11. For brittle materials (GFRP, fail at σ_y), a safety factor is applied such that 1/3 of the yield stress is not exceeded ($\sigma_{design} = 0.33\sigma_y$). Knowing the kinetic energy E_{kin} and area of impact A_{impact} , the thickness of the fairing can be computed with $t = V/A_{impact}$. Using the toughness of GFRP, impact area and energy of impact the

²National Severe Storm Laboratory - hail, [cited on 14 June 2023]

required minimal thickness is found to be 0.55 mm along the entire fairing.

$$T = \frac{E}{V} = \int_0^{\epsilon_f} \sigma d\epsilon = 0.5 \cdot \sigma_y \cdot \epsilon_y \quad (7.11)$$

Because of the brittleness and small thickness of the fairing, the panels should be reinforced. The box loading doors are sized to withstand a closing force equivalent to $10 \cdot 9.81$ N inducing a moment by the hinge, using Equation 7.8. To withstand this bending moment, hat stringers with the dimensions shown in Figure 7.10 are added along the perimeter of the door. These stringers are made out of GFRP and are glued to the fairing sheet, for ease and weight reasons. Next to that, four additional vertical (top to bottom) stringers of the same dimensions are equally spaced over the opening doors, resulting in a stringer pitch of 19 cm (20cm for the 1 m door). The bottom fairing panel is reinforced with four stringers along the longitudinal edges of the holes spanning the entire length of the main fuselage part. Additionally, the lateral edges of all holes are also reinforced, these however only span between the longitudinal stringers as additional connections to the bottom lateral fuselage trusses dissipate the remaining loads (see Figure 7.9). Again, the GFRP does not carry any structural box load, but protect the fuselage bottom from the environment. It should be bolted to the fuselage bottom lateral and longitudinal struts. Lastly, the top section has no additional stringers added, as little to no interaction with this section is expected. Next, it is reinforced by additional connections to the truss structures as diagonal trusses are available here for connection, as also shown in Figure 7.5.

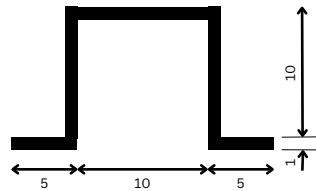


Figure 7.10: Dimensions of selected hat stringer, in millimeters.

To limit manufacturing complexity, no stringers are added to the nose or tail cones. Moreover, because of their complex shape stringer design and manufacturing could have significant costs. However, because of the mere 0.55 mm required for hail impact, the thickness of the cones is increased to 2 mm. This is done to withstand other loads such as its own weight, potential interactions with the ground crew and runway debris impact. It is noted that room for improvement lies within the cone sections, however due to limited resources the design is not detailed further. A more in depth study is thus advised for further design. The combined mass of both cones is only 13.0 kg and thus limited gain is expected here, whereas cost is regarded more important at this stage.

Lastly, 3 kg is added on the total mass as contingency for reinforcement around the bolts used for connection with the fuselage structure. Combining this contingency with the mass of all stringers and sheets results in a total mass of the fairing of 25.5 kg. The loading doors, main section's bottom, main section's top, nose cone and tail cone have a mass of 5.4, 1.7, 2.4, 8.7 and 4.3 respectively.

Finally, because of the relative fragility of the fairing, it is recommended to weld handles to the fuselage, via which the aircraft can be pushed/pulled on the ground, so that no force is transferred from the fairing onto the fuselage. The handles can be placed on the vertical frames, around the mid-height of the fuselage, where the frame is not hidden by a payload door (1, 2, 4, 5). The wing truss, propeller and landing gear are also suitable places to apply ground handling force vectors. Additionally, more failure modes of the fairing should be assessed, such as aerodynamic pressure suction. The specific properties of the opaque nose and fuselage top shall be investigated.

Wing Subsystem

One of the main elements of any aircraft is the wing subsystem. This subsystem will be designed for the mission profile it is required to fly. The appropriate characteristics of the wing will be selected in Section 8.1, where the wing is designed from airfoil to 3D planform. In the following Section 8.2, the wing box structure is determined. This is done using the wingbox approximation. Lastly, in Section 8.3 and Section 8.4 the aileron design and high-lift are designed consecutively.

8.1. Design of the wing

In this section, several characteristics of the design of the wing will be discussed, such as the airfoil selection, taper ratio, sweep, dihedral, etc. Simulation tools will be used to estimate the most accurate value for these characteristics.

8.1.1. Airfoil Selection

The selection of an airfoil comes down to a trade-off between drag, lift, stability and structural weight performance. However, more aspects can be important such as stall behaviour or fuel storage capacity. To take all aspects into account aerodynamic and stability considerations are combined with mission-specific parameters. Moreover, general aerodynamic and stability parameters are captured in Equation 8.3 and mission-specific parameters are considered in Equation 8.4 [22]. Values for (τ) and eta (η) are found for nine different airfoil through data collected by XFLR5 analyses. This was done for cruise condition at the MAC, meaning a Reynolds number of $3.928 \cdot 10^6$ and a Mach number of 0.184 as calculated by Equation 8.1 and Equation 8.2 respectively.

$$Re = \frac{\rho \cdot v \cdot l}{\mu} = \frac{0.9046 \cdot 60.49 \cdot 1.020}{1.421 \cdot 10^{-5}} = 3.928 \cdot 10^6 \quad (8.1)$$

$$M = \frac{V_c}{a} = \frac{60.49}{328.4} = 0.1842 \quad (8.2)$$

The nine considered airfoils can be found in the first column of Table 8.1. These were selected by analysing commonly used airfoils on reference aircraft [23].

Data Collection using XFLR5

Due to time and resource limitations within this project, it was not possible to obtain the airfoil data from windtunnel testing. To assure consistency in the collected data a simulation model has been used rather than windtunnel experiments performed in previous research. This was decided as the airfoils considered differ significantly making it hard to find a source that covers all airfoils at the required Reynolds numbers. Furthermore, simple simulation tools like XFLR5 have proven their use as an "excellent airfoil design and analysis tool" [24], although this applies to low Reynolds numbers around $2.0 \cdot 10^5$. However, it has been shown that also for Reynolds numbers of $2.0 \cdot 10^6$ XFLR5 shows very well accuracy [25]. Where the biggest deviations were found in the prediction of $C_{l,max}$ with errors up to 15%. This is caused by limited capabilities of the program to model stall, as the flow is assumed inviscid. It was shown that XFLR5 shows the best results out of similar prediction methods and was thus chosen within this analysis [25]. However for the selected airfoil, as will be explained later to be the NACA4415, an error of 10% in pressure data occurs by using XFLR5 relative to windtunnel testing [26]. Thus, for a more detailed airfoil selection windtunnel tests are recommended in the future, especially since the considered Reynolds number is relatively high. However as all airfoils follow a similar deviation, the accuracy of XFLR5 is assumed sufficient for the current scope of airfoil trade-off.

The 2D analysis of airfoils in XFLR5 is performed using the underlying code of XFOIL. XFOIL solves the 2D Laplace's equation, which solution is used to solve the boundary layer flow by use of IBL (Interactive

Boundary Layer) methodology. The total viscous drag is then solved using a Squire–Young formula [27]. A result of this modelling choice is the inability to correctly compute the behavior beyond stall angles, flow separation at the trailing edge and laminar separation bubbles [28]. Therefore, viscous drag estimations and transition point determination are the main source of inaccuracies in the computed coefficients.

Airfoil Trade-off Parameters

To capture both the aerodynamic and stability performance of an airfoil in a single parameter an airfoil efficiency parameter (τ), given in Equation 8.3, is used [22]. For each coefficient ($\frac{C_l}{C_d}$, α_{stall} , etc.) the value is normalised with the maximum value of this parameter out of all airfoils. This is done as the order of magnitude between coefficients can vary significantly, altering the weight of each in case normalisation is not performed. For C_{d_0} and C_{m_0} the minimum values are however selected as these coefficients should be minimized. Using the maximum and minimum values presented in Table 8.1 this thus results in Equation 8.3. An overview of the values of τ for the nine considered airfoils can be found in Table 8.2.

$$\tau = \frac{(\frac{C_l}{C_d})_{max}}{164} + \frac{(\frac{C_l^{3/2}}{C_d})_{max}}{170} + \frac{(\frac{C_l^{1/2}}{C_d})_{max}}{166} + \frac{C_{l_{max}}}{1.86} + \frac{\alpha_{stall}}{20.5} + \frac{0.00456}{C_{d_0}} + \frac{C_{l_0}}{0.620} \cdot \left(\frac{C_{l_\alpha}}{0.136} + \frac{C_{m_\alpha}}{0.0105} + \frac{-0.0992}{C_{m_0}} \right) \quad (8.3)$$

Next, to include the mission profile in the airfoil selection an airfoil performance parameter (η) is computed by Equation 8.4 [22]. The mission is split into cruise, descend, ascend and loitering. Each section has a different time fraction and performance parameter as can be seen in Equation 8.4. For example, 51.9% of the mission is spent in cruise where maximum range is desired so each airfoil's $(\frac{C_l^{1/2}}{C_d})_{max}$ is evaluated. The values for η for the considered airfoils are found in Table 8.2.

$$\begin{aligned} \eta &= t_{cruise} \cdot \left(\frac{C_l^{1/2}}{C_d} \right)_{max} + t_{descend} \cdot \left(\frac{C_l}{C_d} \right)_{max} + t_{ascend} \cdot \left(\frac{C_l}{C_d} \right)_{max} + t_{loiter} \cdot \left(\frac{C_l^{3/2}}{C_d} \right)_{max} \\ &= 0.519 \cdot \left(\frac{C_l^{1/2}}{C_d} \right)_{max} + 0.249 \cdot \left(\frac{C_l}{C_d} \right)_{max} + 0.191 \cdot \left(\frac{C_l}{C_d} \right)_{max} + 0.041 \cdot \left(\frac{C_l^{3/2}}{C_d} \right)_{max} \end{aligned} \quad (8.4)$$

Trade-off Summary and Selection

All gathered data from XFLR5 is given in Table 8.1 where the optimum value for each parameter is highlighted in bold. These are used in the normalisation of Equation 8.3 as explained before.

Table 8.1: Overview of airfoil coefficients for all nine considered airfoils with most optimum values highlighted in bold.

Airfoil	$\frac{C_l}{C_d}_{max}$ [-]	$\frac{C_l^{3/2}}{C_d}_{max}$ [-]	$\frac{C_l^{1/2}}{C_d}_{max}$ [-]	$C_{l_{max}}$ [-]	α_{stall} [deg]	C_{d_0} [-]	C_{l_0} [-]	C_{l_α} [1/deg]	C_{m_α} [1/deg]	C_{m_0} [-]
NACA 2412	123	134	147	1.80	18.0	0.00541	0.248	0.114	0.00578	-0.0538
NACA 4412	121	140	109	1.72	15.0	0.00884	0.467	0.141	0.00801	-0.0992
NACA 4415	164	170	166	1.74	18.0	0.00595	0.457	0.103	0.00748	-0.0941
NACA 23012	141	154	142	1.77	17.5	0.00641	0.135	0.114	0.00490	-0.0107
NACA 23015	140	165	134	1.79	18.0	0.00623	0.131	0.114	0.00645	-0.00924
NACA 63215	97.1	102	103	1.40	19.0	0.00479	0.181	0.117	0.00886	-0.0405
NACA 64415	99.9	105	140	1.36	20.5	0.00456	0.361	0.136	0.0105	-0.0818
Clark Y	155	151	162	1.79	16.5	0.00604	0.404	0.113	0.00627	-0.0844
USA 35B	124	146	112	1.86	14.5	0.00851	0.620	0.108	0.00731	-0.0875

Substituting the values of Table 8.1 in Equation 8.3 and Equation 8.4 gives the values for τ and η as presented in Table 8.2. Since different airfoils score highest in the two parameters they were both normalised once again and added to obtain Σ , thus $\Sigma = \tau/\tau_{max} + \eta/\eta_{max}$.

Table 8.2: Overview of τ , η and Σ for nine considered airfoils.

Airfoil	τ	τ/τ_{max}	η	η/η_{max}	Σ
NACA 2412	13.9	0.695	135	0.824	1.51
NACA 4412	20.0	1.00	115	0.699	1.70
NACA 4415	19.8	0.986	164	1.00	1.99
NACA 23012	8.97	0.448	141	0.860	1.31
NACA 23015	9.06	0.452	137	0.837	1.29
NACA 63215	11.9	0.593	100	0.607	1.20
NACA 64415	17.9	0.895	121	0.734	1.63
Clark Y	18.2	0.908	158	0.959	1.87
USA 35B	19.0	0.948	119	0.720	1.67

From Table 8.2 it is clear that the NACA 4415 is the best option following from this analysis. Moreover, the Clark Y airfoil is a clear second best.

Reflection of Selected Airfoil

The selected NACA 4415 airfoil has a relatively high thickness. It is expected that this preference for high thickness is built into the airfoil selection method, because of the nature of XFLR5 to over-predict $C_{l_{max}}$ and under-predict $C_{d_{min}}$, therefore favouring thickness. The high thickness however also brings with it advantages in structural weight, fuel capacity and stall behaviour. The high maximum lift coefficient shows to be valuable and critical later in the design stage when designing the high-lift devices in Section 8.4, thus ruling out the option of airfoils with lower $C_{l_{max}}$ without considerable redesign of the wing planform. To conclude, the NACA 4415 airfoil is thus selected as the best option.

8.1.2. Sweep

Firstly, the decision to implement wing sweep is a trade-off between drag decrease and manufacturing cost increase while taking into account other aspects such as stall behaviour. The increase in total manufacturing cost by adding sweep is around 15%, while the expected decrease in total aircraft drag comes down to 2% for low subsonic aircraft [19]. The decrease in drag reduces the fuel cost per sortie. The added manufacturing cost and reduced fuel cost give the inclusion of sweep a 0.00044 euro increase in cost per kg of payload delivered. This is a marginal difference. However, combining this with the disadvantageous effect sweep has on stall behaviour it was decided to not include sweep for the main wing.

8.1.3. Dihedral

Secondly, it was analysed if applying dihedral to the wing would be beneficial for the stability of the aircraft. In the case of the high wing, it is common to implement negative dihedral or anhedral to the main wing. However, general aviation aircraft such as the Cessna 208 or 172 are also common to have positive dihedral [19]. The dihedral angle mainly influences the stability coefficient C_{l_β} , which models the effect a sideslip angle has on roll. Using this coefficient, it can be checked if the requirement for spiral stability, which is shown in Equation 8.5, is met.

$$C_{l_\beta} C_{n_r} - C_{l_r} C_{n_\beta} > 0 \quad (8.5)$$

To model the current design's value of this derivative as later described in Section 8.1.7, AVL software is used. First of all, its limitation should be carefully analysed as done in Section 8.1.7 and therefore its output should also be handled with great caution. Where in the case of modelling C_{l_β} the biggest inaccuracy originates from the inability to model fuselage interactions well. Additionally the high pressure zone created underneath the downward going wing in roll is not modelled. This lack of interaction modelling has the effect that the absolute value of C_{l_β} likely to be under predicted, in the disadvantage of the design compared to reality. Nevertheless, its accuracy is deemed sufficient for initial sizing.

Initial simulations, with zero dihedral angle, showed C_{l_β} to have a value of -0.026 whereas the Cessna 172 has a value of -0.089. This difference was regarded too large and thus simulations with different dihedral angles were run in AVL. This gave the results shown below in Table 8.3. The effect on other stability derivatives is small, less than 5% between the most extreme cases considered, except for C_{Y_p} which changes very significantly but does so in a advantages manner converging to the Cessna 172's value

of -0.037. The DATCOM method was also investigated to validate the values from AVL [29]. However, this gave values in the order of 10^{-5} regardless of the dihedral angle (restricted at 10°). This was thus deemed unrealistic and its results were discarded. It is expected that this inaccuracy originates from the low half chord sweep angle of the design and the inability of the DATCOM method to incorporate this.

Table 8.3: Effect of dihedral angle (Γ) on C_{l_β} and C_{Y_p} where all other design parameters are kept constant with the final design as presented in Chapter 13 for cruise condition, with the elevator set to trim the aircraft.

$\Gamma[\text{deg}]$	$C_{l_\beta} [-]$	$C_{Y_p} [-]$
0.0	-0.026	0.050
0.5	-0.032	0.037
1.0	-0.038	0.025
1.5	-0.044	0.012
2.0	-0.051	-0.000
2.5	-0.057	-0.013
3.0	-0.063	-0.026

The dihedral angle was finally chosen by trading off the added weight and drag with the added spiral stability. Since the spiral is a relatively slow eigenmotion, recovery is easy using the correct autopilot. Thus, it was decided that some inherent spiral stability in cruise condition is acceptable. As a result the requirements for the dihedral angle were set such that the spiral stability fraction in Equation 8.5 is at least 0.5 and the magnitude of C_{l_β} is no less than half that of the Cessna 172. This results in adding a dihedral of 1.5° to the current design. In case it is desired to have a C_{l_β} within 5% of the Cessna 172 it is recommended to apply a dihedral angle of 5° . However, due to the interference modeling inaccuracies in AVL this is advised to be investigated further in later stages.

8.1.4. Twist

Finally, the twist angle is considered. This is the difference in the angle of attack between the root and chord. Its most important function is preventing tip stall from happening before the root stalls. A negative twist reduces the tip angle of attack and thus delays stall locally. Although manufacturing costs are increased when adding twist, the added safety in stall is regarded to outweigh this cost increase as it will reduce the number of crashes happening. Moreover, this is vital to the mission as a crash is both very expensive and bad for brand image. An angle of -2° is chosen which, including the later explained maximum wing twist from the applied loads of 0.5° , results in a twist of at least -1.5° .

The application of twist is done using geometric twist. That is, the angle of attack of the tip is 2° lower with respect to the root and in between α is linearly interpolated. This makes the manufacturing more complex as the spars will need to be twisted. Aerodynamic twist could prevent this, but an airfoil with a higher stall angle of attack for the tip section will have to be selected. As the root airfoil already is good in stall conditions, finding an efficient airfoil with better characteristics is difficult.

8.1.5. Aspect Ratio, Taper Ratio and Incidence Angle

The main wing is analysed using lifting line theory. This is a mathematical model to predict the lift distribution over a wing from a given geometry [30]. Conceptual circulations are placed in several locations distributed over the wing span. The circulation over the wing is a function of a set of coefficients A_1, \dots, A_N where N is the number of circulations placed over the wing. Equation 8.6 is Prandtl's wing equation and shows the relation between the coefficients and wing geometry.

$$\frac{4b}{a_0 c} \sum_{n=1}^N A_n \sin(n\theta) + \sum_{n=1}^N n A_n \frac{\sin(n\theta)}{\sin(\theta)} = \alpha - \alpha_{L=0} \quad (8.6)$$

Here, b is the wing span, a_0 the airfoils lift slope, c the local chord length, θ a parameter that determines where along the wing span you are and α is the angle of attack. This equation has to be solved numerically by evaluating it at N different locations to get N equations and N unknowns. From the coefficients, a circulations distribution and thus a lift distribution can be obtained. The lift distribution is analysed to obtain parameters such as the span efficiency factor, induced drag and lift coefficient.

The planform design is seen as an input to this mathematical model. Some of the design parameters can already be chosen based on trivial trade-off where it is obvious which options can be discarded. Then, important planform parameters are varied until a lift distribution is obtained that satisfies the requirements. The planform is optimised to obtain minimise drag, while taking into account the total weight and cost of the design. The surface area is already known since $10.4 \text{ m}^2 \pm 5\%$ is required to satisfy the wing loading of the aircraft as shown in Figure 3.7a.

As described above lifting line theory is used to determine the aspect ratio, taper ratio, twist and incidence angle. All parameters influence one another, so iterations are done to converge towards a final design. Below, the process for one iteration is shown, starting with choosing an aspect ratio and ending with setting the incidence angle.

- **Aspect Ratio:** Reducing the aspect ratio below eight results in compatibility issues with the aileron and flap sizing, discussed in Section 8.3 and Section 8.4. Moreover, reducing the aspect ratio reduces the span which reduces both the moment arm, limiting aileron effectiveness and the space available for the aileron and flap. Lower aspect ratios would thus require more expensive, heavy and complex flaps and or ailerons. This was thus not further investigated. It was however analysed what the effect is of increasing the aspect ratio. The aspect ratio is set by selecting the minimum in terms of cost per kilogram delivered, as this is the end objective. Moreover, the entire iteration has been run for different aspect ratios to see the effect on cost per kilogram payload deliver, while keeping all other variables constant. By increasing aspect ratio the lift induced drag of the wing reduces, while the weight of the wing increases since the bending moment increases. For an incidence angle of 0 degrees, a taper ratio of 0.65 and angle of twist of 2 degrees, the cost per kg payload delivered increases from 1.4 to 1.43 going from an aspect ratio of 8 to 10. From this it is clear that an aspect ratio of eight is the best option.
- **Taper Ratio:** With an initial value for the aspect ratio known, the taper ratio will now be varied. The main advantage of modifying the taper ratio is to change the lift distribution over the wing. Figure 8.1 shows how the lift distribution changes as the taper ratio changes, at a constant wing twist of -2° . An elliptical lift distribution is also shown as this is associated with the least induced drag. The taper ratio is chosen such that the lift curve has the minimum absolute mean difference with the elliptical lift distribution to an accuracy of 0.1. This method results in a chosen taper ratio of 0.66. With the value for the taper ratio known, the length of the chord at every span position y can be calculated using the following equation.

$$C(y) = C_r \left(1 - \frac{1 - \lambda}{b/2} y \right) \quad (8.7)$$

Equation 8.7 will be used in Section 8.4 to size the High Lift Devices and to model the wing planform in AVL and CAD.

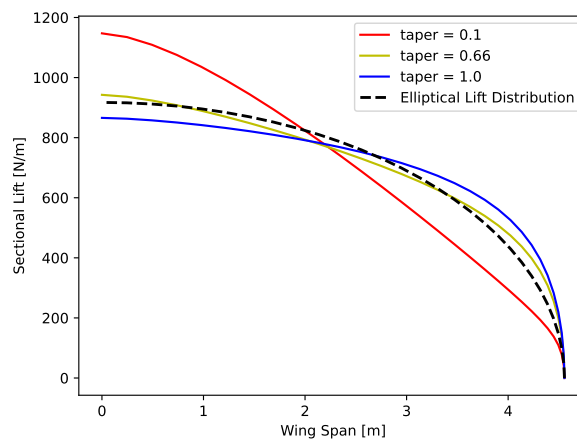


Figure 8.1: Spanwise lift distribution over half span with changing taper ratio at $AR = 8$, $\Lambda_{c/4} = 0$, $\alpha_t = -2^\circ$ and optimised i_w for required lift in cruise, 2.12° .

- **Incidence Angle:** The incidence angle is set such that the wing generates exactly the required lift during cruise. The incidence angle is optimised for this condition as it, therefore, does not require the fuselage to be at an angle of attack during cruise, reducing drag. Cruise is chosen as most of the mission will take place during this phase. The optimization for the required lift gives an incidence angle of 2.12° .

8.1.6. Winglet Consideration

Because of the difference in pressure between the upper and lower surface of the wing required for lift generation wing tip vortices will always exist. The drag this creates, lift-induced drag as described by Equation 13.3, can, however, be limited. Moreover, by adding winglets the effective aspect ratio of the wing is increased without adding extra span and thus no added parasitic drag [31]. Winglets are expected to increase the Oswald efficiency factor of the wing by 32% as a first estimate [32]. It should be noted that this estimate seems high and is thus treated as an upper limit.

However, winglets can generally not be added to existing wing designs as the induced loads, such as extra weight and new spanwise aerodynamic forces, are too high. [33] Also, the induced loads are often predicted too low, therefore requiring in-depth studies and/or experiments when implemented. The weight of the wing thus increases when adding winglets. For similar aircraft, this added weight is approximated to be around 20% of the wing weight.

As a very first cost estimate, the case of the Boeing 737-700 is used. The addition of winglets costs around \$500,000 ¹ whereas the total unit cost is \$89.1 million ², coming down to an cost increase of 0.56%.

Implementing an Oswald efficiency increase of 32% and a wing weight increase of 20% in the full iteration program results in a change in MTOW of 8.89 kg, and even more importantly an added fuel weight per sortie of 0.265 kg. Clearly, from the fact that the required fuel per sortie increases by the addition of winglets it is not worth adding winglets to the design, especially since the estimated Oswald factor increase is higher than expected.

This 20% wing weight increase is however a very rough estimate and it is thus recommended to investigate this further in later design stages. Next, it should also be investigated whether simple winglets show more benefit, such as Hoerner winglets.

8.1.7. AVL Refinement

In order to refine the aerodynamic analysis use was made of AVL (Athena Vortex Lattice). AVL was chosen as a modelling software, because of its relatively high accuracy and the limited resources required. Moreover, comparison with Ansys Fluent and test flights show that AVL (Athena Vortex Lattice) has smaller errors than other comparable software such as XFLR5 in 3D [34]. Moreover, the relative error of Oswald factor and induced drag estimations of a wing using AVL never exceed 7.5% compared to Hoerner's function [35] [36]. Besides lift and drag analysis AVL has also been shown to perform stability analysis at sufficient accuracy for this stage of the design [37].

AVL is a Vortex Lattice Method (VLM) as the name suggests. It has been developed by Mark Drela at MIT ³. Calculations are performed by solving the Laplace equations for the strength of singularities on the lifting surface. A constraint of AVL is that it focused on thin lifting surfaces, as a result, the effect of thickness on the pressure distribution and thus lift and drag is not predicted correctly. Therefore limiting the accuracy as thickness is increased. Another constraint is the inability to model flow separation, viscosity and turbulence, similar to XFLR5 as explained in Section 8.1.1. On the other hand, AVL computations include the leading edge suction force which more sophisticated panel methods do not include. AVL therefore does not require Trefftz-plane theorem and as a result models this more accurately [38]. Also, its computational efficiency was regarded as a big advantage as the estimated amount of iterations required in the design was high. To tackle the inability to model viscosity parasitic drag is inputted manually from the drag calculation explained

¹Winglet added cost.

²Unit cost B737-700.

³Author AVL software.

later in Section 13.1. Surface interactions and interference is not modelled accurately either. However, parasitic drag of the aircraft is modelled separately and the lift generated by the fuselage is insignificant to the total aircraft lift. Thus, the fuselage and landing gear are not modeled in AVL. Its masses and centers of gravity are included for stability analyses.

Wing fuselage interactions are generally not modelled well in AVL and modelling of the aircraft with only its lifting surfaces is often regarded more accurate. For this reason the fuselage and other components such as the landing gear have not modeled. This can however have effect on the stability derivatives modeled using AVL. Especially roll derivatives (C_{l_x} and C_{x_p}) can be effected by this significantly as will be explained further in Section 13.2.

The geometry and masses of the aircraft are loaded in AVL as can be seen in Figure 8.2. The run case is set for cruise conditions by setting the Mach number, density, velocity and required lift. The run case is set in steady, horizontal, symmetrical flight, where the aircraft is trimmed by the elevator. With the outputted angle of attack the incidence angle is changed such that the required angle of attack in cruise is zero again. This is done using the Trefftz plot, for which an example is shown in Figure 8.3 which is in cruise condition. In both figures the wing twist applied to the wing is clearly visible. Moreover, it is also visible that horizontal tail is required to generate negative lift in cruise condition from Figure 8.2. Also, the Y-force required from the vertical tail to offset the engine torque is clearly visible, as will be further explained in Section 9.3.2.

The value for $C_{L_{max, clean}}$ is first predicted using the methods of Phillips and Alley [39]. This value is however later in the iteration overwritten by use of AVL simulations which are an integral part of the total iteration loop as further detailed in Section 3.5. This is a required input to seize high-lift devices, which is described in Section 8.4. This is done by analysing the C_l value in the Trefftz plot as shown in Figure 8.3. Moreover, the aircraft's lift coefficient (C_L) is altered such that C_l matches the maximum lift coefficient of the airfoil, as given in Section 8.1.1. These values should however be handled with care, because of the assumption described above. Yet, for this stage of the design this inaccuracy is regarded acceptable. After performing the analysis the aerodynamic properties are shown in Table 8.4.

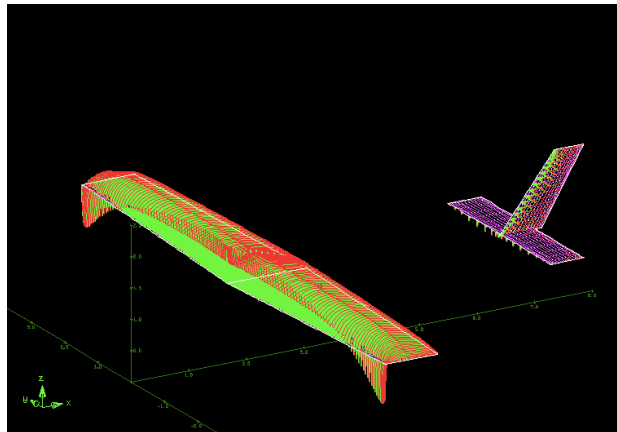


Figure 8.2: Lifting surface's loading in cruise conditions with an elevator angle set for zero pitching moment.

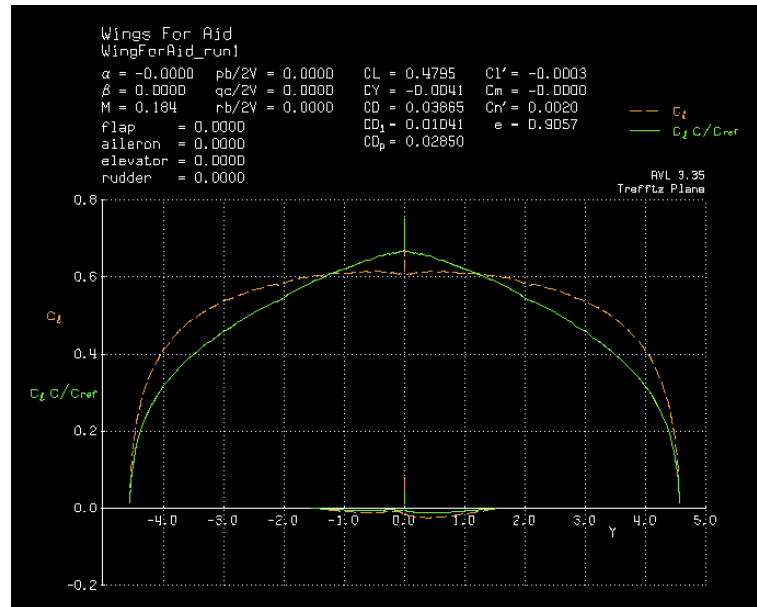


Figure 8.3: Trefftz plot showing spanwise lift distribution in cruise conditions with an elevator angle set for zero pitching moment.

Table 8.4: Summary of final wing planform parameters after AVL refinement.

Air foil	S	b	AR	λ	i_w	α_t	$\Lambda_{c/4}$	C_{root}	MAC	$C_{L_{max, clean}}$
[—]	$[m^2]$	[—]	[—]	[—]	$[deg]$	$[deg]$	$[deg]$	$[m]$	$[m]$	[—]
NACA 4415	10.4	9.11	8.00	0.66	3.10	-2.00	0.00	1.37	1.15	1.42
Contingencies	$\pm 5\%$	$\pm 2.5\%$	-	-	$\pm 25\%$	$\pm 10\%$	-	$\pm 5\%$	$\pm 5\%$	$\pm 10\%$

8.2. Wingbox

With the wing planform and airfoil selected, it is time to design the wingbox structure. The wingbox shall withstand all loads that it could encounter, multiplied with an ultimate load factor of 6.67 (and -3.67). The wingbox will be assumed to consist of a front and aft spar, connected by a top and bottom plate. This means that the leading edge and trailing edge of the airfoil will be neglected. Thus the actual wingbox might turn out to be slightly heavier, but for the current state of design, this level of detail is assumed to be sufficient. The wingbox will be stiffened using stringers and ribs. The first step in the wingbox design is to identify all loads that are present on the wing. This will be covered in Section 8.2.1

8.2.1. Loading Diagrams

A multitude of loads is present on the wing, however for the structural design, two load cases are most important: the load case that has combined the most load pointing upwards (now called 'up case'), and the load case that has combined the most load pointing downwards (now called 'down case'). If the wingbox can withstand these two load cases, then it can withstand the most critical load cases to be encountered in flight. The following loads are accounted for in the wingbox:

- **Lift**, the lift is the biggest load on the wingbox and can both be pointing upwards and downwards. For the up case the lift will be multiplied with an ultimate load factor of 6.67, while for the down case the lift will be multiplied with an ultimate load factor of -3.67.
- **Wing weight**, the weight of the wing is a load that is always present and will always be pointing downwards. The wing weight is assumed evenly distributed as a function of the chord along the span.
- **Flap weight**, the weight of the flap is also included and the location depends on where the flap is placed for control. The flap weight is assumed to be 60% of the control surfaces weight and is evenly distributed over the location of the flap.

- **Aileron weight**, similarly to the flap, the weight of the aileron is also included. The aileron takes up 40% of the control surfaces weight and is also evenly distributed over the location of the aileron.
- **Fuel weight**, for the up case the fuel is left out, as this would relieve the upwards loads. The worst-case scenario is if there is no fuel. For the down case the fuel weight is included, as this worsens the downwards loads. For now the fuel weight is assumed to be distributed equally as a function of chord along the span. Once the fuel tanks are sized and placed, a more accurate fuel weight distribution could be achieved.
- **Strut reaction forces**, since there is also a strut attached to the wing, the forces between the strut and wing need to be accounted for. By removing the strut and replacing it with reaction forces, the effect of the strut on the wing can be calculated.

Applying all loads on the wingbox and solving for the reaction forces both at the root and at the strut location allows to draw the normal, shear, moment and torque diagrams. For the calculation of the reaction forces from the strut, the strut is assumed to be a two force member. A two force member is a body that only has forces in two locations, in this case at the end points of each strut, acting along the strut length. This way the angle of the strut can be used to calculate the components of the force. At this stage it is also very important to define a coordinate system. The coordinate system that is used throughout the wingbox design and which defines the signs for the normal, shear, moment and torque diagrams, is the following: the x-axis points along the fuselage towards the nose, the y-axis points from the wing root to the tip of the right wing, while the z-axis points downwards. Figure 8.4 shows all diagrams as mentioned before for the up case, a similar figure can be made for the down case.

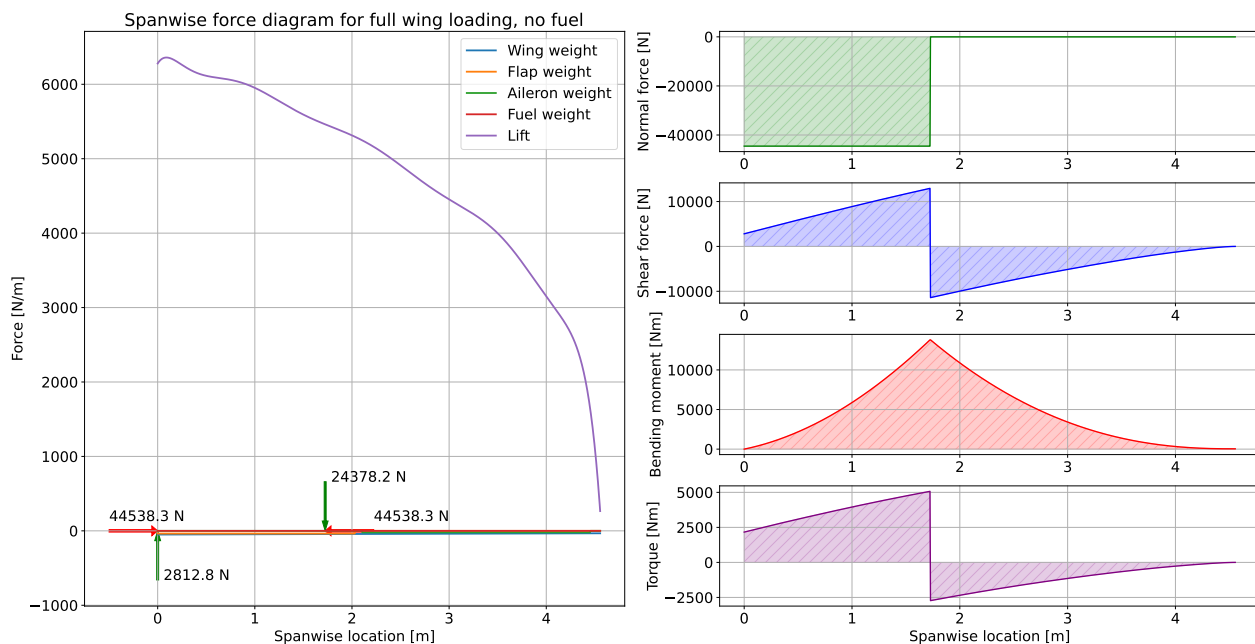


Figure 8.4: Wing spanwise load distribution and wing loading diagrams for up case, $n=6.67$

In the creation of these diagrams, numerous assumptions have been applied:

- The point of application of the lift force is at the center of pressure, which is always assumed to be at 25% of the chord.
- The flexural axis is assumed to coincide with the centroid. Since the main wing has no sweep, this assumption can safely be made.
- Only the shear normal to the chord line is considered. Shear in other directions will be significantly lower and therefore have little effect on the design.
- Only the bending moment about the chord line is considered. Bending moment around other axis will be significantly lower and therefore have little effect on the design.
- The assessed loading cases ignore any effect from the deflection of control surfaces, since these deflection can generate considerable forces, this should be implemented in the future.

- The lift distribution used in the loading diagrams is for cruise, this is however not the most limiting case. Therefore the wingbox could turn out to be slightly underdesigned.
- The fuel and wing weight do not contribute to torsion in the wing, as the flexural axis more or less coincides with the centroid of the weights.

8.2.2. Material

The material choice for the wingbox is made according to the convention described in Section 3.2. The following weights were assigned: raw cost (4), ecological cost (1), CO₂ emissions (0.5), K_{ic} (0.5), material index $E^{\frac{2}{3}}/\rho$ (4). This material index was chosen as it is used for thin plates loaded in bending [10, p. 1193]. These weights returned Aluminium 5052-H38 as the best material. This is the material that will be used for the wingbox.

8.2.3. Structure

The loads as presented in Section 8.2.1 are now used to size the wingbox. As mentioned before the wingbox will consist of a front spar, an aft spar and a top and bottom panel. The wingbox will be stiffened by L-type stringers and ribs shaped as the wingbox cross section. L-type stringers have been chosen as they are simple, readily available and effective in increasing the second moment of area of the wingbox. The base of the stringer, which will be attached to the plates, has half the size of the flange. A Python program is written in order to calculate the optimal wingbox for the given loads. In this program some values can be changed in order to optimise, while other values are fixed. Below a list of parameters will be presented, together with the fact if they are fixed or can change:

- **Airfoil type**, the chosen airfoil is the NACA 4415 and will not be a design variable for the wingbox
- **Location front spar**, the location of the front spar is chosen at 20% of the chord, such that it accommodates proper attachment to the fuselage structure, dependant on the X_{LEMAC}
- **Thickness front spar**, this value can be changed
- **Location aft spar**, the location of the aft spar is chosen at 75% of the chord, in order to accommodate attachment of the control surfaces
- **Thickness aft spar**, this value can be changed
- **Thickness top panel**, this value can be changed
- **Thickness bottom panel**, this value can be changed
- **Base length stringer**, this value can be changed
- **Flange length stringer**, this value will change based on the change of the base length of the stringer
- **Thickness stringer**, this value will change based on the change of the base length of the stringer
- **Number of stringers**, this value can be changed
- **Stringer variation**, as can be seen in Figure 8.4 the highest loads are at the attachment point of the strut. Therefore the wingbox will have the full amount of stringers until this point and decreases at every rib until zero at the tip.
- **Number of ribs**, this value can be changed
- **Thickness of ribs**, this value has been chosen at 1 mm and will not change in the design
- **Twist limit**, this is fixed at 0.5 degree (at a load factor of 2) as the twist due to loads should not cancel out the twist integrated into the wingbox structure

Given all variables above a wingbox cross section can be drawn. In Figure 8.5a this cross section can be seen, in Figure 8.5b the trailing edge of the wingbox is shown a bit more zoomed in.

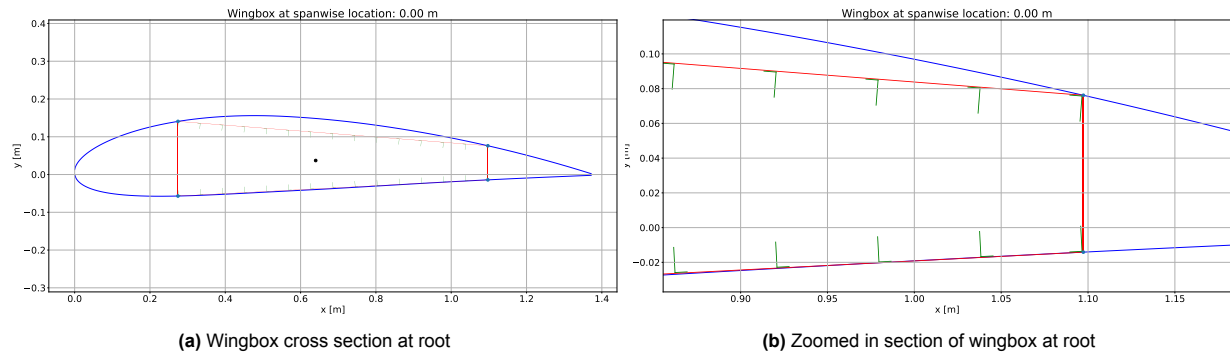


Figure 8.5: Cross section of the wingbox at the root

8.2.4. Calculations

The values of all variable parameters from Section 8.2.3 will be calculated using a Python program. This program will start with certain start values for the parameters (indicated in Figure 8.6). It then checks if the wingbox fails anywhere, and if it does it will increase the thickness of the failing element. It will keep iterating until the wingbox is thick enough everywhere to sustain all loads without failure. It does this for both the up case and down case and afterwards checks if the wing twist limit is not exceeded. The whole process is visualised in Figure 8.6.

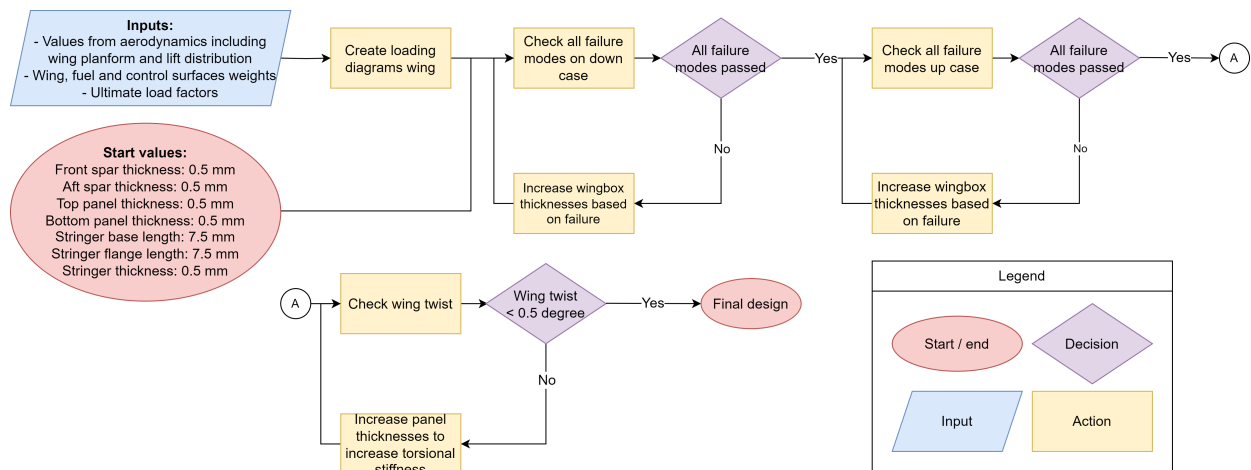


Figure 8.6: Block diagram of wingbox calculation program

The wingbox is tested for a broad range of failure modes, these will be listed below including possible assumptions. All equations used are omitted in this section, however, they can be found on pages 37-42 of the AE2111-I Aircraft Design Reader [40].

- **Shear buckling of spars**, it is assumed that the spars take all the shear stress, such that an average shear stress in the spars can be calculated. This is multiplied with a factor 1.5 to find an estimated maximum shear stress in the spars. This is compared with the critical shear stress for buckling, the material and aspect ratio of the spar play an important role here. Shear follows from both the shear force and torque.
- **Skin buckling of top and bottom panel**, the stress on the top and bottom panel follows from the normal stress and the stresses due to bending. This is compared to the critical buckling stress, also here the material and aspect ratio play an important role.
- **Column buckling of stringers**, for column buckling the stringers at the top have been assumed to buckle as one. This means that in the calculation of the critical stress, the areas of the stringers at the top will be added up. As a conservative approach, a K factor of 1/4 is taken, which is used to take the end conditions of the stringers into account. This corresponds to one free and one fixed end. The same calculations are performed for all bottom stringers.

- **Tensile strength failure all elements**, for all elements the program checks whether the stresses exceed the yield stress for tension anywhere
- **Compressive strength failure all elements**, for all elements the program checks whether the stresses exceed the yield stress for compression anywhere. The yield stress for compression and tension is assumed to be equal.
- **Crack fracture in spars, top and bottom panel**, as part of the damage tolerance, a critical stress is calculated at which the panels fail, given that cracks with a maximum size of 5 mm are present. The stress in the wingbox cannot exceed this stress anywhere. Cracks with a size bigger than 5 mm can be seen with the naked eye, and will need to be repaired or the part needs to be replaced.

For all these failure modes the critical stress can be divided by the actual stress to get the margin of failure. As long as the margin of failure is above one, the element will not fail. This margin of failure can be plotted for all the failure modes as a function for span. Then there should be one failure mode that touches 1, this shows the wingbox is optimally designed and this failure mode is the most critical one. This graph can be found below in Figure 8.7.

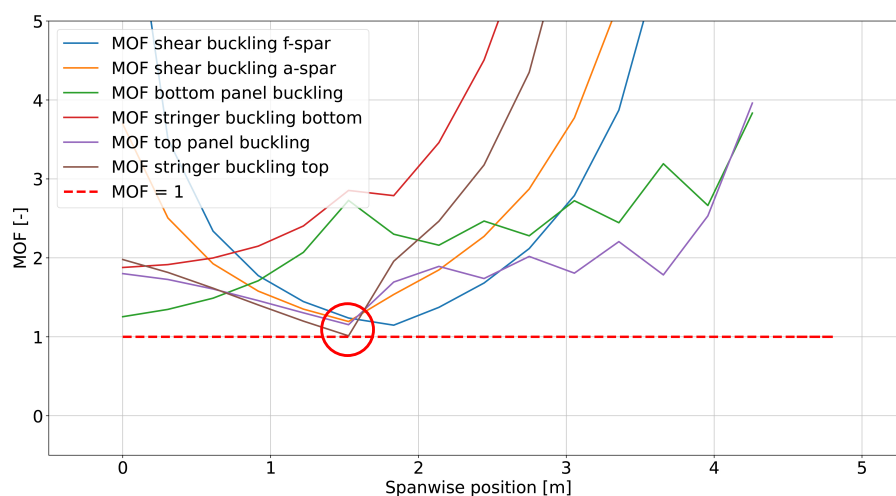


Figure 8.7: Margin of failure of different failure modes along the span

Some failure modes are left out, as those values are significantly above 1. As can be seen, the most critical failure mode is the stringer buckling at the top. The shear buckling of spars and the buckling of the top panel are very close to a margin of failure of 1 too. For now, it is assumed that if one of the elements buckles, the full wingbox fails. In reality, it means that this specific element does not add to the strength of the wingbox anymore. Assuming that the whole wingbox fails in case a single element fails is therefore a conservative approach, which is appropriate for this stage of design.

8.2.5. Optimisation and Final Design

With the whole wingbox design process laid out, it is time to find the optimal wingbox. That is the wingbox with minimum weight, which satisfies all failure modes. To find this the program will look for the optimal combination of stringers and ribs that result in minimum weight. Since using a brute-force method takes up to hours, an optimisation scheme has been written. This is as follows: first a broad range of stringers and ribs is defined (between 0 and 40 for stringers and 0 to 30 for ribs). This range is divided into a grid of 4 by 4 evenly spaced points, each representing a combination of ribs and stringers. At the point which results in minimum weight a new 4 by 4 grid is defined, with the original best point in the middle. The bounds of this new grid are the same as the adjacent points to the original best point. Here again, the point with minimum weight is found. This process is repeated until a single best point is left over, giving the global minimum weight. Afterwards, all datapoints can be plotted to get a 3D surface of all the combinations of stringers and ribs and their respective weight, see Figure 8.8

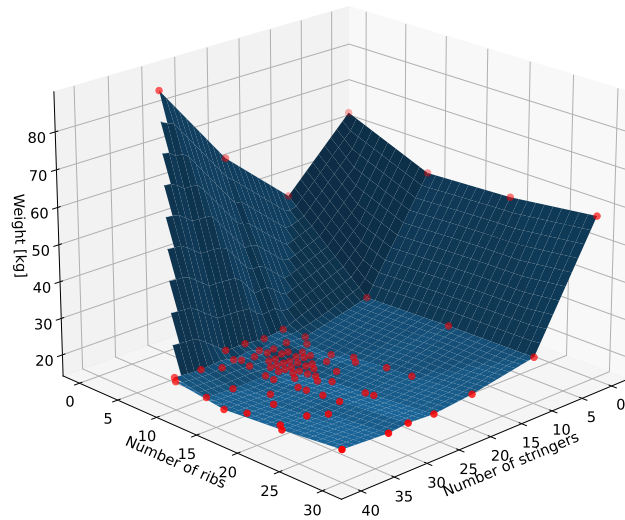


Figure 8.8: 3D surface showing the wingbox weight as a function of the number of stringer and ribs

Choosing the optimum design from this graph leads to all parameters of the final wingbox. These are listed in Table 8.5.

Table 8.5: Summary of structural parameters of the wingbox

Parameter	Value	Unit	Parameter	Value	Unit
Airfoil	NACA 4415	-	Base length stringer	7.5	mm
Location front spar	20%	chord	Flange length stringer	15	mm
Thickness front spar	1.3	mm	Thickness stringer	0.5	mm
Location aft spar	75%	chord	Number of stringers	26	-
Thickness aft spar	1	mm	Number of ribs	14	-
Thickness top panel	0.5	mm	Thickness ribs	1	mm
Thickness bottom panel	0.5	mm	Weight (single wing)	19.21	kg
Stringer type	L-stringer	-			

Given the design in Table 8.5, the performance of the wingbox can be summarised through its tip deflection and tip twist. Figure 8.10 shows this for both loading cases. In Figure 8.9 also the second moment of area in both x and y-direction, the torsional stiffness and the position of the centroid as a function of span can be found. Calculating the maximum tip deflection and tip twist for both cases gives the bounds between which these values will always be. For the deflection, this is between 3.3 and -2.1 cm. For the twist, this is between 1.22 and -1.90°.

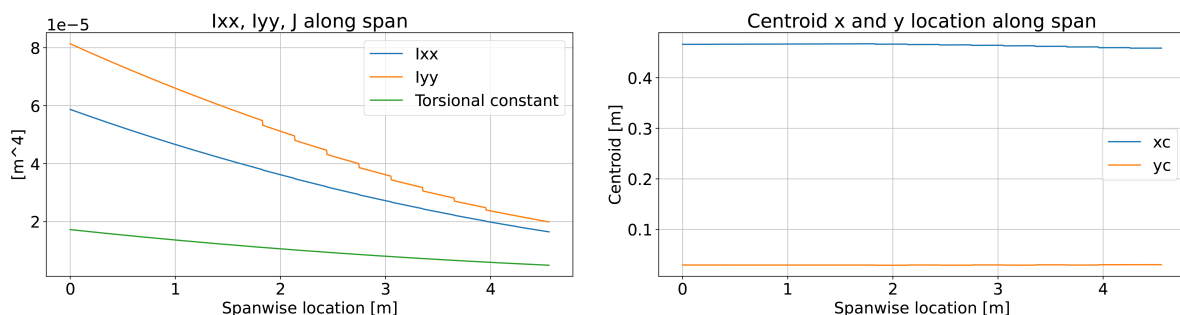


Figure 8.9: Analysis of the wingbox properties I_{xx} , I_{yy} , J and the centroid

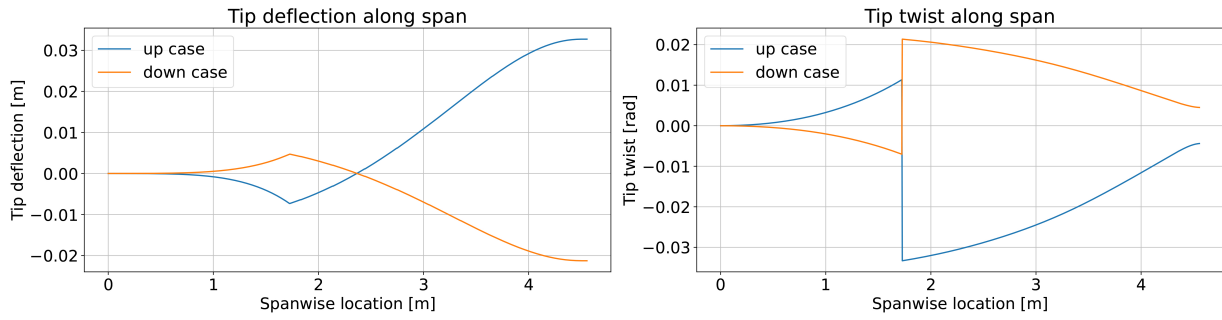


Figure 8.10: Wingbox tip deflection and tip twist

Even though this design does meet all requirements, there is always room for improvement. A few possible improvements for a future iteration include:

- A more thorough study of possible failure modes of the wingbox is advised
- A more detailed design of the wingbox including the leading and trailing edge of the airfoil, together with the geometric twist could be used
- The forces acting on the wingbox in all directions should be considered, for now, it is just the dominant directions

8.2.6. Wing Strut

The wing strut shall be able to partially release the loading from the main wing, while being treated as a truss carrying axial loads only, connected to the wing and fuselage by pins. The geometry can again be sized with Equation 7.5 and Equation 7.6, however, an elliptical cross-section is chosen for aerodynamic purposes so that the ellipse semi-major is aligned with the flow. The location of attachment of the strut on the wing is decided based on a statistical average of braced wing GA aircraft (Cessna Caravan, Skymaster, 152 and 172, Tecnam 2008 and P29, Aviat Husky and Pilatus PC6), being at 44% of the span away from the longitudinal centre line (2.004 m, or 1.504 m from the fuselage), attached directly to the front spar of the wing. It is fixed to the fuselage at the bottom (floor) of the second frame (same longitudinal position as the front wing spar, see Figure 7.3), resulting in a total length of $l=1.65$ m.

After computing the reaction forces (at ultimate loads) of a mid-wing supported by two pints at the root and brace attachment point from the wing loading as described earlier in Section 8.2, the maximum tension and compression loads within the strut are determined. Column buckling is again more constraining than tension, meaning that a minimum weight design urges a large enclosed cross-section. For aerodynamic purposes, a maximum size is put on the ellipse semi-major $a=4$ cm and semi-minor $b=2$ cm.

The material choice is made according to the convention, as described in Section 3.2, with the following weights assigned: raw cost (4), ecological cost (1), CO₂ emissions (0.5), K_{ic} (0.5), material index $\sqrt{(E)}/\rho$ (4). This, with no surprise, outputs steel 4130, followed by Aluminum 5052. The minimum thickness of a steel 4130 strut is $t=1.0$ mm, leading to a mass (single strut) of $m=2.57$ kg. Since buckling is critical, using stainless steel 410 does not save significant mass ($m=2.56$ kg), as it has a similar E to steel 4130.

8.2.7. Attachment to Fuselage

Both attachments of the wing to fuselage and strut to wing/fuselage are realised via pins, allowing for forces P transfer, but no moment transfer. The mounts' (plates) shapes are sized based on where there should be attached, while their thickness is computed so that the attachment withstands pin failure (Equation 8.8), bearing failure (Equation 8.9, critical for strut in compression), net section failure (Equation 8.10) and shear out (Equation 8.11, critical for wing) in both tension and compression. Additionally, a stress concentration factor K_{sc} of 3 is used (Equation 8.12, [10, p. 310]), with $\alpha = 2$ and curvature ρ_{sc} and characteristic dimension c both equal to r_{pin} .

$$\sigma_y = \frac{P}{4\pi r_{pin} t_{pin}} \quad (8.8)$$

$$\sigma_{y,sh} = \frac{P}{2r_{pin} t_{plate}} \quad (8.9)$$

$$\sigma_y = \frac{P}{2t_{plate}(r_{plate} - r_{pin})} \quad (8.10)$$

$$\sigma_{y,sh} = \frac{P}{2t_{plate}(r_{plate} - r_{pin})} \quad (8.11)$$

$$K_{sc} = 1 + \alpha \left(\frac{c}{\rho_{sc}} \right)^{1/2} \quad (8.12)$$

Because of the strut mass and size, its attachment can be realised with a fork-type aligning hole, with locking it with a pin of circular cross section of outside diameter $\varnothing = 12$ mm (full cross section). The mass of a single strut attachment (two used per strut) is $m=0.61$ kg (pin excluded), and is shown on Figure 8.11a. On the other hand, because of the relatively high mass of the wing half and thus trouble with maneuvering with it precisely, a tight fork-type hole aligning should not be used. The plates mounted on the two spars (separated by inter spar separation) should slide in between plates welded to designated fuselage truss corners (two per attachment, as shown on Figure 8.11b), so that once aligned, the order of plates from the front is: fuselage plate 1, front spar plate, small gap, fuselage plate 2, inter spar gap, fuselage plate 3, small gap, rear spar plate, fuselage plate 4. This way, it is easier to "maneuver" the wing half into the attachment, while the attachment still prevents motion in longitudinal direction, once assembled. Here, two short pins should be used (one per spar), with diameter $\varnothing = 40$ mm and minimal thickness $t=0.7$ mm. Both pins' external radius should be around 0.02 mm smaller than the hole diameter⁴, with the lubrication of pins encouraged. The mass of a single wing attachment (two sets used per wing) is $m=0.82$ kg (pin excluded). To ease direct welding onto the fuselage structure, steel 4130 is assumed, although using stainless steel 410 once more allows to save mass, due to the nature of failure modes, where σ_y of the material should be maximised.

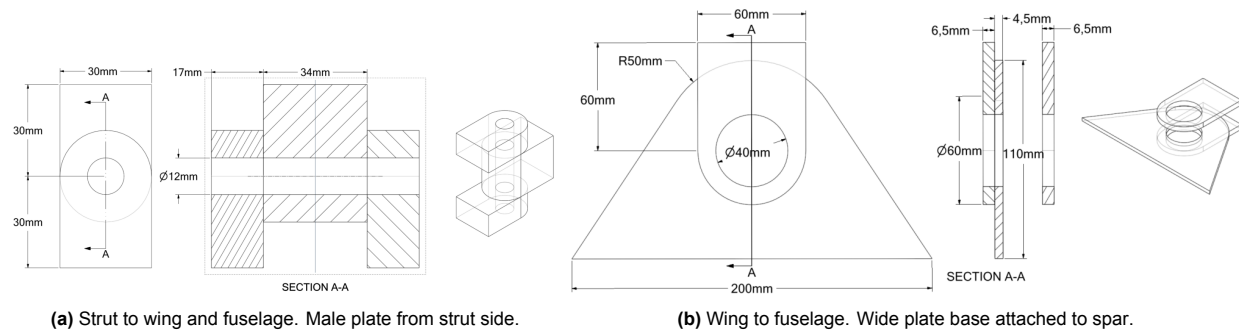


Figure 8.11: Drawing of the attachments of given structure to the fuselage

Drawings presented on Figure 8.11 are a proposition of the design, yet not the only correct one. The minimal thickness of the strut attachment is 34 mm (2×17) from both sides, to prevent bearing failure (critical), given the radii of pin and notch. The minimal thickness of the wing attachment from the fuselage side is 26 mm (4×6.5), while from the wing side 9 mm (2×4.5), given the radii of pin and notches, to prevent shear out (critical).

It is recommended to elaborate on the pin and attachment design for better mass optimisation and integration with the wing and fuselage. Using stainless steel 410 reduces the thickness and mass of the attachments (0.29 kg for wing, 0.24 kg for strut), yet corrosion should be accounted for. Because of time constraints, the current design assumes a single material (same as fuselage) and proposes a solution that might not be the most mass/cost efficient. Ergonomics of pin connection should be looked at. The strut could be elongated or shortened to easily modify the wing dihedral angle.

8.3. Aileron Design

In order to provide the aircraft with a rolling motion, ailerons have to be positioned on the wing planform. As the take-off weight of the aircraft is lower than 6000 kg, the aircraft is also considered a Class-I aircraft and it shall adhere to the requirements in Table 8.6 [19]. Table 8.6 indicates the required bank angles and the time in which these angles need to be achieved for Class-I aircraft according to MIL-F-8785C.

⁴ Metric Standard Bore and Keyway Info, [cited on 26 June 2023]

Table 8.6: Requirements on Class I aircraft to perform bank angle in certain time [41, Table 12.12]

Class I Aircraft				
$\phi_{bank} [deg]$	30	45	60	
$t [s]$	1.3	1.7	1.3	

The ailerons are sized by finding the minimum area of the ailerons for which all three Class-I roll requirements are met and the maximum aileron deflection is not exceeded. In this analysis, a maximum aileron deflection of $\pm 20^\circ$ is used. A safety margin of 10% was included so that the maximum allowed aileron deflection is $\pm 18^\circ$. The turning time is found by estimating the roll moment created by the ailerons and from that estimating the roll rate of the aircraft [19, pp. 677–693]. The chord of the aileron is set to be from the rear spar to the trailing edge which from Section 8.2.3 accounts for 25% of the chord. In Table 8.7, the estimated rolling times for the bank angles of 30, 45 and 60° are shown.

Table 8.7: Design parameters for the aileron and the corresponding roll times for angle of 30°, 45° and 60°

Aileron Parameter	Value	Unit
t_{30°	0.91	s
t_{45°	1.11	s
t_{60°	1.28	s
$y_{aileron_{start}}$	2.10	m
$y_{aileron_{end}}$	4.45	m
$S_{aileron}$	2.43	m ²

As can be seen, the rotation of 60°, from a bank angle of -30° to 30°, is the most limiting. Based on this criterion, the necessary span of the ailerons was determined. The outer end of the aileron was set at 98% of the wing to keep a margin at the tip. At the end of the chapter, the position of the ailerons on the wing planform can be seen in Figure 8.12.

8.4. High-lift Devices

To generate enough lift during take-off and landing whilst keeping the wing planform small, it was chosen to include High-Lift Devices (HLD's) in the design. Flaps are connected to the aft spar and will start at the root of the wing, after which its length is determined based on the required $C_{L_{max}}$ set by Flight Performance in Section 5.1 and 5.5, and the base wing $C_{L_{max}}$ given by Aerodynamics in Section 8.1.7. Subtracting these two results leads to the gap $\Delta C_{L_{max}}$ that needs to be bridged by HLD's. The results from the final iteration can be found in Table 8.8 below.

Table 8.8: Required $\Delta C_{L_{max}}$ High Lift Devices need to provide in different flight conditions

Flight Condition	$C_{L_{max}}$ Required	$C_{L_{max}}$ Wing	$\Delta C_{L_{max}}$ HLD's
Take-Off	1.42	1.42	0
Landing	2	1.42	0.58

Using the information from Table 8.8 the sizing of the HLD's can begin, which starts with selecting the type of HLD used. Table 8.9 shows the types of HLD's considered for this design, together with their lift generating capabilities.

Table 8.9: Additional $\Delta C_{L_{max}}$ generated due to different types of High Lift Devices

HLD type ⁵	Take-Off deflection [deg]	Landing deflection [deg]	$\Delta C_{L_{max}}$ Take-Off [-] ⁶	$\Delta C_{L_{max}}$ Landing
Plain flap	20	60	0.9	0.63
Single slotted flap	20	40	1.3	0.91
Fowler flap	15	40	1.3 c'/c	0.91 c'/c

From Table 8.9, it can be seen that the single slotted and fowler flap are more efficient at generating lift compared to the plain flap, however, this does come at a cost of complexity and/or weight of the design. To keep the design as simple and light as possible, plain flaps will be used as a first estimate.

Using the $\Delta C_{L_{max}}$ calculated previously and the $\Delta C_{l_{max}}$ from Table 8.9 for plain flaps, the required wing surface area S_{wf} that is occupied by flaps can be calculated via the following equation [12, p. 539]:

$$S_{wf} = \frac{\Delta C_{L_{max}} S}{0.9 \Delta C_{l_{max}} \cos(\Lambda_{hingeline})} \quad (8.13)$$

Calculating using the $\Delta C_{L_{max}}$ from Table 8.8, the $\Delta C_{l_{max}}$ from Table 8.9, the surface area from Section 8.1.7 and the $\lambda_{hingeline}$ from the aft spar location as described by Section 8.2.3 leads to the required S_{wf} . Translating this to a flap length is done using the function that describes the chord length over the span of the wing, Equation 8.7. Integrating this function from the root to a distance y , should lead to the area S_{wf} . This accompanying value for y will give the length of the flap, measured from the rootchord.

Performing the calculations described above for both the take-off and landing condition will lead to two required flap lengths, one of which will be more constraining. In order to check the feasibility of the current HLD design, the length of the wing occupied by the flaps and ailerons from Section 8.3 should be less than or equal to half span. When this requirement is not met, a more efficient HLD is chosen and the design steps described above are repeated until this requirement is satisfied.

After iterating using the iteration program, this leads to Table 8.10 below.

Table 8.10: Summary of final design parameters for the High Lift Devices

Flap type	Flap chord	Flap length [m]	Provided $\Delta C_{L_{max}}$ [-]
Single Slotted Flap	22% Local chord ⁷	2.03	0.58

Combining the results from Table 8.7 and 8.10 leads to the fully equipped wing planform, which can be seen in Figure 8.12.

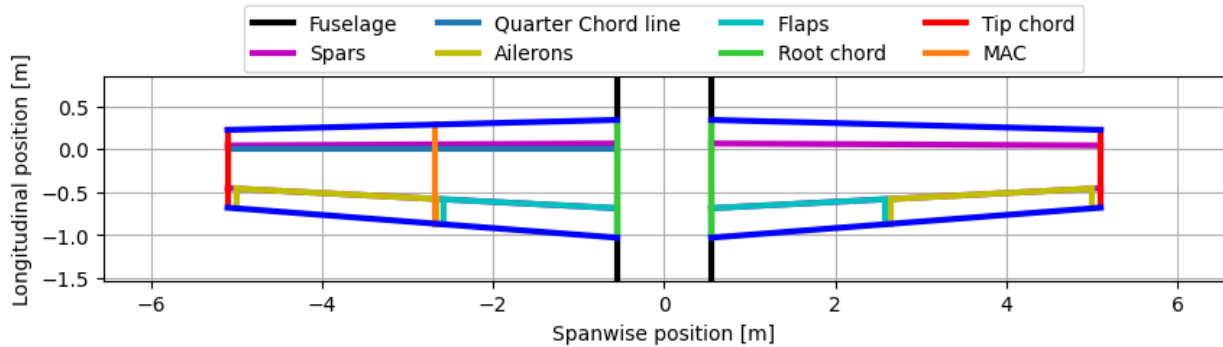


Figure 8.12: Wing planform with indication of control surfaces location and geometrical wing characteristics

From the Tables and Figure 8.12 it can be seen that in order to fit all the control surfaces on the wing, the flaps are connected to the aft spar of the wing, at 75% of the chord. In order to meet the most constraining scenario out of Table 8.6, the ailerons have to occupy a large part of the span which leaves insufficient space for the plain flap. As a result, single slotted flaps will be used to reach the required $\Delta C_{L_{max}}$.

⁵Information from this table is based on [42]

⁶ c'/c is the ratio of the chord with flaps extended (c') over the normal chord length (c)

Empennage Subsystem

Having sized the main elements of the fuselage and wing, a more thorough analysis of the stability and control of the aircraft can be performed. At first, it is needed to estimate the most forward and most after the centre of gravity in Section 9.1. Using this updated range of centre of gravity, the horizontal tail can be sized. Knowing this size, the whole horizontal tail planform can be determined, which is done in Section 9.2. Next, the vertical tail including the rudder is sized in Section 9.3.1. Again, using the sizing the planform is created in Section 9.3.2. Next the rudder design is explained Section 9.3.3.

9.1. Position of Centre of Gravity

As a basis of the sizing of the empennage subsystem, it is necessary to determine the minimum and maximum position of the longitudinal centre of gravity. In order to estimate these accurately, the weight and moment arms of individual subsystems were considered. The weights and moment arms do change throughout the design iteration and thus the position of the centre of gravity is also shifting. In Figure 9.1, a side view of the aircraft after the final iteration is shown.

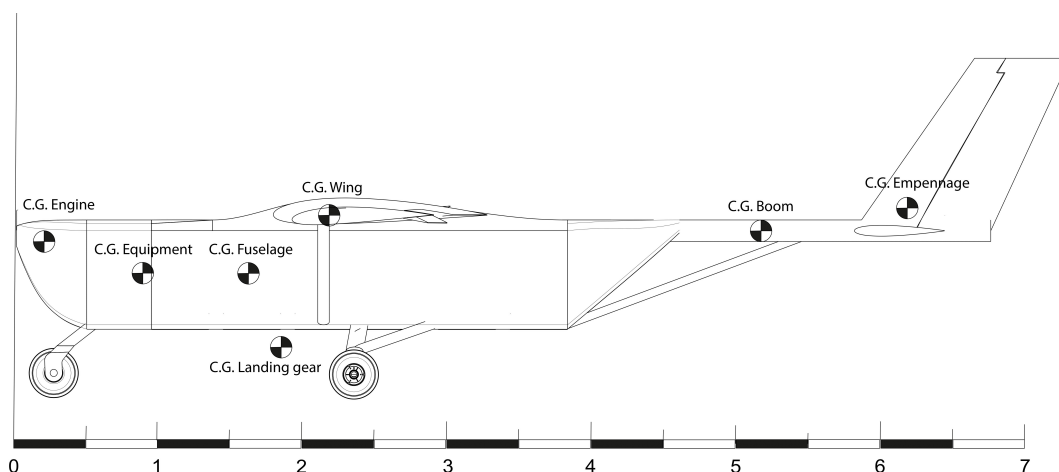


Figure 9.1: Simplified side view of the aircraft, indicating position of centre of gravity of subsystems

During flight, the position of the centre of gravity will shift due to the usage of fuel and the dropping of aid packages. Not all boxes will be dropped at once, which results in a number of loading configurations. These configurations have been given an index, such as '200220', in which each number indicates the number of boxes still present on that row, with the first number being the most forward row in the aircraft. Each of these configurations relates to a different longitudinal position of the centre of gravity, which Figure 9.2 captures in a loading diagram. Using this diagram, the most forward and aft centre of gravity can be estimated as a fraction of the mean aerodynamic chord.

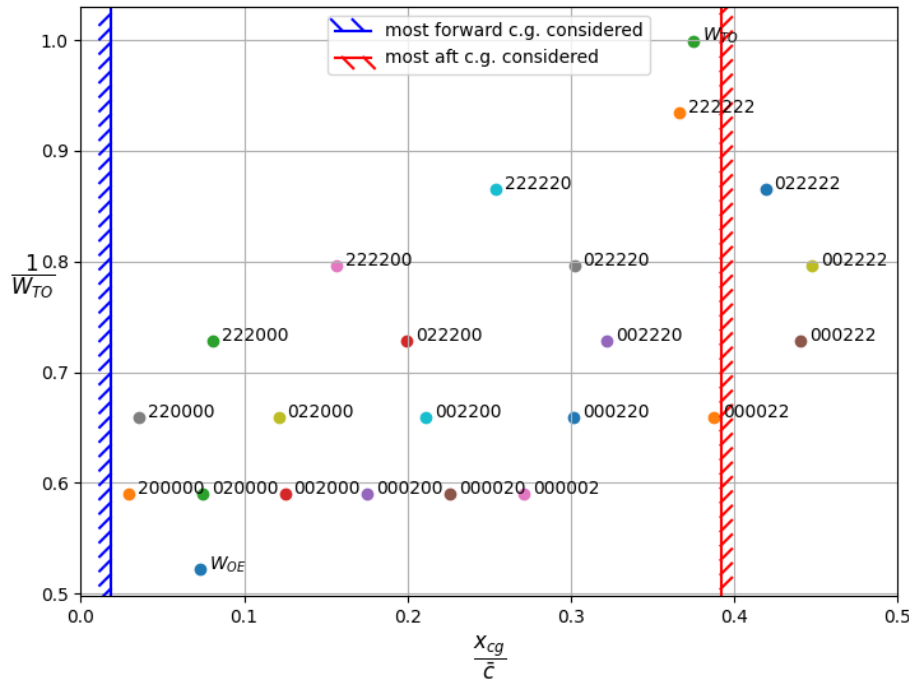


Figure 9.2: Loading diagram of the aircraft as a fraction of take-off weight. Operational constraint set which allows dropping from the back only

The loading diagram in Figure 9.2 starts at the empty weight W_{OE} of the aircraft, which is calculated using Figure 9.1. For the W_{OE} to be calculated, the position of the wing has to be known. It was decided to fixate the location of the wing on the aircraft, as it would reduce the number of variables and therefore complexity in the iterative process of the horizontal tail design, as well as the structural mass of the fuselage. The wing was positioned such that the front spar of the wing is exactly at a node of the second vertical truss of the fuselage as can be seen in Figure 7.3.

This decision results in the wing being placed relatively far forward, which leads to the loading configurations in the diagram skewing backwards, increasing the range in centre of gravity behind the W_{OE} . This large range was reduced by setting an operational limit on the loading configurations attainable in flight, precisely configurations 000022, 000222, 002222 and 022222. As can be seen from Figure 9.2, the operational limit implies the first row of boxes can not be dropped first and that besides 000022 being within the range set, it is too close to the boundary and therefore unadvised to fly with. In general, it is advised to always drop the most aft row, followed by the most forward row, switching back and forth until all payload has been dropped. Packages should always be dropped in pairs to improve lateral stability. In the event of a hatch malfunction in one of the rows, the box in the second front row on the opposite side of the stuck box should be fixed to compensate for this instability. To maximise the amount of payload delivered it could be considered to compensate this instability by deflecting the ailerons, however, this should be checked with rolling requirements.

Applying the restrictions above leads to a smaller centre of gravity range, which is quantified by setting 200000 as the most forward centre of gravity attainable, and W_{TO} as the most aft. A safety margin of 5% of the total range is added to both the most forward and aft centre of gravity to determine the design range. The position of the forward and backward centre of gravity and the distance between them can be found in Table 9.1.

Having determined the position of the most forward and backward centre of gravity, the performance of the aircraft for its stability and control characteristics can be analysed. Following the method described by Torenbeek [43, 44], the stick-fixed neutral stability curve is calculated as follows.

$$\frac{S_h}{S} = \frac{\bar{x}_{cg}}{\left[\frac{C_{L_{\alpha h}}}{C_{L_{\alpha A-h}}} \left(1 - \frac{d\epsilon}{d\alpha} \right) \frac{l_h}{\bar{c}} \left(\frac{V_h}{V} \right)^2 \right]} - \frac{\bar{x}_{ac}}{\left[\frac{C_{L_{\alpha h}}}{C_{L_{\alpha A-h}}} \left(1 - \frac{d\epsilon}{d\alpha} \right) \frac{l_h}{\bar{c}} \left(\frac{V_h}{V} \right)^2 \right]} \quad (9.1)$$

The curve is made for the most constraining case, which for stability is in cruise. To account for stick-free stability, a safety margin of 5% on the distance between the neutral point and aft centre of gravity is added to Equation 9.1, leading to the stability curve for which will be designed.

Next, the controllability curve is calculated as follows.

$$\frac{S_h}{S} = \frac{\bar{x}_{cg}}{\left[\frac{C_{L_h}}{C_{L_{A-h}}} \frac{l_h}{\bar{c}} \left(\frac{V_h}{V} \right)^2 \right]} + \frac{\frac{C_{m_{ac}}}{C_{L_{A-h}}} - \bar{x}_{ac}}{\left[\frac{C_{L_h}}{C_{L_{A-h}}} \frac{l_h}{\bar{c}} \left(\frac{V_h}{V} \right)^2 \right]} \quad (9.2)$$

For controllability, the most constraining case is during landing and will therefore be designed for.

The analysis is performed by generating a scissor plot from which a minimum horizontal tail area can be extracted that will make the aircraft both stable and controllable for a given range in centre of gravity. The plot is made by inserting Equation 9.1 and 9.2 as a function of the centre of gravity location displayed as a fraction of the MAC, \bar{x}_{cg} . Then, the centre of gravity range found in Figure 9.2 is fitted in between the stability and controllability curves. The lowest position on the vertical axis for which the entire centre of gravity range fits between the curves, will be the minimum horizontal tail area S_h displayed as a fraction of the main wing area S . For the design concept after the final iteration, the scissors plot is shown in Figure 9.3 below.

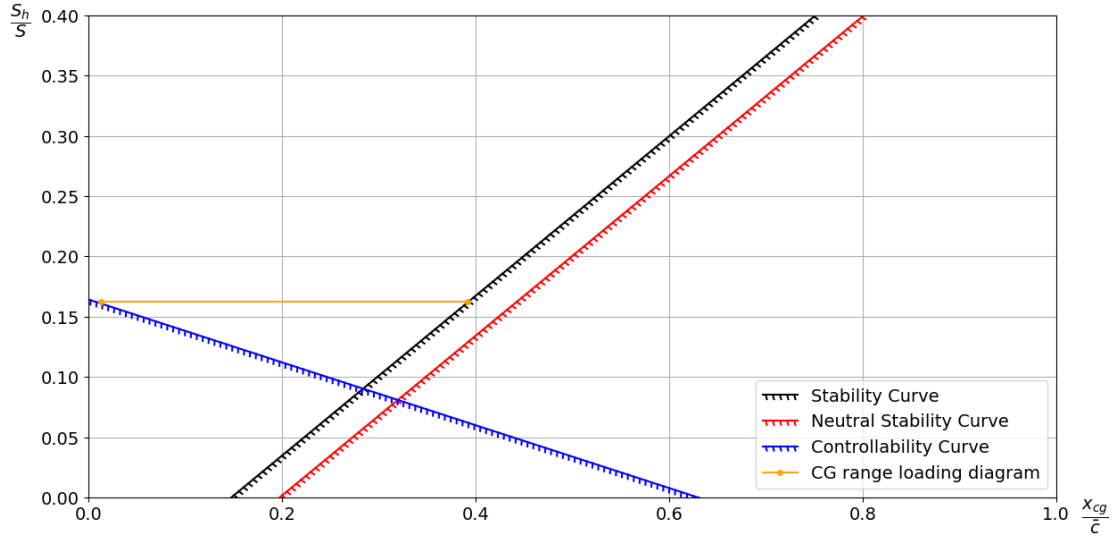


Figure 9.3: Scissor plot constructed for horizontal tail sizing based on limits in controllability and stability for the c.g. range of the aircraft.

As can be seen in the plot, despite the large c.g. range, both the controllability and stability curve are limiting. As a result, the required size of the horizontal tail is as small as it could possibly be, having an area S_h equal to 16.2% of the wing area S .

Concluding, the center of gravity positions found in this section are summarised in Table 9.1. The design value for $\frac{S_h}{S}$ is thus found to be $0.162 \pm 5\%$. In the next sections, the horizontal planform will be sized based on this fraction.

Table 9.1: Estimations of the wing position, the longitudinal positions of the centre of gravity and the sizing of the horizontal tailplane.

Parameter	Estimation	Unit
$X_{xg_{OE}}$	$0.0690 \pm 2.5\%$	$1/\bar{c}$
$X_{cg_{fwd}}$	$0.0120 \pm 2.5\%$	$1/\bar{c}$
$X_{cg_{aft}}$	$0.391 \pm 2.5\%$	$1/\bar{c}$
$X_{cg_{range}}$	$0.379 \pm 5.0\%$	m
$\frac{S_h}{S}$	$0.162 \pm 5.0\%$	-

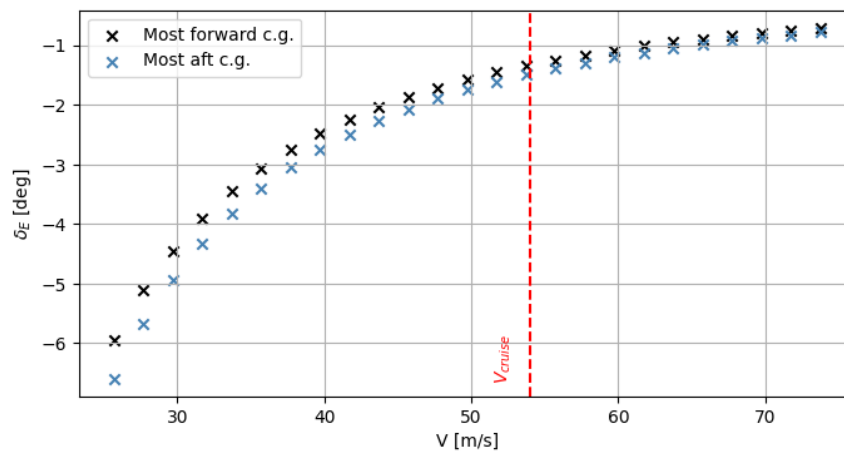
9.2. Horizontal Tailplane

The minimum required area for the horizontal tailplane that was found in the previous section ensures the stability and controllability of the aircraft. In this section, a more detailed design will be performed of the horizontal tailplane.

9.2.1. Elevator Design

An important element of the horizontal tailplane is the elevator which is deflected to stabilise the aircraft. From the detailed trade-off the decision was taken to implement a full-moving or flying tailplane in our design, a configuration in which the whole horizontal tailplane will act like an elevator. Having a full-moving tailplane allows for a more effectively controllable elevator. Next to this, it is easy to manufacture and detach in transport configuration.

As a result, the dimensions of the elevator will be equal to those of the horizontal tailplane. Using this geometry, the maximum required elevator deflection can be found for different velocities, using the methods described in the Aircraft Design book [19]. The result of this analysis can be found in Figure 9.4 below. It should be noted that downwash is modelled only to a limited extend here.

**Figure 9.4:** Maximum rudder deflection needed at velocities from stall velocity to 1.4 of the cruise velocity. Analysis performed for most forward and backward centre of gravity.

Because of the high effectiveness of the full-moving tailplane, for all velocities, the maximum deflection will be smaller than 5° . This is within the capabilities of the elevator, even adding for example 3° additionally to account for downwash. For a complete design of the elevator, a trim tab should be added to the design. However, due to time constraints this was deemed unfeasible and is therefore left as a recommendation for the next design phase.

9.2.2. Planform

Having a combined elevator and horizontal tailplane, the planform of the horizontal tailplane can now be designed. Currently, the design includes a detachment of the horizontal tailplane during transportation to allow for more design freedom and therefore higher aerodynamic efficiency. The case where this mechanism

is not needed is also investigated, this is described in Section 9.2.5.

Downwash

Because of the downwash of the main wing, the horizontal tail experiences a different angle of the incoming flow compared to the (almost) undisturbed flow at the main wing. Thus, the horizontal tailplane should be mounted at an angle α_h rather than i_h , described by Equation 9.3 and Equation 9.4 [19].

$$\epsilon = \epsilon_0 + \frac{\partial \epsilon}{\partial \alpha} \alpha_w = \frac{2C_{L_w}}{\pi \cdot AR} + \frac{2C_{L_{a_w}}}{\pi \cdot AR} \alpha_w \quad (9.3)$$

$$\alpha_h = \alpha_f + i_h - \epsilon \quad (9.4)$$

Airfoil Selection

Throughout the mission, both positive and negative lift are required from the horizontal tailplane, because of center of gravity movement. This requires the tailplane to have similar behaviour in both conditions and thus a symmetrical airfoil is used [19]. This thus limits the selection to the NACA-00XX series.

The thickness of the airfoil is decided by a trade-off between drag and stall angle (α_s). Moreover, increasing thickness increases the stall angle, but also increases the drag. Standard values for the incidence angle are between -1 and -2° and normal stall angles are around $\pm 15^\circ$ [19]. Like the main wing, the horizontal tail is angled to optimise the design for cruise conditions. This is done by setting the angle such that the required lift for pitch stability is produced. This assures that minimal force will be required for pitch stability throughout the entirety of the sortie. Because of the effect of downwash described above not the angle of attack (α_h), but the incidence angle (i_h) is set to this angle. Since the stall of the horizontal tailplane is detrimental, the angle of attack can not exceed this fraction of $\frac{2}{15}$ of the stall angle. To reduce skin friction drag, it was also decided to limit the minimal angle to $\frac{1}{15}$ of the stall angle. Lower angles would indicate the thickness could be reduced, which in turn reduces drag. Thus $\frac{1}{15} \leq \left| \frac{\alpha_h}{\alpha_s} \right| \leq \frac{2}{15}$, for cruise condition (α_h) to find a good balance between high stall and low drag.

Throughout the design iteration the airfoil thus changes between the NACA0006, NACA0009 and NACA0012 to meet the above stated requirement. For the final design this results in the selection of the NACA0012 airfoil.

Sweep

Like the main wing, the horizontal tail will have no sweep. Employing horizontal tail sweep has similar benefits to adding sweep to the main wing. It can improve the stability, move the center of gravity location or delay compressibility effects. Due to the low cruising speed, compressibility is not a concern. Furthermore, stability is taken care of by the surface area and tailplane location. Aerodynamic advantages are not enough to justify the increased manufacturing cost as explained in Section 8.1.2.

Aspect Ratio, Taper Ratio and Incidence Angle

The horizontal tailplane is analysed using lifting line theory similar to the main wing, as described in Section 8.1.5. The model takes geometry inputs and outputs the lift distribution, lift coefficients and induced drag. The geometry has been optimised to obtain an efficient lift distribution. However, slight modifications are made to the way it is applied to the horizontal tailplane. These modifications are listed below:

- **Aspect Ratio:** Again the aspect ratio was chosen by trading off the induced drag decrease but weight increase as the ratio increases. Many different options were computed and an aspect ratio of $\frac{2}{3}AR_w = 5.33$ was decided upon as the induced drag decrease of increasing it further did not outweigh the added weight and complexity. Moreover, increasing AR from 4 to 5.16 results in a induced drag decrease of 21.9% whereas increasing it further to 6 only sees an induced drag decrease of 15%. Since the induced drag of the horizontal tailplane is small portion of the total aircraft lift it was decided to not increase the aspect ratio further. Also, $\frac{2}{3}AR_w$ is a commonly used and well proven value [19].
- **Taper Ratio:** From plotting the lift distribution, it is found that adding taper has very little effect on reducing drag while it does increase tooling cost by approximately 5% and also increases complexity [45]. Moreover, even changing the taper ratio from 1 to 0.1 only saw a decrease in induced drag of the horizontal tailplane of 0.1 %.

- **Incidence Angle:** As mentioned above in the downwash and airfoil selection the angle with which the horizontal tail is mounted is the incidence angle i_h , whereas it experience and angle off attack α_h due to the effect of downwash. This angle of attack is sized by finding the required lift of the horizontal tailplane to counteract the moment induced by the main wing on the aircraft in cruise condition. Rewriting Equation 9.4 then gives i_h with which the tailplane should be mounted such that it does not require any force to sustain this angle in flight.

AVL Refinement

The reasoning, limitations and use of the AVL software have been described in Section 8.1.7. Using AVL the incidence angle and effective angle of attack of the horizontal tail have been refined, next to validating the overall planform and its performance. Also, AVL has also been used to validate the stability characteristics of the aircraft, presented in Section 13.2.

The final geometry and aerodynamic characteristics of the horizontal tailplane are found in Table 9.2.

Table 9.2: Summary of final horizontal tailplane parameters after AVL refinement.

<i>Airfoil</i> [—]	S_h [m ²]	b_h [—]	AR_h [—]	λ_h [—]	i_h [deg]	α_h [deg]	α_{th} [deg]	$\Lambda_{c/4h}$ [deg]	C_{root_h} [m]	MAC_h [m]
NACA 0012	1.79	3.09	5.33	1.00	2.44	-0.0555	0.00	0.00	0.580	0.580
Contingencies	± 5%	± 2.5%	-	-	±50%	± 50%	-	-	± 5%	± 5%

Potential Later Addition of Vortex Generators

Currently the design does not require the horizontal to fly near stall angles. If however, this turns out to be necessary in test flights, vortex generators could be added later to the design. Even after entering the manufacturing stage these can be added [19]. This however comes at a drag penalty and is therefore not added in the current design. Vortex generators energize the boundary layer flow by inducing circulation near the edge of the boundary layer. By energizing (in terms of kinetic energy) the boundary layer it gives the boundary layer more 'strength' to handle higher pressure gradients without separation. Thus, delaying separation at high angles of attack, and thus delaying stall of the horizontal stabilizer.

9.2.3. Structure

Because the horizontal tail needs to rotate as an integral body with respect to the tail boom, it cannot be simply fixed onto the boom. Instead, a circular thin-walled tube is used to constitute a single, common spar for both horizontal tail surfaces, passing through the tail boom on two plain bearings (since tail boom is thin-walled, the spar passes through two surfaces). The control mechanism can thus be mounted inside of the tail boom, for instance, two parallel cables running through the entire tail boom, attached to the top and bottom tubular surface of the tail spar.

Assuming that the net aerodynamic force acts 1/3 of the horizontal tail half-span away from the boom, the spar length is $l = 1/3 b_h$ with 10 cm as a margin from both sides, giving a total $l=1.23$ m. The horizontal tail ribs supporting the aerodynamic surface should then be directly fixed on the rotating spar. The sizing loads induce a shear force F_s within the spar (Equation 7.7), maximum bending moment M at the bearing location (Equation 7.8) as well as torsion T (Equation 9.5), causing twist (Equation 9.6). Here, the shear modulus G is estimated with Equation 9.7, where the Poisson's ratio ν is approximated as 0.33 for metals.

$$T = \frac{c_h}{4} \Delta P_h = 2t A_m \sigma_{y,sh} \quad (9.5)$$

$$\frac{d\theta}{dz} = \frac{T}{4A_m^2 G} \frac{2\pi r}{t} \quad (9.6)$$

$$G = \frac{E}{2(1 + \nu)} \quad (9.7)$$

Because the centre of pressure changes with angle of attack, the maximum load ΔP_h (as computed by Equation 7.4, critical) is assumed to act maximum a quarter chord away $0.25c_h$ from the spar, which itself is located at $0.25c_h$, to minimise the need to complex trimming. Once more, the spar cross-sectional area and moment of inertia (bending is critical) shall be maximised, however imposing a maximum value on the radius $\varnothing_{max} = 7.0$ cm is necessary, also because of the tail boom diameter of 15 cm. Although the bending

moment is critical in this case, the twist shall be checked, with a limit imposed by the control and stability department of 1° .

The standard material choice procedure has been used, with weight: raw cost (4), ecological cost (1), CO_2 (0.5), fracture toughness (0.5), twisting material index G/ρ (2), tension material index σ_y/ρ (3). The tension material index is ranked higher than the twisting one, as for most design iterations, the twisting requirement has been met. This results in the steel 4130 scoring the highest, followed by stainless steel 410. Aluminum 5052 (used for wing box) scores fifth, following other steels. Because the spar has to interact with the aluminium aerodynamic structure and bearing material, anti-corrosion coating is encouraged. The steel 4130 spar thickness is $t=0.6$ mm, with a total mass of $m=1.27$ kg and twist $\theta = 0.81^\circ$. Interestingly, for stainless steel 410, the twist angle is critical, and thus a minimal thickness for $\theta_{twist} < 1^\circ$ is $t=0.6$ mm with $m=1.27$ kg.

In future design steps, the same method and tools developed for the wingbox design (Section 8.2.3) should be tuned to the application of the horizontal and vertical tail. The vertical tail can have an integral wingbox, while the full turning horizontal tail shall be attached to the rotating spar.

9.2.4. Aeroelastic behaviour

The aeroelastic behaviour of the horizontal tail can briefly be addressed by analytically assessing the divergence speed and flutter occurrence. A single horizontal tail half is then modelled as the designed spar, with the load (half of maximum expected, ΔP_{man} , applied at its tip (as designed for, see Section 9.2.3). Its bending stiffness can then be computed as $k_h = 3EI/L^3$ and torsional as $k_\theta = \Delta P/\theta_{twist}$. Implications of changes in these assumptions are addressed at the end of this section.

Divergence

For a static divergence analysis, the horizontal tail can be modelled as supported on a torsional spring support of twisting stiffness k_θ (from twist of the spar), with its local weight W at CG at distance d from support, lift L at distance from support e . By moment balance around the support can be described by Equation 9.8 [46][47]:

$$M_{ac} + L \cdot e - W \cdot d - k_\theta \cdot \theta = 0 \quad (9.8)$$

With small angle approximation, the angle of deformation by aerodynamic load can be computed by [46] [47]

$$\theta = \frac{qScC_{Mac} + qSeC_{L,\alpha}\alpha_0 - Wd}{k_\theta - qSeC_{L,\alpha}}$$

The deformation approaches infinity (divergence), when the divergence speed U_D is reached, and can be derived by solving for the dynamic pressure q .

$$U_D = \sqrt{\frac{2k_\theta}{\rho S e C_{L,\alpha}}} \quad (9.9)$$

The divergence speed occurs at $U_D = 600.3$ m/s (698.5 m/s at cruise air density), which is outside of the flight envelope. U_D decreases to 424 m/s when doubling the tail span (currently, the spar extends to just above 1/3 of the tail span, and is supported by the tail boom plain bearing), to 150 m/s when halving the spar thickness and radius, to 351 m/s when changing the material to Al 5052, but is independent of maximum tail load (see Equation 9.9). It is therefore recommended to carefully sizing the spar, although the safety margin for divergence is significant.

Flutter

Flutter refers to the self-sustained oscillations arising from a fluid-structure interaction. It is a dynamic, two-degree of freedom oscillatory mode, assumed as an amplified harmonic. An attempt is made to identify the velocity conditions, at which the amplification factors transition from negative (damping) to positive (growing). For this, the horizontal tail can be modelled as supported on a transitional spring of stiffness k_h , and torsional spring of stiffness k_θ . The lift and moment as a function of deformation angle $\theta(t)$ can be expressed as [47, p. 30]:

$$L(t) = qSC_{L,\alpha}\theta(t)$$

$$M(t) = 2ebqSC_{L,\alpha}\theta(t)$$

This leads to the following coupled system of equation [47, p. 31]:

$$m\ddot{h} + S_\theta\ddot{\theta} + k_h h + qSC_{L,\alpha}\theta(t) = 0$$

$$S_\theta\ddot{h} + I_\theta\ddot{\theta} + k_\theta\theta - 2eqbSC_{L,\alpha}\theta(t) = 0$$

With the static moment S_θ , mass moment of inertia I_θ , half tail chord b and time derivatives of the vertical displacement h and angular displacement θ . The characteristic equation can be solved for complex roots, which subsequently are plotted as a function of air speed on Figure 9.5.

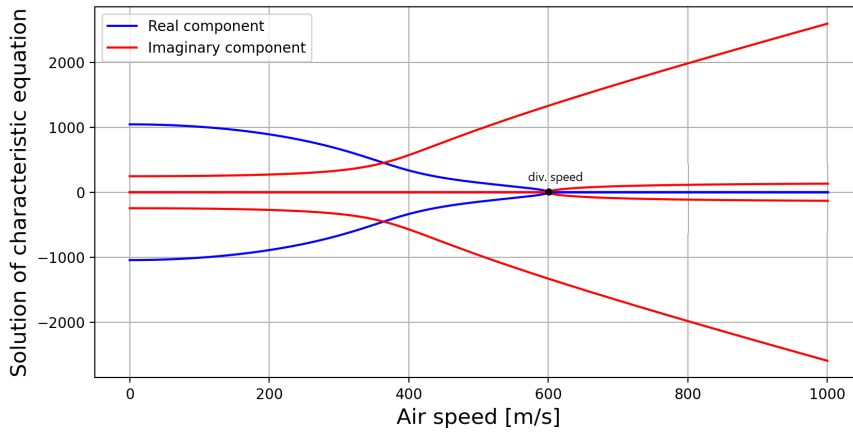


Figure 9.5: Flutter diagram, showing the real and imaginary part of characteristic equation roots, with indicated divergence speed

The imaginary component corresponds to the oscillation frequency, thus its negative part should be ignored. The real part corresponds to the mode growth rate. The behaviour shown by Figure 9.5 shows a separated frequency branches, thus flutter does not occur. The divergence mode appears at high air speed, U_D , as computed. Changing the sign of e , thus causing the force application point to move behind the spar, changes the shape of the curves, yet flutter does not occur.

The analysis is made based on the final design geometry of the aircraft, yet the assumptions of aerodynamic load application on the tail and its mass are rough. It is advised to elaborate on the aeroelastic analysis of the aircraft, by considering more detailed structure and aerodynamic load description, increasing the degrees of freedom of potential motions and confirming analytical results by experimental tests. Additionally, the tail boom is also a beam that can enter in resonance, thus full tail and boom analysis should be performed. The aileron reversal shall also be addressed.

9.2.5. Option Without Detachment

It has also been investigated what the penalty would be by limiting the horizontal tailplane's span to the width of the 40 ft ISO containers. This limits the aspect ratio to 2.77 and with that approximately doubles the lift-induced drag of the horizontal tailplane. More importantly, it reduces the $C_{L_{\alpha_p}}$ by a factor of nearly two, this increases the required surface area of the horizontal tail by such an amount that the design becomes unfeasible. To prevent this the boom length should be increased to increase the moment arm, or the wing position should be altered. Repositioning the wing however causes the vertical loads to no longer be induced in vertical elements directly anymore as described in Section 8.2.7. Limiting the wing span of the horizontal tail thus requires a considerable redesign of the structure and does thus not seem feasible within this design stage. This could be looked into in more detail in later stages if this added benefit is considered significant enough. But it would require redesigning the fuselage truss structure around this new wing position.

9.3. Vertical Tailplane

After the horizontal tailplane has been sized to improve longitudinal stability, the vertical tailplane will now be sized to improve lateral stability. So at the start of the section, in Section 9.3.1, the minimum required size of the vertical tail is determined. Then, in Section 9.3.2, a decision is made on the wing planform of the vertical tail. And at last, in Section 9.3.3, the rudder will be sized based on cross-wind requirements.

9.3.1. Sizing

The vertical tail is crucial for the directional stability of the aircraft. From the system requirements, a minimum directional stability coefficient, C_{n_β} , can be found. Based on this design stability coefficient, a required tail volume can be found [12]. This is achieved by separating the directional stability effect in the effect caused by the vertical tail and the effect caused by other elements of the aircraft, as can be seen in Equation 9.10.

$$C_{n_\beta} = (C_{n_\beta})_{A-h} + \eta_v c_{Y_{v\alpha}} \left(1 - \frac{d\sigma_v}{d\beta}\right) \left(\frac{V_v}{V}\right)^2 \frac{S_v \cdot l_v}{S_w \cdot b} \quad (9.10)$$

It is assumed that $\frac{V_v}{V} = 1$ and $\frac{d\sigma_v}{d\beta} = 0$. The interference between the wing and the fuselage is captured in the term $(C_{n_\beta})_{A-h}$. The derivation of this term can be found in Equation 9.11.

$$(C_{n_\beta})_{A-h} = C_{n_{\beta_{fus}}} + C_{n_{\beta_{prop}}} + \Delta_i C_{n_\beta} \quad (9.11)$$

As can be seen from Equation 9.11, the stability coefficient, $(C_{n_\beta})_{A-h}$, consists of three factors, namely interference caused by the fuselage, the propeller and the wing position. The required directional stability coefficient, C_{n_β} was chosen to be 0.065, as it is stated by REQ-USER-AC-SC-01, plus a safety margin of 10%. Concluding, in Table 9.3 estimations for the directional stability coefficients are given. Next to this, the design size of the vertical tail has been selected based on these stability coefficients.

Table 9.3: Estimations of the directional stability coefficients and the required size of the vertical tail

Parameter	Estimation	Unit
$C_{n_{\beta_{req}}}$	0.065	-
$C_{n_{\beta_{fus}}}$	-0.0237	-
$C_{n_{\beta_{prop}}}$	-0.0047	-
$\Delta_i C_{n_\beta}$	-0.017	-
$(C_{n_\beta})_{A-h}$	-0.0454	-
$\frac{S_v}{S}$	0.074	-

9.3.2. Planform

Using the required vertical tailplane size from directional stability requirements the full planform can be sized. An important design driver here is the ability of the vertical tailplane to resist the engine torque. This influences the incidence angle of the vertical tailplane. Vertical tail sizing and design is a difficult subject and due to the high uncertainty in the design the possible later attachment of a dorsal fin after experimental flight is also explored.

Airfoil Selection

Airfoil selection has been performed in a similar matter as the horizontal tailplane, explained in Section 9.2.2. However, for the vertical tail there is no effect of downwash of the main wing. Next to that, the downwash of the propeller wake is assumed zero at this stage of the design. This method gives an airfoil selection for the vertical tail of the NACA 0009.

Sweep

Adding sweep to the vertical tail increases the yaw moment arm and therefore increases the directional controllability. However, this therefore also worsens the directional stability. This angle was thus derived from the required moment arm for the direction stability found using methods described in Section 9.3.2, together with the boom length. The quarter chord sweep angle of the vertical tail is 35° , as this gives the correct balance between directional controllability and stability. This is also a common value for general aviation aircraft [19], indicating the method is correct. In case this is insufficient the effective sweep can be altered by adding a dorsal fin as explained more in Section 9.3.2.

Aspect Ratio, Taper Ratio and Incidence Angle

- **Aspect ratio:** The aspect ratio is limited by the maximum span of the vertical tail. The span is limited to 1.2 m due to the height of the transport container as shown in Figure 14.3. As the surface area is also fixed by stability requirements, the aspect ratio comes out to be 1.92.
- **Taper ratio:** Taper ratio on the vertical wing reduces the bending stresses on the structure, positively effecting its weight. However, it also reduces the yaw moment arm as a bigger proportion of the lift is generated near the root. Taking these two considerations into account together with the spanwise efficiency factor resulted in a optimum being selected at a taper ratio of 0.7 for the vertical tail.
- **Incidence Angle:** The incidence angle of the vertical tail is designed such that sufficient force is generated to counteract the torque of the engine in cruise condition. The moment of this torque is found by Equation 9.12, where P is the power in watts and ω the rotational speed in radians per second. The incidence angle is set such that this moment around the aircraft's x-axis is generated in cruise condition. Currently the wake of the propellers is not taken into account in the planform and assumed insignificant. This should however be looked into more in later design stages.

$$T = \frac{P}{\omega} \quad (9.12)$$

AVL Refinement

The reasoning, limitations and use of the AVL software has been described in Section 8.1.7. Using AVL the performance of the rudder and vertical tail as a whole has been verified. Also, AVL has also been used to validate the stability characteristics of the aircraft, described in Section 13.2.

The final geometry and aerodynamic characteristics of the vertical tailplane are found in Table 9.4.

Table 9.4: Summary of final horizontal tailplane parameters after AVL refinement.

<i>Air foil</i>	S_v	b_v	AR_v	λ_v	i_v	$\Lambda_{LE_{c/4}}$	C_{root_v}	MAC_v
[—]	[m ²]	[m]	[—]	[—]	[deg]	[deg]	[m]	[m]
NACA 0009	0.76	1.20	1.92	0.70	1.44	35.00	0.74	0.63
Contingencies	± 5%	± 2.5%	-	-	±25%	-	± 5%	± 5%

Dorsal Fin

As aforementioned, a dorsal fin can be added in case the vertical tail sizing turns out to be insufficient during test flights. A dorsal fin not only increases the surface area of the vertical tail, it also reduces the minimum control speed during take-off. The big advantage of a dorsal fin is the fact that it can be added to design while already being in manufacturing stage already.

9.3.3. Rudder Design

The requirements for the design of the rudder are based on directional control. For single-engine low-weight aircraft, there are three relevant requirements on the performance of the aircraft that have to be fulfilled by the aircraft [19, pp. 685-713][41].

1. Cross-wind landing: for a Class-I aircraft, a cross-wind of at least 20 kts is considered. At the flight condition, the aircraft shall have to counteract the sideslip angle, β , by deflecting the rudder without exceeding its maximum deflection of $\pm 30^\circ$.
2. Coordinated turn: the aircraft shall be able to perform a coordinated turn by deflecting the rudder. A coordinated turn is defined as a turn with no net lateral acceleration, a constant turn rate, and a constant turn angle.
3. Adverse yaw: in a coordinated turn, aileron deflection will cause a yaw moment. The rudder is required to counter this yaw moment.

As the aircraft considered is a small single-engine aircraft, the cross-wind landing criterion is usually the most critical. It is expected that this will also be the case for this type of aircraft as it will operate in difficult weather conditions during operation. Coordinated turns will also be able to be performed without rudder deflection. Next to that, adverse yaw can also be countered by differential aileron deflection. Hence, a

first estimation of the rudder will be performed based on this requirement. The maximum side slip angle is calculated from the velocity of the cross-wind and the approach velocity of the aircraft. Next, the stability derivatives with respect to side slip angle β are estimated. Then a fraction of the total chord of the vertical tail is assumed and for this fraction, the required rudder deflection is calculated. The minimum required fraction of the chord is then found to be the fraction of the chord for which the required rudder deflection is just below its maximum deflection. It has been decided to make the span of the vertical rudder equal to the span of the vertical tail as it is desired to have a large moment arm. Figure 9.6 shows the required rudder deflection to produce a moment that counters the cross-winds of 18, 20, and 22 kts for a range of chord fractions. In the figure, the maximum required is indicated by the red line at 30° . A margin is included and a maximum design rudder deflection was chosen to be 27° .

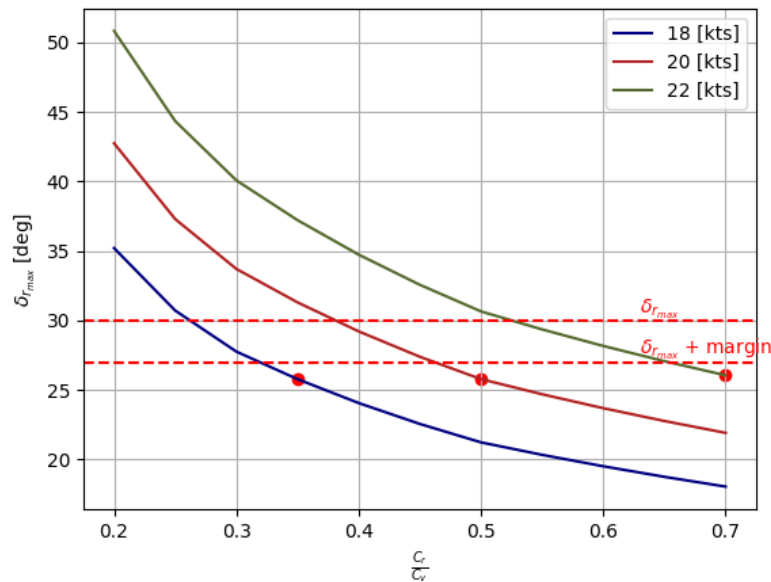


Figure 9.6: Required rudder deflection to counter a cross-wind requirement of 18, 20, 22 kts for different $\frac{C_r}{C_v}$

As can be seen from the figure, for a cross-wind of 20 kts, a design point was chosen of $\frac{C_r}{C_v}$ of 0.50. As has been mentioned before the span of the rudder will be equal to the span of the vertical tail. The area of the rudder will then be 0.39. The chosen geometry for the rudder can be found in Table 9.5.

Table 9.5: Characteristics of rudder design

Parameter	Estimation	Unit
$\frac{C_r}{C_v}$	0.50	-
\bar{c}_{rudder}	0.41	m
b_{rudder}	1.20	m
S_{rudder}	0.49	m ²
$\delta_{r_{max}}$	25.77	deg

Undercarriage Subsystem

Having a better idea of the longitudinal and vertical range in the centre of gravity, a more accurate estimation can be made for the undercarriage subsystem. In this chapter, the design of the landing gear will be separated into three parts. At first in Section 10.1, a type of landing gear is selected. Then using this type of landing gear and the requirements for landing gear, the landing gear was positioned in Section 10.2. Then at last, the structure of the landing gear will be discussed in Section 10.3.

10.1. Landing Gear Selection

Different aircraft require different types of landing gear. Hence, first, the landing gear configuration that is appropriate for the design concept and the type of landing gear are selected.

10.1.1. Landing Gear Configuration

As a start to the design of the landing gear, a landing gear configuration has to be chosen. This was done by comparing the performance of five different landing gear configurations by cost, weight, manufacturability, landing/take-off and stability characteristics. These criteria were then weighted based on their relevance. Cost and manufacturability were considered as most crucial in the design of the landing gear. Four types of landing gear configurations were considered, namely the bicycle, tail-gear, nose-gear and quadricycle. Figure 10.1 shows the results of the performed trade-off between the landing gear configurations. The scores in the matrix are based on the sizing method discussed by M. H. Sadraey [19]. At the top of the matrix, a simplified bottom view for each configuration is shown.

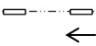

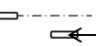
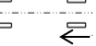
					
	Weight	Bicycle	Tail-gear	Nose-gear	Quadricycle
Cost	0.4	7	6	4	2
Aircraft Weight	0.15	4	6	7	9
Manufacturability	0.2	4	5	7	9
Take-off/landing run	0.1	4	6	10	5
Stability on ground	0.1	2	7	9	10
Stability while taxing	0.05	3	1	8	10
Total	1	4.95	5.65	6.35	5.95

Figure 10.1: Trade-off matrix comparing landing configurations, scored on six criteria on a scale of 1-10.

As can be seen, for the given weights, the nose-gear configuration outperforms the other configurations. It scores especially well in landing performance as the loads at landing are better distributed.

10.1.2. Landing Gear Storage

Now that the landing gear configuration is known, an appropriate way of storing the landing gear can be chosen. A choice has to be made between fixed or (partially) retractable landing gear. Fixed landing gear has the main advantages of being cheaper, lighter, and easier to manufacture and maintain in comparison to retractable landing gear. On the other hand, the fixed landing gear will cause a significant increase in drag. Hence, more fuel will be needed to perform the same mission profile. Next to this, the cruise speed of the aircraft will also be lower, which increases the mission duration. Given the mission profile and design space, in which cost and manufacturability are of great importance, the fixed landing gear was considered the most suitable.

10.2. Placement

As a next step in the design of the undercarriage subsystem, the longitudinal and lateral positions of the front and main landing gear have to be determined. From this determination follow the position of the wheel axes of the landing gear. The longitudinal and lateral positions are constrained by a number of limits, which are presented below [12, pp. 349-360].

- I Limit of main landing gear position caused by tip-back angle
- II Limit of main landing gear position to prevent turnover
- III Limit on nose wheel caused by minimum load of 8% of MTOW: the aircraft will have controllability issues if the load on the nose wheel is less than 8%
- IV Limit on nose wheel caused by maximum load of 15% of MTOW: the force needed for steering and braking will become too large if the load on the nose wheel is larger than 15%.

In the design process, once every two iterations, the front and main landing gear have to be positioned on a plot in which these limits are indicated. This dynamic model continuously updates the location of the limits based on the design parameters. In Figure 10.2, for the final iteration, the limits on the longitudinal and lateral position of the landing gear are shown. Also, the design positions of the front and main landing gear are indicated by a dark green colored triangle and crosses respectively.

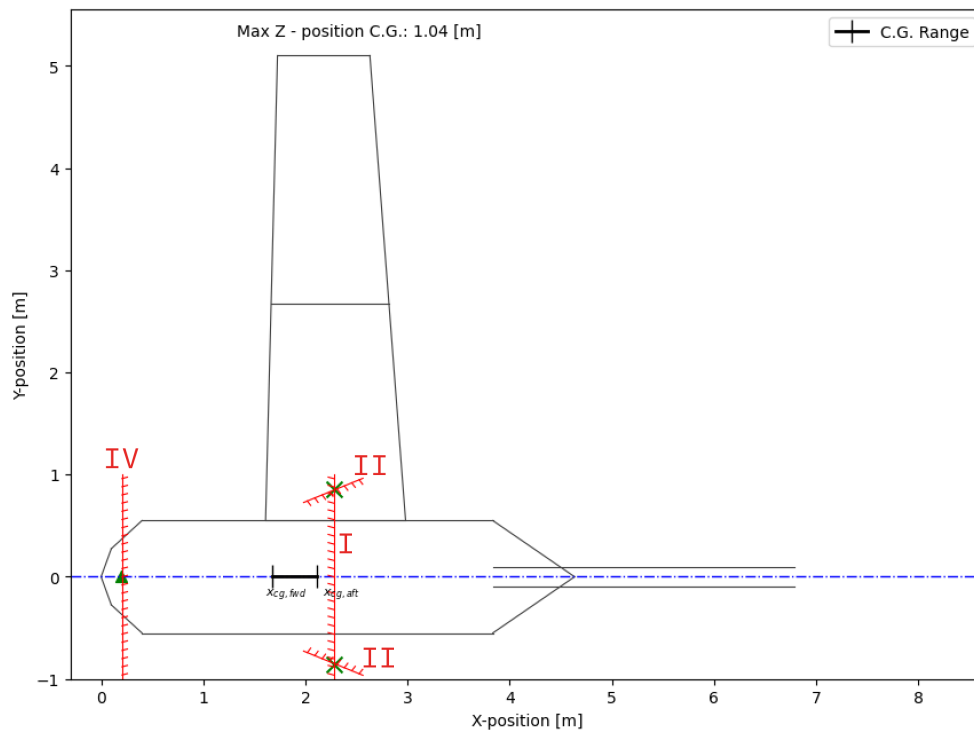


Figure 10.2: Undercarriage position and limits

The design numbers for the landing gear position can be found in Table 10.1. As the nose-gear configuration was chosen, the y-position of the main landing gear will be symmetrical around the longitudinal axis of the aircraft.

Table 10.1: Estimations of the landing gear position

Parameter	Estimation	Unit
$X_{lg_{nose}}$	0.20	m
$Y_{lg_{nose}}$	0	m
$X_{lg_{main}}$	2.28	m
$Y_{lg_{main}}$	± 0.86	m

10.3. Structure

Because the landing gear is fixed, it can be attached to the fuselage truss structure directly. However, because of its relative slenderness, as the tail boom, the landing gear members are considered beams, which means they are sized for axial, shear forces and bending moments.

10.3.1. Critical Load and Geometry

The landing gear transfers static ground and landing impact loads onto the fuselage, therefore it is sized for some of the ground critical loads described in Section 7.1.3, namely a $n=2.0$ single main gear landing at 0.95 MTOW [18, p. 11], 46% of MTOW static load at each of the main gears [12, pp. 356–357], as well as $n=2.25$ nose wheel static load [18, p. 12] assuming 15% of MTOW is carried by it.

With the position of the landing gear known (see Table 10.1), its geometry can be determined. The point of wheel attachment is placed at a distance of wheel radius (r_w) above the landing gear ground track position (for tire dimensions, see Section 10.3.3). The gear structure starts 5 cm below that point (to allow for brake attachment) and extends vertically to r_w above the wheel attachment point, where it bends towards the fuselage (see Figure 10.3b). Figure 7.3 shows to which fuselage frames the main and front gear structure is attached. Because of a relatively forward nose wheel position, an additional structure is needed below and within the engine mount, as presented on Figure 7.3. The near-to-horizontal layout of the main landing gear aims to absorb impact loads by elastic deformation and provide ground clearance. Two attachment points of each main gear to the fuselage provide longitudinal rigidity of the structure.

The cross-sectional sizing of the tubes are computed from the internal maximum shear force F_s (Equation 7.7), axial force F_a (Equation 7.5) bending moment (Equation 7.8) and buckling constraint (Equation 7.6), which are an output of the FEA calculation, double checked by analytical calculations. A path is defined along a selected straight section of the structure, along which the internal loading diagrams are computed, as shown in Figure 10.3a. Here an internal shear force and bending moment diagram output, for reference.

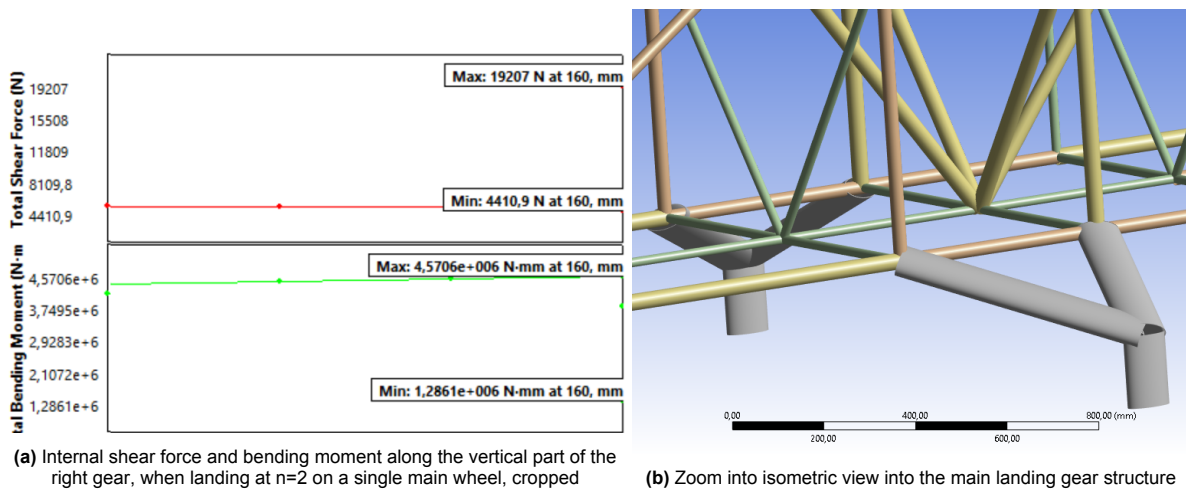


Figure 10.3: Sizing of the landing gear and its layout

It should be noted that for this sizing, the analytical correction has been applied, since the FEA model weight does not realistically match MTOW. The loads are multiplied by a factor of 1.7, which is a ratio between the desired MTOW and the actual FEA model weight. Since the model requires a fixed support applied at the ground contact point, the indicated max value on Figure 10.3a is off, which is confirmed by the constant shear force and steady bending moment increase.

Bending moment is most critical for the landing gear sizing, which implies maximising the cross sectional moment of inertia for minimum mass design. Once more, upper limits on the structure shape must be applied. It is aerodynamically beneficial for the main gear to be made of elliptical tubes, with the semi-major aligned with the flow, and thus $a=0.06$ m and $b=0.04$ m (for steel 4130). The nose gear is made of circular tubes with diameter $\varnothing = 0.05$ m (for steel 4130).

10.3.2. Materials and Integration

The standard material choice procedure has been used, with weight: raw cost (4), ecological cost (1), CO₂ (0.5), fracture toughness (2), buckling material index \sqrt{E}/ρ (1), tension/bending material index σ_y/ρ (4). Because of particular exposure to debris impact, the fracture toughness is given more weight, while since bending is found to be critical, its material index carries the maximum weight. Stainless steel 410 wins the trade-off, followed by steel 4130. Table 10.2 summarizes the required dimensions of the landing gear structure.

Table 10.2: Summary of the landing gear dimensions and structural mass, with alternative material

Structure	Shape [cm]	Thickness [mm]	Material	Corrosion	Mass [kg]
Nose gear	\varnothing 5.0	1.0	Steel 4130	No	0.63
Nose gear	\varnothing 4.0	0.7	S. steel 410	Yes	0.35
Main gear	$a=6, b=4$	2.5	Steel 4130	No	14.15
Main gear	$a=5, b=2.5$	2.0	S. steel 410	Yes	8.71

The default material choice is steel 4130, which allows for direct welding of the structure to the fuselage (same material), however, due to significantly lower mass, using stainless steel 410 can be of an advantage, thus an alternative design is proposed in Table 10.2. Corrosion protection coating and bolt connections between the gear and fuselage shall be used in that case. It is recommended to explore potential use of single-membered pre-bent beam, such as the one used in the current Wings For Aid prototype, together with employment of composite materials.

10.3.3. Tires and Shock Absorber

Since the aircraft should be able to operate from unprepared surfaces (type I), the tire pressure should be around 230-300 kPa [48]. Based on that, the minimum tire size can be estimated from empirical relations and available tire sizes (British sizes, [12, p. 358]). The nose tire is thus 8 cm wide (3 inches minimum) and has a radius of 12 cm radius (3.5 inches of inner diameter minimum). The main tires are 12 cm wide (4 inches minimum) and have a radius of 16 cm radius (3.5 inches of inner diameter minimum).

In case energy absorbers are decided to be used, they can be selected based on the kinetic energy of the aircraft touching the runway. This can be estimated by Equation 10.1 [12, p. 360], with w as the ultimate descent velocity described by Equation 10.3.3, all in SI units.

$$E = \frac{W}{2g} w^2 \quad (10.1)$$

$$w = 0.9 \left(\frac{W}{S} \right)^{0.25} \quad (10.2)$$

In the case of Wings for Aid, $E = 6,624$ J (with $w=4.39$ m/s). The absorbers can subsequently be chosen based on the estimated weight fraction supported by every gear member. In future stages of the design, the implementation of shock absorbers should be assessed, together with the potential influence of the steering mechanism on the structure. A nose wheel fork shall be designed to centre the nose wheel on the nose wheel strut.

Onboard Equipment

Equipment in an aircraft can account for a significant part of the total manufacturing cost. The following section details the sizing of communications (COM), on-board computer (OBC) and power (PWR) subsystems. The chapter will start discussing the system-wide interactions in Section 11.1. In the following sections, the main types of equipment will be analysed, starting with the onboard computer in Section 11.2. Then in Section 11.3, the communications subsystem will be discussed. After, the performance of the control actuators is discussed in Section 11.4. Lastly, Section 11.5 analysis the electrical components onboard.

11.1. System Interactions

In order to understand the relationships between subsystems that will be discussed in the upcoming section, it will be of great help to visualise the entire aircraft system. In Figure 11.1, the hardware diagram of the aircraft is presented.

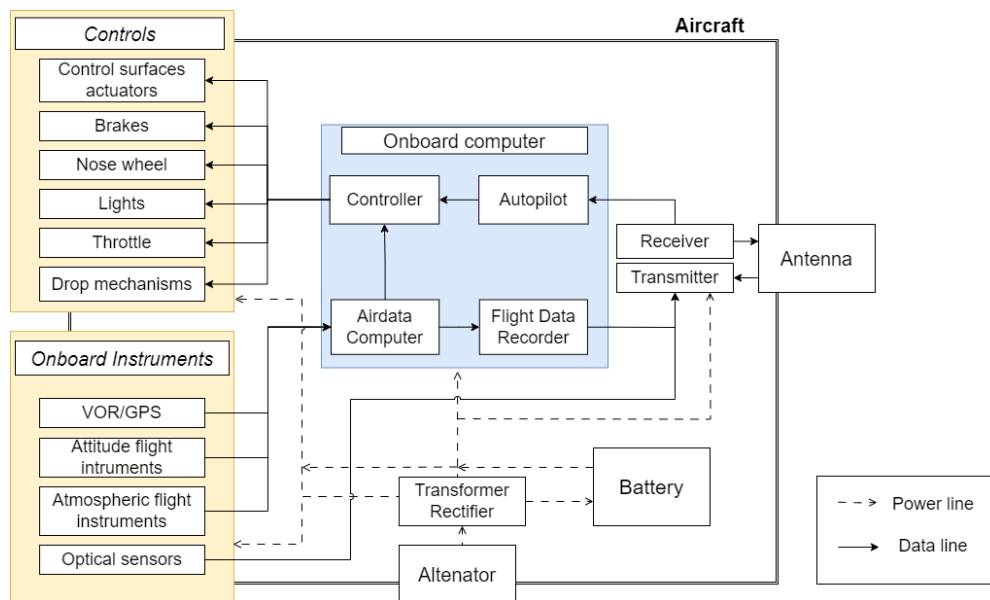


Figure 11.1: Hardware diagram of the aircraft

The main power source of the aircraft will be an alternator. The alternator is driven by the shaft of the propeller. All blocks that are in the blue section of the diagram are part of the onboard computer. The equipment that is part of the onboard computer is required to perform all decision-making and controlling within the aircraft. More detail about this onboard computer is found in Section 11.2. The raw data that is measured by the onboard instruments will be the inputs to the onboard computer. Onboard instruments include GPS, attitude and atmospheric flight instruments and optical sensors. Based on the input data to the computer, a control output will be sent to the controls of the aircraft. Control systems do include actuators that allow the control surfaces to move. Next to this, the brakes, nose wheel steering, lighting, throttle setting and the dropping mechanism are controlled by the computer. In Section 11.4 these will be discussed in more detail. On the right of the diagram, the communication subsystem can be found, consisting of the receiver, transmitter and antenna. Using this antenna, the data is sent to and from the system's satellite. This will also be discussed in more detail in Section 11.3. Lastly, the diagram also shows an overview of the main power lines that will be part of the system. In Section 11.5, the system will be analysed from an electronics perspective.

Moreover, the interactions between the aircraft and the other elements of the system can also be analysed in terms of the data flow. In Figure 11.2, all important data flows within the system are visualised.

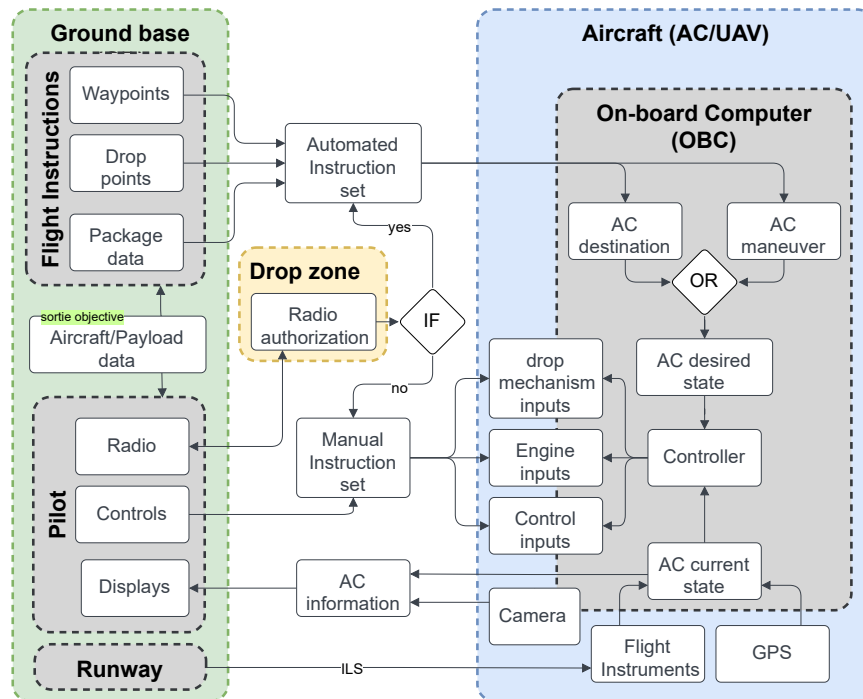


Figure 11.2: Data handling flow diagram

11.2. Onboard Computer

As discussed in Section 5.7 and Section 4.1, the aircraft is semi-autonomous and requires some on-board computer and navigation systems. In Figure 11.3, the software diagram is presented. This diagram gives a more detailed version of the onboard computer that was shown before in Figure 11.1.

In the diagram, the functions that connect the most important elements of the onboard computer are shown. For the design aircraft, the following four elements were considered as the main elements.

- The Airdata Computer (ADC) gathers, processes and corrects data from instruments before sending the information to the navigation and control computers
- Navigation unit (NAV): uses short-range VHF signals (VOR) and GPS to determine the UAV's position and velocity.
- The Flight Data Recorder (FDR) locally stores and broadcasts the aircraft's data for telemetry
- The Autopilot (GNC) must be able to compute a flight profile and follow long-range maneuvers as well as executing the drop maneuver and possibly the take-off and landing.

Then using statistical relations based on COTS data, an estimation was made of the mass, power, volume and most importantly the cost of these four elements. Because the Wings for Aid UAV will be semi-autonomous, it can be assumed that the required GNC computer will be more complex than average. As such, a factor of 1.5 is applied to its values. The results of this analysis can be found in Figure 11.4.

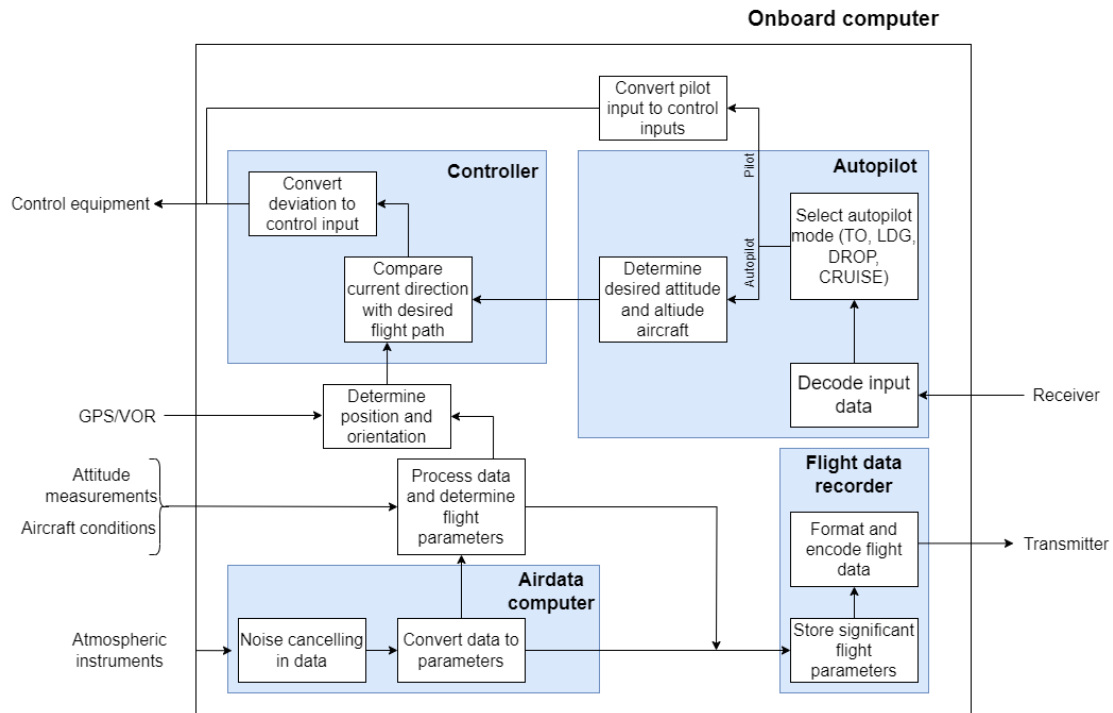
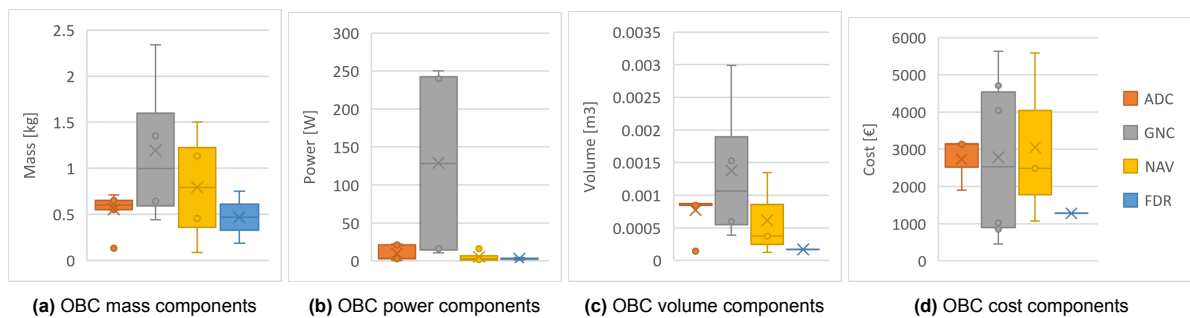


Figure 11.3: Software diagram

Figure 11.4: On-Board Computer sizing. The cost estimations are gathered from commercial data^{1234 56}

As a result, it is estimated that the mass of the entire onboard computer is $3.6\text{kg} \pm 1.7\text{kg}$, the power required is $210\text{W} \pm 130\text{W}$, the volume estimated is $3.6\text{L} \pm 1.5\text{L}$ and the cost to be $\text{€}11300 \pm \text{€}4300$. There is a significant deviation as the available systems differ widely in their capabilities and applications.

11.3. Communications Subsystem

Because the aircraft is to be semi-autonomous instead of relying on simple ADS-B emissions and a pilot like other planes, communications sizing is needed in order to ensure a reliable connection and a sufficient design budget for mass and power.

The communications concept starts with the Communication flow concept shown in Figure 11.5. This details the various links between the system's elements and their nature. Most important is that the split in telecommands source between the autonomous and manual mode is done locally on the aircraft's computer, this implies both sets of instructions should be able to be broadcasted simultaneously. It can be seen that no link is required between the UAV and the drop-zone (DZ) since the drop authorization has to be done between the ground-operator (GO) and the responsible-pilot.

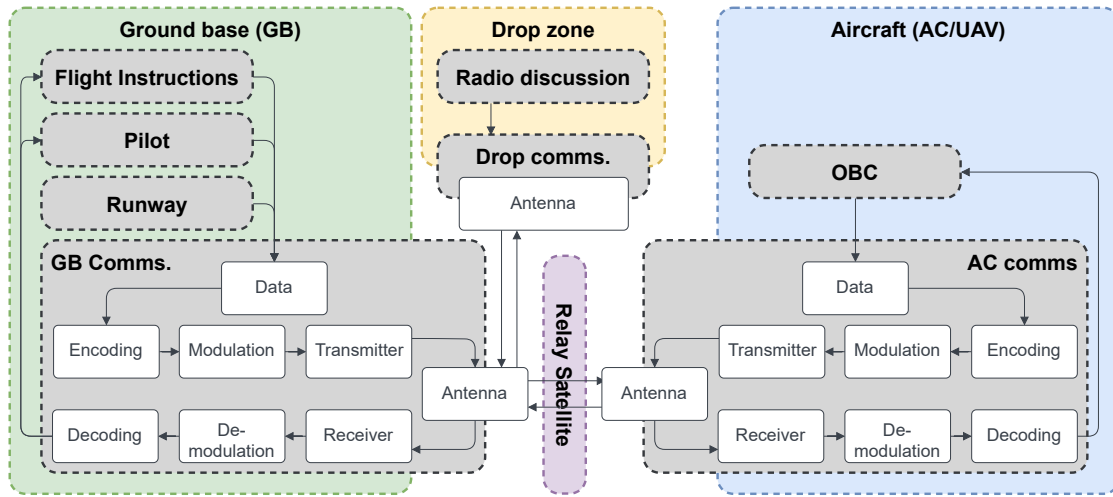


Figure 11.5: Communications flow diagram

This information allows an allocation of data and an estimation of the expected packet size (PC) depending on datatype (telemetry, telecommand, video and voice) and contents.

- AC-GB telemetry: 500 channels with 32 bits resolution (pc = 32,000 bits), an optional video feed of 240x320 pixels with an 8-bit (256 colour values) channel can activate as a contingency for dropping clearance (pc = 614,400 bits)
- GB-AC 50 telecommand channels with 32 bits resolution (pc = 3,200 bits)
- GB-DZ a radio channel: 64 bit/s [49]

Assuming a refresh rate of 15 Hz implies a transmission frequency of at least 30 omnidirectional Hz (Nyquist) which, along with a compression factor (CF) of 10 in the case of video and 5 for data, yields a signal data rate of $DR_s = f_{tr} \cdot pc / CF$. The GB and each UAV are assumed to have omni-directional antennas (gain of 1) since many aircraft will fly simultaneously and moving parts in the airframe would have negative reliability consequences allow to estimate.

In order to size the power required by the aircraft's transmission system to reach the satellite and the antenna size needed to receive the relay's telecommands, the method outlined in [49] Equation 11.1 is used as a basis and re-arranged for input power and antenna size Equation 11.5:

$$EIRP = (P_{in} \cdot \eta_P) \cdot L_l \cdot G_t \quad (11.1)$$

$$W_f = \frac{EIRP}{4\pi d^2} \quad (11.2)$$

$$P_r = W_f \cdot A_{an} \cdot \eta_{an} \quad (11.3)$$

$$\frac{E_b}{N_0} = \frac{P_r / DR_s}{k_B \cdot T_{noise}} \quad (11.4)$$

$$P_{in} = \frac{\frac{E_b}{N_0} \cdot N_0 \cdot R \cdot (4\pi d^2)}{\eta_{an} \cdot A_{an} \cdot L_l \cdot G_t \cdot \eta_P} \quad (11.5)$$

$$A_{an} = \frac{\frac{E_b}{N_0} \cdot N_0 \cdot R \cdot (4\pi d^2)}{\eta_{an} \cdot L_l \cdot G_t \cdot \eta_P \cdot P_{in}} \quad (11.6)$$

The results for a low-earth orbit satellite (maximum distance of 1500 km) yield a power required from the UAV of about 4 W for the radio and telecommand link, the telemetry would amount to 2 W. The video feed, however, would need an estimated 22 W of continuous power for the duration of the stream. Since this is way above standard aviation hardware capabilities and video is optional, the camera is omitted from the design. The resulting link budget is shown in Figure 11.6b

Sizing the mass and volume of the transmitter and receiver (assumed 2 W can then be done using a statistical relation from [49] with respect to their power, while their cost is estimated from COTS data Figure 11.6a. Assuming an helix antenna, its mass can be estimated using its density per area (11 kg/m²). Finally, a cable fraction of 10% is assumed for each metric.

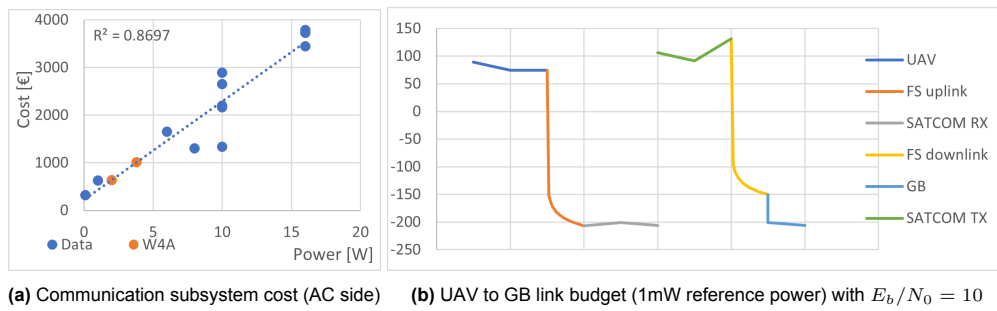


Figure 11.6: COM sizing: With the power and mass determined around 1.8kg and 4.5W respectively, the volume is estimated around 3.6L following the same method from [49] and the cost is approximated to be 1500€.

Since the design of the communications subsystem heavily depends on the satellite choice, a few typical options are considered: A geostationary satellite (GEO) based on Immarsat ⁷, a classical low-earth orbit relay such as Iridium ^{8 9} and a constellation such as Starlink ^{10 11}

Table 11.1: Characteristics of communication satellite available options

	GEO	Iridium	Starlink
Altitude [km]	36000	780	1100
Gain [-]	5	3.5	-
Antenna [m2]	3.14	0.282	-
Power [W]	4000	50	-
UAV			
Power (TM) [W]	1067	3.79	50
Power (TM+video) [W]	11310	40.2	75
Antenna [m2]	0.335	0.01226	0.1545
Antenna [cm]	65.3	12.5	44.4

11.4. Controls Actuators

Since the aircraft is not piloted, the force required to control the UAV needs to be provided by actuators. In order to limit the complexity of the aircraft and provide reasonable reliability, the sizing will be computed assuming COTS electro-mechanical actuators (EMA) driving a screw linked to the control hinge as seen on Figure 11.8a.

The controls will include actuators for two plain flaps, two ailerons, the elevator and rudder, and the nose gear. The approach to determining the necessary redundancy follows the recommendation from [11] "CS23.1329-a1: The automatic pilot system must be designed so that a single malfunction will not produce a hardover (The condition where a control surface or actuator has moved to its extreme limit) signal in more than one control axis". A hardover on a single axis is in itself a significant event but Figure 11.7 explores the effects of any single control failure on the system and the expected response of other controls.

Because of the high weight of EMAs, minimising the number of extra actuators is desirable. It is thus decided that only the elevator requires a redundant EMA while the others will be software-augmented to compensate accordingly. Angle-meters should be attached to all motor shafts and trigger a failure mode if the measured angle deviates too much from the controller input. This failure mode should include physical brakes that stop the control surface from changing its deflection and a circuit breaker to isolate the issue. Furthermore, in order to decrease cost and weight, the elevator EMAs will be used in parallel, both contributing to the total force, such that a failure leads to the deflection rate being effectively halved.

⁷ Immarsat - Global Mobile Broadband[cited 22 June 2023]

⁸ EO portal - Iridium Next[cited 22 June 2023]

⁹ HighSpeedSat - Iridium[cited 22 June 2023]

¹⁰ Starlink specification[cited 22 June 2023]

¹¹ StarlinkHardWare - dish and mast measurements[cited 22 June 2023]

	compensation						
	nose gear	flap L	flap R	aileron L	aileron R	elevator	rudder
failure (+dir)							
nose gear							-
flap L			+			-	
flap R		+				-	
aileron L			+		-		-
aileron R		+		-			+
elevator							
rudder	-			-	+		

Figure 11.7: Effect of control failure on UAV: all failures are indicated for a control surface stuck in the positive direction. Compensation in the same direction is indicated with a +, opposite direction with -. The immediate response is in bold.

The actuator's sizing is based on [50]: it uses deflection angle δ , rate, acceleration and inertia of the control surface along with its maximum hinge moment M_h as inputs. The deflection angle is taken from Section 8.3, Section 9.2 and Section 9.3.3. The rates from statistics used in [51] and the maximum angular acceleration are derived such that the maximum rate achieved within the deflection: $\ddot{\delta} = \frac{\dot{\delta}^2}{2\delta}$. The moment of inertia J is obtained from the CAD model of the control surfaces using the construction described in Section 14.1.1. The hinge moments are found by multiplying the maximum resultant force on the surface by the quarter-chord i.e. assuming a center of pressure at $c/4$ and a hinge at the leading edge. The elevator is the exception since it is full-flying and thus requires special attention on the hinge placement: the position is optimized such that the maximum magnitude of the hinge moment over the full deflection range is minimized, taking into account the significant shift in center of pressure ¹². The optimal hinge position is found to be at 0.45 chord length, resulting in Figure 11.8. The tabulated inputs are found in Table 11.2.

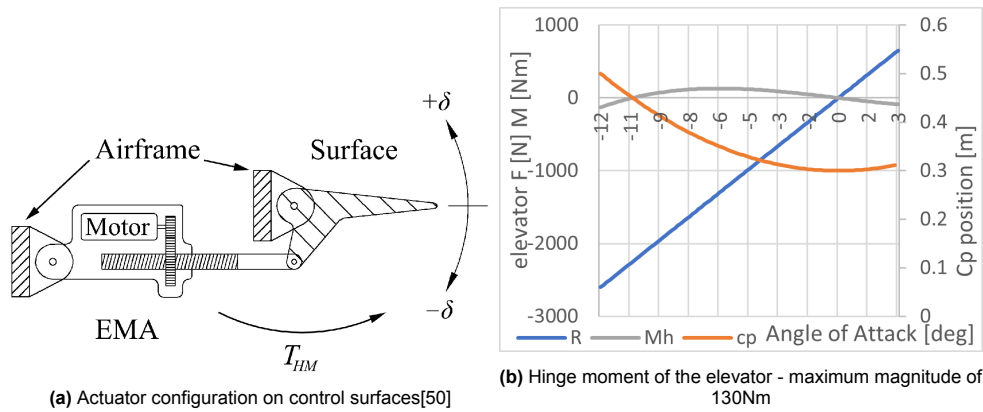


Figure 11.8: Configuration of aileron and optimum hinge moment of actuator

Table 11.2: Summary of parameters used as inputs to the actuator sizing

Actuator	N	J [kgm ²]	F [N]	c [m]	M _h [Nm]	d [deg]	$\frac{d\delta}{dt}$ [deg/s]	$\frac{d^2\delta}{dt^2}$ [deg/s ²]
Nose gear	1	0.0179	-	-	30	45	50	28
Flaps	2	0.0091	5000	0.62	780	45	10	1.1
Aileron	2	0.0091	1500	0.31	117	15	80	214
Elevator	2	0.0173	2600	1	130	12	80	267
Rudder	1	0.0179	1500	0.33	125	27	80	119

¹²CoP shift with respect to AoA

- Nose gear: no effect until landing - then compensate with rudder
- HLD's: set other flap to same deflection and reduce airspeed
- Ailerons: immediately compensate with opposite aileron, effectively reducing allowable deflection. Flaps can then be used to increase the leftover authority. note: flaps can only deflect in one direction.
- Elevator: no possible counteraction - requires redundancy in the actuators.
- Rudder: compensate with sideslip (ailerons) and nose-gear on landing

Required torque is computed assuming mechanical friction F_f of 0.59 Nm, transmission efficiency μ_{tr} of 0.71 and motor efficiency μ_{EMA} of 0.9, as in the case study from a similar aircraft in [50], using $T_{HM} = J\ddot{\delta} + F_f + M_h$. Peak power is obtained with $P_{peak} = \frac{T_{HM}}{\mu_{tr}} \cdot \dot{\delta} / \mu_{EMA}$. That is the power required when the controller requires a full deflection. On average, over a complete sortie, the power will be lower as surfaces are often stationary. Until a complete six degrees-of-freedom model of the UAV is available, a power fraction derived from the results of [50] defined as $EMA_f = \frac{E \cdot \Delta t}{\Sigma P_{peak}}$ is used to approximate it as $P_{avg} = P_{peak} / EMA_f$. Finally, mass and cost were estimated using a linear-relation Figure 11.9 with respect to power using COTS components for small linear actuators (ITT) ¹³ and high-power brushless DC motors (BLDC) ¹⁴. Combining the results, the final characteristics of the actuators are summarised below in Table 11.3

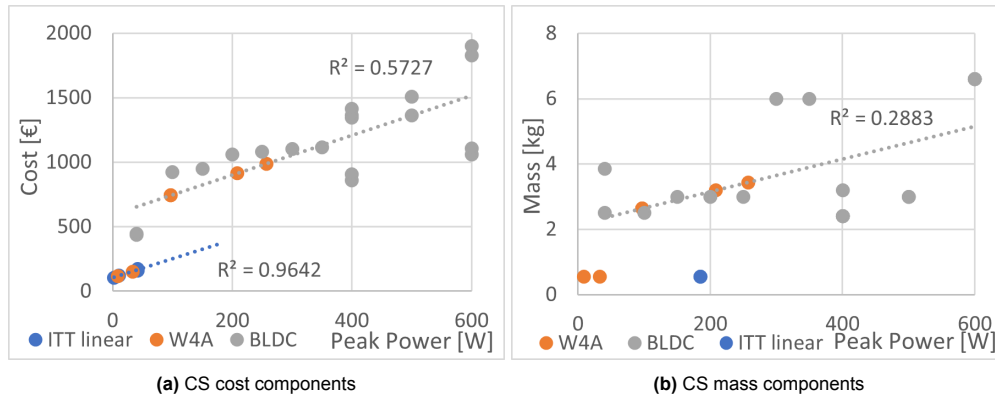


Figure 11.9: Control Surfaces EMAs sizing

Table 11.3: Summary of results of the actuator sizing

	N	M [kg]	CST [€]	P _{peak} [W]	P _{avg} [W]
Nose gear	1	0.55	117	8.9	0.11
Flaps	2	0.55	152	33	0.42
Aileron	2	3.43	988	257	3.3
Elevator	1+1	2.63	742	97.0	1.23
Rudder	1	3.19	914	209	2.66
Total		17.0	4790	4790	12.6

11.5. Power Electronics

The last type of equipment that will still be discussed is the electrical power and electronics onboard. This subsystem is responsible for all interactions between the different subsystems along with their supply in energy. In Figure 11.10, the electrical block diagram of the aircraft system is presented. The loop in the diagram begins at the master switch. If switched on the battery will start providing power to the battery contactor which delivers the power to the starter of the engine. Next to this, the alternator control unit will start operating using power from the battery. The alternator control unit will then start up the alternator. From that moment onwards, the alternator will start generating alternating currents. This current will then flow to the primary bus in which the power will be distributed over all electrical elements of the system. A number of important electrical elements include the actuators, sensors, lights, dropping mechanism, flight computer and communication elements. The primary bus will also include a transformer rectifier that converts the current from alternating to direct current. In case of a surplus of energy generation, the alternator control unit can decide to store this surplus in the battery. The battery will also be used to support the generator in supplying energy to the primary bus.

The battery is sized by following [11] "CS23.1353-h: In the event of a complete loss of the primary electrical power generating system, the battery must be capable of providing 30 minutes of electrical power to those loads that are essential to continue safe flight and landing." along with losses in power conditioning and distribution which are estimated to be 10 and 3.5 % respectively. The battery itself has conditioning, storage

¹³ AeroExpo - moog animatics

¹⁴ ATO high-torque BLDC motors

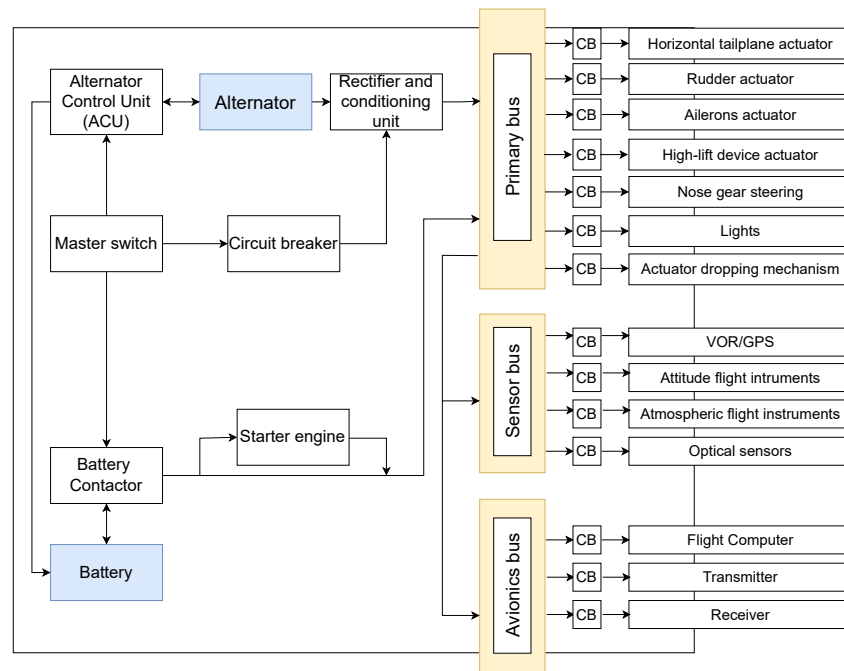


Figure 11.10: Electrical Block Diagram of design aircraft

and discharge efficiencies of 95%. The depth of discharge is chosen as high as 90% since a 30-minute power loss is not the regular operating condition and as such would not overly degrade its lifetime. With a power sum required for all equipment and actuators on the aircraft of 460 W, this accounts for 265 Wh of total capacity. Assuming Li-On cells with a specific energy of 110 Wh/kg and specific density of 285 Wh/L [52] yields a sizing of 5.9 kg, €100¹⁵ and 0.93 L. Assuming that the battery should recharge within a single sortie, the power required is about 89 W.

The alternator thus needs to provide 635 W (using the same conditioning and distribution losses) and is sized using a linear relationship with respect to power using COTS components for generators¹⁶ and alternators^{17 18}. Because of their higher throughput and lower cost above 500 W, an alternator was chosen. The results of this statistical analysis can be seen in Figure 11.11. Furthermore, the generator itself is about 85% efficient and requires 747 W or 1 shaft-horsepower from the engine.

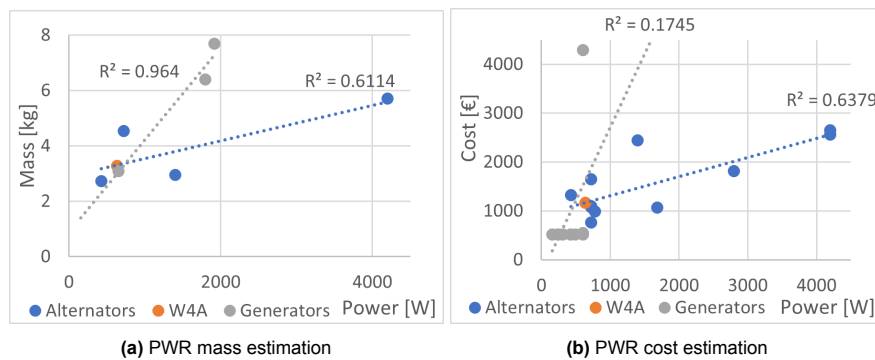


Figure 11.11: Generator sizing: an alternator of 746, 3.28kg and about 1170€.

Finally, the distribution system is sized with respect to the peak power required of 1450 W and amounts to 10.5 kg [52], €1000 along with an added cable fraction of 5%.

¹⁵Bloomberg NEF - LiOn average battery pack prices

¹⁶QAA - aircraft generators

¹⁷AirPowerInc - alternators and generators

¹⁸Boeing aviation

Verification & Validation

At the centre of the used design process, an iterable and flexible model was used. Before the results of this model were calculated, the model was verified by performing static and dynamic testing in Section 12.1 and Section 12.2. Afterwards, system verification was performed by an expected value analysis, a sensitivity analysis, and FEA Verification in Section 12.3, Section 12.4 and Section 12.5.

12.1. Static Testing

The first step in verifying the code will be to perform static testing. During static testing, the code will not be run. Instead, the structure and variables of the design model are evaluated as discussed in the Midterm Report [3]. For a large part, this includes fixing syntax errors which are mostly detected by the used Integrated Development Environments. In addition, outdated variables can be found when comparing them to the file containing all variables. At the end of this phase, a full list of unique and correct variables is left. These will be updated throughout the iteration. Only after this phase of verification was performed, the dynamic testing phase can start.

12.2. Dynamic Testing

During dynamic testing, the code will be verified by running modules of code in increasing sizes. First, only units of code will be verified. Afterwards, larger modules of code will be checked. And at last, the entire code will be executed and compared to expected values.

Block 1: Load Data

1. U-LOAD-01

- **Description:** Specifically for the object that is created after running the file containing all variables, 'parameters.py'. Are the results of all variables as expected and/or described in the right unit.
- **Result:** Test passed for all variables in parameters.py.
- **Accuracy:** Sufficient - very high

Block 2: Aerodynamic Analysis

1. U-AERO-01

- **Description:** XFLR5 results are checked if they are as expected and make sense.
- **Result:** Test passed. Values fall within expected order of magnitude and signs are correct. For example, the moment coefficient is negative which is expected for an airfoil. Performance parameters containing $\frac{C_l}{C_d}$ came out higher than expected. This could be attributed to the differentiation scheme used and did not influence the final results.
- **Accuracy:** Sufficient

2. U-AERO-02

- **Description:** Lift distribution outputs are checked for expected results and whether varying inputs give expected change in outputs.
- **Result:** Test passed. The lift distribution is integrated over the wing and gives a total lift equal to the lift required. Changing inputs also gives logical output changes, examples: Higher aspect ratio makes the distribution end at a higher span, lower taper ratio reduces the sectional lift at root sections and adding twist lowers the lift near the tip.
- **Accuracy:** Sufficient - high

3. U-AERO-03

- **Description:** Boundary value test on section lengths. Test is performed separately on nose- and tailcone. For both, the zero-lift drag is calculated for lengths starting at 0 m increasing to 7 m.
- **Result:** Test passed. Both have positive zero-lift drag at the boundaries with a minimum and parabolic behavior in between. This is expected as it shows the transition in dominating effects. At first, the drag decreases as the optimum $\frac{L}{D}$ is reached, then the surface area becomes dominant.
- **Accuracy:** Sufficient

4. U-AERO-04

- **Description:** The calculated required incidence angles are checked whether give realistic values for the given case.
- **Result:** Passed test. Expected incidence angles are between 1 and 2° in magnitude. Both the main wing and vertical tail incidence angle fall within this range. The horizontal tail does not due to the downwash from the main wing. After removing this effect, the horizontal tail also complies.
- **Accuracy:** Sufficient

Block 3: Stability and Control Analysis

1. U-STAB-01

- **Description:** Logic tests for sizing of empennage and control surfaces. Increase or decrease a parameter from which its impact on the result is known
- **Result:** Logical results. Increasing e.g. the length of the boom increases l_h which decreases the slope of both the stability and controllability curve, and increases structural mass as expected. For the control surfaces, lowering the $C_{L_{max}}$ of the wing increases the flap length or changes HLD type if space is limited, as expected.
- **Accuracy:** Sufficient

2. U-STAB-02

- **Description:** The calculation of the horizontal tail fraction $\frac{S_h}{S}$ and tail volume coefficient $\frac{S_h l_h}{S \bar{c}}$ are compared to similarly configured aircraft.
- **Result:** Test passed. A tail volume coefficient of 0.641 was found for the design aircraft. This is comparable to other aircraft with a full-moving horizontal tailplane such as the Cessna 177 which has a horizontal tail volume coefficient of 0.600 [12, p. 329].
- **Accuracy:** Sufficient accuracy

3. U-STAB-03

- **Description:** The calculation of the vertical tail fraction $\frac{S_v}{S}$ and tail volume coefficient $\frac{S_v l_v}{S \bar{c}}$ are compared to similarly configured aircraft.
- **Result:** Test passed. A tail volume coefficient of 0.036 was found for the design aircraft. This is comparable to other aircraft with a full-moving horizontal tailplane such as the Cessna 177 which has a horizontal tail volume coefficient of 0.041 [12, p. 334].
- **Accuracy:** Sufficient accuracy

4. U-STAB-04

- **Description:** Verifying the position of the centre of gravity visually by plotting all elements that contribute to the centre of gravity.
- **Result:** Test failed initially. Centre of gravity position of empennage was calculated to be outside of the aircraft. This was then modified in the code after which the test did pass.
- **Accuracy:** High accuracy.

5. U-STAB-05

- **Description:** Sensitivity analysis of sizing aileron by varying the values of the mass moment of inertia, the chord length of the aileron and the roll requirement. Results are also compared to similar aircraft.
- **Result:** Test passed. Increase in the mass moment of inertia does result in an increase in the

required size of the aileron. An increase in chord length does decrease the required length of aileron. And a stricter roll requirement does increase the required length.

- **Accuracy:** Sufficient

Block 4: Structural analysis

1. U-STRU-01

- **Description:** The loading diagram is generated for varying load inputs and strut locations, the diagram should change accordingly
- **Result:** Test passed. An increase in load factor increases the lift, and keeps other loads the same. A shift in control surface positions change the application area of the control surface loads. A shift in the attachment point of the strut leads to the reaction forces shifting to that point.
- **Accuracy:** Sufficient

2. U-STRU-02

- **Description:** The sign convention for the normal, shear, moment and torque diagram should be all the same and match the loading diagram from which they are derived
- **Result:** Test passed. Compression leads to a negative internal force. An upwards reaction force leads to an upwards jump in internal shear force, while a downwards reaction force does the opposite. The slope of the moment diagram corresponds to the shear diagram. The reaction force at the strut should relieve the torque, which is exactly what it does once the torque diagram passes the attachment point.
- **Accuracy:** Sufficient

3. U-STRU-03

- **Description:** Positioning of all elements is very important for the calculation of parameters of the wingbox. Therefore the centroids of all individual elements and of the entire wingbox are calculated and plotted. The locations can then be verified with the position of the element itself.
- **Result:** Test passed. The centroids which are used in the calculations are correctly placed, based on the spanwise location and the amount of stringers. This is very important since the centroids are used in the calculation of the second moment of area and the internal stresses.
- **Accuracy:** Sufficient

4. U-STRU-04

- **Description:** Without taking loads into account, an increase in thickness of any element should lead to an increase of weight of the wingbox. The loads should be left out, since otherwise thickening one element could allow another element to be thinner.
- **Result:** Test passed. Without loads present, the weight of the wingbox always increases when a single element increases in size.
- **Accuracy:** Sufficient

5. U-STRU-05

- **Description:** Increasing the ultimate load factor should lead to a heavier wingbox
- **Result:** Test passed. An increase of the load factor of 10% lead to an 8.9% increase in wingbox weight
- **Accuracy:** Sufficient

6. U-STRU-06

- **Description:** At least one of the failure modes should touch a margin of failure of 1, and the most critical failure modes are expected to be at the top of the wingbox. The latter is because the lift multiplied with a load factor of 6.67 is the most critical load case.
- **Result:** Test passed. As Figure 8.7 already showed, the stringer buckling at the top touches a margin of failure of 1. Also the margin of failure of buckling of the top panel is very close to 1.
- **Accuracy:** Sufficient

Block 5: Flight Performance Analysis

1. U-PERF-01

- **Description:** Take-off runway length equations are verified and results are checked if they are in the expected range and make sense. It has also been plotted with varying values to check if the trend is correct.
- **Result:** Test passed. Values fall within expected order of magnitude and signs are correct. For example, a runway length of approximately 160 m is needed in nominal conditions. And the plots trend make sense.
- **Accuracy:** Sufficient

2. U-PERF-02

- **Description:** Descending rate and angle of descent equations are verified and results are checked if they are in the expected range and make sense. It has also been plotted with varying values to check if the trend is correct.
- **Result:** Test passed. Values fall within a reasonable order of magnitude of 2.6 m/s for descending rate and 3.3° for descending angle, and signs are correct. And the plots trend make sense.
- **Accuracy:** Sufficient

3. U-PERF-03

- **Description:** Throttle setting while landing equations are verified and results are checked if they are in the expected range and make sense. It has also been plotted with varying values to check if the trend is correct.
- **Result:** Test passed. Values fall within a reasonable order of magnitude of 17%, and signs are correct. And the plots trend make sense.
- **Accuracy:** Sufficient

4. U-PERF-04

- **Description:** Landing runway length equations are verified and results are checked if they are in the expected range and make sense. It has also been plotted with varying values to check if the trend is correct.
- **Result:** Test passed. Values fall within expected order of magnitude and signs are correct. For example, a runway length of approximately 225 m is needed in nominal conditions. And the plots trend make sense.
- **Accuracy:** Sufficient

5. U-PERF-05

- **Description:** The output of the sortie simulation is checked against varying inputs. The output is compared with expected values and the sensitivity of the result to the inputs is checked to be logical
- **Result:** Test passed. The relation between inputs and outputs is logical and the values are as expected. For context, the fuel use for a sortie lies around 60 l for a sortie that takes 3 hrs. Comparing this with usual fuel consumption values for the selected engines (18 l/hr) and adjusting for bad quality fuel, the result is as expected.
- **Accuracy:** Sufficient - high

6. U-PERF-06

- **Description:** The ferry range of the aircraft is calculated as a boundary value test.
- **Result:** Logical result, the required ferry range is 1000 km, the result is 1176.96 km. The fuel tank volume was selected to be 75 l, this is higher than the sorties with payload require including reserve. This explains the 176.96 km of extra range.
- **Accuracy:** Sufficient - high

7. U-PERF-07

- **Description:** Boundary value test on the sortie simulation. Inputs are zero boxes and no drop manoeuvres with a 1200 s loiter at range, 12 boxes with 12 drops, 12 boxes with 6 drops in a drop region of 10 l, and 12 boxes with 6 drops in a 200 km dropzone.

- **Result:** Logical result, fuel use is highest when flying with max payload the longest. Sorties with a larger number of drops take more time. The difference in fuel use between the sortie profiles is small as sortie parameters like altitude are automatically adjusted based on the number of drops and the drop region
- **Accuracy:** Sufficient

8. U-PERF-08

- **Description:** The calculations used in the sortie simulation are applied to a Cessna 172R aircraft with maximum range and maximum fuel. The results are checked to be logical.
- **Result:** Logical result, the maximum range is obtained with 2.31 kg, or 3.21 l of fuel remaining
- **Accuracy:** Sufficient - high

9. U-PERF-09

- **Description:** The calculation of the climb performance over altitude is verified to be feasible. Additionally, the service ceiling is calculated and verified
- **Result:** Logical result, the maximum climb rate with maximum fuel and maximum payload is 6.44 m/s. This is higher than other aircraft, this is a result of the design point selection from the W/P - W/S diagram. At the design point, climb is not the limiting factor. Meeting the climb requirement would thus require less power.
- **Accuracy:** Sufficient - high

Block 7: Operations Analysis

1. U-OPER-01

- **Description:** Expected value test, compares the outputs of the cost/time estimation to the requirements and previous estimations
- **Result:** The cost per kg of payload delivered is close to the objective
- **Accuracy:** Sufficient

2. U-OPER-02

- **Description:** Sensitivity analysis, the parameters should increase or decrease the cost as expected
- **Result:** The inputs-outputs slope derivative is the right direction for each variable and the magnitude seems accurate
- **Accuracy:** Sufficient-High

Block 8: Save Data

1. U-OUTP-01

- **Description:** Since it is crucial to save and export the correct values, a check is done by every department whether all necessary values are present in the output. At the same time, it is checked whether values that are supposed to stay constant actually do, while values that are supposed to change do so too. This is done by comparing the value at the start and end.
- **Result:** All values were present and changed as expected
- **Accuracy:** Sufficient - very high

12.3. Design Output Comparison

In an expected value analysis, the parameters of the final design are compared to existing aircraft. Similar values showcase feasibility of the design. Large differences can indicate flaws or may showcase a difference in design approach but should be explained in order to get a validated model. Table 12.1 shows important parameters of the final design and those of aircraft in a similar category and weight class.

Table 12.1: Overview of the averaged model output and reference aircraft data.

Parameter	Final design	Piper PA 18-150	Piper PA 22	Cessna 152
L/D [-]	11.4	11.0 ¹	7.0 ²	-
MAC [m]	0.58	1.6 ³	1.5 ^{4 5}	1.5 ⁶
P [hp]	100	95 ⁷	160 ⁴	110 ⁸
$S_{w,wetted}$ [m ²]	22.2	33	27	30
S_w [m ²]	10.4	17 ⁷	14 ⁴	15 ⁸
W_F [kg]	43.4	98 ⁹	100 ⁴	67 ¹⁰
W_{wing} [kg]	38	70 ¹¹	-	-
OEW [kg]	350	420 ⁷	500 ⁴	490 ¹⁰
$MTOW$ [kg]	669	790 ⁷	910 ⁴	760 ¹⁰
M_f [-]	0.1	0.12 ⁹	0.11 ⁴	0.088 ¹⁰
$X_{cg_{aft}}$ [% MAC]	39	19 ¹²	23 ¹³	-
$X_{cg_{fwd}}$ [% MAC]	2	12 ¹²	18 ¹³	-
$X_{cg_{range}}$ [% MAC]	34	6.7 ¹²	5.5 ¹³	9.2 ¹⁰
b [m]	9.1	11 ⁷	8.9 ⁵	10 ⁸

Below, an overview of the most important differences and an explanation is given:

- **MAC:** The relatively small mean aerodynamic chord can be explained by the lower total wing area and higher aspect ratio of the design. The reason for a higher aspect ratio has been explained in Section 8.1.5.
- **Surface area ($S_{w,wetted}$ & S_w):** The design has a lower surface area due to having a lower take-off weight and thus requiring less lift.
- **Fuel weight:** This is the fuel weight calculated for a typical operation. The real fuel weight will be higher. The typical aircraft also have a different mission profile that do not involve the dropping of boxes. This is clearly reflected in the higher range they have.
- **W_{wing} :** The wing weight comes out quite low. This can be explained by the model used as it uses a simplified wing with only the wing box, stringers and stiffeners. In reality, there will also be a fuel tank, control surfaces, root reinforcement and other integral parts. This shows a weakness in the model and will need to be improved.
- **MTOW & OEW:** As all previous parameters are lower than expected, it is logical this is also reflected in the take-off weight and operational empty weight.
- **CG location:** The middle of the CG range is similar to other aircraft. However, the range of the design is relatively large. This is explained by the forward wing position. With a more forward placed wing, the CG will have a large shift aft-wards as most loading takes place behind the CG location.

For all major design differences, there is a sensible explanation. Some can be attributed to different design approaches. However, others are due to model limitations such as the wing weight calculation being over-simplified. This is not a failure of the entire model as it is only a preliminary design tool. However, for further design stages, the model will have to be expanded in these areas.

¹ Flight Testing of the Piper PA 28 Cherokee Archer II Aircraft, [cited 23 May 2023]

² Piper PA-18 Super Cub Drawings - Short Wing Pipers, [cited 23 May 2023]

³ Piper PA-18 Super Cub Drawings - Supercubproject, [cited 23 May 2023]

⁴ Piper PA-22 - Wikipedia, [cited 23 May 2023]

⁵ Piper PA-22 - Ninelima, [cited 23 May 2023]

⁶ Everything explained - weight and balance - Flyingmag, [cited 23 May 2023]

⁷ Piper PA-18 Super Cub - Wikipedia, [cited 23 May 2023]

⁸ Cessna 150 - Flugzeuginfo, [cited 23 May 2023]

⁹ Piper PA-18 Super Cub - Aerocomer, [cited 23 May 2023]

¹⁰ Pilot Operating Handbook Cessna 152 - Long Island Aviators, [cited 23 May 2023]

¹¹ How much does a Cub wing weigh? - Supercub, [cited 23 May 2023]

¹² Piper PA-18 Super Cub - Lausanne Aeroclub, [cited 23 May 2023]

¹³ PA-22 center of gravity limits - Avcanada, [cited 23 May 2023]

12.4. Global Input-Output Analysis

The code has also been tested on its sensitivity to input changes. Moreover, inputs such as load factor, aspect ratio and number of boxes dropped have been varied to see the effect on the total design.

To test the overall operation of the code, a few logical changes will be made, such that their output can validate the program. The first of these is an increase in load factor, which should lead to a heavier aircraft. Increasing the load factor indeed leads to a heavier wing and fuselage, which in turn leads to more fuel needed. Adding this all together shows that the entire aircraft becomes heavier with an increase of load factor. A second change can be made by increasing the aspect ratio, this is expected to increase the wing weight, decrease the fuel weight and decrease the size of the aileron. The latter is expected because the moment arm for the ailerons becomes larger as the span increases. This span increase is also the reason for the wing weight increase. The fuel weight decreases, because lift induced drag decreases. Running the program with different aspect ratios indeed shows the expected changes as mentioned before.

The model shows to have a limited snowball effect due to the large amount of weights being fixed, instead of being updated throughout the iteration. Moreover, as the fuselage and landing gear are analysed using Ansys Mechanical these are currently not incorporated in the iteration. Next, the engine mass is set, as a specific engine is chosen rather than this changing as the power required changes. Lastly, also the equipment weight is currently a fixed value rather than depending on hinge moments or power required for example. Reflecting on this, some parts of the design approach would be changed if performed again, which are worked out more in Section 15.1

Overall the design behaves as expected on input changes, but the snowball effect is smaller than expected. As a result the code shows the behaviour as expected around the design point, however changing inputs significantly should be done with caution.

12.5. FEA Model Verification

The fuselage, tail boom and landing gear have been modelled with Ansys Mechanical, a Finite Element Analysis software. Because of limited computational power, resources, experience and time, the model has limitations, which are addressed as follows. Some verification has also been performed in order to increase the confidence of the results.

12.5.1. Setup

Because a truss structure is modelled, a 3D line body (no volume) body is initially created in Design Modeler CAD tool. An arbitrary, uniform cross section and material is assigned to the body, giving every truss mechanical properties. The body is subsequently meshed, by dividing each truss into elements of equal size. Under the assumption of a line body, the mesh is one-dimensional, which helps reducing the computational power required. Loads are applied to the line body, as specified in Section 7.1.3. In flight, reaction forces from wings and struts are applied to their points of attachment, and fixed supports are placed on the longitudinal axis, in between the attachment points, while at landing, the fixed support is placed at a particular landing gear, while the remaining loads are placed at respective points. The payload mass is simulated by distributing it on a plate, attached to the fuselage floor, while all remaining forces act on points (connections of trusses). The load factor n is altered by modifying the direction and magnitude of the acceleration. The assumed ambient temperature is 22°C.

The solver assumes small deflections, as well as inertia relief and quasi-static solution settings are off. The problem is static, meaning no step control is required. The mesh is refined in a single loop, with a double refinement depth. The desired output is axial forces for truss members and internal shear and moment for beams. These are independent of cross-sections, thus original cross-section assignment is negligible. Based on the output, the cross sections for individual trusses and beams are designed.

12.5.2. Convergence Study

A convergence study is performed in order to investigate how dependent the result is on the mesh element size, and is shown on Figure 12.1. The vertical axis shows the non-dimensionalised node deformation

(taken at maximum deflection of the structure, the tip of the tail boom). Its value refers to how much the deformation at a given mesh element size is with respect to the deformation at a minimum mesh element size.

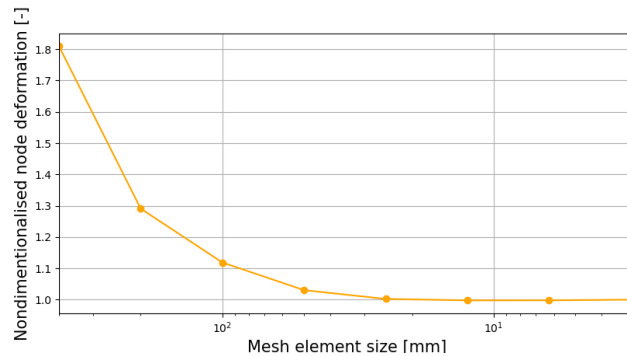


Figure 12.1: Nondimensionalised deformation as function of mesh element size

Initially, the mesh element length is set to 50 mm, which gives an error of 3% with respect to deformation at mesh element size of 3 mm. For the final iteration, the mesh element length is halved to 25 mm, giving an error of 0.2%. This is considered sufficient, given the limited accuracy of other design parameters. It should be noted, that the convergence study is realised on deformation on an arbitrary point, while the used output of the program are internal forces, which is still applicable as deformation originates from internal forces.

12.5.3. Analytical Value Comparison

In order to verify the values outputted by the FEA software, a comparison between numerical and analytical results of a simple canter lever beam loaded at the tip is performed, as shown on Figure 12.2. Figure 12.2a shows the deformation of shortened tail boom tip fixed at root, while Figure 12.2b shows the internal bending moment at the root, under different loads. The reference analytical relations for canter lever beam tip deformation v_{max} and internal bending moment M at root are given by Equation 12.1 [53, p. 830] and Equation 12.2, respectively. For reference, $L=1$ m, $E = 2 \cdot 10^{11}$ Pa and $I_{xx} = 7.67 \cdot 10^{-7}$ m⁴.

$$v_{max} = \frac{PL^3}{3EI} \quad (12.1)$$

$$M = L \cdot P \quad (12.2)$$

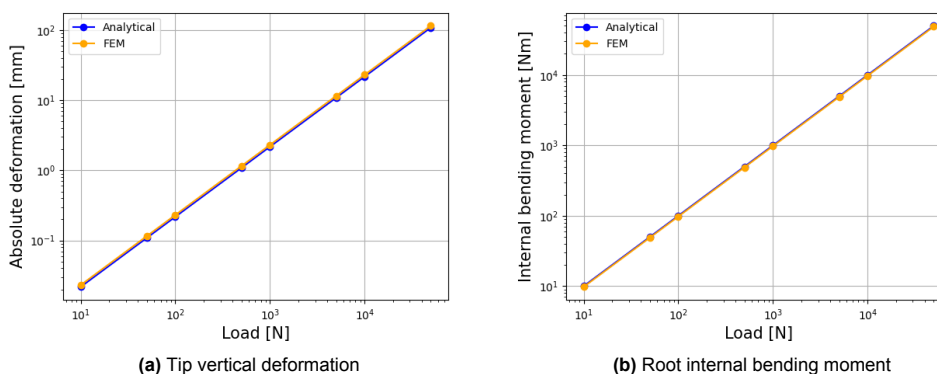


Figure 12.2: Analytical and numerical results for simple canter lever beam loading

The analytical and numerical curves nearly overlap, which confirms the purpose of using the FEA software. The small difference observed is believed to lie in the discretisation of the beam into nodes. Since the study has been done on an element of $L=1$ m with mesh size of 25 mm, the difference should be smaller with regard to the entire fuselage, which is an order of magnitude larger, while keeping the same mesh size.

Final design overview

This chapter will present the integration and final design overview of the UAV. The design choices made for each subsystem respectfully are combined and put into context. Some top-level system parameters, like total drag and the aircraft stability parameters, are computed. Firstly, some important design parameters are shown in Table 13. Next to that, a three-view diagram is shown in page 114.

Table 13.1: Aircraft final design parameters

Parameter	Value	Unit	Parameter	Value	Unit
A	8	[-]	C_{D_0}	0.0303	[-]
$CL_{max_{clean}}$	1.42	[-]	C_{M_α}	-1.08	1/rad
MAC	1.15	m	S_w	10.37	m ²
Range	250	km	SFC	9e-08	kg/J
V_{cruise}	105	kts	V_{stall}	50	kts
OEW	349.83	kg	$m_{payload}$	276	kg
MTOW	669.26	kg	Wing span	9.109	m
Service ceil- ing	20,000	ft	Oswald effi- ciency	0.775	[-]
η_p in cruise	0.82	[-]	Fuel capacity	70	L
$P_{br_{max}}$	100	hp	λ	0.6	[-]
Runway length	750	m	Engine	Rotax	[-]
				912	

13.1. Total Drag

The drag can be split up into zero lift drag (or parasitic) and lift induced drag, as shown in Equation 13.1 [30]. The total drag of the aircraft is thus found by a summation of the zero-lift drag of each component and the lift induced drag.

$$C_D = C_{D_0} + C_{D_i} \quad (13.1)$$

Zero Lift Drag

Zero lift drag (C_{D_0}) gives an indication of how streamlined a body is. It is build up from skin friction drag (C_{f_c}), pressure drag due to viscous separation, captured in the form factor (FF), and interference drag caused by disturbance in the airflow due to interactions between subsystems (wing and fuselage for example), captured by the interference factor (IF). This is given in Equation 13.2 [54].

$$C_{D_0} = \frac{1}{S_{ref}} \cdot \sum_{c=1}^7 C_{f_c} \cdot FF_c \cdot IF_c \cdot S_{wet_c} + \sum_{c=1}^7 C_{D_{misc_c}} \quad (13.2)$$

In the calculation of the zero lift drag it is assumed that all non-lifting components have similar flow characteristics. That is, the flow is assumed fully turbulent, whereas lifting surfaces have 10 % laminar flow [54]. Furthermore, the interference drag of the boom and landing gear strut is assumed to be similar to that of the wing strut. Due to the deviations from a smooth surface a factor of 20% is added, called excrescence drag. This accounts for all additional deviations from a smooth surface. This for example includes misalignment of sheets, but also from antenna or skin roughness [55]. This is a relatively high factor as usual values lay between 5 and 10 % for general aviation aircraft [54]. However, due to the many deviations from a smooth surface over the entire aircraft and the overall not fully aerodynamically optimized shape an higher factor is taken. An overview of the zero lift drag breakup for each component is given in Table 13.2.

Table 13.2: Overview of the drag contributions to every system, including the total aircraft's zero lift drag.

	C_f [-]	FF [-]	IF [-]	S_{wet} [m ²]	$C_{d,misc}$ [-]	C_{D_0} [-]
Wing	0.003238	1.235	1.00	22.20	0.000000	0.008559
Horizontal Tailplane	0.003238	1.221	1.05	3.566	0.000000	0.001427
Vertical Tailplane	0.003238	1.221	1.05	1.602	0.000000	0.000641
Landing Gear Strut	0.003514	1.160	1.10	0.055	0.000000	0.000024
Landing Gear Wheels	0.000000	0.000	0.00	0.000	0.005090	0.005090
Fuselage	0.003514	1.817	1.00	14.02	0.000768	0.009400
Strut	0.003514	1.108	1.10	0.058	0.000000	0.000024
Boom	0.003514	1.148	1.10	0.017	0.000000	0.000007
Excrescence Drag	-	-	-	-	-	+20%
Total Drag	-	-	-	-	-	0.0303

Lift Induced Drag

Lift induced drag however originates from the redirection of the airflow as lift is generated, causing a downwash behind the aircraft. This is given by Equation 13.3.

$$C_{D_i} = \frac{C_L^2}{\pi \cdot AR \cdot e} \quad (13.3)$$

Here the Oswald efficiency factor (e) is derived from the spanwise efficiency factor (e_{theo}) and correction factors for the fuselage ($k_{e,F}$), zero lift drag ($k_{e,C_{D_0}}$) and compressibility effects ($k_{e,M}$) [36]. However the correction factor for compressibility equals one due to the low Mach number. Next, the zero lift correction follows from statistics and the spanwise efficiency factor is computed by lifting line analysis as described in Chapter 8. The values for the wing span (b) and fuselage diameter (d_F) are derived in Chapter 8 and Chapter 7 respectively. This gives an Oswald efficiency factor of 0.7748.

Total Drag

Using the found zero lift drag, aspect ratio of all lifting surfaces and their respective span efficiency factor, or Oswald efficiency factor for the lift and fuselage, the total drag is obtained using Equation 13.4. In cruise condition this gives Equation 13.5.

$$C_D = C_{D_0} + C_{D_{i_w}} + C_{D_{i_h}} + C_{D_{i_v}} = 0.0303 + \frac{C_{L_w}^2}{\pi \cdot AR_w \cdot e_w} + \frac{C_{L_h}^2}{\pi \cdot AR_h \cdot e_h} + \frac{C_{L_v}^2}{\pi \cdot AR_v \cdot e_v} \quad (13.4)$$

$$C_D = 0.0303 + \frac{C_{L_w}^2}{\pi \cdot 8 \cdot 0.7748} + \frac{-0.2766^2}{\pi \cdot 5.1333 \cdot 0.9696} + \frac{0.07178^2}{\pi \cdot 1.9176 \cdot 0.9966} \quad (13.5)$$

$$= 0.0303 + 0.0514 C_L^2 = 0.0303 + 0.0514 \cdot (0.4794)^2 = 0.0421$$

13.2. Stability and Control of Entire Aircraft

As described in Section 8.1.7 AVL has been used to perform stability analysis of the aircraft. To meet REQ-USER-AC-S&C-01, stating "the aircraft should be as stable as a Cessna 172" all derivatives that could be found of this aircraft have been computed in AVL for comparison. These are listed in Table 13.3 where the relative difference of the current design is given w.r.t. the Cessna 172 derivatives [56]. Overall, relative errors are within acceptable bounds. However, some show bigger than expected differences, which will be analysed in more depth.

Control surface derivatives ($C_{x_{\delta_a}}$, $C_{x_{\delta_e}}$ and $C_{x_{\delta_r}}$, with x indicating 'any') are not listed here due to the differences in size of the Wing For Aid design and the Cessna 172. Moreover, for example the elevator of the design is a full moving tailplane whereas the Cessna 172 only uses part of the horizontal tail. Logic tests have however been performed on the control surface derivatives to test the accuracy of the simulation. Moreover, the coefficients for the elevator deflection are for example indeed bigger for the design compared

to the Cessna.

The difference in C_{l_β} and C_{Y_p} has already been extensively covered in Section 8.1.3. In short, the current design is spirally unstable whereas the Cessna 172 is not. This can be changed by adding an higher dihedral angle (current 1.5). However, wing fuselage interactions are not modeled in AVL, therefore lowering the values for C_{l_β} and C_{Y_p} compared to real-life. Spiral instability is however a slow eigenmode and correct implementation of the auto-pilot should assure for plenty of time before the spiral diverges significantly. In case this is however still not desired dihedral can easily be added by increasing the strut length, due to the pinned wing. This could even be altered at late stages of the design when test flights have already been performed. Next to that, a dorsal fin could also show beneficial effects, which is explained in more detail in Section 9.3.2.

The design also under performs in terms of the vertical tails effectiveness in case of sideslip compared to the Cessna 172. Moreover, the force in spanwise direction generated by the vertical tail increases less with increasing sideslip angle compared to the Cessna. For now this is however considered acceptable, as the created yaw moment is sufficient because of the relatively long moment arm. This can however easily be altered if in later stages this is desired to be changed. This can be done by increasing the surface area of the vertical tail, either directly or by use of an dorsal fin, described in Section 9.3.2.

Overall, stability of the design is thus comparable with the Cessna 172. The design is considered slightly less stable overall however due to the spiral instability characteristics described above, yet statically it is more stable.

Derivative	AVL	Cessna 172 [56]	Relative Difference in %
C_{L_α}	4.6	5.1	-9.8
C_{m_α}	-1.08	-0.89	+24
C_{Y_β}	-0.18	-0.31	-42
C_{l_β}	-0.044	-0.089	-51
C_{n_β}	0.078	0.065	+20
C_{Y_p}	0.012	-0.037	+132
C_{l_p}	-0.41	-0.47	-13
C_{n_p}	-0.026	-0.030	-13
C_{Y_r}	0.18	0.21	-14
C_{l_r}	0.099	0.096	+3.1
C_{n_r}	-0.090	-0.099	-9.1

Table 13.3: Overview of all stability derivatives of the entire aircraft with the absolute relative error of the AVL model with respect to the Cessna 172 values.

13.3. Friendly-Look Assessment

Wings for Aid listed a user requirement for the aircraft to look friendly. To assess whether this requirement is met, the design was shown to a number of people. Their thoughts on the design were captured. In total, 59 people responded to the assessment. 56 people responded that the aircraft does not look scary or intimidating. Additionally, one of the respondents replied that the aircraft looks "Teddybear friendly". Three respondents mentioned that a remotely piloted aircraft can be scary or intimidating by default, especially considering the recent use in wars around the world. Because of this, it is extra important that the UAV looks friendly. Transparency is one of the key values of Wings for Aid, the respondents were asked whether implementing transparent fairings in the design adds to the friendliness of the aircraft. The results of this question are shown in

Are the see-through doors more confidence inspiring than the white doors?

59 antwoorden

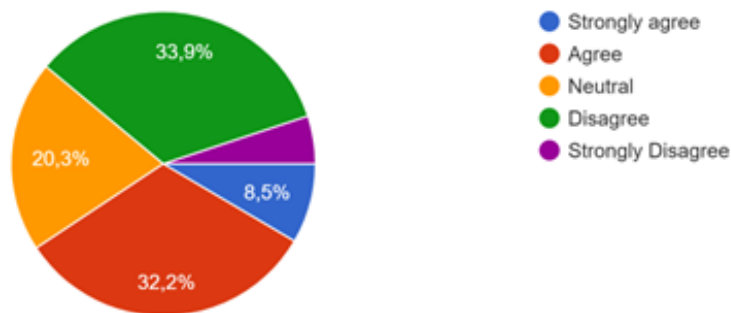


Figure 13.1: Responses to the question "Are transparent doors confidence inspiring?"

Following these results, it is safe to conclude that the aircraft does not look scary or intimidating. The respondents were also asked whether they had any recommendations to add to the 'friendliness' of the design. Out of these recommendations, the one that was mentioned most often was to add human characteristics, like a face, to the aircraft.

13.4. Resource budgeting

Concluding, the final values for mass, cost, power and volume of the main components are presented in Table 13.4 and Table 13.5 The cost per subsystem is presented in Table 13.6.

Table 13.4: Summary of aircraft manufactured components characteristics

Sub- system	Part	Manufactured				
		# Units	Mass [kg]	Cost [€]	Power [W]	Volume [L]
STR	frame	1	45.0	710	0	0
STR	panels	1	12.8	570	0	0
STR	boom	1	7.6	(STR)	0	0
STR	interfaces	1	10.7	360	0	0
STR	landing gear	1	14.8	100	0	0
STR	strut	2	2.6	0	0	0
STR	wing	2	19.2	3714.5	0	0
STR	empennage	1	31.7	770	0	0
STR	assembly	1	12.1	5580	0	0
PRO	Tanks	2	4.9	1170	0	50
PRO	Fuel system	1	3.5	1000	0	10
GNC	electronics	1	0.2	130	0.4	0.3
PWR	cables	1	0.8	50	0	0

Table 13.5: Summary of aircraft commercial components characteristics

COTS						
Sub- system	Part	# Units	Mass [kg]	Cost [€]	Power [W]	Volume [L]
PRO	Engine	1	67.7	10000	100	0
PRO	Propeller	1	10	2500	0	0
GNC	Instruments	34	0.1	200	1	0.1
GNC	Actuators	1	17.1	4870	13.3	0
COM	transmitter	1	0.9	660	2.1	1.9
COM	antenna	1	0	100	0	0
COM	receiver	1	0.7	640	2	1.4
PWR	generator	1	3.8	1530	1135.7	0
PWR	battery	1	5.9	100	217.9	2.3
PWR	controls	1	15.6	1000	0	0
OBC	ADC	1	0.6	2730	9.8	0
OBC	NAV	1	0.8	3050	5.5	0
OBC	FDR	1	0.5	1280	3	0
OBC	GNC	1	1.8	4180	193.7	0

Table 13.6: Aircraft system characteristics summary

	Mass [kg]	Cost [€]	Power [W]	Volume[L]
STR	193	9210	0	0
PRO	86.1	14670	100	60
GNC	21.8	6350	2	0.2
COM	1.8	1530	4.5	3.6
PWR	27.5	2680	1353.6	2.3
OBC	3.7	11240	212	0
UAV OEW	333.9	45680	1672.1	6.1
COTS		34120		

The subsystem and total sum is shown in Table 13.6. The total equipment weighs almost 60kg and takes about 10 L which fits between the nosecone firewall and the first batch of boxes. Overall, an estimated 34,000€ is COTS out of 54,000€ total or 64% which is fitting with the customer's desire to have as much as possible already designed.

13.5. Requirement Compliance

With the final design values known, the requirement compliance can be analysed. This analysis is done through the requirement compliance matrix seen in Table 13.7 in which for each user requirement it is indicated whether the requirement is met.

Table 13.7: User requirements compliance matrix

Code	Requirement	Compliance
REQ-USER-OPS-01	The aircraft shall be able to be disassembled so that it can be fitted into a 40 ft ISO container.	
REQ-USER-OPS-02	The aircraft shall be able to operate 24/7.	
REQ-USER-OPS-03	The aircraft and its systems shall be operable in a temperature range of -5 to 50°C.	Requires thermal performance investigation in all sub-systems
REQ-USER-OPS-04	The aircraft and its systems shall be able to operate during rain.	

REQ-USER-OPS-05	The aircraft shall be able to perform at least three aid missions within 24 hrs.	
REQ-USER-OPS-06	The aircraft without payload shall have an endurance of at least 10 hrs.	Endurance = 12.84 hrs
REQ-USER-OPS-07	The aircraft shall be able to operate in conditions similar to a UH1 helicopter.	Not specific enough
REQ-USER-OPS-08	The aircraft shall be able to operate in mountainous regions.	
REQ-USER-OPS-09	The aircraft shall be able to operate in desert conditions.	
REQ-USER-OPS-10	The design of the aircraft shall guarantee the cargo loading to be performed outside of the propulsion system zone.	
REQ-USER-OPS-11	The design of the aircraft shall guarantee fueling to be performed outside of the propulsion system zone.	
REQ-USER-OPS-12	The visual inspection of the cargo bay shall be possible by opening hatches or clear windows.	
REQ-USER-OPS-13	The aircraft shall look friendly.	Requires further investigation
REQ-USER-OPS-14	The aircraft shall be able to take off and land on paved runway surface.	
REQ-USER-OPS-15	The aircraft shall be able to take off and land on grass runway surface.	Type I airfield
REQ-USER-OPS-16	The aircraft shall be able to take off and land on gravel runway surface.	Type I airfield
REQ-USER-OPS-17	The aircraft shall be able to take off and land on unprepared runway surface.	Type I airfield
REQ-USER-OPS-18	The avionics system of the aircraft shall be swarm compatible.	Requires further investigation of autopilot capabilities
REQ-USER-OPS-19	The aircraft shall use as many standard of the shelf parts as possible	Not specific enough
REQ-USER-MANV-01	The aircraft shall be able to fly at a minimum altitude of 15 <i>m</i> within fly-in and drop zone.	
REQ-USER-MANV-02	The aircraft shall be able to accurately deliver a package within a drop-zone of 25 by 25 m.	
REQ-USER-MANV-03	The aircraft shall be operable at a visibility condition of at least 100 m during take-off and landing.	Required further investigation of autopilot capabilities
REQ-USER-MANV-04	The maximum runway length for take-off and landing shall be 750 <i>m</i> .	Worst condition: $L_{runway} = 742 \text{ m}$
REQ-USER-MANV-05	The aircraft shall have a maximum stall speed at an airspeed of 50 <i>kt</i> at its maximum take off weight.	Minimum stall speed = 50 kts
REQ-USER-MANV-06	The aircraft shall be able to climb at a rate of at least 500 <i>ft/min</i> at sea level.	Climb rate: 1280 ft/min

REQ-USER-COST-01	The unit cost of one aircraft shall not exceed €25,000.	Unit cost: €41300
REQ-USER-COST-02	The operational costs shall at maximum be 2-4 times the operational costs of a truck per delivered <i>kg</i> .	Operational cost: €1.50 per kg payload (6 times price truck)
REQ-USER-AC-S&C-01	The aircraft shall be at least as stable as a Cessna 172.	Aircraft is spiral unstable
REQ-USER-PL-01	The aircraft shall be able to carry a payload of at least 10-12 boxes of 20 kg each.	
REQ-USER-PL-02	The total operational aid delivery capacity per 24 <i>hrs</i> shall be comparable with the aid delivery capacity of a C-130 Hercules.	Total operational aid delivery capacity per 24 <i>hrs</i> for a fleet of 19 aircraft is 20480 kg.
REQ-USER-FENV-01	The aircraft that is loaded with payload shall have a range of at least 500 km.	
REQ-USER-FENV-02	The aircraft shall have a ferry range of at least 1000 km.	Ferry range = 1077 km
REQ-USER-FENV-03	The aircraft shall have a maximum operational altitude of 18000 ft.	Service ceiling 20694.38 ft
REQ-USER-FENV-04	The aircraft shall have a cruise speed in the range of 100 to 110 kts.	$V_{cruise} = 105$ kts
REQ-USER-AC-PROP-01	The aircraft shall be powered by an engine equivalent to the Rotax-912.	Engine: Rotax-912 (100 hp)
REQ-USER-AC-PROP-02	The aircraft propulsion unit shall be powered by AV-GAS or gasoline.	Gasoline

13.6. Feasibility Analysis

From the requirement compliance matrix, it was concluded that a number of user requirements were either not met or not analysed in this stage of the design. In this section, the feasibility of the design will be discussed regarding the requirement with which the design did not comply.

- **REQ-USER-COST-01:** The proposed design exceeds the requirement of keeping the unit cost below €25,000 by 65%. The main components of the cost are the engine and the equipment onboard. In consultation with the client, the agreement was made that exceeding the cost requirement is acceptable as long as there is compensation for it in other aspects. In further design, the possibility of cost reduction by mass ordering or production will have to be analysed. The mitigation of cost are discussed in more detail in Figure 14.1.2.
- **REQ-USER-COST-02:** The operational cost of the proposed aircraft exceeds the cost per kilogram of payload requirement of €0.96 per kilogram by 56%. Hence, the user requirement is not met. To the client it was given as a suggestion that a driving aspect of the operational cost is the transport to the affection region. Having aircraft already stored or operable in other businesses close to high-risk regions, can significantly decrease this cost. However, by having the aircraft more spread the company will be more decentralised which can also result in unforeseen costs.
- **REQ-USER-AC-SC-01:** As was discussed in Section 13.2, for most of the stability characteristics the stability and control derivatives were in the same order as the derivatives of the Cessna-172. Only for spiral stability does the aircraft not meet the performance of the Cessna-172. The choice was made to design the aircraft with spiral instability which will be compensated by the autopilot. In that way, the

spiral instability does not influence the performance of the aircraft during operation. Next to this, also more analysis can be done into the implementation of a higher angle of dihedral or other solutions.

- REQ-USER-OPS-03: During the design analysis, the range in temperature is only taken into account in the material trade-off. For other aspects such as thermal loads, functioning of equipment and thermal management onboard were not addressed in the design analysis so far.
- REQ-USER-OPS-13: The aircraft is also required to look friendly in operation. There are two ways in which friendliness are implemented in the design. Firstly, the structure of the payload bay was made transparent to show the company does not have anything to hide. Secondly, by implementing certain colour profiles the look of the aircraft is less threatening. These suggestions were however not tested and because of that there is no proof of how they affect the friendliness of the aircraft.
- REQ-USER-OPS-18: This user requirement states that the design shall be swarm-compatible. From the operations perspective, this requirement has been taken in mind to optimise the loading and fuelling time. The ground base shall be set-up so that an entire fleet of aircraft can be operated from it. On the other hand, no analysis was performed on the equipment needed to have the autopilots of different aircraft communicating together.
- REQ-USER-OPS-19: During the design, the user requirement to make use of as many product that are sold of the shelf was interpreted by using product that are easily available and supplied to Wings for Aid. This has mainly been taking into account for the selection of the engine and equipment. For other materials in the aircraft structure no analysis was performed about the availability of the products. It is expected though that because of the simplicity of the design, no parts of the design will be difficult to access.
- REQ-USER-MANV-03: For visibility, it was required that the aircraft shall be able to operate at visibility levels of lower up to 100 meter. In principal, the aircraft will not operate based on visual information but based on the instructions of the autopilot. However, the take-off, landing and dropping performance at low-visibility shall be analysed.

13.7. Modularity

One of the advantages of this design is its modularity. This property allows for many parts to be taken apart from the aircraft and switched with a new part in case there is a damage, with minimum complexity.

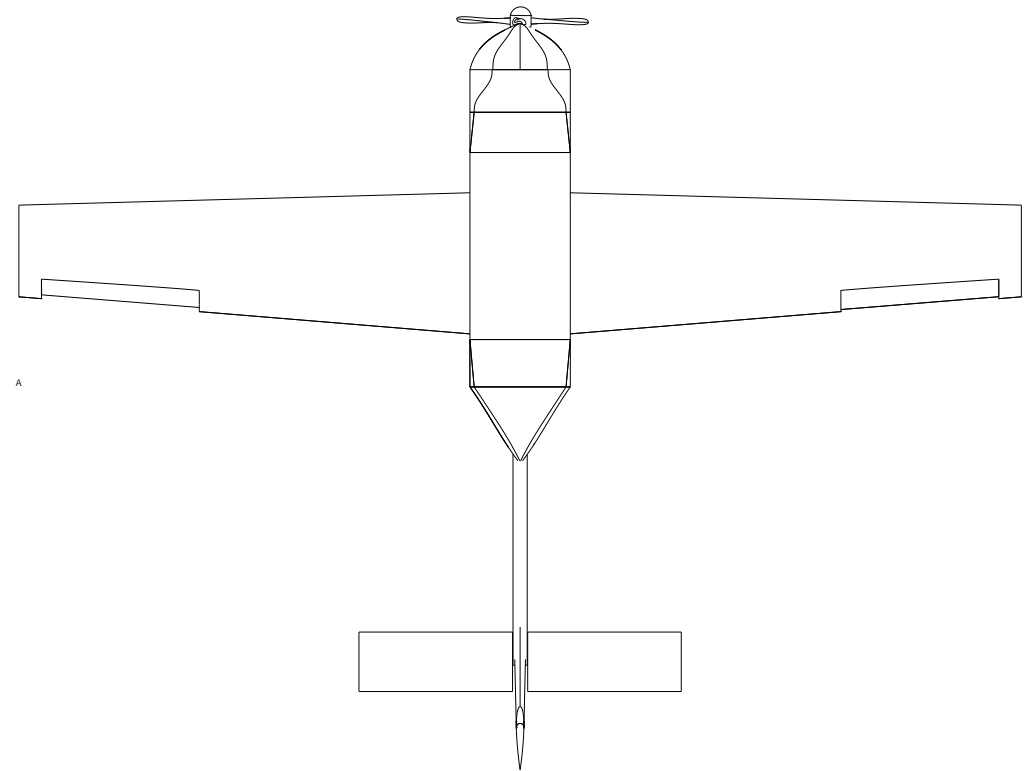
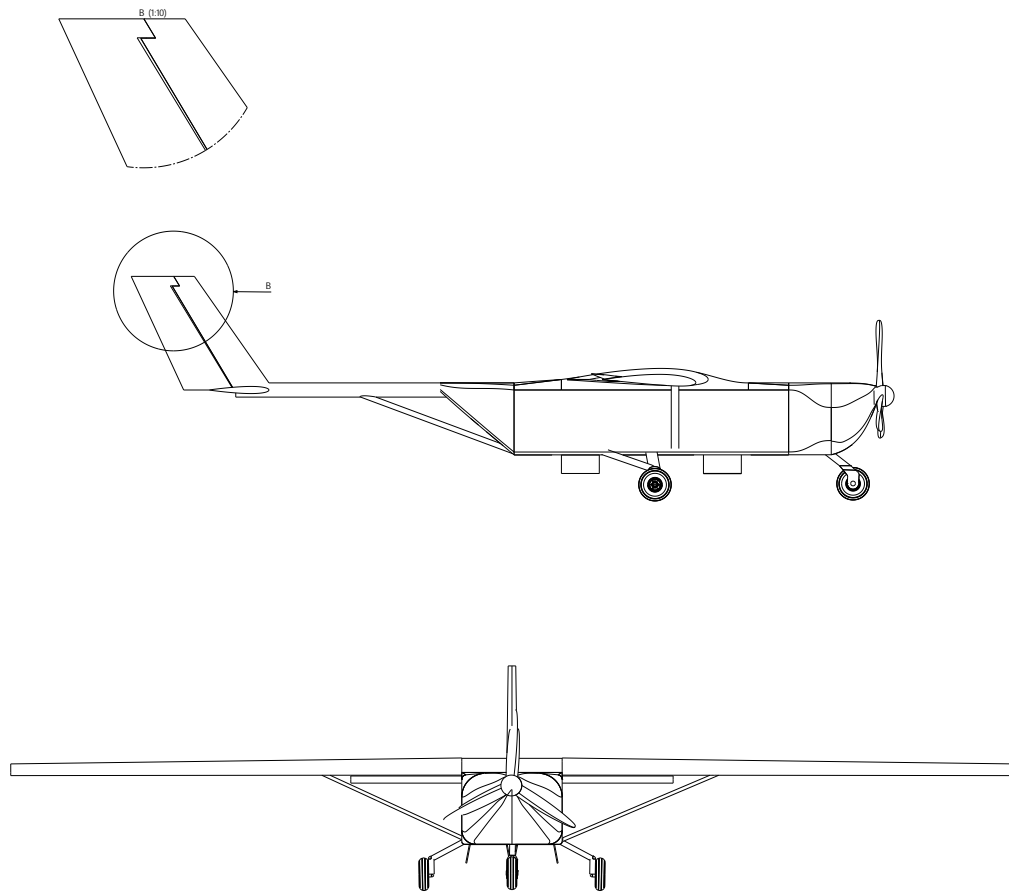
The modular parts in this design are as follows:

- The wing
- The horizontal tailplane
- The struts
- The propeller
- The engine

Both the wing and the horizontal tailplane are pin connected to the fuselage which facilitates the option of removal and replacement. Furthermore, the struts of the structure are all modular and possible to be exchanged in any case of failure and prevent the failure from propagating to the entire fuselage structure. Next to that, the choice of ground adjustable propeller makes the replacement of the propeller in case of a damage very easy, even though the probability of the propeller failing is small. The engine is integrated in the structure in a way for it to be possible to be taken out and replaced in case of failure.

For future design, the boom can be used to swap out different tails for different application areas.

Three View Drawing of the Final Design



Final Design Evaluation

This chapter aims to evaluate the design as summarised in Chapter 13. The evaluation entails the production plan, operational cost assessment, return on investment analysis and RAMS analysis. Among other things, the unit cost of an aircraft is calculated in the production plan. The operational cost assessment breaks down expenditures that occur in the operational lifetime. Subsequently, the return on investment analysis assesses whether the project is worth investing in. Finally, the RAMS analysis is performed. This analysis covers the reliability, availability, maintenance and safety of the current design.

14.1. Production Plan

The present section covers the production plan. The production plan is built up out of the manufacturing of parts, the assembly of the aircraft, the unit cost assessment based on the parts used, container fitting and end-of-life procedures.

14.1.1. Manufacturing

In the context of this production plan, parts are manufactured in-house by one of two processes: welded tube frame or joined (rivets / bolts) panels. Alternatively, they are acquired from suppliers (COTS). Each process's associated cost and weight penalty will be discussed in the following section.

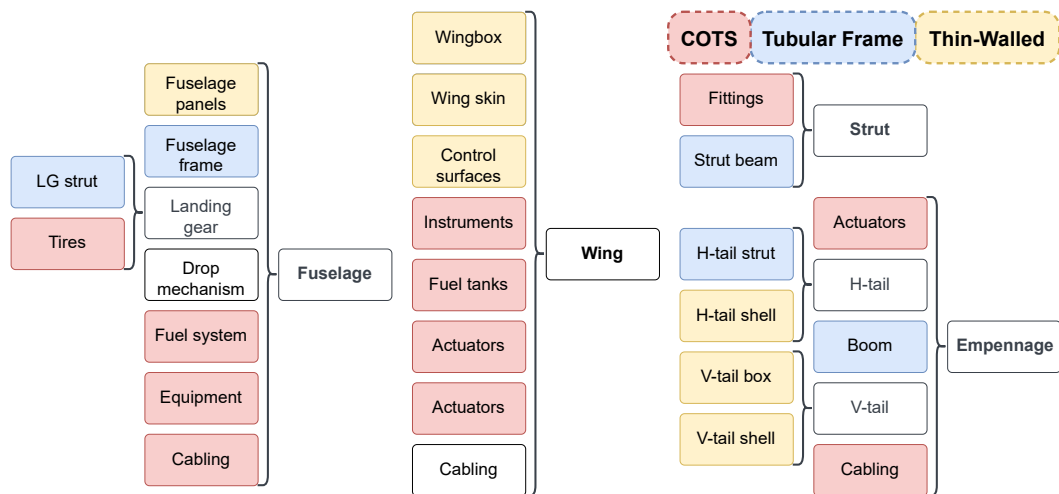


Figure 14.1: Manufacturing chain of the aircraft's parts into components

Tubular frames are obtained by cutting the tubes to size, and welding them. The costs associated are as follows:

- material: proportional to the mass of the tube stock acquired
- Cutting: assumed cost of 2€ per operation i.e. 4€/tube
- welding: the costs associated with a welding operations contain many operations. However, statistics¹ show that an approximation proportional to the perimeter of the weld of about 30€/m is reasonably accurate. A similar method considering the welded volume is used in conjunction with rod density² to estimate the weight deposited in the process (0.09kg/m).

¹parametric cost components of welding

²Twi-Global - calculating weld volume and weight

Computing for each part of the frame structure Section 7.1.4, Section 10.3, Section 9.2.3 and summing up yields a fuselage sub-assembly of 55.5kg (570€) and a total of 84kg and 715€ for the truss structure.

Table 14.1: Frame welding summary (Steel 4130)

	N part [#]	Dimensions					Cost [€]			
		t [mm]	r [mm]	p [mm]	A[m ²]	M [kg]	Cutting	Welding	Material	Assembly
fuselage	35	0.6	10	63	3.77E-05	70	66.15	7.01	143.16	
	35	0.7	15	94	6.60E-05	70	98.7	15.99	184.69	
	25	0.9	18	113	1.02E-04	50	84.75	18.57	153.32	
	7	1	24	151	1.51E-04	14	31.71	10.58	56.29	
	1	1.2	30	188	2.26E-04	2	5.64	4.18	11.82	
fuselage	0	0	0	0	0.00E+00	0	286.95	56.33	549.28	
main gear	6	2.5	50	314	8.01E-04	12	56.52	17.59	86.11	
nose gear	2	1	25	157	1.57E-04	4	9.42	0.86	14.28	
elevator spar	1	1	35	220	2.20E-04	2	6.6	2.58	11.18	
tail boom	1	1.4	75	471	6.60E-04	2	14.13	14.27	30.4	
Frame	113								691.25	

Panels are estimated using the same approach with a different set of processes. Each part is cut, formed if flanges, bends or reinforcements are needed and riveted to the sub-assembly or frame. Costs are estimated as follows:

- Forming: Encompasses a few different processes yielding the same result depending on the material, size and complexity of the operation. In the case of composite construction for the fairings, the forming process includes every part of the manufacturing ³Technical cost modelling and efficient design of lightweight composites in structural applications at 150€/kg. Metal panels are assumed to follow the 80/20 rule ⁴ i.e. a fourth of the material cost.
- Cutting: except in the case of thick parts (>10mm) the cost is assumed to be 5€/panel
- Riveting: the number of rivets is set to be proportional to the perimeter of each panel, the pitch is assumed to be 10 cm for all parts at this stage of the design. Taking the average of the cost of rivets (15-50€/1000) ⁵ and a labor of 10s/rivet at 17€/h yields 0.08€/rivet.

Computing for the fairings Section 7.2.3, wing-box Section 8.2.3 and empennage. Each set of parts is put together in sub-assemblies as seen below:

Table 14.2: Fuselage fairing manufacturing summary (GFRP)

	N part	Dimensions							M [kg]	Cost [€]				
		b [m]	l [m]	t [mm]	p [m]	A [m ²]	rivet [/m]	N rivets		Cutting	Forming	Joining	Material	Part
loading panels	2	1.102	4.6342	0.5	11.5	1.90E+00	5	57	1.805	0	270.73	4.54	52.35	327.62
drop panel	12	0.45	0.45	0.5	1.8	2.65E-01	5	9	0.251	0	37.65	0.7175	7.279	45.65
fuselage top	1	1.102	4.6342	0.5	11.5	3.25E+00	5	57	3.083	0	462.42	4.544167	89.407	556.37
nosecone	1	1.102	1.102	0.5	4.4	1.00E+00	5	22	0.95	0	142.49	1.753889	27.55	171.79
tailcone	1	1.102	1.102	0.5	4.4	1.42E+00	5	22	1.347	0	202.04	1.753889	39.063	242.86
stiffeners	40	0.02	1	0.55	2	2.00E-02	5	10	0.021	0	3.15	0.797222	0.609	4.56
Fuselage	57								12.8					2840

³Technical cost modelling and efficient design of lightweight composites in structural applications

⁴Dallan - manufacturing cost of sheet metal

⁵TWI global - cost of self-piercing riveting system

Table 14.3: Wingbox manufacturing summary (AI-5052-H38)

	Dimensions									Cost [€]					
	N part	b [m]	l [m]	t [mm]	p [m]	A [m2]	rivet [/m]	N rivets	Cutting	Forming	Joining	Material	Part		
skin	2	1.16	8.62	0.5	19.6	5.97E+00	10	196	8.001	150	5.62	15.63	22.48	193.73	
front spar	1	0.164	8.62	1.3	17.6	1.41E+00	10	176	4.925	30	3.46	14.03	13.84	61.33	
aft spar	1	0.0902	8.62	1	17.4	7.78E-01	10	174	2.084	30	1.47	13.87	5.86	51.2	
stringers	26	0.0225	3.45	0.5	6.9	7.76E-02	10	69	0.104	5	0.07	5.5	0.29	10.86	
stringers	23	0.0225	0.575	0.5	1.195	1.29E-02	10	11	0.017	5	0.01	0.88	0.05	5.94	
stringers	20	0.0225	0.575	0.5	1.195	1.29E-02	10	11	0.017	5	0.01	0.88	0.05	5.94	
stringers	17	0.0225	0.575	0.5	1.195	1.29E-02	10	11	0.017	5	0.01	0.88	0.05	5.94	
stringers	14	0.0225	0.575	0.5	1.195	1.29E-02	10	11	0.017	5	0.01	0.88	0.05	5.94	
stringers	11	0.0225	0.575	0.5	1.195	1.29E-02	10	11	0.017	5	0.01	0.88	0.05	5.94	
stringers	8	0.0225	0.575	0.5	1.195	1.29E-02	10	11	0.017	5	0.01	0.88	0.05	5.94	
stringers	5	0.0225	0.575	0.5	1.195	1.29E-02	10	11	0.017	5	0.01	0.88	0.05	5.94	
stringers	2	0.0225	0.575	0.5	1.195	1.29E-02	10	11	0.017	5	0.01	0.88	0.05	5.94	
stringers	0	0.0225	0.575	0.5	1.195	1.29E-02	10	11	0.017	5	0.01	0.88	0.05	5.94	
ribs	14	0.175	1.16	1	2.7	7.91E-02	20	54	0.212	20	0.15	4.31	0.6	25.06	
Wing	144							4392	30.4					2950	

Table 14.4: Empennage manufacturing summary (AI-5052-H38)

	Dimensions									Cost [€]			
	N part	b [m]	l [m]	t [mm]	p [m]	A [m2]	rivet [/m]	N rivets	Cutting	Forming	Joining	Material	Part
bottom shell	2	1.1	0.275	0.0005	2.75	3.03E-01	15	82	5	0.63	6.54	2.51	36.36
top shell	2	1.1	0.275	0.0005	2.75	3.03E-01	15	82	5	0.63	6.54	2.51	36.36
skin	2	1	0.25	0.001	2.5	2.50E-01	15	75	5	1	5.98	3.98	38.92
front spar	1	1	1	0.001	4	1.00E+00	15	60	5	1.91	4.78	7.62	22.81
aft spar	1	1	1	0.001	4	1.00E+00	15	60	5	1.91	4.78	7.62	22.81
stringers	10	0.06	1	0.002	2.12	6.00E-02	15	318	5	3.38	25.35	13.5	507.3
ribs	3	0.1	1	0.005	2.2	1.00E-01	15	99	5	2.93	7.89	11.71	93.09
Empennage	21							4075					757.65

14.1.2. Aircraft Unit Cost

Once every component has been put together into a sub-assembly, the aircraft can be test-fitted and packaged into its container awaiting an operation. Assembly cost in the aircraft industry has been estimated to be as high as 40% of the total price ⁶. Since the UAV has been designed with the goal of simplicity in assembly and lean-manufacturing in mind, the assembly fraction is assumed to be around 20% (i.e. half the maximum expected in worst-case conditions).

An estimate of the aircraft cost can be obtained using the information from Section 14.1.1 into the part-wise sum in Section 13.4 along with the assembly cost discussed. The initial value totals at 50,600€ per set of parts per unit of which 32,770 are COTS parts. This accounts for 63,250€ when adding the 20% assembly cost fraction: $C_1 = \frac{C_{manuf} + C_{COTS}}{1 - 0.2}$. However, the production scale of 500 units as asked by the client offer some ways to reduce the costs.

For the parts manufactured and assembled by Wings for Aid, two scaling factor can be applied: the production scale flows down from the factory scale, equipment and production chain, according to the amount of UAVs the OEM intends to produce - it affects all aircraft made in that factory and drives the investment costs. The learning curve factor is related to the increase in skill and optimization of the production chain with time. As such, the effect changes over time and the factor applied for this estimation is the cumulative average ⁷. The learning curve for the aerospace industry being around 85% ⁸ leads to a reduction of $C_{Manuf,N} = C_{Manuf,1} (1 + \frac{\log_{10}(0.85)}{\log_{10}(2)})$.

In the case of COTS, a discount can be applied when buying parts in batches. Furthermore, deals and agreements can be made directly from the manufacturer in order to reduce intermediates and associated costs for both parties. The discount model used assumes a 5% reduction for 50 units, 10% for 100 and 15% for

⁶FARO - trends in aerospace assembly

⁷AIAA DOI

⁸NASA learning curves [2012]

200 or, using a logarithmic model similar to manufacturing, $C_{COTS,N} = C_{COTS,1}(1 - (0.0721 \ln(n) - 0.2322))$, which can of course be adjusted per supplier's offers.

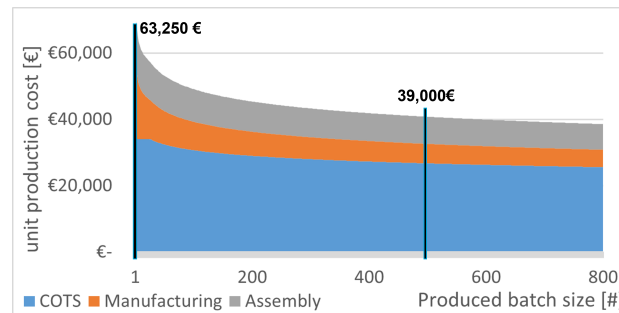


Figure 14.2: Production scaling with batch size

As shown in Figure 14.2, increasing batch size from 1 to 50 has a sizeable effect on the unit cost due to the manufacturing decrease. The COTS discounts starting at 50 then reduce it further until it levels out. The final unit cost for 500 units would be 42,000€, the last UAV costing only 39,000€. These figures still exceed the initial goal of 25,000€ but some measures can be taken to drive it down:

- non-certified electronics: the OBC and COM currently costs a combined 12,700€, which is mainly due to the certification cost of aircraft electronics. Switching to uncertified drone or UAV options could reduce it to as low as 5,000€ (Figure 11.4).
- open-source software: a large share of the cost comes from the licensed and verified software used in aircraft systems, sometimes dating decades. Using recently developed, open-source and free software such as MavLab's autopilot⁹ would reduce this to zero.
- cheaper engine option: see Table 6.1
- reliability concessions: components such as the battery and actuators are sized according to CS23 crewed aircraft regulations. Increasing the allowable risk would have little to no safety consequences at the cost of increased maintenance and repairs, lower availability and possible hurdles when shipping the aircraft to new countries. Careful study of these could allow for a reduction of up to 1,000€ (cost of redundant systems)
- manufacturing and assembly: the current estimate is based on aerospace-grade manufacturing standard and include many procedures, tests and documentation that may not be needed for a UAV, if some operational penalties can be accepted.

Applying these measures, however, have an adverse effect on reliability, complexity and most-importantly: operational cost. In this case, a decision should be made by weighing the customer's capacity for initial investment against the will to be competitive in the "last-mile" delivery market.

14.1.3. Container fitting

Once the aircraft is assembled, it is put in a 40 ft container. A visualisation of the container fitting can be found in Figure 14.3. In order to easily get the aircraft in and out of the container, a step-by-step plan is necessary. Assuming the aircraft is assembled before going in the container, it will have to be disassembled. Before the aircraft is put in the container, all other tools and spare parts which should be in the front of the container are fastened in their appointed locations. After this is completed, the horizontal tail is removed and attached to the designated hooks on the container walls. The next step is to remove the struts between the fuselage and the wings. This has to be done with at least three people, as the main wing will need to be held up by hand. Once the strut is removed, the wing will rotate at the root, where it is hinged to the fuselage. It is then slowly lowered until the tip rests on the ground. At this point, the root of the wing is detached from the fuselage and hung on the container wall. This is repeated on the other side.

Everything that is inside the container at this point in time should be checked to see if there are no loose parts that could potentially move around during transport. If everything is attached, the aircraft is rolled

⁹MavLab - LisaS world's smallest open source autopilot

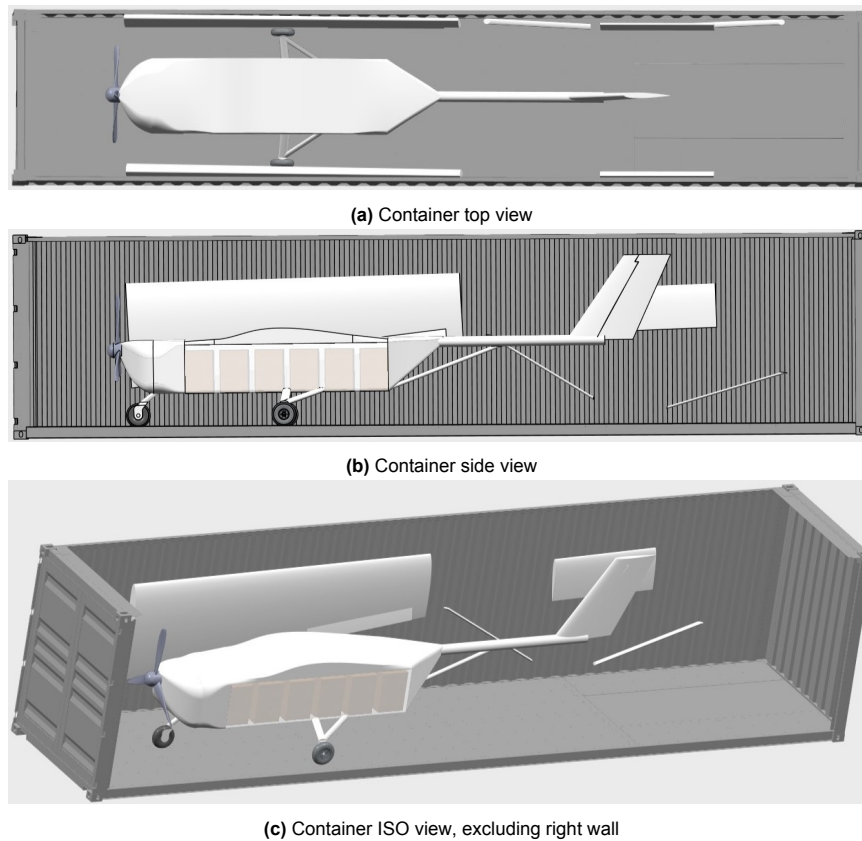


Figure 14.3: CAD render showing how the disassembled aircraft fits into the 40 ft ISO container

inside. There are latches on the floor to which the wheels can be fastened. Once these are locked in place, the excess empty space is filled with folded up aid boxes.

When the aircraft arrive at their desired ground base, the opposite steps can be followed to take everything out of the container and assemble the aircraft.

14.1.4. End-Of-Life Procedures

Finally, some considerations have to be taken for the end-of-life (EoL) plan of the aircraft. COTS components are often complex and contain a multitude of different materials, which make them hard to recycle. The airframe, however, is mostly made of steel and aluminium which be separated and melted with ease because of the modularity and simple disassembly built into the UAV. Other components could be upcycled and reused in a different airframe if enough lifetime is left (such as the computers, designed for 20,000 fh compared to the structure's 10,000 fh) effectively halving their environmental impact.

14.2. Operational Cost

Over the lifetime of the aircraft, the operational costs make up the biggest portion of the total cost. The longer the aircraft is in operation, the bigger the percentage of cost will be spent on operations. This also means that a big part of finding cost saving solutions is spent on operations. In this section, these costs and ways to minimise them are discussed. The section is divided into three parts, the facilities, ground base and sortie costs. All values are based on the defaults defined in Section 4.4.

The functions and activities defined in Chapter 4 are assigned the following parameters and their cost are computed according to The activity cost is then computed using: $CST = R(N \cdot C_u + ppl \cdot t \cdot W)$.

- Number N : of aircraft or parts related to said activity - e.g. 23 AC on GB and 18 operational AC for the sortie or 410 parts required fixing.

- Cost/unit C_u : cost of parts, elements such as transport cost or storage and manufacturing (unit AC cost)
- Recurrence R : how many times an activity takes place. Multiplying the activity cost and time along with its subparts. This is used in cases such as number of operations (178) or transport (1 for air, 2 for sea and back).
- time t : the time for a single instance of the activity to be executed, e.g. 35 hrs to ship the aircraft or 15 min to load the payload.
- People ppl : the number needed for that task. This can be derived from the labour hours needed divided by the time allocated.
- Wage W : depending on the task and qualifications required, a different wage is given per labour hour.

Costs are split in three categories: namely facilities (or external), ground-base and sortie.

Facility costs include storage, transport and extensive maintenance. When the aircraft are not in operation or undergoing maintenance, they are stored in strategically located storage facilities around the globe. Assuming a rate of 0.28 €/h-container along with enough UAVs ready at each harbour and the central airport for the required number of concurrent operations, storage accounts for up to 15% of the external costs. The extensive repairs can be either recurring (overhaul every 1500 h) or unplanned (UAVs shipped back from the GB). The number of aircraft which needs attention per operation comes from Section 14.4.3 and the parts cost is estimated to be €1000 for fixes and half that for planned activities on top of the labour (4 skilled people for 40 and 20 hours respectively).

The transport costs take up the biggest portion of facility costs at around 45%. Each aircraft does most of the distance from its storage location by ship or planes and the last part via truck. Shipping costs are calculated per km-kg (from Section 2.7) using a distance $d = C \frac{p_{earth}}{2N+1}$ (earth circumference p of 40,075 km) where the world coverage C (%) and number of bases N plays an important role for ships or planes and 500 km from shore to GB for trucks. The time component is based on the respective speed of each transport ¹⁰. Because of the extremely high cost penalty of air transport, this option should only be used for a very select number of aircraft if it is crucial that the first sortie starts within a very short time frame.

The cost for the ground base is split into three parts. The set-up, packing and on-base maintenance. These activities make up 15% of the operation costs. Similarly to the facilities cost, the maintenance takes up the biggest portion of the ground base cost (60%) and is computed similarly using only 2 people and parts of 100 €/fix. The expected type of fixes are tailplanes or engine swaps, oil and filters changes, fuse resets and the like. The setup and end-of-operation costs are driven by the labour required, namely: a qualified crew wage of 20 €/h and a local labour cost of 5 €/h for GB setup (10h with 10 people) and aircraft (un-)packing or (dis-)assembly. Overseeing personnel from Wings for Aid (50 €/hrs) is also present 24/7 until the last aircraft is made operational, which makes for over 85% of the setup costs.

The biggest portion of the operational costs are spent on the sortie itself, which is the useful and money-making part of the endeavour. Over half of this cost is spent on fuel which is computed using the simulation from Section 6.3 along with the time to first drop and total time along with estimations for ground operations - 50 min/sortie for inspection, loading, fuelling, taxi and clearance. The rest is spent on personnel. The pilot's time controlling the UAV includes taxi, take-off, landing and a potential (20% chance) visual clearance for drops which accounts for 45 minutes/sortie at a wage of 80 €/hrs. Inspection loading and fuelling is done in 50 minutes by local labour and makes up 6% of the sortie cost.

Adding to that the manufacturing which includes the aircraft (as per Section 14.1.2) and the ground base along with a rough estimate of end-of-life costs yields the following cost distribution over a typical operation: The total accounts for 123 million € over the lifetime of the 500AC produced. This includes over 160 operations, each with 100–150 sorties and 20-30 aircraft, which accounts for 500,000 tons of payload and thus a cost per delivery of 1.481 €/kg or 5.92 times the price of a truck. Other important parameters computed here include the time to first delivery of 67 and a sortie time of 5h30 (i.e. 4.34 sorties per day).

¹⁰ MaritimePage - the speed of a cargo ship [Cited May 22 2023]

¹¹ RAF - Hercules C130J [Cited May 22 2023]

Finally, other business cases were explored by varying the main parameters from Section 4.4. A longer operation time (e.g. a year) implies lower costs given that the fleet is replaced and that the GB is sufficiently large to accommodate the increased number of UAVs. The commercial case looks at the possibility of using the aircraft to deliver non-aid, high-value packages to customers who might need parts rapidly in places without much infrastructure or established logistics, such as wind farms. The last option had each parameter optimized in a way to reduce cost and represents a theoretical minimum for the current design.

Table 14.5: Results per case

Parameters	Default	Long	Commercial	Cheap
Packages per drop	6	6	1	12
aircraft shipped to GB	34	60	10	29
AC shipped by plane	2	2	0	0
AC shipped per boat	20	20	10	3
fleet replacement threshold	NA	1	NA	0.25
concurrent operations	2	2	2	1
operation duration [days]	28	365	7	2000
storage time [days]	30	30	0	0
world coverage in 72h [%]	70	70	0	50
operational cost [€/kg]	1.575	1.447	1.342	1.196
payload rate [kg/day]	20,400	20,400	9,000	10,000
sorties per day	4.34	4.34	4.34	3.95
TTFD [h]	67	67	35	104
fleet availability [%]	58	33	87	36

14.3. Return on Investment

In order to have a successful business model, the profits have to be maximised whilst keeping the price competitive. In order to calculate the ideal price, certain steps are taken. First, the revenue is plotted compared to the amount of aircraft manufactured per year. It is estimated that operations will start once 30 aircraft are manufactured. The plot can be found in Figure 14.4, on the horizontal axis is the amount of years starting with 30 aircraft in year zero (start up operations), and on the vertical axis the revenue per year in €. The code takes all parts of operations into account, from manufacturing costs, maintenance, end-of-life procedures and shipping costs to the risk of an aircraft failing beyond repair. So as the amount of aircraft increase, the amount of operations increase and with that the aircraft which have to be retired increase. Due to this decrease in aircraft, the revenue does not increase per year every year.

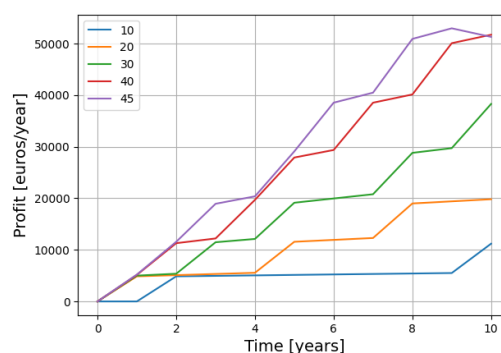
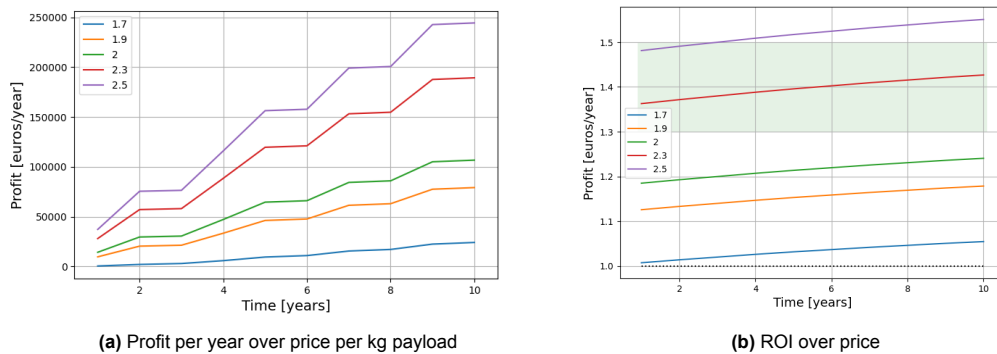


Figure 14.4: Revenue per year over number of aircraft manufactured per year

The minimum aircraft necessary for an operation are 45. Because the amount of aircraft at the start of the first year (0,0) is equal to 30, when manufacturing 10 extra aircraft per year the first two years no operations will commence. The decrease, at the end of the 50 extra aircraft per year revenue line, is due to the maximum amount of aircraft, which is set to 300. Once this number is exceeded, no new aircraft are produced until the

total amount of aircraft is lower than this maximum again. This means for one to two years, whilst no new aircraft are manufactured, but old aircraft still retire, the revenue appears to go down a bit for those years. If the retiring aircraft are still manufactured and replaced, the revenue will stay the same as it reached at 300 aircraft.

From Figure 14.4 combined with the manufacturing logistics, it is decided that manufacturing around 40 aircraft per year is the ideal amount. Going further with this amount, the ideal price has to be decided. In Figure 14.5a, the vertical axis is the profit per year and the horizontal axis the time in years, with each line using a different price per kg payload. In Figure 14.5b, these same prices are then shown as a ROI (return on investment). If the ROI value is one, that means the same amount is spent as comes in (break-even). If the ROI is two, then the income is twice as much as the costs (for example, if you spent 500 € but make 700, your ROI value is $\frac{700}{500} = 1.4$). A value lower than one means a loss is made.



The ROI decreases over time, as the price remains constant, but the costs increase with more aircraft to maintain. Because the price has to be competitive and profitable, a ROI around 1.3-1.5 is advised. This is indicated by the green rectangle in Figure 14.5b and results in a price around 1.25 to 1.35 €/per kg of payload delivered.

In Figure 14.6 the total revenue for the prices 1.25, 1.3 and 1.35 €/per kg payload are shown. From these figures, it becomes clear that Wings For Aid is a profitable business. If more income is required for any reason, the ROI can be increased and a new price may be decided upon. The prices of competitive companies should be taken into account when considering a price increase.

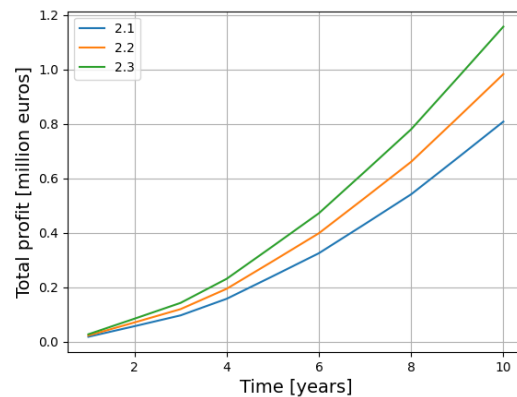


Figure 14.6: Total revenue over time

14.4. RAMS

To round off the project, a RAMS analysis is conducted. Now that the design is more refined, a better estimation of reliability can be done using a part-wise, repairable model Figure 14.7. It uses each component's mean time between failure (MTBF) multiplied by the part's current hazard rate (Figure 14.8) to obtain the expected number of failures of each set of component per sortie. The consequences (unplanned maintenance at the GB, at external facilities or crash) of a failure is determined using inspection, redundancy, criticality and repairability criteria.

Once the expected number of failures per sortie over time is known, the availability and maintenance (planned and unplanned) are evaluated for an operation, yielding the number of aircraft and parts required. A cost estimate can be obtained when combined with a mean time to repair for small (GB) or large (EXT) repairs and labor costs.

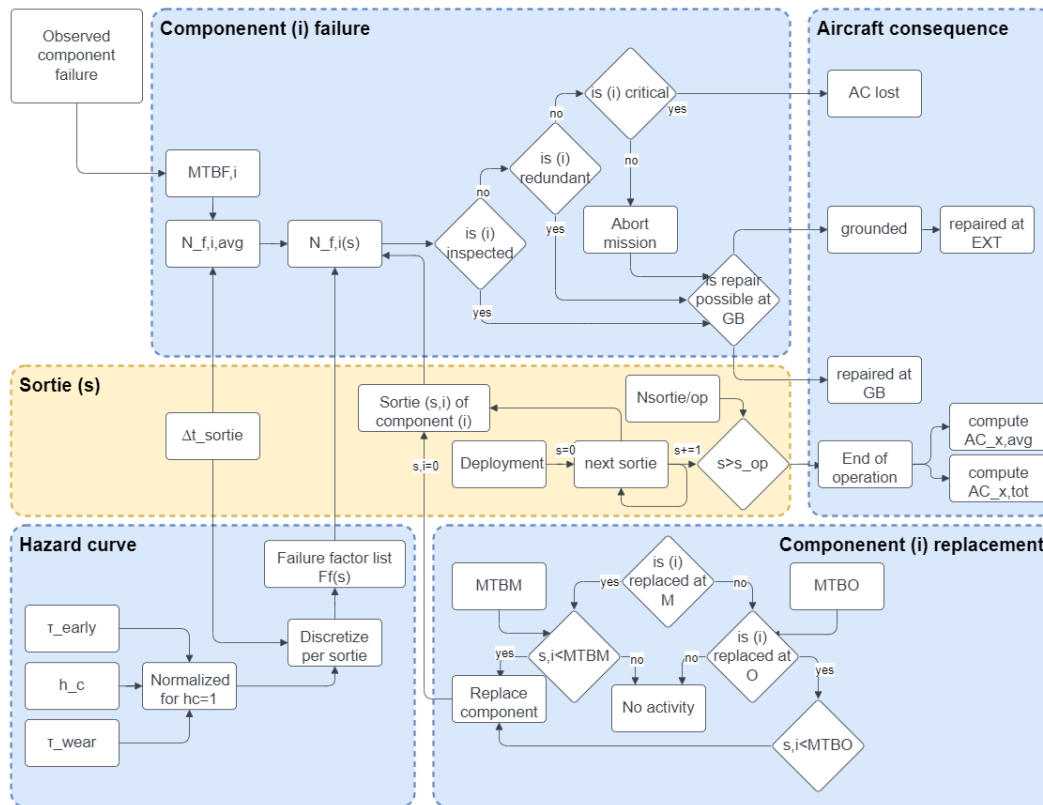


Figure 14.7: Repairable system model implementation

14.4.1. Reliability

In order to estimate the level of contingency and expected time to failure, probability of some of the subsystems is researched and presented in Table 14.6. The reliability over the lifetime $R [Lt]$ of a subsystem is $1 - P_{fail} [Lt]$, where P_{fail} , the failure likelihood, expresses the probability of failure during the lifetime (10,000 flight hours, see Chapter 4). The probability of failure per flight hour $P_{fail} [fh]$ can be computed as $P_{fail} [Lt]/lifetime$. The mean time between failure in flight hours MTBF [fh] is then the inverse of $P_{fail} [fh]$. This means, that if the MTBF of a subsystem is smaller than the lifetime of the aircraft, $P_{fail} [Lt] > 0$.

Table 14.6: Failure per lifetime, flight hour and Mean Time Between Failure of some aircraft subsystems

Subsystem	$P_{fail} [Lt]$	$P_{fail} [fh]$	MTBF [fh]
Engine ¹²	$7.00 \cdot 10^{-2}$	$7.00 \cdot 10^{-6}$	$1.43 \cdot 10^5$ (100 ¹³)
Propeller ¹⁴	-	-	(1500 ¹⁵)
Electric actuators [51]	$2.46 \cdot 10^{-2}$	$2.46 \cdot 10^{-6}$	$4.05 \cdot 10^5$
Power generators [57]	$1.67 \cdot 10^1$	$1.67 \cdot 10^{-3}$	600
Ground and UAV comms. [58]	$1.00 \cdot 10^0$	$1.00 \cdot 10^{-4}$	10000
ADC [59]	$4.20 \cdot 10^{-7}$	$4.20 \cdot 10^{-11}$	$2.38 \cdot 10^{10}$
VOR NAV/COM ¹⁶	$4.55 \cdot 10^{-1}$	$4.55 \cdot 10^{-5}$	22000.00
Flight data recorder [60]	$1.98 \cdot 10^0$	$1.98 \cdot 10^{-4}$	5053
Landing gear [61]	$5.70 \cdot 10^{-3}$	$5.70 \cdot 10^{-7}$	$1.75 \cdot 10^6$
Airframe [62]	$1.00 \cdot 10^{-4}$	$1.00 \cdot 10^{-8}$	$1.00 \cdot 10^8$

A limited number of aircraft subsystems is analysed in the table. The airframe (wing, fuselage, tail) is designed with a similar philosophy to withstand ultimate load factors. Those are defined so that "loss of one aircraft due to structural overload shall be expected in 1000 aircraft lifetimes" [62]. The landing gear, although designed for predefined extreme loads, can sustain fatigue damage, should abnormal landings occur too often, with the assumption that the aircraft performs 3000 take-off and landing cycles throughout the lifetime. The engine and propeller, as well as electric and electronic on board equipment are off the shelf products, which can have their reliability expressed by the manufacturer, or computed. The expected failure rate of a set of components (i) at a point in the aircraft's lifetime or sortie index (s) is computed using:

$$N_f = N_{components} \cdot P_{failure(s,i)} \quad (14.1)$$

$$N_f = \left(\frac{N_{comp}}{N_{AC}} \cdot N_{AC,operational} \right) \left(\Delta_{t,sortie} \frac{H(s)}{MTBF_{(i)}} \right) \quad (14.2)$$

$$(14.3)$$

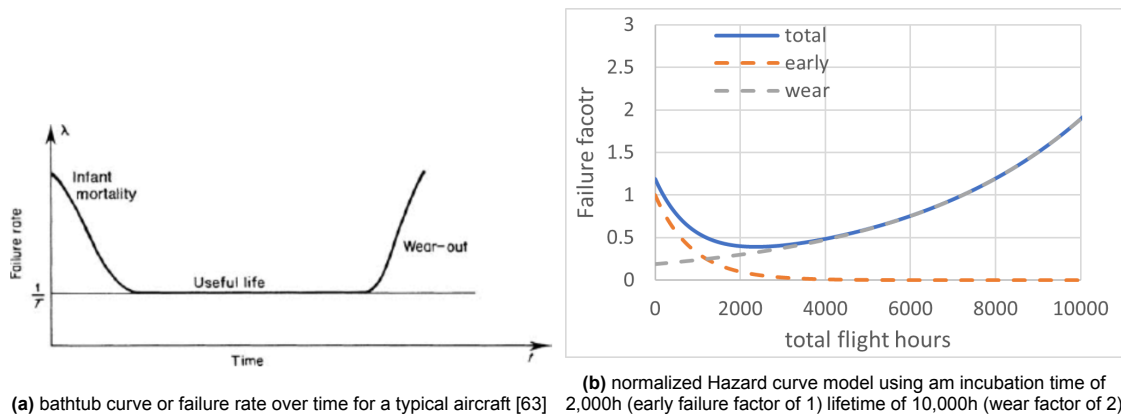


Figure 14.8: Failure rate over time

14.4.2. Maintenance

From the values of MTBF and failure rates in Table 14.6, the most important factors affecting the maintenance approach can be qualified. Table 14.7 presents the number of components of each of the subsystem and qualifies whether each subsystem is redundant (redundancy implemented in the design), is critical (flight impossible with failure), is inspectable (check before operation allowing to spot upcoming failures, reducing the consequence by a single level), and is repairable (at ground base, if not, grounded). Based on these qualification, the consequence (status) of an aircraft with a failure of the given subsystem can be expressed: maintained (on local ground base), grounded (sent away for major repair) or crashed (lost). The maintenance of a given subsystem can be major (overhaul, sent to away for major repair) or performed at ground base.

¹²Kitplanes - Homebuilt accidents, [cited on 20 June 2023]

¹³flight hour service interval

¹⁴Aircraft Propeller Works, [cited on 20 June 2023]

¹⁵flight hour overhaul interval

¹⁶Aeroexpo - Gables products, [cited on 20 June 2023]

Table 14.7: MTB and consequence of failure of selected aircraft subsystems

Subsystem	MTBF [fh]	Redundant	Critical	Inspectable	Repairable	Consequence	Maintained at
Engine	$1.43 \cdot 10^5$	No	Yes	Yes	Yes	Maintenance	Ground base
Propeller	(1500)	No	Yes	Yes	Yes	Maintenance	Ground base
Electric actuators	$4.05 \cdot 10^5$	Yes	Yes	No	No	Grounded	Overhaul
Power generators	600	Yes	Yes	No	Yes	Maintenance	Ground base
Ground comss.	10000	No	Yes	Yes	Yes	Maintenance	Ground base
UAV comss.	10000	No	Yes	No	No	Crash	Overhaul
ADC	$2.38 \cdot 10^{10}$	No	Yes	No	No	Crash	Overhaul
VOR NAV/COM	22000	No	Yes	No	No	Crash	Overhaul
Flifht data recorder	5053	No	No	No	No	Grounded	Overhaul
Landing gear	$1.75 \cdot 10^6$	No	Yes	No	No	Crash	Ground base
Wing	$1.00 \cdot 10^8$	No	Yes	No	No	Crash	Overhaul
Fuselage	$1.00 \cdot 10^8$	No	Yes	No	No	Crash	Overhaul

Since two separate wing parts exist, the airframe can be separated into fuselage and two wings. Because of lack of data on propeller reliability, only the overhaul interval is given. The maintenance scenarios can be translated into aircraft availability, described in Section 14.4.3.

14.4.3. Availability

The availability of the fleet is defined as the fraction of aircraft in an operational state out of the aircraft present at the ground base (GB). Figure 14.10a shows the availability distribution over the complete lifetime of an aircraft which, as expected, tends to zero. Figure 14.10 shows the distribution of the fleet in an actual operation: it can be clearly seen that the first two aircraft arrive immediately, while the others arrive in batches by ship Figure 4.1 (note the peaks) until the desired number is stored. The maintenance fraction is initially high since it takes some time (hours to days) between an aircraft is found to fail and its repair being completed which causes a backlog of UAVs under maintenance. If the repair can be done at GB, they go back into the operational fleet (note the bump around the 50th sortie set which indicates the first batch of repairs). If not, they are grounded, stored safely in their containers and eventually shipped back to undergo more extensive or delicate repairs at the external facilities.

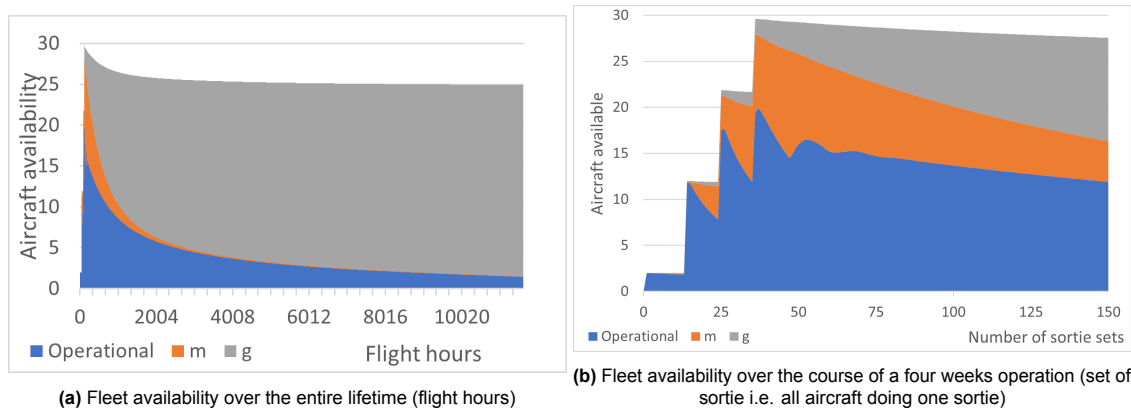


Figure 14.9: Fleet availability indicating the fraction of aircraft under maintenance (at the ground base) with "m" in orange, the part awaiting extensive repairs i.e. grounded with "g" in grey and the operational (useful fleet) in blue - the crashed UAVs account for the decreasing total

The current design and parameters yield a four-week fleet availability (starting at the last shipment) of about 65%. This figure could be improved by making components easily interchangeable and replaceable at the ground base using spare parts: up to 75% if all components can be repaired at GB. Alternatively, reducing to mean time to repair (MTTR) could increase the fleet availability to 72%. Combined measures give a theoretical maximum of 90% given the reliability figures. Longer operations can be optimized using a fleet replacement throughout the operation i.e. exchanging the grounded UAVs with new ones once a certain proportion of the fleet is grounded. This measure decreases the amount of on-site storage needed and spread-out the shipments more efficiently.

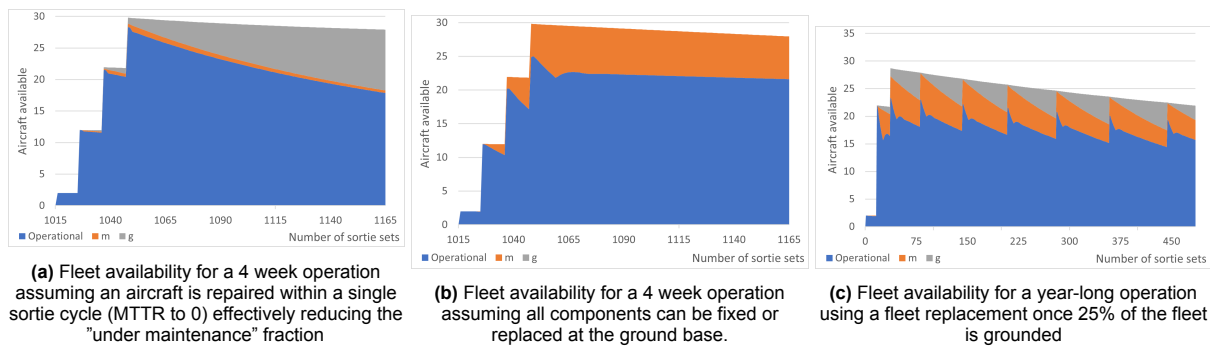


Figure 14.10: Fleet availability mitigation measures

This parameter drives the number of UAVs that need to be shipped at the start of an operation such that the average operational fleet can fulfill the payload delivery rate requirement of 20,000 kg/day. Since the number of operational aircraft over time is exponential (see Figure 14.10a), the number shipped can be estimated given the expected length of the operation. For 4 weeks, 21 AC shipped, or 18 operational, can accomplish 21,000 kg/day. In case the operations runs for much longer (e.g. conflicts for a year), the grounded part of the fleet will need to be replaced to ensure continued operations (the fleet availability drops to 27% otherwise).

Finally, the aircraft availability is defined as the fraction of time a given UAV is flying per day. This comes down to about 16 h/day, 68%, or 4.8 sorties per aircraft per day.

14.4.4. Safety

Safety qualitatively identifies events that can lead to loss of health or lives of human beings. It can be split into the aircraft crashing, posing a danger to people related and non-related to the Wings for Aid operations, as well as ground handling safety, which affects the Wings for Aid ground crew. Moreover, the aircraft itself can be damaged during ground operations, which can results in failures in flight, if unnoticed.

Likelihood of crash

Crashing likelihood can be addressed by computing the total number of aircraft that statistically will crash over a time of single operation (see Chapter 4 for operation definition), assuming that crash occurs when failure of ground and UAV communication, ADC, VOR NAV/COM, landing gear, wing or fuselage occurs. From Section 14.4.2 and Section 14.4.3, 1.38 aircraft out of the overall fleet crashes during an entire operation, translating to a probability of 0.0012 of crash per flight hour. This is considered significant, meaning that cruising routes should avoid populated areas.

Ground handling injury

The rotating propeller, aircraft velocity at take-off and landing, box impact as well as engine heat can pose a danger to the ground operators. They are briefly addressed individually, with an operational recommendation given to mitigate the risk of occurrence.

- The propeller is positioned as the most forward part of the aircraft, with the rotating axis at 1.1 m above the ground and diameter of 1.44 m and tip speed of over 230 m/s. It can easily cause serious or fatal injuries to humans and living creatures. The aircraft should be approached only when the engine is off and the propeller reaches full stop. Before turning the engine on, clearance should be checked and anyone in proximity warned ("clear prop" shout out).
- The aircraft kinetic energy can reach 0.25 MJ at take off and landing. The avoiding maneuvers at those flight phases are not precise, because of the large speeds, therefore the presence on the designated landing and taxi strip should be avoided at all time.
- A dropping box can reach the ground at around 14 m/s, and thus 4.4 kJ. It poses a critical danger to anyone in proximity of the dropping zone, also the ground operator. The operator's responsibility is to ensure no dropping zone intrusion occurs, and that him/herself stays away from the range of box drops (see Chapter 4).

- The engine heats up significantly during long operation, as the cylinder head temperature reaches 150°C¹⁷. In order to avoid burns, engine maintenance should only be performed once the engine has cooled down to ambient temperature. Additional care should be taken when loading the front box row, as it is placed 0.4 m behind the engine, with no firewall.

Other ground handling injury risks can be identified (for instance finger pinching with loading doors, foot crush by aircraft tire etc), however are omitted in this report. It is recommended to use common sense when around the aircraft. All personnel should be trained to these procedures within the first week by the overseers sent by Wings for Aid.

Ground damage

In commercial aviation, one aircraft is damaged per 5000 flight due to ground handling incidents [64]. Because lack of specialised equipment and potentially limited training and procedures, this number can be more significant for Wings for Aid. Some unique features of the aircraft cause particular failure risk, other, more general caution habits should also be applied.

Some damage specific to the aircraft includes:

- Glass composite fairing damage, if excess pressure is applied on a fuselage wall. The aircraft should be pushed and pulled by struts, propeller, landing gear structure or handles (see Section 7.2.3). No items should be temporarily placed on top or against the sides of the fuselage. Loading doors should be handled with normal force, handing items from the handles or pulling on them excessively is unacceptable.
- Dropping mechanism damage, if boxes are loaded with insufficient care. This also includes correct placement of the boxes, so that their deployment does not damage the fairing nor the dropping mechanism. Care should be taken when handling of the loading trolley (cart), so that it does not exert force on the fairing, loading doors, fuselage truss structure or tires.
- The wing and strut attachments are designed to withstand high loads, however alignment of notches should be careful, so that inserting the pin is not forced. Pin lubrication is recommended. All pins should be secured before operations. In order to reduce required assembly forces, wings should not contain any fuel during that process.

Additionally, the following common practises are recommended [65].

Firstly, a safety and just culture is encouraged. Management should understand that mistakes are and will be made. Therefore employees should not be punished for accidental mistakes and reporting any potential damage should be encouraged. This allows to prevent potential in-flight failure and eventually leads to savings. When waling airside, it is necessary to remain aware of all operations, and not simply rely on noise. When operating with a vehicle, the operator should remember that any trailers do not strictly follow the leading vehicle path. The vehicle height should be remembered when operating under the wing. All vehicles should be brought to standstill and parking brakes should be on, when servicing the aircraft. FOD (Foreign Object Debris) should never be ignored and always picked up. When refuelling, the aircraft, fuel pump and tank should be grounded with a wire, to prevent any static discharges. All hatches and engine air inlets should be closed or covered for precipitation, dust storm and heavy weather, the aircraft should be stored under roof if possible. Boxes with aid should not be stored inside the aircraft, unless for operations, especially if they contain corrosive fluids or dangerous goods. The communication between ground crew should be concise, clear and not open to interpretation. Ideally, confirmation of instructions should always be received, to confirm the understanding [65].

For further improvement of the RAMS analysis, more precise and accurate reliability data should be researched for more aircraft subsystems. Empirical data from the real Wings for Aid project can be taken to compare with initial estimations, A ground handling instruction and aircraft user manual should be issued.

¹⁷Rotax 912 cylinder head temperature

Post Project Plan

In order to guide the further development of the design, an outline has been created for post project activities. The first stage includes client recommendations, which follow from the design process undertaken in this report. After, all activities are examined and their flow for post project activities indicated in Section 15.2. Next, time indications of these activities are presented in Section 15.3. Lastly, cost allocations have been made of these activities made to give a first indication of the cost involved in further development of the project.

15.1. Client Recommendations

With the entire conceptual design process done and the final design evaluation performed, there is some time to look back at the process. With any design process there are a lot of obstacles and almost everything comes after a long iteration of methods and approaches. However, with this phase done, there are some recommendations for when the client decides to use this design for further development. It is assumed the client will start over themselves, but using the ideas and processes developed in this report. This way, the client can get a relatively quick yet accurate design for their specific mission needs.

The first recommendation is to change the man power per department, or adjust the tasks assigned per department. Departments such as aerodynamics and structures needed to do a lot of work compared to other departments. This meant more effort was needed in order to get the work of these departments done in the same time. This was not always achieved and therefore led to an unbalance in design phase and maturity. This design maturity is the basis for the next recommendation. It is very important to keep track of the design maturity of every department and make sure this progresses evenly for all departments. One of the things that should have been incorporated earlier is the sizing and placement of equipment, such as flight computers or actuators.

The creation of a fully integrated calculation program, which takes the parameters of all departments into account, is also highly recommended. However, the way this was approached in this report can definitely use improvements. From the start a clear parameter naming convention should be agreed on, and all departments should actively be checking and monitoring their parameters, in order to prevent any duplicate parameters. All calculations should also be written while keeping in mind that they become part of a larger iteration process, which might require many iterations. Therefore, any manual calculations should be avoided if possible. It is also advised to add many checks throughout the program, which throw a warning once a value exceeds a certain threshold.

Lastly, it is also recommended to have more reflection on the requirements throughout the entirety of the design process. Moreover, reviewing of the requirements should happen within shorter time intervals. This allows for faster responses in case parts of the design are overlooked or contingencies are exceeding their estimated thresholds. This also includes increasing the interactions with the stakeholders to optionally renegotiate certain requirements.

15.2. Project Design and Development Logic

After the preliminary design stage performed in this report, many steps still need to be taken in order to reach a fully operational aircraft, able to perform missions. These steps are presented in a logical order, reflecting the technical characteristics of the project. The Project Design and Development Logic can be found in page 130. After the preliminary design, the detailed design phase will be entered. After this phase, the aircraft should be ready to undergo numerous tests. If the aircraft passes these tests, the aircraft can be certified and the manufacturing process can be started. Following preparation such as obtaining contracts

and logistical planning, the market roll-out can be performed. The final step is the operation phase, in which Wings for Aid will be delivering humanitarian aid in regions affected by disasters.

15.3. Project Gantt Chart

A time indication of the full development stage up to market roll-out is given in page 131. Generally, once the design has reached sufficient maturity, the certification rules for the aircraft need to be specified. This will be done after the conceptual design is finished. The period for compliance demonstration given by EASA is five years¹, which is why the next steps in the total design add up to five years. One and a half year is allocated for familiarization and preliminary design. Two years are estimated for detailed design, which is finished with a testing phase of one year. Lastly, about a year is assigned to market roll-out preparation, including the logistics. An important note is the fact that 10 engineers are estimated to work on this design. If this number is different, time should be changed accordingly.

15.4. Cost Breakdown Structure

Up until the end of the DSE part of the project, no development costs were accounted for. Future continuation of the design process, however, will come at a cost of monetary resources. In order to account for these expenditures, a post-DSE cost breakdown structure has been made. It is shown in Figure 15.1. The manufacturing of the aircraft is part of the cost breakdown structure. It is not, however, part of the development costs.

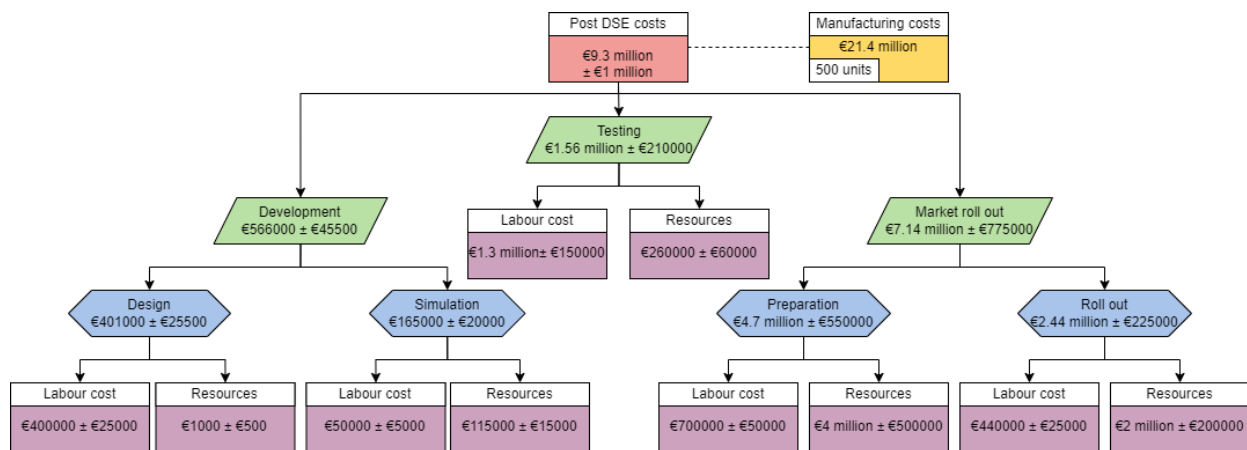
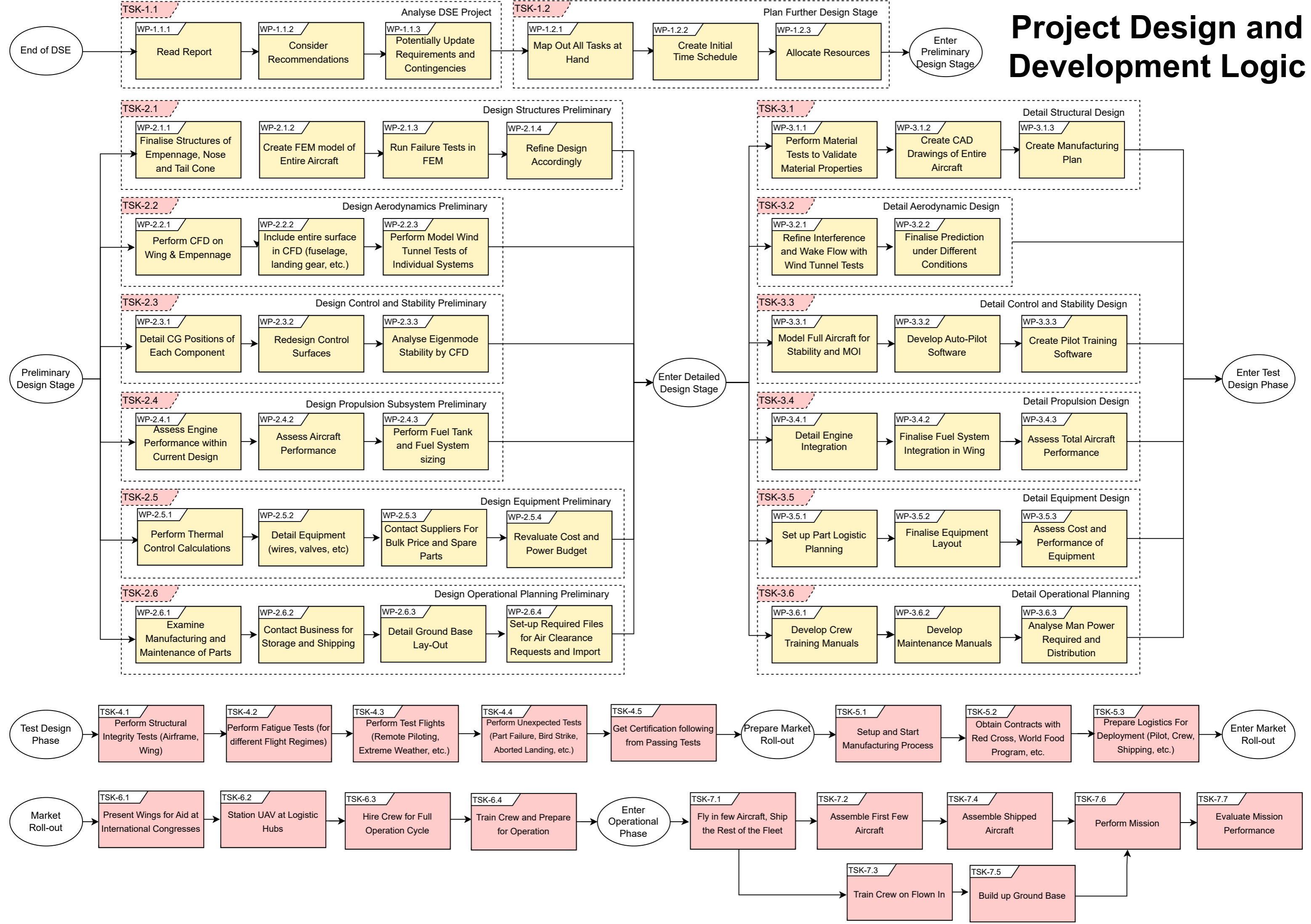


Figure 15.1: Post DSE Cost Breakdown Structure

¹EASA - Aircraft Certification

Project Design and Development Logic



Post Design Gantt Chart

[illegible]

Conclusion & Recommendations

The present report describes and justifies the design process of a remotely-piloted aircraft that is able to deliver 10 to 12 boxes containing 20 kg of humanitarian aid with pinpoint accuracy at a range of 250 km. One of the main objectives is minimizing the cost. This goes for aircraft unit cost and the cost of a kilogram of payload delivered. Apart from designing an aircraft to perform this mission, the aircraft are integrated into an operation that has the same daily payload capacity as a C-130 Hercules aircraft.

At this design stage, there is compliance with all user requirements except the requirements for cost and the requirement for stability. The unit cost for the current design concept is up to €41,300. This cost is strongly dependent on the unit cost of the engine. Next, the cost per kilogram of payload delivered, considering the entire picture, is more than four times higher than that of a truck. Besides the cost, it was concluded that the current design concept is spirally unstable. Measures have to be taken to reduce these cost parameters as well as the spiral stability, which will be given in the next paragraph. In order to visualise the final design, an isometric view of the aircraft is presented in Figure 16.1.



Figure 16.1: Isometric view of conceptual solution

The design process as experienced by the design team has brought some insights forward. These insights are left as recommendations for future design teams to incorporate in their work. It should be mentioned that time as a resource was limited during this design process. Because of this, the deepness of the analyses performed was limited.

- For the structures subsystem, the compromise of material performance and cost should be analysed further, with potential to reduce structural mass and employment of composites. Elaborating on joining methods and corrosion protection allows to save mass by combining steel 4130 and stainless steel 410. The structural analysis can be refined by applying the finite element analysis with more accurate and elaborate loading distributions. In the refinement of the structure, the optimisation criteria should also be re-evaluated. Considering the stringent cost requirement, opting for a slightly heavier design could outweigh further optimisation in terms of structural mass.

- The current design is able to operate in South-Sudan, or regions having a similar landscape. To operate in more mountainous regions, the amount of payload brought by the aircraft needs to be reduced. If more payload would like to be brought, it is recommended to tailor the design to a certain operating area. An example of this could be adding forced induction to the engine in order to reduce power loss at altitudes. This could be beneficial for operating areas like the Himalayas.
- The aerodynamics of the design is currently estimated using lifting line theory and vortex lattice theory. In order to more accurately predict the drag and stability of the aircraft, computational fluid dynamics analyses could be performed. A windtunnel test of a scale model could also be used to analyse this. These analyses will reduce the contingency on the values mentioned. Especially as the interactions between surface and subsystems gets modelled in more detail using these methods. The design and sizing of control surface actuators should be analysed, to check the feasibility of current control surface sizes for the surfaces they are part of. In addition, this will increase the accuracy of the weights and their corresponding centre of gravity location for each control surface, improving the overall accuracy of the design.
- If the stability requirement is to be met, it is recommended to consider design alterations that improve spiral stability such as increasing dihedral, or by looking more into the capabilities of available auto pilots to deal with unstable slow eigenmotions.
- As an overall recommendation, future design teams could consider certifying the airframe with aviation authorities. This would make deployment and clearance in airspace less cumbersome and more reliable. This would add to the strategic position of Wings for Aid in the market, providing another competitive edge. [66]
- To lower the cost of manufacturing as well as the cost per kilogram, it is recommended to make deals with suppliers to receive goods at a lower rate by buying in larger quantities, or by buying solely from the same supplier. Other measures that can be taken are accepting lower quality materials, such as used engines. For the example of used engines, the lower cost of the part is reflected in lower lifetime remaining and uncertainty on previous operating conditions.
- The design can be altered to accommodate more payload. This can be done by stretching the fuselage and choosing a more powerful engine while using the same "blueprint". This makes the design future-proof and resilient to changes in the market by changing with it.

References

- [1] B. Nielsen and A. L. R. Santos. "Key challenges of product development for humanitarian markets". In: *2013 IEEE Global Humanitarian Technology Conference (GHTC)*. 2013, pp. 411–415. DOI: 10.1109/GHTC.2013.6713721.
- [2] AE3200 Group 18. *DSE baseline report - Wings for Aid*. Tech. rep. TU Delft, Apr. 2023.
- [3] AE3200 Group 18. *DSE Miterm Report - Wings for Aid*. Tech. rep. TU Delft, May 2023.
- [4] J. Melkert. *Project Guide Design Synthesis Exercise, Wings for Aid*. Unpublished. Faculty of Aerospace Engineering, TU Delft. 2023.
- [5] Shaman Gupta and Sanjiv Kumar Jain. "A literature review of lean manufacturing". In: *International Journal of Management Science and Engineering Management* 8.4 (2013), pp. 241–249.
- [6] B. vad Mathiesen, D. Connolly, and H. Lund. *CEESA 100 Renewable Energy Transport Scenarios towards 2050*. Aalborg University, 2014.
- [7] AE3200 Group 18. *DSE Baseline Report - Wings for Aid*. Tech. rep. TU Delft, May 2023.
- [8] A. K. Kundu. *Aircraft Design*. 3rd. Cambridge University Press, 2010.
- [9] J. Roskam. *Airplane Design Part I: Preliminary Sizing of Airplanes*. Design, Analysis and Research Corporation (DARcorporation) 1440 Wakarusa Drive, Suite 500 Lawrence, Kansas 66049 U.S.A, 1985.
- [10] M. Ashby, H. Shercliff, and D. Cebon. *Materials Engineering, Science, Processing and Design*. 4th. Butterworth-Heinemann.
- [11] *Easy Access Rules for Normal, Utility, Aerobatic and Commuter Category Aeroplanes (CS-23)*. EASA. 2018.
- [12] E. Torenbeek. *Synthesis of subsonic airplane design*. Delft University Press, 1982.
- [13] P.C. Roling and M. Voskuilj). *Lecture 4: Airfield performance [powerpoint slides]*.
- [14] D. P. Raymer. *Aircraft Design: A Conceptual Approach*. 3rd. American Institute of Aeronautics and Astronautics, 2018.
- [15] Sept. 2016. URL: <https://www.eaa.org/ea/news-and-publications/ea-news-and-aviation-news/bits-and-pieces-newsletter/09-13-2016-aviation-word-service-ceiling#:~:text=The20definition20of20the20service,minute20under20standard20air20conditions..>
- [16] A. Kundu, M. A. Price, and D. Riordan. *Conceptual aircraft design: an industrial approach*. Wiley.
- [17] *Certification Specifications for Normal, Utility, Aerobatic, and Commuter Category Aeroplanes, Amendment 3*. EASA. July 2012.
- [18] *Standard Specification for Design Loads and Conditions*. ASTM International; Jan. 2021.
- [19] H. S. Mohammad. *Aircraft design: a systems engineering approach*. John Wiley and Sons, Ltd., 2013.
- [20] J. Jang et al. "Preparation of high-performance transparent glass-fiber reinforced composites based on refractive index-tunable epoxy functionalized siloxane hybrid matrix". In: (2021).
- [21] W. B. Soboyejo. *Mechanical properties of engineered materials*. Marcel Dekker, 2003.
- [22] T. A. Shams et al. "Airfoil selection procedure, wind tunnel experimentation and implementation of 6dof modeling on a flying wing micro aerial vehicle". In: *Micromachines* 11.6 (2020), p. 553.
- [23] D. Lednicer. *The Incomplete Guide to Airfoil Usage*. University of Illinois at Urbana-Champaign, 2023.
- [24] J. Morgado et al. "XFOIL vs CFD performance predictions for high lift low Reynolds number airfoils". In: *Aerospace Science and Technology* 52 (2016), pp. 207–214.
- [25] M. D. Maughmer and J. G. Coder. *Comparisons of theoretical methods for predicting airfoil aerodynamic characteristics*. Tech. rep. AIRFOILS INC PORT MATILDA PA, 2010.

- [26] A. V. Popov et al. "Variations in Optical Sensor Pressure Measurements due to Temperature in Wind Tunnel Testing". In: *Journal of Aircraft* 46.4 (2009), pp. 1314–1318.
- [27] J. G. Coder and M. D. Maughmer. "Numerical validation of the Squire–Young formula for profile-drag prediction". In: *Journal of Aircraft* 52.3 (2015), pp. 948–955.
- [28] N. K. Hieu and H. T. Loc. "Airfoil selection for fixed wing of small unmanned aerial vehicles". In: *AETA 2015: Recent Advances in Electrical Engineering and Related Sciences*. Springer. 2016, pp. 881–890.
- [29] John E Williams and Steven R Vukelich. *The USAF Stability and Control Digital DATCOM. Volume III. Plot Module*. Tech. rep. McDonnell Douglas Astronautics Co St Louis Mo, 1979.
- [30] J. D. Anderson and M. L. Bowden. *Introduction to flight*. Vol. 582. McGraw-Hill Higher Education New York, 2005.
- [31] R. Faye, R. Laprete, and M. Winter. "Blended winglets". In: *Aero, Boeing*, (17), January (2002).
- [32] R. Cosin et al. "Aerodynamic analysis of multi-winglets for low speed aircraft". In: *27th International congress of the aeronautical sciences*. 2010, pp. 1622–1631.
- [33] R. V. Gifford and C. P. Vandam. "The design integration of wingtip devices for light general aviation aircraft". In: *ICAS/AIAA Aircraft Systems and Technol. Conf.* NASA-TM-83252. 1982.
- [34] O. Dantsker and M. Vahora. "Comparison of aerodynamic characterization methods for design of unmanned aerial vehicles". In: *2018 AIAA Aerospace Sciences Meeting*. 2018, p. 0272.
- [35] K. Budziak. *Aerodynamic Analysis with Athena Vortex Lattice (AVL)*. Hamburg: Aircraft Design and Systems Group (AERO), Department of Automotive..., 2015.
- [36] M. Nictua and D. Scholz. *Estimating the Oswald factor from basic aircraft geometrical parameters*. Deutsche Gesellschaft fur Luft-und Raumfahrt-Lilienthal-Oberth eV, 2012.
- [37] S. D. Iyaghighba, A. Hamza, and A. E. Ogaga. "Investigation of the Dynamic Stability for a Light Aircraft". In: *American Journal of Electrical and Computer Engineering* 2.2 (2018), pp. 37–55.
- [38] P. Okonkwo and P. Jemitola. "Integration of the athena vortex lattice aerodynamic analysis software into the multivariate design synthesis of a blended wing body aircraft". In: *Heliyon* 9.3 (2023).
- [39] W. F. Phillips and N. R. Alley. "Predicting maximum lift coefficient for twisted wings using lifting-line theory". In: *Journal of aircraft* 44.3 (2007), pp. 898–910.
- [40] W.A. Timmer and S.J. van Elsloo. *AE2111-I Systems Design - Project Reader - Work Package 4*. Delft University of Technology, 2021.
- [41] Department of Defence. *Flying Qualities of Piloted Aircraft*. 1997.
- [42] F. Oliviero. *AE2111-II Aerospace Design and System Engineering Elements II, Mobile Surfaces of the Wing*. Delft University of Technology, 2022.
- [43] F. Oliviero. *AE3211-I System Engineering and Aerospace Design, Requirement Analysis and Design principles for A/C stability control P1*. Delft University of Technology, 2023.
- [44] F. Oliviero. *AE3211-I System Engineering and Aerospace Design, Requirement Analysis and Design principles for A/C stability control P2*. Delft University of Technology, 2023.
- [45] C. N. Eastlake and H. W. Blackwell. "Cost estimating software for general aviation aircraft design". In: *2000 Annual Conference*. 2000, pp. 5–173.
- [46] M. Farhat. *ME-435 Aeroelasticity and fluid-structure interaction*. Ecole Polytechnique Federale de Lausanne, 2022.
- [47] S. J. Hulshoff. *AE4930 Aeroelasticity*. TU Delft, 2023.
- [48] R. Vos and M. Hoogreef. *Aerospace Design and Sysetms Engineering Elements I - Landing Gear and Empennage Design*. Delft University of Technology, 2020.
- [49] J.A. Melkert, R. Vos, and B.T.C. Zandbergen. *AE1222-II Aerospace Design and Systems Engineering Elements - Part: Spacecraft (bus) design and sizing*. Delft University of Technology, 2020.
- [50] Jingcheng Fu, Albert Stevan Johan Van Heerden, and Craig P. Lawson. "A Generic Mission-Level Flight Control Surface EMA Power Consumption Simulation Tool". In: (2022).

- [51] J. Fu et al. "A Generic Mission-Level Flight Control Surface EMA Power Consumption Simulation Tool". In: (2021). URL: https://www.researchgate.net/figure/An-illustration-of-BLOS-provided-through-the-Satellite-BLOS-communication-overcomes-L0S_fig1_338000340.
- [52] *Reader 1222 - Spacecraft Design*, v2.3 – 1(*total*). Tech. rep. TU Delft, 2020.
- [53] R. C. Hibbeler. *Mechanics of Materials*. Pearson Education, 2017.
- [54] F. Oliviero. *AE2111-I Systems Engineering and Aerospace Design, Aircraft aerodynamic analysis – Lift and Drag*. Delft University of Technology, 2019.
- [55] R. Root. *Fuel Conservation, Airframe Maintenance for Environmental Performance*. ICAO, 2002.
- [56] C. Kasnakoglu. "Investigation of multi-input multi-output robust control methods to handle parametric uncertainties in autopilot design". In: *PloS one* 11.10 (2016), e0165017.
- [57] D. Lee and D. Choi. "Analysis of the Reliability of a Starter-Generator Using a Dynamic Bayesian Network". In: (2019). URL: https://www.researchgate.net/publication/336077211_Analysis_of_the_Reliability_of_a_Starter-Generator_Using_a_Dynamic_Bayesian_Network.
- [58] D. Dessoay et al. "Satellite-Based ADS-B for Lower Separation-minima Application". In: (2018). URL: <https://ec.europa.eu/research/participants/documents/downloadPublic?documentIds=080166e5b8b29706&appId=PPGMS>.
- [59] A. Lerro and M. Battipede. "Safety Analysis of a Certifiable Air Data System Based on Synthetic Sensors for Flow Angle Estimation". In: (2021). URL: <https://www.mdpi.com/2076-3417/11/7/3127>.
- [60] S. Srivastava and A. K. Chauhan. "Reliability Analysis and Prediction of Mean Time Between Failure of Flight Data Recorder". In: (2015). URL: https://www.academia.edu/21612930/RELIABILITY_ANALYSIS_and_PREDICTION_OF_MEAN_TIME_BETWEEN_FAILURE_OF_FLIGHT_DATA_RECORDER.
- [61] H. Wang, C. J. Xue, and W. T. Jiang. "Fuzzy Fatigue Reliability Analysis for a Landing Gear Structure". In: 1 (2010), pp. 112–115. DOI: 10.1109/CS0.2010.130.
- [62] H. A. William. "Application of Rational Probability Analysis for Determination of Ultimate Design Loads on Large, Flexible, Military Aircraft". In: (1964). URL: <https://apps.dtic.mil/sti/tr/pdf/AD0601777.pdf>.
- [63] A. S. Verma et al. "Measurement of reliability and availability of satellite communication links: Progress and challenges". In: (2013), pp. 268–271. DOI: 10.1109/ISSP.2013.6526916.
- [64] A. D. Balk. *Safety of ground handling*. National Aerospace Laboratory NLR, 2008.
- [65] S. Dupin, T. Thiebaut, and N. Turcot. *Ground Handling and Flight Safety*. Direction Generagle de l'Aviation civile, 2015.
- [66] S. M. Ali, S. M. Kumar, and V. Sumalatha. "Computational Bayesian Approach to Dependency Assessment in System Reliability of Electro-Mechanical Actuator". In: (2021).

A

Task division

Task	Student Name(s)
Executive Overview	All
Introduction	Torben
System Engineering	
Project Description	Linda
Functional Analysis	Linda, Torben, Tim, Jan V.
User Requirements	Linda, Théo, Torben
Contingencies	Théo
Technical Risk Assessment	Linda, Jan V., Jan W.
Sustainable Development	Linda
Strategy	
Market Analysis	Linda, Jarno, Jan W.
Design Approach	
Design Options	Linda, Tim, Jan V.
Trade-off	Linda, Jarno, Ties, Jan W., Jan V., Tim, Bram
First Order estimation	Jarno, Jan W., Tim
Design Organisation	Jan W.
Iteration Description	Tim Jan V.
Operations	
Operations Model	Théo, Torben, Maxime
Ground Base Layout	Maxime
Box Loading	Maxime
Operational parameters	Théo
Flight Performance	
Take-off	Linda
Climb Performance	Ties
Cruise	Ties
Descent	Linda, Ties
Approach & Landing	Linda
Sortie Performance	Ties
Drop Manoeuvre	Théo
Propulsion Subsystem	
Engine Selection	Linda
Propeller Selection	Linda
Fuel Equipment Sizing	Théo, Ties
Fuselage Subsystem	
Frame Structure and Boom	Jan W., (Tim)
Outside Fairing	Jan W., Jan V., Jarno
Wing Subsystem	
Design of the Wing	Jarno, Jan V.
Wingbox	Tim, (Jan W.)
Strut and Attachments	Jan W., (Tim)
Geometry Determination	Ties
Aileron Design	Bram, Torben
High-Lift Device	Bram, Torben

Empennage Subsystem	
Position of Centre of Gravity	Torben, Bram, Tim
Horizontal Tailplane	Jarno, Jan V., Torben, Bram
Vertical Tailplane	Jarno, Jan V., Torben, Bram
Tailplane Spar	Jan W., (Tim)
Aeroelastic behaviour	Jan W.
Undercarriage Subsystem	
Landing Gear Selection	Torben
Placement	Torben, Bram
Structure	Jan W., (Tim)
Onboard Equipment	
System Interaction	Torben
Onboard Computer	Théo, Torben
Communications Subsystem	Théo
Controls Actuators	Théo
Power Electronics	Théo, Torben
Verification & Validation	
Static Testing	Torben
Dynamic Testing	Bram, Ties, Jarno, Jan V., Linda
Design Output Comparison	Jarno
Global Input-Output Analysis	Tim, Jan V.
FEA Model Verification	Jan W.
Final Design Overview	
Total Drag	Jarno, Jan V.
Stability and Control of Entire Aircraft	Jan V.
Resource budgeting	Théo
Requirement Compliance	Torben
Design Evolution	Théo
Feasibility Analysis	Torben
Final Design Evaluation	
Production Plan	Théo
Operational Cost	Théo, Maxime
Return on Investment	Maxime
RAMS Analysis	Linda, Jan W., Théo
Post Project Plan	
Client recommendations	Jan V., Tim
Project Design and Development Logic	Jan V., Tim
Project Gantt Chart	Jan V., Tim
Cost Breakdown Structure	Ties
Conclusion and Recommendation	Bram, Ties, Torben, Jan V.
Jury Summary	Ties
Poster	Tim, Jan V
CAD Model	Maxime